Transcriptomic Studies of Atlantic Salmon Responses to Dietary Omega-3 Long-Chain Polyunsaturated Fatty Acids, *Piscirickettsia salmonis* Infection, Immunogens, and Functional Feed

by

© Xi Xue, B.Sc. (Hons), M.Sc.

A thesis submitted to the

School of Graduate Studies

in partial fulfillment of the requirements for the degree of

Doctor of Philosophy

Marine Biology

Department of Ocean Sciences

Memorial University of Newfoundland

September 2022

St. John's, Newfoundland and Labrador, Canada

ABSTRACT

Atlantic salmon farming faces several issues and challenges such as disease outbreaks and the limited supply of fish oil, affecting the sustainability of the industry. The current thesis aimed to gain a better understanding of the dietary requirement of omega-3 long-chain polyunsaturated fatty acids (ω3 LC-PUFA; i.e. DHA+EPA), immune responses against *Piscirickettsia salmonis* or immunogens, and the immune-modulating properties of a functional feed in Atlantic salmon. In **Chapter 2**, I studied the impact of varying levels of DHA and EPA (0, 1.0, and 1.4% of the diet) on the hepatic transcriptome. My data suggested that ~1.0% of dietary ω3 LC-PUFA is sufficient to sustain the optimal growth performance of Atlantic salmon, but may not be enough to maintain good health and survival compared with fish fed diets containing a higher amount of DHA and EPA. In **Chapter 3**, Atlantic salmon parr were infected with an EM-90-like isolate of *Piscirickettsia salmonis* through intraperitoneal injection. I used microarray and qPCR analyses to study the head kidney transcriptomic differences between high and low infection individuals at 21 days post-injection (DPI). Many innate and adaptive immune processes were dysregulated in *P. salmonis*-infected Atlantic salmon. In contrast, a small number of general physiological processes was affected. Furthermore, the comparison of individuals with differing infection levels has provided insights into the biological processes possibly involved in natural resistance against *P. salmonis*. In **Chapter 4**, I used small RNA deep sequencing and qPCR analyses to characterize Atlantic salmon head kidney miRNA expression responses to polyriboinosinic polyribocytidylic acid [pIC; a synthetic double-

stranded RNA (dsRNA) analogue, to elicit antiviral-like responses] and formalin-killed typical *Aeromonas salmonicida* (a bacterin, to elicit antibacterial responses) stimulations. I identified and qPCR confirmed nine miRNA biomarkers of Atlantic salmon response to pIC and/or bacterin stimulations. I also found that dietary CpG ODN 1668 may be helpful in modulating the bacterin-triggered antibacterial immune response. In **Chapter 5**, as a follow-up study to Chapter 4, I found that pIC and/or bacterin stimulations significantly modulated the expression of many immune-relevant predicted target genes of previously identified miRNAs. Significant down-regulation of immune-relevant transcripts (e.g. *tlr9*, *irf5*, *il1r1*, *hsp90ab1*, *itgb2*) by dietary CpG ODN 1668 were evident, especially among pre-injection and PBS-injected fish. Significant correlations between the changes in mRNA and miRNA expression representing putative miRNA-target pairs provided insights into how miRNAs might fine-tune the expression of immune-relevant mRNAs. Overall, this thesis has provided new insights into the dietary requirement of ω3 LC-PUFA, immune responses against *P. salmonis* infection and immunogens, and the immunomodulatory functions of dietary CpG in Atlantic salmon. The novel results and molecular biomarkers generated by this thesis will be valuable in future research aimed at improving aquaculture sustainability.

ACKNOWLEDGEMENTS

First and foremost, this thesis could not have been completed without an unwavering source of the love, encouragement and support from my wife Wanjun and son Owen during the last tough five years. To my family in China, thank you for being an endless source of encouragement and support.

My deepest gratitude goes to Dr. Matt Rise, my supervisor, for his continuous guidance, support and encouragement throughout the course of my Ph.D. program, and for providing the platform to begin my career as a scientist for so many years. I am forever grateful for his dedication to his students. Acknowledgements are extended to the supervisory committee members, Drs. Chris Parrish and Javier Santander, for their valuable suggestions throughout this thesis.

During the course of my research, I received help from many groups. I thank all past and present members of the Rise lab, Drs. Albert Caballero-Solares, Umasuthan Navaneethaiyer, Khalil Eslamloo, Tomer Katan, Mohamed Emam, Surendra Kumar and Nicole Smith, as well as Sabrina Inkpen, Eric Ignatz, Sindy Cove, Hoda Rajabi and Kathleen Parrish for their support and help over the last many years. You guys have turned our lab into a friendly and enjoyable workplace. I am grateful to Dr. Jennifer Hall (Aquatic Research Cluster, CREAIT Network, MUN) for helping with molecular assays. I would like to thank Cara Kirkpatrick from Genome Atlantic and Dr. Richard Taylor from Cargill Innovation for their support and project management. Special thanks go to the Dr. Joe Brown Aquatic Research Building (JBARB) and Cold-Ocean Deep-Sea Research Facility

(CDRF) staff at the Ocean Sciences Centre, who assisted with the maintenance and sampling of fish.

I am grateful to Dr. Rune Andreassen at the Oslo Metropolitan University (Oslo, Norway) for the opportunity to work on salmon miRNA research in his lab in 2018, as well as to Dr. Nardos Tesfaye Woldemariam for her help during my visit to Dr. Andreassen's lab. I particularly want to thank two great scientists for the support that I received at the end of my Ph.D. research program. I am grateful to Dr. Ian Fleming (OSC, MUN) for the opportunity to contribute to his research on the impact of aquaculture on wild fish populations and for providing such a nice and quiet office space for creating this thesis. I would also like to thank Dr. Cynthia McKenzie (DFO, St. John's) for the opportunity to work in her Aquatic Invasive Species research team and to contribute to green crab population genetics and eDNA research.

This research was supported by two Genomic Applications Partnership Program (GAPP) projects [the Biomarker Platform for Commercial Aquaculture Feed Development project (#6604) and the Integrated Pathogen Management of Co-infection in Atlantic salmon (IPMC) project (#6607)], funded by the Government of Canada through Genome Canada and Genome Atlantic, and EWOS Innovation (now part of Cargill, Incorporated). The IPMC project was also funded by InnovateNL (Government of Newfoundland and Labrador, Department of Tourism, Culture, Industry and Innovation; Leverage R&D award #5401-1019-108). Funding was also provided by two Natural Sciences and Engineering Research Council of Canada (NSERC) Discovery Grants (341304-2012 and 2020-04519) to Dr. Matt Rise, a Norwegian Research Council grant (280839/E40) to Dr. Rune

Andreassen, and a High North Programme grant (HNP-2015/10026) of Norway to Drs. Rune Andreassen and Matt Rise. I was supported by a Postgraduate Scholarship-Doctoral (PGS D) from NSERC, a Memorial University of Newfoundland SGS Fellowship, a Scholarship Award from Aquaculture Association of Canada, and a Dr. Joe Brown Graduate Research Award in Aquatic Ecology and Aquaculture.

The completion of this thesis has involved numerous contributions from many people. I want to take this chance to express my gratitude and appreciation to all of them, even when it is not possible to list each of them here.

TABLE OF CONTENTS

LIST OF TABLES

LIST OF FIGURES

LIST OF SUPPLEMENTAL FILES

LIST OF ABBREVIATIONS

°C	degrees centigrade
µL	microlitre
AFI	apparent feed intake
ALA	α-linolenic acid (18:3ω3)
AMP	antimicrobial peptide
ANOVA	analysis of variance
APC	antigen-presenting cell
ARA	arachidonic acid (20:4ω6)
aRNA	anti-sense amino-allyl RNA
BKD	bacterial kidney disease
BLAST	basic local alignment search tool
bp	base pair
BP	biological process
BW	body weight
campb	*cathelicidin antimicrobial peptide b*
cDNA	complementary DNA
CDRF	Cold-Ocean Deep-Sea Research Facility
CF	condition factor
cGRASP	consortium for Genomic Research on All Salmonids Project
CHSE-214	chinook salmon embryo cell line
clra	*C type lectin receptor A*
contig	contiguous sequence
CpG ODN	cytosine–phosphate–guanine oligodeoxynucleotide motifs
C_T	threshold cycle
cxcr3	*C-X-C chemokine receptor type 3*
DEP	differentially expressed probe
DHA	docosahexaenoic acid (22:6ω3)
DNA	deoxyribonucleic acid
dNTP	deoxyribose nucleotide triphosphate
DPI	days post-injection
dsRNA	double-stranded RNA
EFA	essential fatty acid
elovl2	*elongation of very long chain fatty acids 2*
EPA	eicosapentaenoic acid (20:5ω3)
EST	expressed sequence tag

fadsd5	*delta-5 fatty acyl desaturase*
FC	fold-change
FCR	feed conversion ratio
FDR	false discovery rate
FM	fish meal
FO	fish oil
g	gram
GAPP	Genomic Applications Partnership Program
GEO	Gene Expression Omnibus
GO	gene ontology
GOI	gene of interest
h	hour
hampa	*hepcidin a*
HK	head kidney
HSI	hepatosomatic index
HSP	heat shock protein
hsp90ab1	*heat shock protein HSP 90-beta*
ID	identity
IFN	interferon
ifng	*interferon gamma*
igmb	*immunoglobulin mu heavy chain b*
Ig	immunoglobulin
il10rb	*interleukin-10 receptor beta chain precursor*
il1r1	*interleukin-1 receptor type I*
il8a	*interleukin 8a*
IPMC	Integrated Pathogen Management of Co-infection in Atlantic salmon
IPNV	infectious pancreatic necrosis virus
irf3	*interferon regulatory factor 3*
irf5	*interferon regulatory factor 5*
irf7a	*interferon regulatory factor 7a*
irf9	*interferon regulatory factor 9*
ISAV	infectious salmon anemia virus
ISG	IFN-stimulated genes
itgb2	*integrin beta-2*
ITS	*16S-23S ribosomal RNA internal transcribed spacer*
JAK	janus kinase
JBARB	Dr. Joe Brown Aquatic Research Building
KEGG	Kyoto Encyclopedia of Genes and Genomes
L	litre

LA	linoleic acid (18:2ω6)
LC-PUFA	long-chain polyunsaturated fatty acid
lect2a	*leukocyte cell-derived chemotaxin 2 a*
LPS	lipopolysaccharides
lyz2	*lysozyme CII*
mapk3	*MAP kinase-activated protein kinase 3*
MAVS	mitochondrial antiviral-signalling protein
mg	milligram
mgst1	*microsomal glutathione S-transferase 1*
MHC	major histocompatibility complex
min	minute
miRISC	miRNA-induced silencing complex
miRNA	microRNA
mL	millilitre
mM	millimolar
M-MLV	moloney murine leukemia virus
MMP	matrix metalloproteinase
mRNA	messenger RNA
MUFA	monounsaturated fatty acid
MUN	Memorial University of Newfoundland
mxa	*interferon-induced GTP-binding protein Mx a*
mxb	*interferon-induced GTP-binding protein Mx b*
MyD88	myeloid differentiation primary response gene 88
NADPH	nicotinamide adenine dinucleotide phosphate
NCBI	National Center for Biotechnology Information
ncRNA	non-coding RNA
NF-κB	nuclear factor kappa B
ng	nanogram
NGC	Norwegian Genomics Consortium
nr	non-redundant
NSERC	Natural Sciences and Engineering Research Council of Canada
nt	nucleotide
NTC	non-template control
oligo	oligonucleotide
OSC	Ocean Sciences Centre
p	p-value
PAMP	pathogen-associated molecular pattern
PBS	phosphate-buffered saline
PCA	principal component analysis

PCoA	principal coordinate analysis
PCR	polymerase chain reaction
PERMANOVA	permutational multivariate ANOVA
PFP	percentage of false-positives
pIC	polyriboinosinic polyribocytidylic acid
PMT	photomultiplier tube
PPP	pentose phosphate pathway
pre-miRNA	precursor miRNA
pri-miRNA	primary miRNA
PRR	pattern recognition receptor
PUFA	polyunsaturated fatty acid
QC	quality check
qPCR	quantitative reverse transcription-polymerase chain reaction
r	Pearson's correlation coefficient
r^2	coefficient of determination
RLR	retinoic acid-inducible gene I (RIG-I)-like receptor
RNA	ribonucleic acid
RNA-seq	RNA sequencing
ROS	reactive oxygen specie
RP	rank products
RQ	relative quantity
RT	reverse transcription
SAM	significance analysis of microarrays
SAV	salmonid alphavirus
SD	standard deviation of the mean
SE	standard error of the mean
SGR	specific growth rate
SHK-1	salmon head kidney-1
SIMPER	similarity of percentages analysis
SRA	Sequence Read Archive
srebp1	*sterol regulatory element-binding protein 1*
srk2	*tyrosine-protein kinase SRK2*
SRS	salmonid rickettsial septicemia
ssRNA	single-stranded RNA
STAT	signal transducers and activators of transcription
$TCID_{50}$	median tissue culture infective dose
TCR	T cell receptor
TLR	Toll-like receptor

tlr5a	*toll-like receptor 5a*
TMS	tricaine-methane-sulfonate (MS-222)
tnfa	*tumor necrosis factor alpha*
TRIF	TIR domain-containing adaptor inducing IFN-β
U	units
UTR	untranslated region
VHSV	viral hemorrhagic septicemia virus
VO	vegetable oil
VSI	viscerosomatic index
ω3	omega-3
ω6	omega-6

CO-AUTHORSHIP STATEMENT

I am the first author on all of the manuscripts generated from this thesis. I was primarily responsible for experimental design, implementation of the experiments, sampling, molecular analyses, data analyses and drafting the manuscripts. Exceptions are: 1) the *P. salmonis* disease challenge trial, fish sampling, and RNA extraction in **Chapter 3** were performed at the Cargill Innovation Center (Colaco, Chile); and the small RNA sequencing and data analysis were conducted by Dr. Rune Andreassen and his research group at the Oslo Metropolitan University (Oslo, Norway). Throughout my work, I benefitted from collaborating with a supportive and dedicated group of co-authors. The detailed contributions by co-authors to each chapter are as follows:

Chapter 2

Myself, A. Caballero-Solares, R.G. Taylor, C.C. Parrish, and M.L. Rise designed project; Myself, J.R. Hall, and A. Caballero-Solares collected the data; myself, A Caballero-Solares, and K. Eslamloo analyzed the data; myself, A. Caballero-Solares, K. Eslamloo, R.G. Taylor, C.C. Parrish, and M.L. Rise interpreted the data. I led the writing of the manuscript. All authors contributed critically to the drafts and gave final approval for publication.

A version of this paper was published in Marine Biotechnology as:

Xue, X., Hall, J.R., Caballero-Solares, A. Eslamloo, K., Taylor, R.G., Parrish, C.C., Rise, M.L., 2020. Liver transcriptome profiling reveals that dietary DHA and EPA levels influence suites of genes involved in metabolism, redox homeostasis, and immune function in Atlantic salmon (*Salmo salar*). Mar. Biotechnol. 22, 263–284. doi.org/10.1007/s10126-020-09950-x

Chapter 3

Myself, A. Caballero-Solares, N. Umasuthan, E. Jakob, R.G. Taylor, and M.L. Rise designed project; myself, J.R. Hall, N. Umasuthan, E. Jakob, and C. Hawes collected the data; myself and A. Caballero-Solares analyzed the data; myself, A. Caballero-Solares, N. Umasuthan, S. Kumar, E. Jakob, S. Skugor, J. Santander, R.G. Taylor, and M.L. Rise interpreted the data. I led the writing of the manuscript. All authors contributed critically to the drafts and gave final approval for publication.

A version of this paper was published in Frontiers in Immunology as:

Xue, X., Caballero-Solares, A., Hall, J.R., Umasuthan, N., Kumar, S., Jakob, E., Skugor, S., Hawes, C., Santander, J., Taylor, R.G., Rise, M.L., 2021. Transcriptome profiling of Atlantic salmon (*Salmo salar*) parr with higher and lower pathogen loads following *Piscirickettsia salmonis* infection. Front. Immunol. 12, 789465. doi.org/10.3389/fimmu.2021.789465

Chapter 4

Myself, A. Caballero-Solares, N. Umasuthan, M.D. Fast, R.G. Taylor, M.L. Rise, and R. Andreassen designed project; myself, N.T. Woldemariam, A. Caballero-Solares, N. Umasuthan, and R. Andreassen collected the data; myself and N.T. Woldemariam analyzed the data; myself, N.T. Woldemariam, A. Caballero-Solares, N. Umasuthan, M.D. Fast, R.G. Taylor, M.L. Rise, and R. Andreassen interpreted the data. I led the writing of the manuscript. All authors contributed critically to the drafts and gave final approval for publication.

A version of this paper was published in Cells as:

Xue, X., Woldemariam, N.T., Caballero-Solares, A., Umasuthan, N., Fast, M.D., Taylor, R.G., Rise, M.L., Andreassen, R., 2019. Dietary immunostimulant CpG modulates microRNA biomarkers associated with immune responses in Atlantic salmon (*Salmo salar*). Cells 8, 1592. doi:10.3390/cells8121592

Chapter 5

Myself, K. Eslamloo, A. Caballero-Solares, N. Umasuthan, R.G. Taylor, M.D. Fast, R. Andreassen, and M.L. Rise designed project; myself, A. Caballero-Solares, T. Katan, and N. Umasuthan collected the data; myself analyzed the data; myself, K. Eslamloo, and M.L. Rise interpreted the data. I led the writing of the manuscript.

A version of this paper is being prepared for submission to Fish & Shellfish Immunology as:

Xue, X., Eslamloo, K., Caballero-Solares, A., Katan T, Umasuthan N, Taylor, R.G., Fast, M.D., Andreassen R, Rise, M.L., Characterization of the impact of dietary immunostimulant CpG on the expression of mRNA biomarkers involved in the immune responses in Atlantic salmon (*Salmo salar*).

CHAPTER 1: General Introduction

1.1 Aquaculture production of Atlantic salmon

The flesh of finfish provides important components of human diets (Morais et al., 2011). It provides not only high-quality proteins, vitamins, and minerals, but is also the primary source of essential omega-3 long-chain polyunsaturated fatty acids ($\geq C_{20}$; ω3 LC-PUFA) in human diets (Morais et al., 2011). With a variety of finfish species being farmed, Atlantic salmon (*Salmo salar*) is one of the most important species in aquaculture (Kiron, 2012). The global production of farmed Atlantic salmon increased from approximately 1.4 million metric tonnes in 2010 to 2.4 million metric tonnes in 2018 (FAO, 2020). The salmon aquaculture industry has made significant contributions to food, economic and employment security in many countries, especially Norway, Chile, the United Kingdom, and Canada (Houston and Macqueen, 2019). Worldwide demand for seafood for human consumption, with a significant contribution from aquaculture (~50%), continues to climb due to flat or decreasing global wild fisheries in the face of the rising human population (Tocher et al., 2006; FAO, 2020). Consequently, there is great potential for the aquaculture industry, including salmon farming, to expand.

1.2 Fish diseases and outbreaks

The significance of aquaculture production for global food security is well recognized (FAO, 2014). However, infectious diseases have resulted in substantial mortality and losses to aquaculture worldwide, affecting the growth, public acceptance and sustainability of the industry (Rodger, 2016). This might be due to high stocking density in the farm setting, which favours pathogen transmission and induces stress (Caballero-Solares et al., 2017). Fish are exposed to a broad range of bacterial, viral, fungal and

parasitic pathogens (Tacchi et al., 2011). Bacterial pathogens are the most common causative agents of infectious diseases in farmed fish (54.9%), followed by viruses (22.6%), parasites (19.4%) and fungi (3.1%) (Kibenge et al. 2012). Bacterial pathogens that have a severe impact on salmonid aquaculture include *Piscirickettsia salmonis* [Gram-negative; the cause of piscirickettsiosis or salmonid rickettsial septicaemia (SRS)] (Rise et al., 2004), *Renibacterium salmoninarum* [Gram-positive; the cause of bacterial kidney disease (BKD)] (Eslamloo et al., 2020a; Fryer and Sanders, 1981), *Aeromonas salmonicida* (Gram-negative; the cause of furunculosis) (Ewart et al., 2005), and *Moritella viscosa* (Gram-negative; the cause of winter-ulcer disease) (Løvoll et al., 2009). For example, SRS is one of the most economically significant diseases of Atlantic salmon aquaculture (Rise et al., 2004; Rozas and Enríquez, 2014). SRS is characterized by an aggressive systemic infection including liver lesions, and head kidney necrosis and inflammation (Rise et al., 2004). *P. salmonis* has been identified in farmed salmonids in Canada, Ireland, Chile, and Norway (Rozas and Enríquez, 2014). Attempts to control SRS have been unsuccessful thus far due to the ineffectiveness of existing vaccines, as well as the failure of antibiotic treatments.

In addition to bacterial disease, several well-known viruses that cause severe diseases in Atlantic salmon include salmonid alphavirus (SAV), infectious salmon anemia virus (ISAV), viral hemorrhagic septicemia virus (VHSV), piscine orthoreovirus (PRV), infectious pancreatic necrosis virus (IPNV), salmon gill poxvirus (Lang et al., 2009; Krasnov et al., 2021). For instance, while ISAV outbreaks were first detected in Norway its presence has been observed in all major salmon farming counties, including Canada

(Thorud and Djubvik, 1988; Rodger and Richards, 1998; Keleher et al., 1999; Godoy et al., 2008). It is classified as a notifiable disease by the World Organization for Animal Health, and culling of infected farms remains the current practice to prevent the spread to nearby farms (Gagne and LeBlanc, 2018).

1.3 Fish oil (FO) in aquafeeds and its benefits

In addition to disease, another key issue affecting the sustainability of the aquaculture industry is the limited supply of fish oil (FO, a marine-derived ingredient). Until recently, FO has been the preferable source of lipid in aquafeeds due to its excellent content of essential fatty acids (EFAs) such as eicosapentaenoic acid (EPA, 20:5ω3) and docosahexaenoic acid (DHA, 22:6ω3) (Torstensen et al., 2008; Morais et al., 2011). The demands for FO to meet the expansion of the aquaculture industry will exceed the supply from capture fisheries (e.g. herring, anchovies, capelin) which are in a static phase (FAO, 2020). The increasing demand and limited supply and rising prices of FO have pressed aquaculture companies to find alternative ingredients for feed production such as vegetable oils (VO). However, VOs from conventional terrestrial plants often lack LC-PUFAs ($\geq C_{20}$; e.g. DHA and EPA) but are usually rich in short chain PUFAs ($<C_{20}$) such as α-linolenic acid (ALA; 18:3ω3) and linoleic acid (LA; 18:2ω6) (Xue et al., 2015). Nevertheless, research efforts have been made to produce *de novo* LC-PUFAs from microalgae and genetically engineered oilseed crops in order to fill the gaps of LC-PUFA supplies (Sprague et al., 2017).

Dietary lipid and fatty acids are the predominant source of energy for teleost fish (Leaver et al., 2008a). Essential fatty acids, especially LC-PUFAs, in dietary oils play

important roles in the structure of cell membranes, ion balance, cell synthesis, neural development, immune function and reproduction (Glencross, 2009; Rosenlund et al., 2016). Hence, any dietary alternative to FO must satisfy the nutritional needs of the fish (e.g. supplying lipids and essential fatty acids used for optimal growth) without having a negative impact on the fish health or on quality of the flesh for human consumption. Studies have demonstrated that VOs (either singly or as blends) can be used to replace up to 100% of FO in diets containing minimal levels of fish meal without negatively influencing growth in salmonids (Bell et al., 2001; Torstensen et al., 2005; Bell et al., 2010; Hixson et al., 2014; Xue et al., 2015). Replacement of FO with VOs in fish diets has been suggested to affect lipogenesis in teleosts (Morais et al., 2011; Xue et al., 2015). For example, Atlantic salmon fed FO-based diets showed lower triacylglycerol levels in the liver compared to vegetable oil-fed fish (Jordal et al., 2007). A number of other lipid metabolic processes, for example, fatty acid β-oxidation, cholesterol and fatty acid biosynthesis, were also linked to intake of VO-based diets (Leaver et al., 2008b; Xue et al., 2015; Hixson et al., 2017).

Altering the fatty acid composition of the immune cells from changing dietary lipids might influence immune cell functions in a variety of ways such as alterations in the fluidity of the plasma membrane, cell signalling mechanisms and eicosanoids production (Calder and Grimble, 2002). Dietary ω3 and ω6 fatty acids [e.g. EPA, DHA, arachidonic acid (ARA; 20:4ω6)] are precursors to various classes of eicosanoids, which have important roles in the regulation of inflammation and immune responses (Saini and Keum, 2018). In general, ω3 fatty acids (e.g. EPA and DHA) exhibit anti-inflammatory functions (Calder, 2015). In contrast, ω6 fatty acids (e.g. ARA) promote the formation of pro-

inflammatory eicosanoids (Patterson et al., 2012). ARA can be converted to 2-series prostaglandins, 4-series leukotrienes, thromboxane, lipoxins and epoxyeicosatrienoic acids by cyclooxygenase (COX) and lipoxygenase (LOX) (Holen et al., 2015). In contrast to ARA, EPA is metabolized to 3-series prostaglandins and 5-series leukotrienes, while DHA can be converted to non-classical eicosanoid derivatives such as resolvins, maresins and protectins (Saini and Keum, 2018). Holen et al. (2015) has shown that combining EPA, DHA and ARA affected the transcript expression of inflammation markers and eicosanoid secretion (i.e. prostaglandin E2) in Atlantic salmon head kidney cells *in vitro* (Holen et al., 2015). The changes in the fatty acid profiles of diets due to the replacement of FO by VOs have been shown to affect fish health, immune function and pathogen resistance (Bransden et al., 2003; Montero et al., 2003; Mourente et al., 2005; Xue et al., 2015; Yan et al., 2020). For example, Montero et al. (2010) have shown that gilthead seabream (*Sparus aurata*) fed complete FO replacement diets had higher expression of transcripts encoding pro-inflammatory cytokines (*tumor necrosis factor-α* and *interleukin 1β*) after exposure to a bacterial pathogen (*Photobacterium damselae*). Atlantic salmon fed diets supplemented with high levels of rapeseed oil (rich in ω6 and ω9 fatty acids) and plant protein had enhanced innate antiviral-like response (Caballero-Solares et al., 2017). These studies confirm that dietary fatty acids (e.g. EPA, DHA, and ARA) play important roles in inflammation and immune responses.

Several studies have examined the dietary requirement of ω3 LC-PUFA in Atlantic salmon under different physiological conditions and at different life stages (Ruyter et al., 2000; Glencross et al., 2014; Rosenlund et al., 2016; Sissener et al., 2016; Bou et al., 2017a;

Bou et al., 2017b). A level of ≥ 1.0% (i.e. 10 g/kg) of ω3 LC-PUFA for optimal growth of Atlantic salmon has been suggested (Ruyter et al., 2000; Rosenlund et al., 2016; Sissener et al., 2016). Under laboratory conditions, 1.0% of ω3 LC-PUFA in feed seemed to be sufficient for post-smolt Atlantic salmon during long-term growth trials (Rosenlund et al., 2016). In contrast, Bou et al. (2017b) have found that post-smolt Atlantic salmon fed a diet containing 1.0% DHA + EPA had poor survival compared with fish fed a 1.7% DHA + EPA diet when the fish were under demanding environmental conditions (e.g. high water temperature, sea lice infection, and handling stress) in sea cages. Studies on the determination of ω3 LC-PUFA requirements in Atlantic salmon were mostly conducted based on growth performance. Other aspects, including fish health and immunity, need to be considered when determining the nutritional requirement of EPA and DHA. Recently, a study evaluated the impact of ω3 LC-PUFA on Atlantic salmon performance and midgut health under normal and challenging condition (Løvmo et al., 2021). This study showed that 0.8% of ω3 LC-PUFA is sufficient to sustain growth in Atlantic salmon under normal conditions; however, fish fed this diet had a reduced intestinal health (e.g. impaired intestinal transport) in response to chronic stress when compared with fish fed 3.0% of ω3 LC-PUFA diet.

1.4 Fish immune system

As in other vertebrates, fish immunity is typically divided into two distinct components: the innate immune response and the adaptive immune response (Martin and Król, 2017). Innate immunity is the first and most effective line of defense against a large array of pathogens; it includes physical barriers such as the skin, humoral components [e.g.

antimicrobial peptides (AMPs), lysozyme, complement proteins], and cellular responses (e.g. phagocytosis and respiratory burst activity) (Ellis, 2001). The adaptive immune system is engaged when a pathogen persists. In contrast to innate immunity, adaptive immunity is highly specific to a particular antigen and mediated by the actions of two types of lymphocytes, B cells that mediate antibody responses (humoral) and T cells that mediate cell-mediated immune responses (Secombes and Wang, 2012). The major lymphoid tissues in teleost fish include the thymus, head kidney, spleen, as well as mucosa-associated lymphoid tissues (e.g. skin, gill, gut) (Press and Evensen, 1999; Salinas, 2015). Recently, a new organ, the salmonid bursa (a thick lymphoepithelium dominated by T cells), has been described in Atlantic salmon (Bjørgen and Koppang, 2021).

The first line of defense in the innate immune system is physical barriers such as skin (e.g. scales and mucus) and epithelial layer of gills and intestines that prevent the entry of pathogens (Magnadóttir, 2006; Smith et al., 2019). For example, the mucus secreted by the mucosal surface plays an essential role in the innate defense mechanisms. It creates a physical and chemical barrier to any offense from the environment (Ellis, 2001). The most abundant molecules in mucus are mucins, high molecular weight glycoproteins; the chemical characteristics of mucins give mucus its viscosity for trapping pathogens (Salinas and Magadán, 2017). Many other molecules implicated in innate immunity are also present in fish mucosal secretions (Gomez et al., 2013). These include lysozymes, complement components, cytokines, AMPs, and others (Salinas and Parra, 2015).

If a pathogen makes its way through the physical barriers, it will face the cellular and humoral components of the innate immune system. Many different cell types such as

macrophages, granulocytes, dendritic cells, non-specific cytotoxic cells, and natural killer cells are involved in the cellular components of the innate immune system (Secombes and Wang, 2012). These innate immune cells can participate in various responses depending on cell type including, but not limited to, phagocytosis, activation of humoral components (e.g. complement pathway), and activation of the adaptive immune system through antigen presentation (Smith et al., 2019).

The innate immune response is initiated when germline-encoded intracellular or extracellular pattern recognition receptors (PRRs) of an immune cell detect and respond to pathogen-associated molecular patterns (PAMPs) present on a pathogen, such as lipopolysaccharides (LPS; endotoxins found on the outer membrane of Gram-negative bacteria), peptidoglycans (found on the cell wall of both Gram-positive and Gram-negative bacteria), viral RNA, and bacterial DNA (Secombes and Wang, 2012; Gomez et al., 2013; Smith et al., 2019). Some of the PRR groups identified in teleosts include Toll-like receptors (TLRs), C-type lectins, and nucleotide-binding oligomerization domain (NOD)-like receptors (NLRs) (Peatman et al., 2015).

Among various PRRs, the family of TLRs are the best characterized innate immune receptors (Zhang et al., 2014). TLRs are type I transmembrane proteins that are characterized by three major domains: a leucine-rich repeat (LRR) extracellular domain, a cytoplasmic TIR domain, and a transmembrane domain (Secombes and Wang, 2012). In mammals, a number of PAMPs from different microbes (e.g. virus *vs* bacteria) can be detected by TLRs. For instance, lipoprotein is recognized by TLR1, 2 and 6, LPS by TLR4, flagellin by TLR5, double-stranded RNA by TLR3, single-stranded RNA by TLR7/8, and

CpG DNA by TLR9 (Mogensen, 2009; Secombes and Wang, 2012). In general, TLR signaling pathways can be classified into two distinct pathways [i.e. the myeloid differentiation primary response gene 88 (MyD88)-dependent and the MyD88-independent (TIR domain-containing adaptor inducing IFN-β (TRIF)-dependent)] (Rauta et al., 2014). All mammalian TLRs except TLR3 interact with adaptor protein MyD88 to activate the transcription factor nuclear factor-κB (NF-κB) and mitogen-activated protein kinases (MAPKs), which then induce the production of inflammatory cytokines [e.g. tumor necrosis factor-α (TNF-α), interleukin-1β (IL-1β)] (Zhang et al., 2014). Interestingly, the MyD88-mediated TLR7, 8 and 9 signaling also induces the production of type I interferons (IFNs) (Zhang et al., 2014). In the MyD88-independent (TRIF-dependent) pathway, TLR3 and 4 interact with TRIF and activate the transcription factors IRF3 and NF-κB, which then induce genes encoding type I IFNs and inflammatory cytokines (Kanwal et al., 2014).

The production of IFNs and the proteins encoded by IFN-stimulated genes (ISGs) confers the antiviral innate immune responses (Rauta et al., 2014). The IFN pathways are initiated by the binding of IFN-α/IFN-β to interferon alpha and beta receptors (i.e. IFNAR1 and IFNAR2) or IFN-γ to interferon gamma receptors (i.e. IFNGR1 and IFNGR2) to transduce signals via Janus kinases (JAKs) and signal transducers and activators of transcription (STATs), resulting in expression of a wide range of ISGs (e.g. viperin, interferon-induced GTP-binding protein, interferon stimulated gene 15) (Mogensen, 2009). IFNs also play important roles in adaptive immune defenses. For example, IFN-γ or type II interferon exerts regulatory roles in both innate and adaptive immunity, including

activating macrophages, enhancing antigen presentation and promoting T cell differentiation and activation (Wang and Secombes, 2013)

Pathogen recognition through PRRs can also regulate leukocyte activation and their recruitment to sites of infection (Mogensen, 2009). For instance, pathogen recognition by PRRs activate phagocytosis in cells termed phagocytes such as macrophages, monocytes, neutrophils and dendritic cells (Pérez et al., 2010). Respiratory burst activity, an indication of the oxidative potential of reactive oxygen species (ROS; e.g. hydrogen peroxide), is an important innate defense mechanism in fish (Nayak, 2010; Wang et al., 2019). It occurs in phagocytes to degrade internalized particles and bacteria by ROS.

The humoral part of the innate immune system is mediated by macromolecules released into the extracellular fluids by immune cells following infection (Magnadóttir, 2006; Uribe et al., 2011). Some of the well-known examples in fish include AMPs (e.g. cathelicidins, hepcidins), lysozyme, lectins, complement proteins, and acute phase proteins (e.g. C-reactive protein and serum amyloid proteins) (Magnadóttir, 2006; Uribe et al., 2011). AMPs, also known as host defence peptides, exhibit antibacterial, antifungal and antiparasitic activity through a wide range of mechanisms including but not limited to disruptive or pore-forming actions against microbial membranes and protein aggregation (Romo et al., 2016). Lysozyme is a lytic enzyme that is able to bond to the peptidoglycan layer of bacterial cell walls resulting in lysis of the bacterium (Magnadóttir, 2006). In vertebrates including fish, two types of lysozyme have been described: (chicken) c-type and (goose) g-type (Smith et al., 2019). The complement system is composed of serum proteins that react against pathogens through three activation pathways: the classical

pathway, the alternative pathway and the lectin pathway (Romo et al., 2016). The complement system eliminates the pathogens through opsonization, enhanced inflammatory response and phagocytosis (Romo et al., 2016; Smith et al., 2019).

The adaptive immune system of fish includes immunoglobulins (Igs; i.e. antibodies), B cells, T cells, and major histocompatibility complex (MHC), and its activation relies on antigen-specific receptors distributed on the surfaces of T and B cells (Medzhitov and Janeway Jr, 1998). The main role of B cells is to produce Igs against foreign antigens, and to act as antigen-presenting cells (APCs) to present antigen to T cells (Secombes and Wang, 2012; Smith et al., 2019). A typical Ig is comprised of two heavy chains and two light chains, each of which contains one N-terminal variable (V) domain and one or more C-terminal constant (C) domains (Mashoof and Criscitiello, 2016). The V domains of the heavy and light chains are generated by gene rearrangement during B cell development, leading to the diversification of Igs (Secombes and Wang, 2012; Smith et al., 2021). B cells will secrete antigen-specific Igs in response in antigen. Three classes of Ig have been identified in many teleost fish: IgM, IgD and IgZ/T (Hikima et al., 2011). Previous studies suggest a compartmentalization of Ig isotypes into mucosal (IgT/Z) and systemic (IgM) sites in response to pathogenic challenge (Zhang et al., 2010; Austbø et al., 2014). IgT/Z, an Ig isotype analogous to IgA in mammals, can be secreted via polymeric Ig receptor (pIgR) present on epithelial cells into mucus (Merrifield and Rodiles, 2015). T cells express T cell receptors (TCRs) which recognize a specific antigen that has been processed and presented by APCs via their MHC proteins (Flajnik and Kasahara, 2010). The TCRs on the surface of helper ($CD4^+$) and cytotoxic ($CD8^+$) T-cells recognize MHC

class II- and MHC class I-bound antigens, respectively (Somamoto et al., 2014). The activated T cells eliminate pathogen via cytotoxicity of infected host cells; they also regulate immune response through cytokine production (Chen and Flies, 2013; Somamoto et al., 2014).

1.5 miRNAs and their regulation of immune response in fish

MicroRNAs (miRNAs) are a class of small (usually 20-24 nucleotides in length), non-coding RNAs that regulate gene expression at the post-transcriptional level (Andreassen and Høyheim, 2017; Woldemariam et al., 2019). The miRNA genes are firstly transcribed in the nucleus by RNA polymerase to produce primary miRNAs (pri-miRNAs), which then are cleaved by Drosha into shorter miRNA precursors (pre-miRNAs; ~70 nucleotides in length) (Herkenhoff et al., 2018). Thereafter, pre-miRNAs are exported out of the nucleus and further processed by Dicer to produce two mature miRNAs (i.e., 5p and 3p) (Woldemariam et al., 2019). One of the mature miRNAs is then assembled into the miRNA-induced silencing complex (miRISC), and this complex can form an imperfect complementary base-pairing mainly in the 3' untranslated region (UTR) of target mRNA and mediate the suppression of translation or degradation of the target mRNA (Herkenhoff et al., 2018). The most important part of a miRNA that contributes to the binding of target mRNAs is the so-called “seed sequence” or “seed region”, which is mostly situated at positions 2-8 in the 5' end (Hausser and Zavolan, 2014). Thousands of miRNAs have been identified in vertebrates, and they may potentially regulate a very large number of genes due to the short seed sequence (the most crucial part of the miRNA) as well as the imperfect

complementary base-pairing between miRNA and its target (Andreassen and Høyheim, 2017).

In higher vertebrates, a set of miRNAs has been previously found to play important roles in different immune-related mechanisms and processes such as inflammation, TLR signaling, cytokine production, complement and coagulation cascades, and B- and T-cell development (Momen-Heravi and Bala, 2018). To date, a variety of miRNAs have been characterized in teleosts to be involved in antibacterial and antiviral responses (Wang et al., 2018). A common approach used in the initial search for miRNAs that may play key roles in immune responses is to analyze miRNA expression between a healthy group (i.e. control) and a challenged group (i.e. fish that have been exposed to a pathogen or other immune stimulus) (Andreassen and Høyheim, 2017; Wang et al., 2018). For instance, miRNA-based transcriptomic analyses of Atlantic salmon tissues infected with *P. salmonis* revealed 84 and 25 differentially expressed miRNAs in the head kidney and spleen, respectively (Valenzuela-Miranda et al., 2017). Moreover, these differentially expressed miRNAs were predicted to target genes involved in immune-related pathways, such as chemokine-mediated signaling pathway and neutrophil chemotaxis (Valenzuela-Miranda et al., 2017). In contrast, a limited number of miRNAs in fish have been further characterized by directly studying their effect on the target genes (i.e. experimental validations of target genes) (Andreassen and Høyheim, 2017; Wang et al., 2018).

1.6 Immunostimulants and immune modulation

As discussed in the previous sections, the aquaculture industry has suffered significant economic losses due to bacterial and viral diseases (Rodger, 2016). The most

common countermeasures to prevent or contain the disease outbreaks include vaccines, breeding, chemicals, and antibiotics (Newaj-Fyzul et al., 2014; Dawood et al., 2018). However, several limitations such as public health concerns on food contamination, bacterial drug resistance and adverse effects on the environment have arisen in using some of these products (Manzetti and Ghisi, 2014; Hernández et al., 2016). It is therefore essential to develop alternative methods for preventing or mitigating infectious disease outbreaks that threaten aquaculture sustainability. One of the alternative approaches to improve fish health and performance is to incorporate functional feeds into health management (Tacchi et al., 2011; Kiron, 2012; Martin and Król, 2017). Significant advances within the aquafeed sector have been made, with diets being more specifically designed to meet the nutritional needs of species, stage of the life cycle, and health status of the fish (Tacchi et al., 2011).

Functional feeds are diets designed to enhance the health and/or growth of the animals by supplying additional functional ingredients (i.e. additives) beyond the basic nutritional requirements of the animal (Martin and Król, 2017). The most common additives used in aquaculture diets are algae, herbs, plant extracts, probiotics, prebiotics, micronutrients (e.g. selenium), nucleotides, and microbial cell components (i.e. PAMPs) (Kiron, 2012; Vallejos-Vidal et al., 2016; Martin and Król, 2017; Dawood et al., 2018). Many of these additives have been shown to mitigate fish diseases by enhancing the non-specific immune system; therefore, they have also traditionally been defined as immunostimulants (Tacchi et al., 2011; Kiron, 2012; Vallejos-Vidal et al., 2016). For example, orally administered peptidoglycan enhanced the rainbow trout (*Oncorhynchus*

mykiss) innate immune system, particularly by increasing the expression of AMP-encoding genes (Casadei et al., 2013; Casadei et al., 2015). Improved resistance against *Vibrio anguillarum* challenges has been reported in Japanese flounder (*Paralichthys olivaceus*) fed with dietary peptidoglycan (Zhou et al., 2006).

Another type of PAMP used as an immunostimulant in aquaculture is unmethylated DNA with cytosine–phosphate–guanine oligodeoxynucleotide motifs (CpG ODN) (Covello et al., 2012; Purcell et al., 2013). CpG motifs in vertebrate genomes are suppressed and methylated; however, they are prevalent and often unmethylated in bacterial and some viral genomes (Carrington and Secombes, 2006; Strandskog et al., 2007). Recognition of CpG ODN is mediated through a PRR called Toll-like receptor 9 (TLR9), which is present on the cell surface or within endosomal compartments of different immune cells (e.g. macrophages) (Cuesta et al., 2008). CpG ODNs have been divided into three classes (i.e. A-, B-, and C-classes) based on the backbone structure and sequences, and each class carries its own immunostimulatory properties (Carrington and Secombes, 2006). CpG ODN A-class contains only one unmethylated CpG motif within a palindromic sequence on a phosphodiester backbone and is known to induce large amounts of IFN-α (Strandskog et al., 2007). CpG ODN B-class contains at least one unmethylated CpG motif with a phosphorothioate backbone and has been shown to stimulate B-cell proliferation and natural killer (NK) cell activation. The third class of CpG ODNs, CpG C-class, has some characteristics from the first two classes and contains a central palindromic sequence similar to that present on A-class (Carrington and Secombes, 2006). CpG C-class can

stimulate B-cells, NK cells, and dendritic cells (Carrington and Secombes, 2006; Strandskog et al., 2007).

The immunostimulatory properties of CpG ODNs as vaccine adjuvants and feed additives have been evaluated in several fish models (Carrington and Secombes, 2006; Strandskog et al., 2007; Purcell et al., 2013; Xue et al., 2019). For example, a B-class ODN, CpG ODN 205, has been shown to enhance the immune system of turbot (*Scophthalmus maximus*) and induce protection against *Edwardsiella tarda* challenge (Liu et al., 2010). CpG ODN 1668 (another B-class ODN) induced both the innate and adaptive immune responses of rock bream (*Oplegnathus fasciatus*) against iridovirus infection (Jung and Jung, 2017). Further, a study in Pacific red snapper (*Lutjanus peru*) revealed that CpG ODN 1668 enhanced the immune response of animals exposed to *Vibrio parahaemolyticus* (Cárdenas-Reyna et al., 2016). Finally, CpG ODN 1668 has been reported to provide protection against sea lice (*Lepeophtheirus salmonis*) infection in Atlantic salmon via feed as an immunostimulant (Covello et al., 2012; Purcell et al., 2013).

1.7 Functional genomics approaches: microarrays, next-generation sequencing, and qPCR.

Functional genomic approaches [microarray hybridization, next-generation sequencing (NGS) based methods such as RNA-sequencing (RNA-seq), and qPCR] have been shown to be useful for the identification of genes and molecular pathways that are altered in fish (e.g. Atlantic salmon) that were subjected to dietary manipulation (e.g. Xue et al., 2015; Jalili et al., 2019; Ytrestøyl et al., 2021), immune stimulation (e.g. Caballero-Solares et al., 2017; Stenberg et al., 2019; Eslamloo et al., 2020b) and disease challenge

(e.g. Rozas-Serri et al., 2018; Eslamloo et al., 2020a; Umasuthan et al., 2020). The consortium for Genomic Research on All Salmonids Project (cGRASP)-designed Agilent 4x44K salmonid oligonucleotide microarray [Gene Expression Omnibus (GEO) accession # GPL11299], with each slide containing four ~44,000-feature (44K) arrays, is a platform developed by Dr. Ben F. Koop's research team (Jantzen et al., 2011). This array comprises about 22,000 60-mer oligos that are similar (95%) between rainbow trout and Atlantic salmon, plus 14,866 additional Atlantic salmon-specific sequences and 5,661 additional rainbow trout-specific sequences, resulting in a broad representation of transcripts in salmonids with low redundancy (Jantzen et al., 2011). This particular microarray platform has proven to be a useful and robust tool in detecting differentially expressed transcripts in several diet- and immune-related studies in Atlantic salmon (e.g. Xue et al., 2015; Brown et al., 2016; Eslamloo et al., 2017; Caballero-Solares et al., 2018; Eslamloo et al., 2020a; Eslamloo et al., 2020b; Umasuthan et al., 2020; Xue et al., 2020). Compared with DNA microarrays, high-throughput sequencing technology does not typically rely on existing genomics resources of the target organisms. For example, RNA sequencing (RNA-seq) methods can cover all aspects of the transcriptome, allowing for the analysis of novel transcripts, splice variants, and non-coding RNAs (e.g. miRNAs). Advances in small RNA deep sequencing and bioinformatics tools have led to the detection of virus/bacteria-responsive miRNAs in fish (Andreassen et al., 2013; Andreassen et al., 2017; Valenzuela-Miranda et al., 2017; Eslamloo et al., 2018; Woldemariam et al., 2019; Woldemariam et al., 2020).

Real-time quantitative polymerase chain reaction (qPCR), discovered in the early 1990s, has rapidly become the preferred analytical tool to quantify DNA abundance (Higuchi et al., 1992; Higuchi et al., 1993). With the addition of a reverse-transcription (RT) step, the qPCR technique is able to measure the levels of specific target mRNAs or miRNAs. Due to its high performance (i.e. sensitivity, specificity, and reproducibility), qPCR has been extensively used for gene expression analyses in aquaculture-related research. However, unlike microarray or RNA-seq, qPCR typically measures one gene or a few (i.e. multiplex qPCR) in a single reaction. At present, qPCR is the method of choice for analyzing gene expression of a moderate number of target genes with sample sizes of anywhere between a small number and thousands (VanGuilder et al., 2008). Last but not least, qPCR remains an essential and robust approach for validating microarray and RNA-seq experiments.

1.8 Overall research objectives of thesis

Aquaculture is becoming the main supply of seafood for human consumption; therefore, it is important to conduct research that helps to address issues affecting the growth and sustainability of the industry. As discussed earlier, the limited supply of fish oil, as well as infectious diseases, are some of the key challenges faced by Atlantic salmon aquaculture. To these ends, the overall objectives of this thesis were to: 1) determine the optimal dietary requirement of ω3 LC-PUFA for Atlantic salmon that promotes growth and health; 2) explore the head kidney transcriptomic responses of Atlantic salmon parr to an EM-90-like *P. salmonis* isolate and fill the gaps in the current knowledge regarding piscirickettsiosis outbreaks involving such isolates; and 3) characterize Atlantic salmon

head kidney miRNA and mRNA expression responses to immunogens: polyriboinosinic polyribocytidylic acid [pIC; a PAMP-like synthetic double-stranded RNA (dsRNA) analogue, to elicit antiviral-like responses] or formalin-killed typical *Aeromonas salmonicida* (a PAMP-containing bacterin, to elicit antibacterial responses) and evaluate the immune-modulating properties of dietary CpG.

To accomplish these objectives, in **Chapter 2**, a 14-week feeding trial was conducted with salmon fed three different experimental diets containing increasing levels of DHA+EPA (0, 1.0, and 1.4% of the diet, as formulated). I used 44K microarrays to study the impact of dietary DHA and EPA levels on Atlantic salmon growth and liver transcriptome. I also explored connections between the changes in hepatic transcriptome, fatty acid composition, and growth performance using linear regression and multivariate statistical analyses. I hypothesized that different levels of dietary DHA and EPA would significantly alter the growth performance and hepatic transcriptome in Atlantic salmon, with fish fed the highest level of DHA+EPA showing the best growth performance.

In **Chapter 3**, a *P. salmonis* disease challenge trial involving an EM-90-like isolate was conducted; samples collected from multiple time points post-infection (up to 42 days) were included in qPCR analyses to study the temporal patterns of pathogen level and host immune responses. Two infection phenotypes (higher and lower infection levels) at 21 days post-injection (DPI) were detected by multivariate analyses of pathogen load and levels of 4 antibacterial biomarker transcripts. I used 44K microarrays to explore the head kidney transcriptomic differences between high and low infection individuals, and to identify candidate biomarker genes that would be valuable for future SRS-related research.

I hypothesized that comparing the transcriptomic different between high and low infection fish may provide insight into the molecular mechanisms associated with the ability to evade or clear *P. salmonis* infection as well as the dysregulations leading to susceptibility and more adverse outcomes.

In **Chapter 4**, I used small RNA deep sequencing to identify pIC- and/or bacterin-responsive miRNAs in the head kidney of salmon fed a control diet. I also examined the immune-modulating properties of a functional feed (containing CpG ODN 1668) by evaluating the expression changes of putative antiviral and antibacterial responsive miRNAs identified through sequencing in pre- and post-immune stimulation individuals. In **Chapter 5**, I selected a set of immune-relevant mRNAs identified as predicted targets of the pIC- and/or bacterin-responsive miRNAs from **Chapter 4**, and studied the impact of dietary immunostimulant CpG on the expression of these mRNA biomarkers using qPCR. Finally, the connections between the changes in miRNA and mRNA expression were also explored. I hypothesized that the small RNA deep sequencing approach would be able to identify pIC- and/or bacterin-responsive miRNAs in the head kidney of salmon, and that the dietary immunostimulant CpG would result in modifications in the expression of putative antiviral and antibacterial responsive miRNAs as well as mRNAs.

1.9 References

Andreassen, R., Høyheim, B., 2017. miRNAs associated with immune response in teleost fish. Dev. Comp. Immunol. 75, 77-85.

Andreassen, R., Woldemariam, N.T., Egeland, I.Ø., Agafonov, O., Sindre, H., Høyheim, B., 2017. Identification of differentially expressed Atlantic salmon miRNAs responding to salmonid alphavirus (SAV) infection. BMC Genomics 18, 349.

Andreassen, R., Worren, M.M., Hoyheim, B., 2013. Discovery and characterization of miRNA genes in Atlantic salmon (*Salmo salar*) by use of a deep sequencing approach. BMC Genomics 14, 482.

Austbø, L., Aas, I.B., König, M., Weli, S.C., Syed, M., Falk, K., Koppang, E.O., 2014. Transcriptional response of immune genes in gills and the interbranchial lymphoid tissue of Atlantic salmon challenged with infectious salmon anaemia virus. Dev. Comp. Immunol. 45, 107-114.

Bell, J.G., McEvoy, J., Tocher, D.R., McGhee, F., Campbell, P.J., Sargent, J.R., 2001. Replacement of fish oil with rapeseed oil in diets of Atlantic salmon (*Salmo salar*) affects tissue lipid compositions and hepatocyte fatty acid metabolism. J. Nutr. 131, 1535-1543.

Bell, J.G., Pratoomyot, J., Strachan, F., Henderson, R.J., Fontanillas, R., Hebard, A., Guy, D.R., Hunter, D., Tocher, D.R., 2010. Growth, flesh adiposity and fatty acid composition of Atlantic salmon (*Salmo salar*) families with contrasting flesh adiposity: Effects of replacement of dietary fish oil with vegetable oils. Aquaculture 306, 225-232.

Bjørgen, H., Koppang, E.O., 2021. Anatomy of teleost fish immune structures and organs. Immunogenetics 73, 53-63.

Bou, M., Berge, G.M., Baeverfjord, G., Sigholt, T., Østbye, T.-K., Romarheim, O.H., Hatlen, B., Leeuwis, R., Venegas, C., Ruyter, B., 2017a. Requirements of n-3 very long-chain PUFA in Atlantic salmon (*Salmo salar* L): effects of different dietary levels of EPA and DHA on fish performance and tissue composition and integrity. Br. J. Nutr. 117, 30-47.

Bou, M., Berge, G.M., Baeverfjord, G., Sigholt, T., Østbye, T.-K., Ruyter, B., 2017b. Low levels of very-long-chain n-3 PUFA in Atlantic salmon (*Salmo salar*) diet reduce fish robustness under challenging conditions in sea cages. J Nutr Sci 6, E32.

Bransden, M.P., Carter, C.G., Nichols, P.D., 2003. Replacement of fish oil with sunflower oil in feeds for Atlantic salmon (*Salmo salar* L.): effect on growth performance, tissue fatty acid composition and disease resistance. Comp. Biochem. Physiol. Part B Biochem. Mol. Biol. 135, 611-625.

Brown, T.D., Hori, T.S., Xue, X., Ye, C.L., Anderson, D.M., Rise, M.L., 2016. Functional genomic analysis of the impact of camelina (*Camelina sativa*) meal on Atlantic salmon (*Salmo salar*) distal intestine gene expression and physiology. Mar. Biotechnol. 18, 418-435.

Caballero-Solares, A., Hall, J.R., Xue, X., Eslamloo, K., Taylor, R.G., Parrish, C.C., Rise, M.L., 2017. The dietary replacement of marine ingredients by terrestrial animal and plant alternatives modulates the antiviral immune response of Atlantic salmon (*Salmo salar*). Fish Shellfish Immunol. 64, 24-38.

Caballero-Solares, A., Xue, X., Parrish, C.C., Foroutani, M.B., Taylor, R.G., Rise, M.L., 2018. Changes in the liver transcriptome of farmed Atlantic salmon (*Salmo salar*) fed experimental diets based on terrestrial alternatives to fish meal and fish oil. BMC Genomics 19, 796.

Calder, P.C., 2015. Marine omega-3 fatty acids and inflammatory processes: effects, mechanisms and clinical relevance. Biochim. Biophys. Acta, Mol. Cell. Biol. Lipids 1851, 469-484.

Calder, P.C., Grimble, R.F., 2002. Polyunsaturated fatty acids, inflammation and immunity. Eur. J. Clin. Nutr. 56(3), S14-S19.

Cárdenas-Reyna, T., Angulo, C., Hori-Oshima, S., Velázquez-Lizárraga, E., Reyes-Becerril, M., 2016. B-cell activating CpG ODN 1668 enhance the immune response of Pacific red snapper (*Lutjanus peru*) exposed to *Vibrio parahaemolitycus*. Dev. Comp. Immunol. 62, 72-81.

Carrington, A.C., Secombes, C.J., 2006. A review of CpGs and their relevance to aquaculture. Vet. Immunol. Immunopathol. 112, 87-101.

Casadei, E., Bird, S., González Vecino, J.L., Wadsworth, S., Secombes, C.J., 2013. The effect of peptidoglycan enriched diets on antimicrobial peptide gene expression in rainbow trout (*Oncorhynchus mykiss*). Fish Shellfish Immunol. 34, 529-537.

Casadei, E., Bird, S., Wadsworth, S., González Vecino, J.L., Secombes, C.J., 2015. The longevity of the antimicrobial response in rainbow trout (*Oncorhynchus mykiss*) fed a peptidoglycan (PG) supplemented diet. Fish Shellfish Immunol. 44, 316-320.

Chen, L., Flies, D.B., 2013. Molecular mechanisms of T cell co-stimulation and co-inhibition. Nat. Rev. Immunol. 13, 227-242.

Covello, J.M., Friend, S.E., Purcell, S.L., Burka, J.F., Markham, R.J.F., Donkin, A.W., Groman, D.B., Fast, M.D., 2012. Effects of orally administered immunostimulants on inflammatory gene expression and sea lice (*Lepeophtheirus salmonis*) burdens on Atlantic salmon (*Salmo salar*). Aquaculture 366, 9-16.

Cuesta, A., Esteban, M.A., Meseguer, J., 2008. The expression profile of TLR9 mRNA and CpG ODNs immunostimulatory actions in the teleost gilthead seabream points to a major role of lymphocytes. Cell. Mol. Life Sci. 65, 2091-2104.

Dawood, M.A., Koshio, S., Esteban, M.Á., 2018. Beneficial roles of feed additives as immunostimulants in aquaculture: a review. Rev. Aquac. 10, 950-974.

Ellis, A.E., 2001. Innate host defense mechanisms of fish against viruses and bacteria. Dev. Comp. Immunol. 25, 827-839.

Eslamloo, K., Caballero-Solares, A., Inkpen, S.M., Emam, M., Kumar, S., Bouniot, C., Avendaño-Herrera, R., Jakob, E., Rise, M.L., 2020a. Transcriptomic profiling of the adaptive and innate immune responses of Atlantic salmon to *Renibacterium salmoninarum* infection. Front. Immunol. 11, 2487.

Eslamloo, K., Inkpen, S.M., Rise, M.L., Andreassen, R., 2018. Discovery of microRNAs associated with the antiviral immune response of Atlantic cod macrophages. Mol. Immunol. 93, 152-161.

Eslamloo, K., Kumar, S., Caballero-Solares, A., Gnanagobal, H., Santander, J., Rise, M.L., 2020b. Profiling the transcriptome response of Atlantic salmon head kidney to formalin-killed *Renibacterium salmoninarum*. Fish Shellfish Immunol. 98, 937-949.

Eslamloo, K., Xue, X., Hall, J.R., Smith, N.C., Caballero-Solares, A., Parrish, C.C., Taylor, R.G., Rise, M.L., 2017. Transcriptome profiling of antiviral immune and dietary

fatty acid dependent responses of Atlantic salmon macrophage-like cells. BMC Genomics 18, 706.
Ewart, K.V., Belanger, J.C., Williams, J., Karakach, T., Penny, S., Tsoi, S.C., Richards, R.C., Douglas, S.E., 2005. Identification of genes differentially expressed in Atlantic salmon (*Salmo salar*) in response to infection by *Aeromonas salmonicida* using cDNA microarray technology. Dev. Comp. Immunol. 29, 333-347.
FAO, 2014. The state of world fisheries and aquaculture 2014. Food and Agriculture Organization of the United Nations, Rome.
FAO, 2020. The state of world fisheries and aquaculture 2020. Food and Agriculture Organization of the United Nations, Rome.
Flajnik, M.F., Kasahara, M., 2010. Origin and evolution of the adaptive immune system: genetic events and selective pressures. Nat. Rev. Genet. 11, 47-59.
Fryer, J.L., Sanders, J.E., 1981. Bacterial kidney disease of salmonid fish. Annu. Rev. Microbiol. 35(1), 273-298.
Gagne, N., LeBlanc, F., 2018. Overview of infectious salmon anaemia virus (ISAV) in Atlantic Canada and first report of an ISAV North American - HPR 0 subtype. J. Fish Dis. 41, 421-430.
Glencross, B.D., 2009. Exploring the nutritional demand for essential fatty acids by aquaculture species. Rev. Aquac. 1, 71-124.
Glencross, B.D., Tocher, D.R., Matthew, C., Bell, J.G., 2014. Interactions between dietary docosahexaenoic acid and other long-chain polyunsaturated fatty acids on performance and fatty acid retention in post-smolt Atlantic salmon (*Salmo salar*). Fish Physiol. Biochem. 40, 1213-1227.
Godoy, M.G., Aedo, A., Kibenge, M.J., Groman, D.B., Yason, C.V., Grothusen, H., Lisperguer, A., Calbucura, M., Avendaño, F., Imilán, M., 2008. First detection, isolation and molecular characterization of infectious salmon anaemia virus associated with clinical disease in farmed Atlantic salmon (*Salmo salar*) in Chile. BMC Vet. Res. 4, 1-13.
Gomez, D., Sunyer, J.O., Salinas, I., 2013. The mucosal immune system of fish: the evolution of tolerating commensals while fighting pathogens. Fish Shellfish Immunol. 35, 1729-1739.
Hausser, J., Zavolan, M., 2014. Identification and consequences of miRNA–target interactions—beyond repression of gene expression. Nat. Rev. Genet. 15, 599-612.
Herkenhoff, M.E., Oliveira, A.C., Nachtigall, P.G., Costa, J.M., Campos, V.F., Hilsdorf, A.W., Pinhal, D., 2018. Fishing into the MicroRNA transcriptome. Front. Genet. 9, 88.
Hernández, A.J., Romero, A., Gonzalez-Stegmaier, R., Dantagnan, P., 2016. The effects of supplemented diets with a phytopharmaceutical preparation from herbal and macroalgal origin on disease resistance in rainbow trout against *Piscirickettsia salmonis*. Aquaculture 454, 109-117.
Higuchi, R., Dollinger, G., Walsh, P.S., Griffith, R., 1992. Simultaneous amplification and detection of specific DNA sequences. Nat. Biotechnol. 10, 413-417.
Higuchi, R., Fockler, C., Dollinger, G., Watson, R., 1993. Kinetic PCR analysis: real-time monitoring of DNA amplification reactions. Nat. Biotechnol. 11, 1026-1030.

Hikima, J.-I., Jung, T.-S., Aoki, T., 2011. Immunoglobulin genes and their transcriptional control in teleosts. Dev. Comp. Immunol. 35, 924-936.

Hixson, S.M., Parrish, C.C., Anderson, D.M., 2014. Full substitution of fish oil with camelina (*Camelina sativa*) oil, with partial substitution of fish meal with camelina meal, in diets for farmed Atlantic salmon (*Salmo salar*) and its effect on tissue lipids and sensory quality. Food Chem. 157, 51-61.

Hixson, S.M., Parrish, C.C., Xue, X., Wells, J.S., Collins, S.A., Anderson, D.M., Rise, M.L., 2017. Growth performance, tissue composition, and gene expression responses in Atlantic salmon (*Salmo salar*) fed varying levels of different lipid sources. Aquaculture 467, 76-88.

Holen, E., He, J., Espe, M., Chen, L., Araujo, P., 2015. Combining eicosapentaenoic acid, decosahexaenoic acid and arachidonic acid, using a fully crossed design, affect gene expression and eicosanoid secretion in salmon head kidney cells *in vitro*. Fish Shellfish Immunol. 45(2), 695-703.

Houston, R., Macqueen, D., 2019. Atlantic salmon (*Salmo salar* L.) genetics in the 21st century: taking leaps forward in aquaculture and biological understanding. Anim. Genet. 50, 3-14.

Jalili, M., Jin, Y., Bones, A.M., Olsen, Y., Vadstein, O., Østensen, M.-A., Buonocore, F., Gerdol, M., Pallavicini, A., Scapigliati, G., 2019. Dietary fatty acid source has little effect on the development of the immune system in the pyloric caeca of Atlantic salmon fry. Sci. Rep. 9, 27.

Jung, M.-H., Jung, S.-J., 2017. CpG ODN 1668 induce innate and adaptive immune responses in rock bream (*Oplegnathus fasciatus*) against rock bream iridovirus (RBIV) infection. Fish Shellfish Immunol. 69, 247-257.

Kanwal, Z., Wiegertjes, G.F., Veneman, W.J., Meijer, A.H., Spaink, H.P., 2014. Comparative studies of Toll-like receptor signalling using zebrafish. Dev. Comp. Immunol. 46, 35-52.

Keleher, W., Opitz, H., Blake, S., Edwards, K., Nicholson, B., 1999. Isolation of infectious salmon anemia virus (ISAV) from Atlantic salmon in New Brunswick, Canada. Dis. Aquat. Org. 35, 131-137.

Kibenge, F.S., Godoy, M.G., Fast, M., Workenhe, S., Kibenge, M.J., 2012. Countermeasures against viral diseases of farmed fish. Antiviral Res. 95(3), 257-281.

Kiron, V., 2012. Fish immune system and its nutritional modulation for preventive health care. Anim. Feed Sci. Technol. 173, 111 - 133.

Krasnov A., Johansen L.H., Karlsen C., Sveen L., Ytteborg E., Timmerhaus G., Lazado C.C., Afanasyev S., 2021. Transcriptome responses of Atlantic salmon (*Salmo salar* L.) to viral and bacterial pathogens, inflammation, and stress. Front. Immunol. 12, 705601.

Lang, A.S., Rise, M.L., Culley, A.I., Steward, G.F., 2009. RNA viruses in the sea. FEMS Microbiol. Rev. 33, 295-323.

Leaver, M.J., Bautista, J.M., Björnsson, B.T., Jönsson, E., Krey, G., Tocher, D.R., Torstensen, B.E., 2008a. Towards fish lipid nutrigenomics: current state and prospects for fin-fish aquaculture. Rev. Fish. Sci. 16, 73-94.

Leaver, M.J., Villeneuve, L.A., Obach, A., Jensen, L., Bron, J.E., Tocher, D.R., Taggart, J.B., 2008b. Functional genomics reveals increases in cholesterol biosynthetic genes and highly unsaturated fatty acid biosynthesis after dietary substitution of fish oil with vegetable oils in Atlantic salmon (*Salmo salar*). BMC Genomics 9, 299.

Liu, C.-S., Sun, Y., Hu, Y.-H., Sun, L., 2010. Identification and analysis of a CpG motif that protects turbot (*Scophthalmus maximus*) against bacterial challenge and enhances vaccine-induced specific immunity. Vaccine 28, 4153-4161.

Løvmo, S.D., Whatmore, P., Sundh, H., Sigholt, T., Madaro, A., Bardal, T., Olsen, R.E., 2021. Effects of Atlantic salmon (*Salmo salar*) fed low- and high HUFA diets on growth and midgut intestinal health. Aquaculture 539, 736653.

Løvoll, M., Wiik-Nielsen, C.R., Tunsjø, H.S., Colquhoun, D., Lunder, T., Sørum, H., Grove, S., 2009. Atlantic salmon bath challenged with *Moritella viscosa* – Pathogen invasion and host response. Fish Shellfish Immunol. 26, 877-884.

Magnadóttir, B., 2006. Innate immunity of fish (overview). Fish Shellfish Immunol. 20, 137-151.

Manzetti, S., Ghisi, R., 2014. The environmental release and fate of antibiotics. Mar. Pollut. Bull. 79, 7-15.

Martin, S.A.M., Król, E., 2017. Nutrigenomics and immune function in fish: new insights from omics technologies. Dev. Comp. Immunol. 75, 86-98.

Mashoof, S., Criscitiello, M.F., 2016. Fish immunoglobulins. Biology 5, 45.

Medzhitov, R., Janeway Jr, C.A., 1998. Innate immune recognition and control of adaptive immune responses, Seminars in immunology. Elsevier, pp. 351-353.

Merrifield, D.L., Rodiles, A., 2015. The fish microbiome and its interactions with mucosal tissues, in: Beck, B.H., Peatman, E. (Eds.), Mucosal Health in Aquaculture. Academic Press, pp. 273-295.

Mogensen, T.H., 2009. Pathogen recognition and inflammatory signaling in innate immune defenses. Clin. Microbiol. Rev. 22, 240-273.

Momen-Heravi, F., Bala, S., 2018. miRNA regulation of innate immunity. J. Leukoc. Biol. 103, 1205-1217.

Montero, D., Kalinowski, T., Obach, A., Robaina, L., Tort, L., Caballero, M., Izquierdo, M., 2003. Vegetable lipid sources for gilthead seabream (*Sparus aurata*): effects on fish health. Aquaculture 225, 353-370.

Montero, D., Mathlouthi, F., Tort, L., Afonso, J., Torrecillas, S., Fernández-Vaquero, A., Negrin, D., Izquierdo, M., 2010. Replacement of dietary fish oil by vegetable oils affects humoral immunity and expression of pro-inflammatory cytokines genes in gilthead sea bream *Sparus aurata*. Fish Shellfish Immunol. 29, 1073-1081.

Morais, S., Pratoomyot, J., Taggart, J.B., Bron, J.E., Guy, D.R., Bell, J.G., Tocher, D.R., 2011. Genotype-specific responses in Atlantic salmon (*Salmo salar*) subject to dietary fish oil replacement by vegetable oil: a liver transcriptomic analysis. BMC Genomics 12, 255.

Mourente, G., Good, J.E., Bell, J.G., 2005. Partial substitution of fish oil with rapeseed, linseed and olive oils in diets for European sea bass (*Dicentrarchus labrax* L.):

effects on flesh fatty acid composition, plasma prostaglandins E_2 and $F_{2\alpha}$, immune function and effectiveness of a fish oil finishing diet. Aquacult. Nutr. 11, 25-40.
Nayak, S., 2010. Probiotics and immunity: a fish perspective. Fish Shellfish Immunol. 29, 2-14.
Newaj-Fyzul, A., Al-Harbi, A., Austin, B., 2014. Developments in the use of probiotics for disease control in aquaculture. Aquaculture 431, 1-11.
Patterson, E., Wall, R., Fitzgerald, G., Ross, R., Stanton, C., 2012. Health implications of high dietary omega-6 polyunsaturated fatty acids. J Nutr Metab 2012, 539426.
Peatman, E., Lange, M., Zhao, H., Beck, B.H., 2015. Physiology and immunology of mucosal barriers in catfish (*Ictalurus spp*.). Tissue Barriers 3, e1068907.
Pérez, T., Balcázar, J., Ruiz-Zarzuela, I., Halaihel, N., Vendrell, D., De Blas, I., Múzquiz, J., 2010. Host–microbiota interactions within the fish intestinal ecosystem. Mucosal Immunol. 3, 355.
Press, C.M., Evensen, Ø., 1999. The morphology of the immune system in teleost fishes. Fish Shellfish Immunol. 9, 309-318.
Purcell, S.L., Friend, S.E., Covello, J.M., Donkin, A., Groman, D.B., Poley, J., Fast, M.D., 2013. CpG inclusion in feed reduces sea lice, *Lepeophtheirus salmonis*, numbers following re‐infection. J. Fish Dis. 36, 229-240.
Rauta, P.R., Samanta, M., Dash, H.R., Nayak, B., Das, S., 2014. Toll-like receptors (TLRs) in aquatic animals: signaling pathways, expressions and immune responses. Immunol. Lett. 158, 14-24.
Rise, M.L., Jones, S.R.M., Brown, G.D., von Schalburg, K.R., Davidson, W.S., Koop, B.F., 2004. Microarray analyses identify molecular biomarkers of Atlantic salmon macrophage and hematopoietic kidney responses to *Piscirickettsia salmonis* infection. Physiol. Genomics 20, 21 - 35.
Rodger, H., Richards, R., 1998. Haemorrhagic smolt syndrome: a severe anaemic condition in farmed salmon in Scotland. Vet. Rec. 142, 538-541.
Rodger, H.D., 2016. Fish disease causing economic impact in global aquaculture, Fish vaccines. Springer, pp. 1-34.
Romo, M.R., Pérez-Martínez, D., Ferrer, C.C., 2016. Innate immunity in vertebrates: an overview. Immunology, 148(2), 125-139.
Rosenlund, G., Torstensen, B.E., Stubhaug, I., Usman, N., Sissener, N.H., 2016. Atlantic salmon require long-chain n-3 fatty acids for optimal growth throughout the seawater period. J Nutr Sci 5, e19.
Rozas-Serri, M., Peña, A., Arriagada, G., Enríquez, R., Maldonado, L., 2018. Comparison of gene expression in post‐smolt Atlantic salmon challenged by LF‐89‐like and EM‐90‐like *Piscirickettsia salmonis* isolates reveals differences in the immune response associated with pathogenicity. J. Fish Dis. 41, 539-552.
Rozas, M., Enríquez, R., 2014. Piscirickettsiosis and *Piscirickettsia salmonis* in fish: a review. J. Fish Dis. 37, 163-188.
Ruyter, B., Røsjø, C., Einen, O., Thomassen, M., 2000. Essential fatty acids in Atlantic salmon: effects of increasing dietary doses of n-6 and n-3 fatty acids on growth,

survival and fatty acid composition of liver, blood and carcass. Aquac. Nutr. 6, 119-127.
Saini, R.K., Keum, Y.S., 2018. Omega-3 and omega-6 polyunsaturated fatty acids: Dietary sources, metabolism, and significance—A review. Life Sci. 203, 255-267.
Salinas, I., 2015. The mucosal immune system of teleost fish. Biology 4, 525-539.
Salinas, I., Magadán, S., 2017. Omics in fish mucosal immunity. Dev. Comp. Immunol. 75, 99-108.
Salinas, I., Parra, D., 2015. Fish mucosal immunity: intestine, in: Beck, B.H., Peatman, E. (Eds.), Mucosal Health in Aquaculture. Academic Press, pp. 135-170.
Secombes, C.J., Wang, T., 2012. The innate and adaptive immune system of fish, in: Austin, B. (Ed.), Infectious Disease in Aquaculture. Woodhead Publishing, pp. 3-68.
Sissener, N., Waagbø, R., Rosenlund, G., Tvenning, L., Susort, S., Lea, T., Oaland, Ø., Chen, L., Breck, O., 2016. Reduced n-3 long chain fatty acid levels in feed for Atlantic salmon (*Salmo salar* L.) do not reduce growth, robustness or product quality through an entire full scale commercial production cycle in seawater. Aquaculture 464, 236-245.
Smith, N.C., Rise, M.L., Christian, S.L., 2019. A comparison of the innate and adaptive immune systems in cartilaginous fish, ray-finned fish, and lobe-finned fish. Front. Immunol. 10, 2292.
Somamoto, T., Koppang, E.O., Fischer, U., 2014. Antiviral functions of $CD8^+$ cytotoxic T cells in teleost fish. Dev. Comp. Immunol. 43, 197-204.
Sprague, M., Betancor, M.B., Tocher, D.R., 2017. Microbial and genetically engineered oils as replacements for fish oil in aquaculture feeds. Biotechnol. Lett. 39, 1599-1609.
Stenberg, O.K., Holen, E., Piemontese, L., Liland, N.S., Lock, E.-J., Espe, M., Belghit, I., 2019. Effect of dietary replacement of fish meal with insect meal on in vitro bacterial and viral induced gene response in Atlantic salmon (*Salmo salar*) head kidney leukocytes. Fish Shellfish Immunol. 91, 223-232.
Strandskog, G., Ellingsen, T., Jørgensen, J.B., 2007. Characterization of three distinct CpG oligonucleotide classes which differ in ability to induce IFN α/β activity and cell proliferation in Atlantic salmon (*Salmo salar* L.) leukocytes. Dev. Comp. Immunol. 31, 39-51.
Tacchi, L., Bickerdike, R., Douglas, A., Secombes, C.J., Martin, S.A.M., 2011. Transcriptomic responses to functional feeds in Atlantic salmon (*Salmo salar*). Fish Shellfish Immunol. 31, 704-715.
Thorud, K., Djubvik, H., 1988. Infectious anaemia in Atlantic salmon (*Salmo salar*). Bull. Eur. Ass. Fish Pathol 8, 109-111.
Tocher, D.R., Zheng, X., Schlechtriem, C., Hastings, N., Dick, J.R., Teale, A.J., 2006. Highly unsaturated fatty acid synthesis in marine fish: Cloning, functional characterization, and nutritional regulation of fatty acyl Δ6 desaturase of Atlantic cod (*Gadus morhua* L.). Lipids 41, 1003-1016.
Torstensen, B.E., Bell, J.G., Rosenlund, G., Henderson, R.J., Graff, I.E., Tocher, D.R., Lie, Ø., Sargent, J.R., 2005. Tailoring of Atlantic salmon (*Salmo salar* L.) flesh lipid

composition and sensory quality by replacing fish oil with a vegetable oil blend. J. Agric. Food Chem. 53, 10166-10178.

Torstensen, B.E., Espe, M., Sanden, M., Stubhaug, I., Waagbø, R., Hemre, G.-I., Fontanillas, R., Nordgarden, U., Hevrøy, E.M., Olsvik, P., Berntssen, M.H.G., 2008. Novel production of Atlantic salmon (*Salmo salar*) protein based on combined replacement of fish meal and fish oil with plant meal and vegetable oil blends. Aquaculture 285, 193-200.

Umasuthan, N., Xue, X., Caballero-Solares, A., Kumar, S., Westcott, J.D., Chen, Z., Fast, M.D., Skugor, S., Nowak, B.F., Taylor, R.G., Rise, M.L., 2020. Transcriptomic profiling in fins of Atlantic salmon parasitized with sea lice: evidence for an early imbalance between chalimus-induced immunomodulation and the host's defense response. Int. J. Mol. Sci. 21, 2417.

Uribe, C., Folch, H., Enríquez, R., Moran, G., 2011. Innate and adaptive immunity in teleost fish: a review. Vet Med (Praha) 56, 486.

Valenzuela-Miranda, D., Valenzuela-Muñoz, V., Farlora, R., Gallardo-Escárate, C., 2017. MicroRNA-based transcriptomic responses of Atlantic salmon during infection by the intracellular bacterium *Piscirickettsia salmonis*. Dev. Comp. Immunol. 77, 287-296.

Vallejos-Vidal, E., Reyes-López, F., Teles, M., MacKenzie, S., 2016. The response of fish to immunostimulant diets. Fish Shellfish Immunol. 56, 34-69.

VanGuilder, H.D., Vrana, K.E., Freeman, W.M., 2008. Twenty-five years of quantitative PCR for gene expression analysis. BioTechniques 44, 619-626.

Wang, A., Ran, C., Wang, Y., Zhang, Z., Ding, Q., Yang, Y., Olsen, R.E., Ringø, E., Bindelle, J., Zhou, Z., 2019. Use of probiotics in aquaculture of China—a review of the past decade. Fish Shellfish Immunol. 83, 734-755.

Wang, M., Jiang, S., Wu, W., Yu, F., Chang, W., Li, P., Wang, K., 2018. Non-coding RNAs function as immune regulators in teleost fish. Front. Immunol. 9, 2801.

Wang, T., Secombes, C.J., 2013. The cytokine networks of adaptive immunity in fish. Fish Shellfish Immunol. 35, 1703-1718.

Woldemariam, N.T., Agafonov, O., Høyheim, B., Houston, R.D., Taggart, J.B., Andreassen, R., 2019. Expanding the miRNA repertoire in Atlantic salmon; discovery of isomiRs and miRNAs highly expressed in different tissues and developmental stages. Cells 8, 42.

Woldemariam, N.T., Agafonov, O., Sindre, H., Høyheim, B., Houston, R.D., Robledo, D., Bron, J.E., Andreassen, R., 2020. miRNAs predicted to regulate host anti-viral gene pathways in IPNV-challenged Atlantic salmon fry are affected by viral load, and associated with the major IPN resistance QTL genotypes in late infection. Front. Immunol. 11, 2113.

Xue, X., Hall, J.R., Caballero-Solares, A., Eslamloo, K., Taylor, R.G., Parrish, C.C., Rise, M.L., 2020. Liver transcriptome profiling reveals that dietary DHA and EPA levels influence suites of genes involved in metabolism, redox homeostasis, and immune function in Atlantic salmon (*Salmo salar*). Mar. Biotechnol. 22, 263-284.

Xue, X., Hixson, S.M., Hori, T.S., Booman, M., Parrish, C.C., Anderson, D.M., Rise, M.L., 2015. Atlantic salmon (*Salmo salar*) liver transcriptome response to diets

containing *Camelina sativa* products. Comp. Biochem. Physiol. D: Genomics Proteomics 14, 1-15.

Xue, X., Woldemariam, N.T., Caballero-Solares, A., Umasuthan, N., Fast, M.D., Taylor, R.G., Rise, M.L., Andreassen, R., 2019. Dietary immunostimulant CpG modulates microRNA biomarkers associated with immune responses in Atlantic salmon (*Salmo salar*). Cells 8, 1592.

Yan, X.-B., Dong, X.-H., Tan, B.-P., Zhang, S., Chi, S.-Y., Liu, H.-Y., Yang, Y.-Z., 2020. Influence of different oil sources on growth, disease resistance, immune response and immune-related gene expression on the hybrid grouper (♀ *Epinephelus fuscoguttatus* × ♂ E. lanceolatu), to *Vibrio parahaemolyticus* challenge. Fish Shellfish Immunol. 99, 310-321.

Ytrestøyl, T., Afanasyev, S., Ruyter, B., Hatlen, B., Østbye, T.-K., Krasnov, A., 2021. Transcriptome and functional responses to absence of astaxanthin in Atlantic salmon fed low marine diets. Comp. Biochem. Physiol. Part D Genomics Proteomics 39, 100841.

Zhang, J., Kong, X., Zhou, C., Li, L., Nie, G., Li, X., 2014. Toll-like receptor recognition of bacteria in fish: ligand specificity and signal pathways. Fish Shellfish Immunol. 41, 380-388.

Zhang, Y.-A., Salinas, I., Li, J., Parra, D., Bjork, S., Xu, Z., LaPatra, S.E., Bartholomew, J., Sunyer, J.O., 2010. IgT, a primitive immunoglobulin class specialized in mucosal immunity. Nat. Immunol. 11, 827-835.

Zhou, J., Song, X.-L., Huang, J., Wang, X.-H., 2006. Effects of dietary supplementation of A3α-peptidoglycan on innate immune responses and defense activity of Japanese flounder (*Paralichthys olivaceus*). Aquaculture 251, 172-181.

CHAPTER 2: Liver transcriptome profiling reveals that dietary DHA and EPA levels influence suites of genes involved in metabolism, redox homeostasis, and immune function in Atlantic salmon (*Salmo salar*)

The research described in **Chapter 2** has been published in the journal Marine Biotechnology as: Xue, X., Hall, J.R., Caballero-Solares, A. Eslamloo, K., Taylor, R.G., Parrish, C.C., Rise, M.L., 2020. Liver transcriptome profiling reveals that dietary DHA and EPA levels influence suites of genes involved in metabolism, redox homeostasis, and immune function in Atlantic salmon (*Salmo salar*). Mar. Biotechnol. 22, 263–284. https://doi.org/10.1007/s10126-020-09950-x

2.1 Abstract

The optimal dietary requirement of omega-3 long-chain polyunsaturated fatty acids (ω3 LC-PUFA), namely docosahexaenoic acid (DHA) and eicosapentaenoic acid (EPA), for Atlantic salmon that promotes growth and health warrants careful investigation. I used 44K microarrays to study the influence of increasing levels of dietary DHA+EPA (0, 1.0, and 1.4% of the diet, as formulated) in the presence of high linoleic acid (LA) on Atlantic salmon growth and liver transcriptome. After a 14-week feeding trial, Atlantic salmon fed diet ω3LC0 (i.e. 0% of DHA+EPA) showed significantly lower final weight and weight gain, and higher feed conversion ratio compared with the ω3LC1.0 and ω3LC1.4 diet groups. The microarray experiment identified 55 and 77 differentially expressed probes (Rank Products analyses; PFP < 10%) in salmon fed diets ω3LC1.4 and ω3LC1.0 compared with those fed diet ω3LC0, respectively. The comparison between ω3LC1.4 and ω3LC1.0 revealed 134 differentially expressed probes. The microarray results were confirmed by qPCR analyses of 22 microarray-identified transcripts. Several key genes involved in fatty acid metabolism including LC-PUFA synthesis were up-regulated in fish fed ω3LC0 compared with both other groups. Hierarchical clustering and linear regression analyses of liver qPCR and fatty acid composition data demonstrated significant correlations. In the current study, 1.0% ω3 LC-PUFA seemed to be the minimum requirement for Atlantic salmon based on growth performance; however, multivariate statistical analyses (PERMANOVA and SIMPER) showed that fish fed ω3LC1.0 and ω3LC1.4 diets had similar hepatic fatty acid profiles, but marked differences in the transcript expression of biomarker genes involved in redox homeostasis (*mgst1*), immune

responses (*mxb*, *igmb*, *irf3*, *lect2a*, *srk2*, *lyz2*) and LC-PUFA synthesis (*srebp1*, *fadsd5*, *elovl2*). This research has provided new insights into dietary requirement of DHA and EPA, and their impact on physiologically important pathways in addition to lipid metabolism in Atlantic salmon.

2.2 Introduction

Until recently, the finfish aquaculture industry, especially for carnivorous species such as Atlantic salmon (*Salmo salar*), relied heavily on fish oil (FO) for the production of aquafeeds due to its excellent profile of essential fatty acids (EFAs) such as eicosapentaenoic acid (EPA, 20:5ω3) and docosahexaenoic acid (DHA, 22:6ω3) (Torstensen et al., 2008; Morais et al., 2011). The increasing demand and limited supply of FO have caused aquaculture companies to decrease FO in the formulation and find alternatives such as vegetable oils (VO) for feed production. However, VOs lack long-chain polyunsaturated fatty acids (LC-PUFAs) but are often rich in short chain PUFAs such as α-linolenic acid (18:3ω3; ALA) and linoleic acid (18:2ω6; LA) (Xue et al., 2015). It is well known that adequate levels of DHA and EPA, as well as arachidonic acid (20:4ω6; ARA), are needed for normal growth, health and development in all vertebrates including fish (Betancor et al., 2014; Rosenlund et al., 2016). These fatty acids play key roles in the structure of cell membranes, ion balance, regulation of reproduction, and the function of the immune system (reviewed by Glencross, 2009).

A large volume of research in recent years has focused on finding alternative lipid sources to replace (partially or completely) FO in aquafeeds (Montero et al., 2003; Montero et al., 2010; Morais et al., 2012; Xue et al., 2015; Rosenlund et al., 2016; Caballero-Solares et al., 2017; Eslamloo et al., 2017; Hixson et al., 2017; Caballero-Solares et al., 2018; Foroutani et al., 2018). Previous studies have shown that VOs such as linseed oil, canola oil (i.e. genetically modified version of rapeseed plant), camelina oil, and rapeseed oil, can be used to replace up to 100% of FO without negatively influencing growth in Atlantic

salmon when there is still fish meal in the diets providing adequate levels of DHA and EPA (Bell et al., 2001; Torstensen et al., 2005; Bell et al., 2010; Hixson et al., 2014; Xue et al., 2015). Reduced flesh ω3 LC-PUFA content in Atlantic salmon was noted when large proportions of FO were replaced (Hixson et al., 2014; Foroutani et al., 2018). Moreover, VO dietary treatments in salmon frequently influence lipid metabolism including the synthesis of LC-PUFAs (reviewed by Leaver et al., 2008). For example, transcripts encoding enzymes involved in the bioconversion of both ω3 and ω6 PUFAs to LC-PUFAs [e.g., *delta-5 fatty acyl desaturase* (*fadsd5*), *elongation of very long chain fatty acids 2* (*elovl2*)] are often up-regulated in the liver of Atlantic salmon fed diets containing VO (reviewed by Leaver et al., 2008). In addition, a range of other biochemical and metabolic effects of VO inclusion in Atlantic salmon such as altered expression of genes involved in carbohydrate metabolism and immunity was also noted (Morais et al., 2011; Morais et al., 2012; Xue et al., 2015).

LC-PUFAs are known to play important roles in inflammation and immune responses (Calder, 2013; Eslamloo et al., 2017). For instance, ω3 fatty acids (e.g. EPA and DHA) exhibit anti-inflammatory functions through inhibition of activation of the pro-inflammatory transcription factor nuclear factor kappa B (Calder, 2015), while ω6 fatty acids (e.g. ARA) promote the formation of pro-inflammatory eicosanoids (Patterson et al., 2012). Hence, the balance between ω3 and ω6 fatty acids determines whether the inflammatory response is promoted or suppressed. The replacement of FO by VO resulted in changes in dietary fatty acid profiles and ratios (e.g. ω3/ω6), which could affect fish immune systems (Montero et al., 2003; Mourente et al., 2005). For example, Montero et

al. (2008) examined the effect of linseed and soybean oils on hepatic *mx* expression; elevated basal expression, as well as reduced phagocytic and serum alternative complement pathway activities, were noted in gilthead sea bream (*Sparus aurata*) fed VOs. In addition, Atlantic salmon fed diets supplemented with high levels of rapeseed oil and plant protein showed an enhanced antiviral immune response (Caballero-Solares et al., 2017).

During the last two decades, the dietary requirement of ω3 LC-PUFA in Atlantic salmon has been examined in several studies under different conditions (e.g. life stage and dietary formulation) (Ruyter et al., 2000; Glencross et al., 2014; Rosenlund et al., 2016; Bou et al., 2017b). It has been suggested that ≥ 1.0% (i.e. 10 g/kg) of ω3 LC-PUFA (i.e. DHA+EPA) is needed for optimal growth of Atlantic salmon (Ruyter et al., 2000; Rosenlund et al., 2016; Sissener et al., 2016). Previous studies on the determination of EFA requirements were mostly based on fish growth and survival, which might result in underestimates (Bou et al., 2017a). Other aspects such as fish health should be taken into consideration when determining the minimal requirement of ω3 LC-PUFA in Atlantic salmon diets. In a more recent study, Bou et al. (2017b) have found that under demanding environmental conditions (e.g. high water temperature, sea lice infection, and handling stress) in sea cages, Atlantic salmon fed a diet containing 1.0% DHA+EPA had poor survival compared with fish fed a 1.7% DHA+EPA diet. However, the molecular mechanisms involved in poor survival, and the impact of low ω3 LC-PUFA on salmon metabolism, physiology and immune function, are poorly understood.

Recently, a large feeding trial was conducted to evaluate the growth performance and the lipid and fatty acid composition in tissues, of Atlantic salmon fed 7 experimental

diets containing different levels of animal by-products, vegetable proteins, VO, and/or FO (Beheshti Foroutani, 2017; Beheshti Foroutani et al., 2018; Foroutani et al., 2020). Among the 7 experimental diets, 3 had the same levels of feed ingredients except for FO and VO (i.e. rapeseed oil), with graded levels of dietary DHA+EPA (0, 1.0 and 1.4% of the diet, as formulated). These diets were selected for the current study to increase the current knowledge and understanding of the physiological importance of dietary ω3 LC-PUFA in Atlantic salmon using molecular and genomic tools (e.g. DNA microarray). The use of such tools is becoming increasingly important in detecting genes and molecular pathway responses to nutritional variables (e.g. Xue et al., 2015; Caballero-Solares et al., 2018). I investigated the influence of graded levels of dietary DHA+EPA on Atlantic salmon growth and hepatic transcriptome. I also explored connections between the changes in hepatic transcriptome, fatty acid composition, and growth performance using linear regression and multivariate statistical analyses. Liver was chosen due to its roles in metabolizing nutrients as well as detoxification and immunity (Vilhelmsson et al., 2004; Panserat et al., 2009). This study allowed me to assess the impacts of dietary DHA and EPA on salmon physiology and health, and to identify and validate hepatic molecular biomarkers of response to varying levels of DHA+EPA.

2.3 Materials and methods

2.3.1 Experimental diets and animals

The Atlantic salmon post-smolt feeding trial was conducted at the Dr. Joe Brown Aquatic Research Building (JBARB, Ocean Sciences Centre, Memorial University of

Newfoundland, Canada). Three experimental diets were formulated by EWOS Innovation (now Cargill Innovation Center, Dirdal, Norway) to contain different levels of DHA+EPA [0% (ω3LC0), 1.0% (ω3LC1.0), and 1.4% (ω3LC1.4) of the diet, as formulated; 0.75, 3.57 and 4.74% of total fatty acids, as fed] (**Table 2.1**). The levels of DHA and EPA were obtained by including 0 to 7.4% of FO in the diets. The formulation of these 3 diets was published in previous investigations (Foroutani, 2017; Foroutani et al., 2018; Foroutani et al., 2020). However, since diet formulation is pertinent to the current study, it is provided herein (**Table 2.1**).

Atlantic salmon post-smolts (~178 g) were randomly distributed among twelve 620 L tanks (40 fish per tank) supplied with flow-through seawater (~11°C, dissolved oxygen ≥ 10 mg L^{-1}), and all fish were kept on a photoperiod of 12 h. All fish were acclimated to the experimental tanks for 2 weeks. Quadruplicate tanks of fish were fed each experimental diet to apparent satiety, twice each day for a period of 14 weeks. Apparent feed intake (AFI), water temperature and oxygen levels, were recorded daily. At the end of trial, 5 fish from each tank were euthanized by 400 mg L^{-1} tricaine-methane-sulfonate bath (TMS; Syndel Laboratories, Vancouver, BC, Canada) after 24 h of fasting. Liver tissues (50-100 mg $sample^{-1}$) were collected, flash-frozen in liquid nitrogen, and stored at -80°C until RNA extractions were performed. Body weight and fork length of the whole population were measured and recorded. This study was carried out in accordance with Animal Care Protocol (14-71-MR) approved by the Institutional Animal Care Committee of Memorial University of Newfoundland.

Table 2.1. Diet composition.

	ω3LC0	ω3LC1.0	ω3LC1.4
Ingredient[a] (% of diet)			
Fish meal	5.0	5.0	5.0
Poultry by-product meals[b]	21.6	21.4	21.6
Corn gluten	5.0	5.1	5.0
Soy protein concentrate	25.0	25.3	25.0
Wheat gluten	3.3	3.4	3.3
Fish oil	0	5.1	7.4
Rapeseed oil	27.3	22.1	19.9
Raw wheat	10.4	10.3	10.4
Premix[c]	2.4	2.3	2.4
Total	100	100	100
Composition of selected fatty acids (%)[d]			
18:2ω6 (LA)	18.4±1.1	16.6±0.1	15.7±0.1
18:3ω3 (ALA)	7.27±0.74	6.70±0.05	6.34±0.06
20:4ω6 (ARA)	0.10±0.03	0.18±0.01	0.21±0.01
20:5ω3 (EPA)	0.34±0.04	1.82±0.04	2.47±0.03
22:6ω3 (DHA)	0.41±0.05	1.75±0.11	2.27±0.04

Data in this table were published previously by Beheshti Foroutani et al. (2018).
[a]All ingredients were sourced from EWOS stocks. [b]For confidentiality, the nature and proportions of the poultry by-product meals included in the diets are not provided. [c]Premix includes vitamins, trace elements and inorganic phosphorus. Composition in micronutrients of the premix is proprietary information to EWOS. [d]Values are presented as mean area percentage of fatty acid methyl ester ± SD (n = 6-9). LA: linoleic acid; ALA: α-linolenic acid; ARA: arachidonic acid; EPA: eicosapentaenoic acid; DHA: docosahexaenoic acid.

2.3.2 RNA extraction, DNase treatment, and column purification

Liver samples were homogenized in TRIzol reagent (Invitrogen/Life Technologies, Carlsbad, CA, USA) with stainless steel beads (5 mm; Qiagen, Mississauga, ON, Canada) using a TissueLyser (Qiagen) and subjected to RNA extraction according to manufacturer instructions. Due to low 260/230 ratios (i.e. ranging from 0.9 to 1.7) following TRIzol extraction, all RNA samples were re-extracted using the phenol-chloroform phase separation method as described in Xue et al. (2015) and Xu et al. (2013). Total RNA samples were treated with DNase I (Qiagen) to degrade residual genomic DNA, and then purified using the RNeasy Mini Kit (Qiagen) following manufacturer protocols. RNA integrity was verified by 1% agarose gel electrophoresis, and RNA purity was assessed by A260/280 and A260/230 using NanoDrop spectrophotometry (Thermo Fisher, Mississauga, ON, Canada). All column-purified RNA samples in this study showed acceptable purity (i.e. A260/230 > 2 and A260/280 ratios > 1.9) and integrity (i.e. tight 18S and 28S ribosomal RNA bands).

2.3.3 Microarray hybridization and data acquisition

Eight individual fish (2 from each quadruplicate tank) from each experimental diet group were included in the microarray analysis using a common reference design (**Figure 2.1a**). Twenty-four arrays were used in this study, with one array per individual fish. The microarray experiment was performed as previously described (Xue et al., 2015; Brown et al., 2016; Eslamloo et al., 2017; Caballero-Solares et al., 2018). Anti-sense amplified RNA (aRNA) was *in vitro* transcribed from 1 µg of each experimental RNA using the Amino

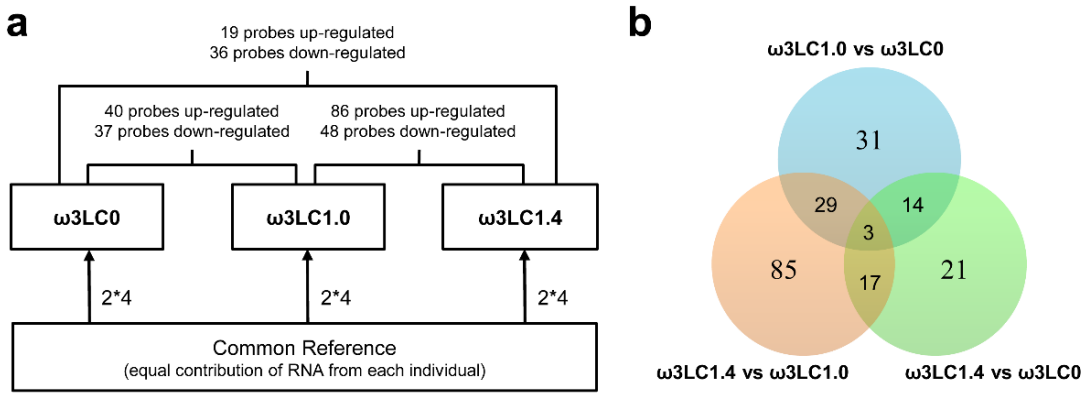

Figure 2.1. (a) Overview of the microarray experimental design and results with the number of differentially expressed probes (PFP < 10%) shown. (**b)** Venn diagram identifying microarray probes that are in common between gene lists.

Allyl MessageAmp II aRNA Amplification kit (Ambion/Life Technologies), following manufacturer instructions. The quality and quantity of aRNA were assessed using NanoDrop spectrophotometry and agarose gel electrophoresis. For each individual fish, 20 µg of aRNA was precipitated overnight following standard molecular biology procedure and resuspended in 9 µl of the manufacturer's coupling buffer. To generate the common reference pool, 5 µg of aRNA from each of the twenty-four samples was pooled, and divided into six 20 µg aliquots which were precipitated and resuspended as above. Resulting aRNA was labeled with either Cy3 (for the common reference) or Cy5 (for the experimental individuals) fluor (GE HealthCare, Mississauga, ON, Canada) through a dye-coupling reaction, following the manufacturer's instructions. The labeling efficiency was measured using the "microarray" function of the NanoDrop spectrophotometer. Equal quantities (825 ng) of each labeled aRNA from one experimental sample and the common reference were pooled, fragmented following the manufacturer's instructions and co-hybridized to a consortium for Genomic Research on All Salmonids Project (cGRASP)-designed Agilent 44K salmonid oligonucleotide microarray (GEO accession # GPL11299) (Jantzen et al., 2011; Sahlmann et al., 2013) as per the manufacturer's instructions (Agilent, Mississauga, ON, Canada). The arrays were hybridized at 65°C for 17 h with 10 rpm rotation in an Agilent hybridization oven. The array slides were washed immediately following hybridization as per the manufacturer's instructions.

Each microarray was scanned at 5 µm resolution and 90% of laser power using a ScanArray Gx Plus scanner and ScanArray Express software (v4.0; Perkin Elmer, Woodbridge, ON, Canada) with photomultiplier tube (PMT) set to balance fluorescence

signal between channels. The resulting TIFF images containing raw microarray data were extracted using Imagene (v9.0; BioDiscovery Inc., El Segundo, CA). Background correction, data transformation (log_2), print-tip Loess normalization, and removal of low-quality/flagged spots were performed using R and the Bioconductor package mArray (Booman et al., 2011; Xue et al., 2015). After spot quality filtering, probes absent in more than 30% of the arrays (i.e. 5 arrays out of 24) were discarded, resulting in a final list of 11,389 probes for statistical analyses. All microarray data have been submitted to Gene Expression Omnibus (GEO) under the accession GSE128472.

2.3.4 Microarray data analysis

Prior to statistical analyses, missing data points for the 11,389 probes were imputed using the EM_array method from LSimpute (Bo et al., 2004; Celton et al., 2010). The differentially expressed genes among diets were determined using Rank Products (RP), a non-parametric statistical method that is less sensitive to high biological variability than Significance Analysis of Microarrays (SAM) (Tusher et al., 2001; Breitling et al., 2004; Jeffery et al., 2006; Brown et al., 2016). RP analysis was conducted at a percentage of false-positives (PFP) threshold of 10%, using the Bioconductor package, RankProd (Hong et al., 2006). The resulting gene lists were annotated in Blast2GO (Conesa et al., 2005) using the contiguous sequences (contigs) from which informative 60mer oligonucleotide probes on the array were designed against the non-redundant (nr) protein database of NCBI (2015.09.30). The best BLASTx hit with an Expect (E) value $<10^{-5}$ and an informatively named protein product was chosen. To ensure the accuracy of gene identification, the probe sequences were also BLASTn aligned against the NCBI nr/nt databases for both Atlantic

salmon and rainbow trout. If BLASTn and BLASTx analyses for a given probe showed different results, then the best BLASTn hit was reported. Gene Ontology (GO) terms mapped to each microarray probe in Blast2GO were collected. For some microarray-identified probes, GO terms were obtained from *Homo sapiens* or *Mus musculus* putative orthologues from UniProt Knowledgebase (http://www.uniprot.org/).

2.3.5 qPCR analysis

I selected 22 genes of interest (GOIs; excluding paralogues) from the list of microarray-identified genes for real-time quantitative polymerase chain reaction (qPCR) analysis. One additional GOI not identified by the microarray analysis (i.e. *elovl2*) was added to the qPCR experiment.

First-strand cDNA templates for qPCR were synthesized in 20 µL reactions from 1 µg of DNaseI-treated, column-purified total RNA using random primers (250 ng; Invitrogen/Life Technologies), dNTPs (0.5 mM final concentration; Invitrogen/ Life Technologies) and M-MLV reverse transcriptase (200 U; Invitrogen/Life Technologies) with the manufacturer's first strand buffer (1× final concentration) and DTT (10 mM final concentration) at 37°C for 50 min. PCR amplifications were performed in 13 µL reactions using 1× Power SYBR Green PCR Master Mix (Applied Biosystems/Life Technologies), 50 nM of both the forward and reverse primers, and the indicated cDNA quantity (see below). The real-time qPCR analysis program consisted of 1 cycle of 50°C for 2 min, 1 cycle of 95°C for 10 min and 40 cycles of 95°C for 15 s and 60°C for 1 min, with fluorescence detection at the end of each 60°C step.

The sequences of all primer pairs used in qPCR analyses are presented in **Table 2.2**. In the case of gene paralogues, the primers were designed in an area with ≥ 3 bp different between the paralogues to ensure specificity. Each primer pair was quality tested using the 7500 Fast Real Time PCR system (Applied Biosystems/Life Technologies). Quality testing ensured that a single product was amplified (dissociation curve analysis) and that there was no primer-dimer present in the no-template control. Amplicons were electrophoretically separated on 2% agarose gels and compared with a 1 kb plus ladder (Invitrogen/Life Technologies) to verify that the correct size fragment was being amplified. Amplification efficiencies (Pfaffl, 2001) were calculated using cDNA synthesized from liver RNA samples (n = 18; 6 from each of the 3 diets) that had been pooled post-cDNA synthesis. Standard curves were generated using a 5-point 1:3 dilution series starting with cDNA representing 10 ng of input total RNA.

Transcript levels of the GOIs were normalized to transcript levels of two reference genes (i.e. normalizers). To select these reference genes, qPCR primer pairs were designed for six candidates [*60S ribosomal protein L32* (BT043656), *β-actin* (BG933897), *elongation factor 1-alpha 1* (AF321836), *elongation factor 1-alpha 2* (BT058669), *eukaryotic translation initiation factor 3 subunit D* (GE777139), and *polyadenylate-binding protein 1* (EG908498)] and quality tested as described above. The fluorescence threshold cycle (C_T) values of 18 samples (6 samples from each of the 3 diets) were measured for each of these genes using diluted cDNA representing 5 ng of input total RNA, and then analyzed using *geNorm* (Vandesompele et al., 2002). Using this software,

Table 2.2. Primers used in qPCR studies.

Transcript (gene symbol)	Primer sequence 5'-3'[a]	Efficiency (%)	Size (bp)[b]	Accession number[c]
Genes of interest				
elongation of very long chain fatty acids 2 (*elovl2*)[d]	F:GATGCCTGCTCTTCCAGTTC R:GCGACTGGACTTGATGGATT	100.8	113	FJ237532[e]
delta 5 fatty acyl desaturase (*fadsd5*)	F:GTCTGGTTGTCCGTTCGTTT R:GAGGCGATCAGCTTGAGAAA	98.9	135	AF478472[e]
delta 6 fatty acyl desaturase a (*fadsd6a*)	F:CCCCAGACGTTTGTGTCAG R:CCTGGATTGTTGCTTTGGAT	97.6	181	AY458652[e]
FAD-linked sulfhydryl oxidase ALR (*gfer*)	F:ACTACCCAGACCAGCCCTCT R:CAGGTCCTCAGCACACTCCT	96.1	101	GE791133
fatty acid synthase b (*fasb*)	F:TGCCATACAAGTGATGTCCTG R:AGTGGGCACCAAACATGAAC	100.3	105	EG872804
sterol regulatory element-binding protein 1 (*srebp1*)	F:TCAACAAGTCGGCAATTCTG R:GACATCTTCAGGGCCATGTT	90.6	100	HM561860
glucokinase (*gck*)	F:CTTTGGAGCCAACGGAGA R:GCACCAGCTCTCCCATGTA	97.4	131	XM_014171080[f]
pyruvate dehydrogenase kinase isozyme 2, mitochondrial precursor a (*pdk2a*)	F:TTGAGTACAAAGACACCTTTGGC R:GTTTCCGTCGAAAACAAGCGTG	93.0	134	XM_014192566
glucose-6-phosphate 1-dehydrogenase a (*g6pda*)	F:GAGCTGCATGATGACAAGGA R:TGTTCAGGGAGGAGACCATC	86.7	137	NM_001141724
beta-enolase a (*eno3a*)	F:CCGCCAAACTGATTGAGAA R:GCAGACCGCCAAAGACAC	100.6	137	NM_001141700
cysteine sulfinic acid decarboxylase a (*csada*)	F:CCCTGTATGGTCAGCAGAATATG R:CTTCTCTTTGACATCTGTGCCT	91.9	128	XM_014200263
cysteine sulfinic acid decarboxylase b (*csadb*)	F:AACCCTATGGTCAGCAGCACC R:TTCTCGTTGACGTCTATGCCC	93.7	127	XM_014154169
phospholipid hydroperoxide glutathione peroxidase, mitochondrial precursor a (*gpx4a*)	F:CCCAATGGGAAAGGCTTACT R:ACCACACTGGGATCATCCAT	93.0	116	DY710063
glutaredoxin-1 (*glrx1*)	F:ACGGGTGTTCATCGGTAAGA R:AGCGATCCGATTGACTTCAG	97.6	102	BT049493
microsomal glutathione S-transferase 1 (*mgst1*)	F:GGAAGACACAGGGATGGCTA R:CGGAGTGATGTTCTCCAGGT	100.4	115	XM_014151199
retinol dehydrogenase 3a (*rdh3a*)	F:CTGCTCTCCACCCTCGGACA R:ACGAATAGATCCTGTTGGTTTGG	94.2	137	BT046546
interferon regulatory factor 3 (*irf3*)	F:ACAAACAGCTGGGAACCAAC R:ATTGGATATTGCCGTTGCTC	98.2	108	NM_001172282[g]
interferon-induced GTP-binding protein Mx b (*mxb*)	F:ACGCACCACTCTGGAGAAAT R:CTTCCATTTCCCGAACTCTG	102.6	184	BT044881[g]
interferon-induced protein with tetratricopeptide repeats 5 (*ifit5*)	F:ATTGGCCTGTGTCACAAACA R:TGGTAGTTGTTCCCGTAGGC	93.1	191	BT046021[g]
leukocyte cell-derived chemotaxin 2 a (*lect2a*)	F:CAGATGGGGACAAGGACACT R:GCCTTCTTCGGGTCTGTGTA	98.3	150	BT059281[f]
lysozyme CII (*lyz2*)	F:ATACGGAATGGATGGCTACG R:AGATGCCATAGTCGGTGGAG	92.5	125	BT047934
GTPase IMAP family member 7 a (*gima7a*)	F:GTGGAGGACAATGGAGGAGA R:CCATACGCTGCCAGTTTACA	103.8	101	BT048289
immunoglobulin mu heavy chain a (*igma*)	F:AGCATTCACTTGCGTGTTTG R:CGGGGTGATCTTAATGACTACTG	103.8	115	BT058702[f]
immunoglobulin mu heavy chain b (*igmb*)	F:GAAGTTTCATTCACTTGCGTGT R:GCGGGATGATGTTAATGACC	99.1	121	BT059185[f]
tyrosine-protein kinase SRK2 (*srk2*)	F:ACCTGAACAACTCCCAGGTG R:GAAAGTGGGCCTGTCATGTT	105.4	140	BT046361
Normalizer genes				

elongation factor 1 alpha 1 (*ef1a1*)	F:TGGCACTTTCACTGCTCAAG R:CAACAATAGCAGCGTCTCCA	97.5	197	AF321836[e]
60S ribosomal protein 32 (*rpl32*)	F:AGGCGGTTTAAGGGTCAGAT R:TCGAGCTCCTTGATGTTGTG	101.7	119	BT043656[e]

[a]F: forward primer; R: reverse primer. [b]Amplicon size. [c]Nucleotide sequence from GenBank used for primer design. [d]*elongation of very long chain fatty acids 2* was not a microarray-identified transcript. [e]Primers previously designed in Xue et al. (2015), and quality-tested again using the reference cDNA template of the present study. [f]Primers previously designed in Caballero-Solares et al. (2018), and quality-tested again using the reference cDNA template of the present study. [g]Primers previously designed in Caballero-Solares et al. (2017), and quality-tested again using the reference cDNA template of the present study.

elongation factor 1-alpha 1 (*geNorm* M = 0.154) and *60S ribosomal protein L32* (*geNorm* M = 0.165) were determined to be the most stable.

When primer quality testing and normalizer selection were completed, qPCR analyses of transcript (mRNA) expression levels of the target genes were performed using the ViiA 7 Real Time PCR system (384-well format) (Applied Biosystems/Life Technologies). Expression levels of GOIs were measured in 24 liver samples [i.e. from 8 individual fish (2 from each quadruplicate tank) from each of the 3 diets]. In all cases, diluted cDNA corresponding to 4 ng of input RNA was used as template in the PCR reactions. On each plate, for every sample, the GOIs and normalizers were tested in triplicate, and a plate linker sample (i.e. a sample that was run on all plates in a given study) and a no-template control were included. The relative quantity (RQ) of each transcript was determined using the ViiA 7 Software Relative Quantification Study Application (Version 1.2.3) (Applied Biosystems/Life Technologies), with normalization to both *elongation factor 1-alpha 1* and *60S ribosomal protein L32* transcript levels, and with amplification efficiencies incorporated. For each GOI, the sample with the lowest normalized expression (mRNA) level was set as the calibrator sample (i.e. assigned an RQ value = 1).

Fold-change values calculated from microarray $\log_2$ ratios, and qPCR RQs, were analyzed for correlation via linear regression (see below). Gene expression fold-changes obtained through microarray analysis were calculated as 2^{A-B} (Hori et al., 2012), where A is the mean of $\log_2$ ratios from a dietary group, and B is the mean of $\log_2$ ratios from another dietary group. For down-regulated genes, fold-change values were inverted (−1/fold-

change). A significant correlation between both datasets was considered as proof of the validity of the microarray results.

2.3.6 Statistical analyses

2.3.6.1 Analyzing growth and qPCR data

All statistical analyses of growth-relevant and qPCR data were performed using Prism v6.0 (GraphPad Software Inc, La Jolla. CA). As mentioned earlier, the growth performance of salmon fed 7 experimental diets from the larger feeding trial was reported previously (Foroutani, 2017; Foroutani et al., 2018). The current study only focused on 3 dietary treatments (i.e. ω3LC0, ω3LC1.0, ω3LC1.4); therefore, growth performance (e.g. weight gain and AFI) data were reanalyzed using one-way ANOVA followed by Tukey's post hoc test for multiple comparisons at the 5% level of significance. qPCR data (i.e. RQ) were $\log_2$-transformed to improve the normality of data distribution, and analyzed using Student's *t*-test in a pairwise manner to determine if there is a significant difference ($p < 0.05$).

2.3.6.2 Linear regression analyses and hierarchical clustering

The three experimental diets under investigation were formulated with different levels of DHA+EPA. These differences could lead to contrasted tissue FA profiles, as well as changes in the liver transcriptome of the salmon. Therefore, I studied the possible connections between the mRNA levels of the qPCR-analyzed GOIs and the liver fatty acid composition. The results from the fatty acid composition analyses are published elsewhere (Foroutani, 2017; Foroutani et al., 2018). I analyzed the relationships between qPCR results

($\log_2$ RQ) and liver fatty acid composition by linear correlation analysis. Among the GOIs, I chose to analyze only those showing significant differences or trends among diets. Fatty acids in the ω3 family (ALA, 18:4ω3, 20:3ω3, 20:4ω3, EPA, 22:5ω3, DHA) and the ω6 family (LA, 18:3ω6, 20:2ω6, 20:3ω6, ARA, 22:4ω6, 22:5ω6), as well as the sums of monounsaturated fatty acids (MUFA), saturated fatty acids (SFA) and PUFA, were included in the analyses. Fish weight gain and other relevant parameters (e.g. EPA/ARA and ω3/ω6 ratios) for the interpretation of the microarray and qPCR results were also included. The linear regression analyses were performed with IBM SPSS Statistics, whereas the hierarchical clustering was carried out with PRIMER (Version 6.1.15; PRIMER-E Ltd, Ivybridge, UK) using Pearson correlation resemblance matrices. The significance of the regression was determined by an F-test ($p < 0.05$).

2.3.6.3 Multivariate statistical analyses

In addition to the statistical analyses described above, principal coordinates analysis (PCoA), permutational multivariate ANOVA (PERMANOVA), and similarity of percentages analysis (SIMPER) were performed using PRIMER to explore differences in liver fatty acid composition and qPCR-analyzed transcript expression among samples from fish fed different levels of DHA+EPA. PCoA is a multidimensional statistical scaling method used to explore and summarize similarities in data sets (Gower, 2014). PERMANOVA is a non-parametric multivariate test with statistical inferences made in a distribution-free setting using permutational algorithms (Anderson, 2014). SIMPER calculates the overall dissimilarity between groups and the contributing variables of

variables to the group dissimilarity (Clarke, 1993). All variables were standardized by the total of each variable in PRIMER prior to analyses.

2.4 Results

2.4.1 Atlantic salmon growth performance

As previously stated, the growth performance, fatty acid and other lipid data for the larger feeding trial involving 7 experimental diets were reported elsewhere (Foroutani, 2017; Foroutani et al., 2018; Foroutani et al., 2020). However, since the growth data are also important to the current study, they were reanalysed including only the 3 relevant diets. These data are briefly described and included in **Table 2.3**. Atlantic salmon fed the experimental diets increased in weight from 176.6-179.3 g fish^{-1} initially to 309.3–341.9 g fish^{-1} after 14 weeks (**Table 2.3**). The growth performance of salmon, as measured by final weight and weight gain, was significantly reduced in the ω3LC0 diet fed group, compared with other diets (i.e. ω3LC1.0 and ω3LC1.4) (e.g. weight gain, 132.7 g fish^{-1} *vs* 160.4-163.8 g fish^{-1}) (**Table 2.3**). In contrast, no significant difference was observed among organ indices such as HSI and VSI. Fish fed ω3LC0 diet had a significantly higher FCR than the other two diet groups (**Table 2.3**).

2.4.2 Microarray profiling of the liver transcriptome

Two hundred differentially expressed probes were detected in the microarray analysis of the liver transcriptome of salmon fed three experimental diets (**Figure 2.1**). Rank Products analysis (PFP < 10%) showed that 55 and 77 differentially expressed

Table 2.3. Growth performance and feed efficiency of Atlantic salmon fed experimental diets for 14 weeks[a].

Diet	ω3LC0	ω3LC1.0	ω3LC1.4
Initial weight[b] (g)	176.6 ± 26.5	179.3 ± 30.1	178.1 ± 27.5
Final weight[b] (g)	309.3 ± 63.7[B]	339.7 ± 73.5[A]	341.9 ± 68.7[A]
Weight gain[b] (g)	132.7 ± 48.6[B]	160.4 ± 59.7[A]	163.8 ± 54.7[A]
HSI[c] (%)	1.09 ± 0.22	1.14 ± 0.22	1.10 ± 0.18
VSI[d] (%)	10.9 ± 1.5	11.3 ± 1.7	11.1 ± 1.3
AFI[e] (g fish^{-1})	145.4 ± 16.7	159.0 ± 11.2	161.5 ± 19.7
FCR[f]	1.10 ± 0.05[A]	0.99 ± 0.03[B]	0.99 ± 0.02[B]

[a]Values are expressed as mean ± SD. Means with different superscript upper-case letters in the same row indicate significant differences among diets ($p < 0.05$). Data in this Table were published previously by Beheshti Foroutani et al. (2018) as a larger study involving seven experimental diets. They were reanalyzed with diets relevant to the current study. [b]n = 135-140. [c]Hepatosomatic index (HSI) = 100 × (liver mass/body mass). n = 30-32. [d]Viscerosomatic index (VSI) = 100 × (viscera mass/body mass). n = 30-32. [e]Apparent feed intake (AFI) = feed consumption/number of fish per tank. n = 4 (calculated by tank means). [f]Feed conversion ratio (FCR) = feed consumption/weight gain. n = 4 (calculated by tank means).

microarray probes were identified in salmon fed diets ω3LC1.4 and ω3LC1.0 compared with those fed diet ω3LC0, respectively. The comparison between ω3LC1.4 and ω3LC1.0 revealed 134 differentially expressed probes. Among all differentially expressed probes, 183 probes had significant BLASTx or BLASTn hits (E-value < 10^{-5}) (**Supplemental Table S2.1**). Based on their associated Gene Ontology (GO) terms and the information available in the literature, 30 of these BLAST-identified and functionally characterized probes were classified as genes involved in metabolic pathways (e.g. carbohydrate and lipid metabolism; **Table 2.4**); while 12 of these microarray probes putatively involved in redox homeostasis were identified (**Table 2.5**). Forty-nine differentially expressed probes were classified as genes involved in immune function (**Table 2.6**). BLAST identification, GO functional annotation, and microarray fold change values for all 200 differentially expressed probes are contained in **Supplemental Table S2.1**.

Among differentially expressed probes classified as metabolism-relevant, 5 were related to nucleotide metabolism (e.g. *adenylate kinase isoenzyme 6*), 2 related to taurine biosynthesis [both probes representing *cysteine sulfinic acid decarboxylase* (*csad*)], 5 related to carbohydrate metabolism [e.g. *glucokinase* (*gck*) and *glucose-6-phosphate 1-dehydrogenase* (*g6pda*)], and 11 related to lipid metabolism [e.g. *fadsd5* and *fatty acid synthase* (*fasb*)] (**Table 2.4**). Overall, microarray probes identified as genes involved in nucleotide metabolism (e.g. *adenylate kinase isoenzyme 6* and *cysteinyl-tRNA synthetase, cytoplasmic*) were down-regulated in salmon fed ω3LC1.4 diet compared with ω3LC0 diet. Of the microarray-identified genes related to carbohydrate metabolism (e.g. glycolytic

Table 2.4. A subset of microarray-identified ω3 LC-PUFA responsive genes involved in nutrient metabolism that were differentially expressed in the liver of Atlantic salmon.

Probe ID[a]	Gene[b]	Functional annotation[c]	Fold-change (FC) values[d]		
			ω3LC1.0 *vs* ω3LC0	ω3LC1.4 *vs* ω3LC0	ω3LC1.4 *vs* ω3LC1.0
Nucleotide metabolism					
C031R072	Adenylate kinase isoenzyme 6	P:nucleotide phosphorylation	-1.27	**-1.88**	-1.48
C135R067	Cysteinyl-tRNA synthetase, cytoplasmic	P:cysteinyl-tRNA aminoacylation	-1.25	**-1.96**	-1.59
C262R126	Stonustoxin subunit beta	F:nucleotide binding	-1.30	1.34	**1.75**
C128R027	Uridine phosphorylase 2	P:nucleotide catabolic process	-1.64	**-1.76**	-1.07
C086R065	Kalirin RhoGEF	P:'de novo' UMP biosynthetic process	**2.06**	1.46	-1.41
Carbohydrate metabolism					
C103R155	Trehalase precursor	P:trehalose catabolic process	1.60	**1.93**	1.21
C052R144	Beta-enolase (*eno3a*)	P:glycolytic process	1.18	-1.44	**-1.70**
C035R008	Glucokinase (*gck*)	P:glycolytic process	**-1.25**	**-1.52**	-1.22
C152R045	Glucose-6-phosphate 1-dehydrogenase (*g6pda*)	P:glucose metabolic process	**-1.76**	1.03	**1.80**
C146R081	Glyceraldehyde-3-phosphate dehydrogenase	P:glycolytic process	**-2.26**	**-1.55**	1.46
Lipid metabolism					
C223R038	Delta-5 fatty acyl desaturase (*fadsd5*)	P:unsaturated fatty acid biosynthetic process†	-1.38	**-1.80**	-1.30
C038R110	PREDICTED: delta-6 fatty acyl desaturase isoform X1 (*fadsd6a*)*	P:unsaturated fatty acid biosynthetic process†	-1.62	**-1.78**	-1.10
C004R046	Fatty acid synthase (*fasb*)	P:fatty acid biosynthetic process	**-1.76**	**-2.03**	-1.16
C220R061	PREDICTED: fatty acid synthase-like*	P:fatty acid biosynthetic process	-1.18	**-2.22**	**-1.88**
C049R002	Perilipin-2	P:long-chain fatty acid transport	-1.12	**-1.69**	-1.50
C251R020	Probable phospholipid-transporting ATPase IA	P:phospholipid translocation	-1.29	1.38	**1.78**
C086R136	Pyruvate dehydrogenase kinase isozyme 2, mitochondrial precursor (*pdk2a*)	P:regulation of fatty acid oxidation	**-1.64**	-1.36	1.21
C255R096	PREDICTED: fatty acyl-CoA hydrolase precursor, medium chain-like isoform X2*	P:fatty acid metabolic process†	**-1.91**	-1.11	**1.73**
C230R060	Very long-chain acyl-CoA synthetase	F:very long-chain fatty acid-CoA ligase activity	**1.73**	1.57	-1.10
C098R149	Sterol regulatory element-binding protein 1 (*srebp1*)	P:positive regulation of lipid biosynthetic process	1.27	-1.39	**-1.77**
C134R089	PREDICTED: diacylglycerol O-acyltransferase 2-like*	P:triglyceride biosynthetic process†	1.18	**-1.45**	**-1.70**
Other metabolic processes					
C054R118	Cysteine sulfinic acid decarboxylase (*csad*)	P:taurine biosynthetic process	**1.86**	1.41	-1.33
C077R080	Cysteine sulfinic acid decarboxylase (*csada*)	P:taurine biosynthetic process	**1.56**	**1.80**	1.15
C023R106	Lysine-specific demethylase 2B-like isoform X1	P:primary metabolic process	-1.29	1.34	**1.73**
C227R133	Putative aminopeptidase W07G4.4	P:proteolysis	-1.19	1.60	**1.91**
C099R009	Receptor-type tyrosine-protein phosphatase F precursor	F:protein tyrosine phosphatase activity	-1.29	1.44	**1.86**
C060R108	Cytochrome c oxidase subunit II	C:respiratory chain complex IV	**1.05**	**1.28**	**1.23**

C097R143	NADH dehydrogenase [ubiquinone] 1 alpha subcomplex subunit 4-like 2	C:mitochondrial respiratory chain complex IV	1.46	-1.10	**-1.60**
C119R046	Isocitrate dehydrogenase [NAD] subunit alpha, mitochondrial precursor	P:tricarboxylic acid cycle	-1.23	1.41	**1.74**
C079R021	Receptor activity-modifying protein 1 precursor	P:positive regulation of cellular biosynthetic process	**-1.67**	-1.26	1.32

[a]Refers to the identifier of the probe on the 44K microarray. [b]The protein name of the best BLASTx hit of microarray probe. BLASTn-identified genes are denoted with an asterisk (*). For qPCR-analyzed genes (underlined), gene symbol is indicated in brackets, differentiating paralogues if possible. [c]Representative gene ontology (GO) term mapped to each microarray probe. Complete GO terms for each probe are shown in **Supplemental Table S2.1**. GO term obtained from *Homo sapiens* or *Mus musculus* putative orthologues denoted with a dagger (†). GO categories: biological process (P), molecular function (F), and cellular component (C). [d]Fold-change (FC) values between two dietary treatments with bold font indicate statistical significance (PFP < 10%).

Table 2.5. A subset of microarray-identified ω3 LC-PUFA responsive genes involved in redox homeostasis that were differentially expressed in the liver of Atlantic salmon.

Probe ID[a]	Gene[b]	Functional annotation[c]	Fold-change (FC) values[d]		
			ω3LC1.0 *vs* ω3LC0	**ω3LC1.4 *vs* ω3LC0**	**ω3LC1.4 *vs* ω3LC1.0**
Redox homeostasis					
C064R163	Glutaredoxin-1 (*glrx1*)	P:cell redox homeostasis	**2.00**	-1.02	**-2.03**
C058R098	Glutaredoxin-1 (*glrx1*)	P:cell redox homeostasis	1.36	-1.38	**-1.88**
C121R018	Glutaredoxin-1 (*glrx1*)	P:cell redox homeostasis	1.24	-1.49	**-1.85**
C224R002	Glutaredoxin-1 (*glrx1*)	P:cell redox homeostasis	1.20	-1.55	**-1.86**
C136R102	Microsomal glutathione S-transferase 1 (*mgst1*)	P:glutathione metabolic process	**1.68**	-1.18	**-1.98**
C013R125	Phospholipid hydroperoxide glutathione peroxidase, mitochondrial precursor (*gpx4a*)	P:response to oxidative stress	**1.54**	1.36	-1.13
C049R143	Alcohol dehydrogenase 1	F:S-(hydroxymethyl)glutathione dehydrogenase activity	-1.14	**1.56**	**1.78**
C247R158	Branched-chain-amino-acid aminotransferase, cytosolic	P:oxidation-reduction process	-1.09	1.64	**1.78**
C061R061	Retinol dehydrogenase 12	P:oxidation-reduction process	-1.25	**-1.70**	-1.36
C042R054	Probable D-lactate dehydrogenase, mitochondrial	P:oxidation-reduction process	-1.45	1.24	**1.80**
C264R033	Retinol dehydrogenase 3 (*rdh3a*)	P:oxidation-reduction process	**-1.71**	1.18	**2.01**
C126R012	FAD-linked sulfhydryl oxidase ALR (*gfer*)	P:oxidation-reduction process	**-2.42**	**-1.35**	**1.79**

[a,b,c,d]All column constructions are as described in **Table 2.4.**

Table 2.6. A subset of microarray-identified ω3 LC-PUFA responsive genes involved in immune function that were differentially expressed in the liver of Atlantic salmon.

Probe ID[a]	Gene[b]	Functional annotation[c]	Fold-change (FC) values[d]		
			ω3LC1.0 *vs* ω3LC0	ω3LC1.4 *vs* ω3LC0	ω3LC1.4 *vs* ω3LC1.0
Antibacterial					
C159R112	Leukocyte cell-derived chemotaxin 2 precursor (*lect2a*)	P:response to bacterium	**-2.33**	1.27	**2.97**
C164R142	Leukocyte cell-derived chemotaxin 2 precursor (*lect2a*)	P:response to bacterium	**-2.00**	1.05	**2.09**
C134R121	Leukocyte cell-derived chemotaxin 2 precursor (*lect2a*)	P:response to bacterium	**-1.99**	1.15	**2.29**
C172R005	Lysozyme C II precursor (*lyz2*)	P:defense response to bacterium	-1.49	1.13	**1.69**
C099R149	Lysozyme C II precursor (*lyz2*)	P:defense response to bacterium	-1.17	1.40	**1.63**
C247R087	Pleiotrophic factor-alpha-2 precursor	P:defense response to bacterium	-1.49	1.19	**1.77**
C195R122	CD59 Glycoprotein	P:defense response to Gram-negative bacterium	-1.15	1.62	**1.86**
C085R091	Serum amyloid A-5 protein precursor*	P:acute-phase response†	**1.15**	1.26	1.09
Antiviral					
C093R102	Interferon regulatory factor 3 (*irf3*)	P:defense response to virus†	1.40	-1.29	**-1.80**
C236R043	Interferon-induced GTP-binding protein Mx b (*mxb*)	P:response to type I interferon	1.44	-1.47	**-2.12**
C055R128	Interferon-induced protein with tetratricopeptide repeats 5 (*ifit5*)	P:defense response to virus†	**1.39**	-1.49	**-2.07**
C058R152	Interferon-induced very large GTPase 1	F:GTP binding	**1.57**	-1.06	**-1.67**
C159R004	Interferon-inducible protein Gig2-like, partial	P:defense response to virus	**-1.77**	-1.22	1.44
C128R041	Galectin-9*	P:cellular response to interferon-gamma†	-1.14	**-1.91**	**-1.68**
C180R027	GTPase IMAP family member 7 (*gima7a*)	F:GTP binding	-1.25	**-2.14**	**-1.71**
C042R095	GTPase IMAP family member 7 (*gima7a*)	F:GTP binding	**1.57**	**-1.25**	**-1.96**
Adaptive immune response					
C027R162	MHC class I antigen	P:antigen processing and presentation of peptide antigen via MHC class I	1.03	1.32	**1.28**
C192R116	MHC class I antigen	P:antigen processing and presentation of peptide antigen via MHC class I	1.51	-1.47	**-2.22**
C197R118	Immunoglobulin light chain precursor	P:antigen processing and presentation of peptide antigen via MHC class I	**1.67**	-1.03	**-1.71**
C166R162	Ig kappa chain V-III region MOPC 63 precursor	P:immune response†	1.37	**1.94**	1.41
C151R068	Ig mu chain C region membrane-bound form (*igm*)	P:adaptive immune response†	1.21	**1.94**	**1.60**
C264R117	Ig mu chain C region membrane-bound form (*igm*)	P:adaptive immune response†	1.28	**2.35**	**1.84**
C205R051	Ig mu chain C region membrane-bound form (*igm*)	P:adaptive immune response†	1.28	**1.75**	1.37
C012R159	Ig mu chain C region membrane-bound form (*igm*)	P:adaptive immune response†	1.36	**1.79**	1.32
C061R085	Ig mu chain C region membrane-bound form (*igm*)	P:adaptive immune response†	1.48	**1.95**	1.32
C075R137	Ig mu chain C region membrane-bound form (*igm*)	P:adaptive immune response†	**1.80**	**2.05**	1.13

C087R072	Immunoglobulin superfamily member 6 precursor	P:cell surface receptor signaling pathway†	**1.72**	-1.04	**-1.79**
Other immune-related					
C190R106	PREDICTED: fucolectin-6-like*	P:regulation of complement activation, lectin pathway†	**-1.85**	-1.42	1.30
C246R052	Nuclear factor of activated T-cells 5-like*	P:positive regulation of NIK/NF-kappaB signaling†	**1.70**	1.65	-1.03
C057R114	PREDICTED: purine nucleoside phosphorylase-like*	P:positive regulation of T cell proliferation	**-1.77**	**-1.81**	-1.03
C127R051	Purine nucleoside phosphorylase	P:positive regulation of T cell proliferation	-1.55	**-1.92**	-1.24
C137R023	4F2 cell-surface antigen heavy chain	P:leukocyte migration†	**-1.78**	-1.36	1.31
C163R079	PREDICTED: C-C motif chemokine 19-like*	P:inflammatory response†	**-1.70**	-1.38	1.24
C068R097	PREDICTED: ladderlectin-like*	F:carbohydrate binding	-1.13	1.55	**1.74**
C134R069	Lectin precursor	P:immune response	1.05	-1.49	**-1.56**
C187R013	Proteasome subunit beta type-6 precursor	P:immune system process	-1.22	**-1.73**	-1.42
C117R007	Caspase recruitment domain-containing protein 9	P:positive regulation of innate immune response	**-1.72**	1.03	**1.77**
C089R017	Rho/Rac guanine nucleotide exchange factor 2	P:innate immune response	**-1.88**	-1.06	**1.76**
C240R145	Tyrosine-protein kinase FRK	P:innate immune response	**1.72**	1.12	**-1.54**
C050R143	Tyrosine-protein kinase SRK2 (*srk2*)	P:innate immune response	**1.76**	-1.27	**-2.24**
C108R011	Stabilin-2 precursor	P:positive regulation of lymphangiogenesis	-1.35	1.21	**1.64**
C156R109	Eukaryotic translation initiation factor 4 gamma 2	P:cytokine-mediated signaling pathway	**2.11**	-1.36	**-2.86**
C029R088	CD9 antigen	C:integral component of membrane	1.30	-1.45	**-1.89**

[a,b,c,d]All column constructions are as described in **Table 2.4.**

process), three were significantly down-regulated (e.g. *gck*, *g6pda*) in fish fed ω3LC1.0 diet compared with ω3LC0 diet; *beta-enolase* (*eno3a*) was down-regulated by ω3LC1.4 diet compared with both ω3LC0 and ω3LC1.0 diets, this down-regulation being statistically significant for ω3LC1.0 diet. Regarding lipid metabolism relevant genes, 6 of them (e.g. *fadsd5* and *fasb*) were significantly down-regulated by ω3LC1.4 diet compared with ω3LC0 diet; *sterol regulatory element-binding protein 1* (*srebp1*) and *very long-chain acyl-CoA synthetase* were up-regulated in fish fed ω3LC1.0 diet compared with ω3LC1.4 and ω3LC0 diets, respectively. In addition, three lipid metabolism-related probes [i.e. *pyruvate dehydrogenase kinase isozyme 2*, *mitochondrial precursor* (*pdk2a*); *fatty acyl-CoA hydrolase precursor*, *medium chain-like isoform X2*; and *fatty acid synthase* (*fasb*)], were down-regulated in fish fed ω3LC1.0 diet compared with ω3LC0 diet. Of the genes related to other metabolic processes, 2 probes encoding *csad* were up-regulated in fish fed ω3LC1.0 and/or ω3LC1.4 diets compared with ω3LC0 group.

Regarding the redox relevant differentially expressed genes, *glutaredoxin-1* (*glrx1*; probe C064R163), *microsomal glutathione S-transferase 1* (*mgst1*), and *phospholipid hydroperoxide glutathione peroxidase, mitochondrial precursor* (*gpx4a*) were up-regulated in fish fed ω3LC1.0 diet compared with fish fed ω3LC0 diet (**Table 2.5**). All probes representing *glrx1* and *mgst1* were also up-regulated in ω3LC1.0 group compared with ω3LC1.4 group. In addition, 5 probes representing genes involved in redox homeostasis [e.g. *alcohol dehydrogenase 1* and *retinol dehydrogenase 3* (*rdh3a*)] were down-regulated by ω3LC1.0 diet compared with ω3LC1.4 diet.

Among the immune-related probes identified as differentially expressed between diet groups, 8 probes were classified as antibacterial [e.g. *leukocyte cell-derived chemotaxin 2 precursor* (*lect2a*) and *lysozyme CII precursor* (*lyz2*)], 8 probes were annotated as antiviral [e.g. *interferon regulatory factor 3* (*irf3*) and *interferon-induced GTP-binding protein Mx* (*mxb*)], and a number of probes were related to adaptive immune response [e.g. *Ig mu chain C region membrane-bound form* (*igm*)] and other immune processes [e.g. *tyrosine-protein kinase SRK2* (*srk2*) and *stabilin-2 precursor*] (**Table 2.6**). Overall, 7 of those classified as antibacterial (e.g. *lect2*, *lyz2*, and *CD59 glycoprotein*) were up-regulated by ω3LC1.4 diet compared with ω3LC1.0 diet. Genes involved in the antiviral response [e.g. *irf3*, *mxb*, and *interferon-induced protein with tetratricopeptide repeats 5* (*ifit5*)] were down-regulated in fish fed ω3LC1.4 diet compared with fish fed ω3LC1.0 diet except for *interferon-inducible protein Gig2-like, partial*. Among microarray-identified genes related to antigen processing and presentation, 7 probes representing immunoglobulin genes (e.g. *igm*) were up-regulated in fish fed ω3LC1.4 diet compared with ω3LC0 group. It is worth noting that *srk2*, classified under "other immune-related", was up-regulated by ω3LC1.0 diet compared with both ω3LC0 and ω3LC1.4 diets.

2.4.3 qPCR validation

Twenty-two microarray-identified genes (excluding paralogues and *elovl2*) were subjected to qPCR validation. Eight of these transcripts (36.4%), namely *fadsd5*, *fadsd6a*, *fasb*, *mgst1*, *glrx1*, *pdk2a*, *lect2a* and *lyz2*, were shown to be significantly affected by dietary DHA and EPA; twelve of the remaining transcripts analyzed agreed with the microarray results in the direction of change (i.e. up- or down-regulation) (**Figures 2.2-**

2.4). In addition, the fold-change values calculated from microarray $\log_2$ ratios and fold-change values calculated from qPCR RQs showed a highly significant correlation (R^2 = 0.5835; $p < 0.0001$), indicating good overall validation of microarray results by qPCR (**Supplemental Figure S2.1**).

Considering metabolism-related transcripts, expression levels of *fadsd5*, *fadsd6a* and *fasb* were significantly lower in fish fed ω3LC1.0 and ω3LC1.4 diets compared with fish fed ω3LC0 diet except for *fadsd5* which only showed a trend ($p = 0.09$) in fish fed ω3LC1.0 (**Figure 2.2b-d**). Transcript expression levels of *elovl2* trended higher ($p = 0.09$) in fish fed the ω3LC0 diet compared with the ω3LC1.0 group (**Figure 2.2a**). Although not statistically significant, *srebp1* transcript levels appeared to be down-regulated by the ω3LC1.4 diet compared with fish fed diets with lower levels of DHA and EPA (**Figure 2.2e**; $p = 0.12$ and $p = 0.06$). In addition, *pdk2a* transcript levels were down-regulated by both ω3LC1.0 and ω3LC1.4 diets, with this down-regulation (~ 2-fold) being statistically significant for the ω3LC1.0 diet (**Figure 2.2f**). There were no significant differences in transcript expression levels of carbohydrate metabolism-related (*gck*, *g6pda*, and *eno3a*) and taurine biosynthetic process relevant (*csada* and *csadb*) genes among dietary groups (**Figure 2.2g-k**); however, the qPCR results did agree with the microarray results in direction of change.

Considering redox-relevant transcripts, *mgst1* expression level was significantly up-regulated by the ω3LC1.0 diet compared with ω3LC0 and ω3LC1.4 (**Figure 2.3b**); the up-regulation of *glrx1* expression by the ω3LC1.0 diet was only significant when compared

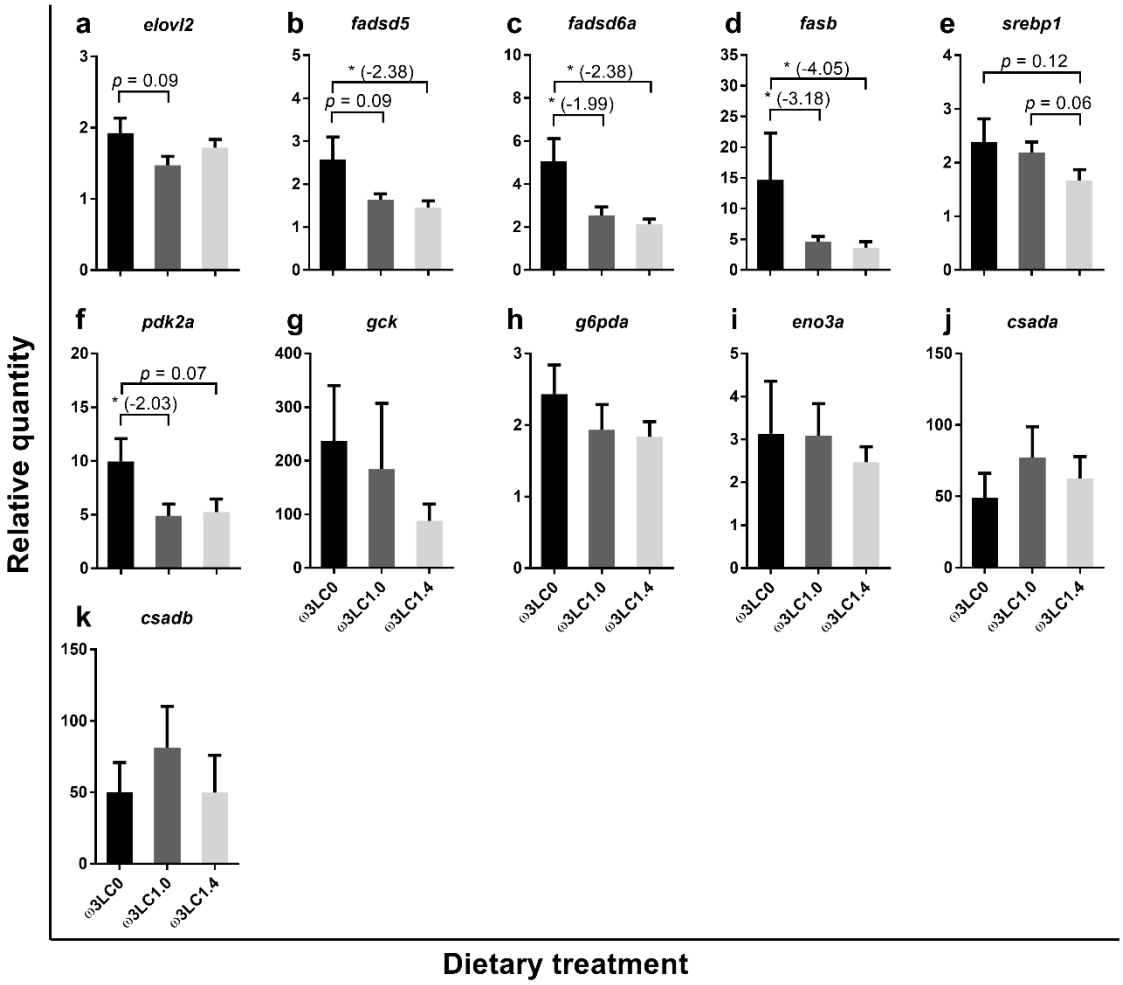

Figure 2.2. qPCR analysis of transcripts with putative roles in lipid (**a-f**), carbohydrate (**g-i**), and taurine (**j-k**) metabolism in the liver of salmon fed diets contain different levels of ω3 LC-PUFA. Columns and error bars represent mean relative quantity (RQ) values and SE, respectively. Significant difference by dietary treatment is indicated with asterisks (Student's t-test: *, $p < 0.05$). Fold-change is shown in brackets next to the asterisks.

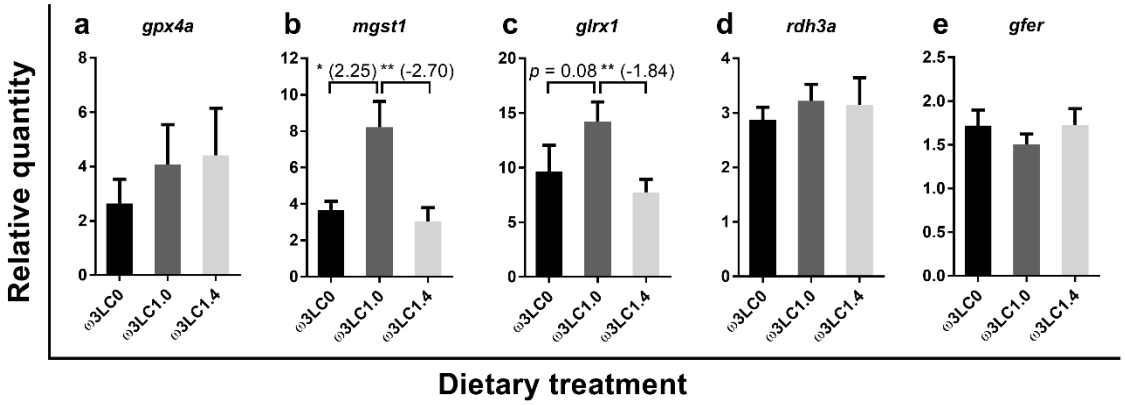

Figure 2.3. qPCR analysis of transcripts with putative roles in redox homeostasis (**a-e**) in the liver of salmon fed diets containing different levels of ω3 LC-PUFA. Columns and error bars represent mean relative quantity (RQ) values and SE, respectively. Significant difference by dietary treatment is indicated with asterisks (Student's *t*-test: *, $p < 0.05$; **, $p < 0.001$). Fold-change is shown in brackets next to the asterisks.

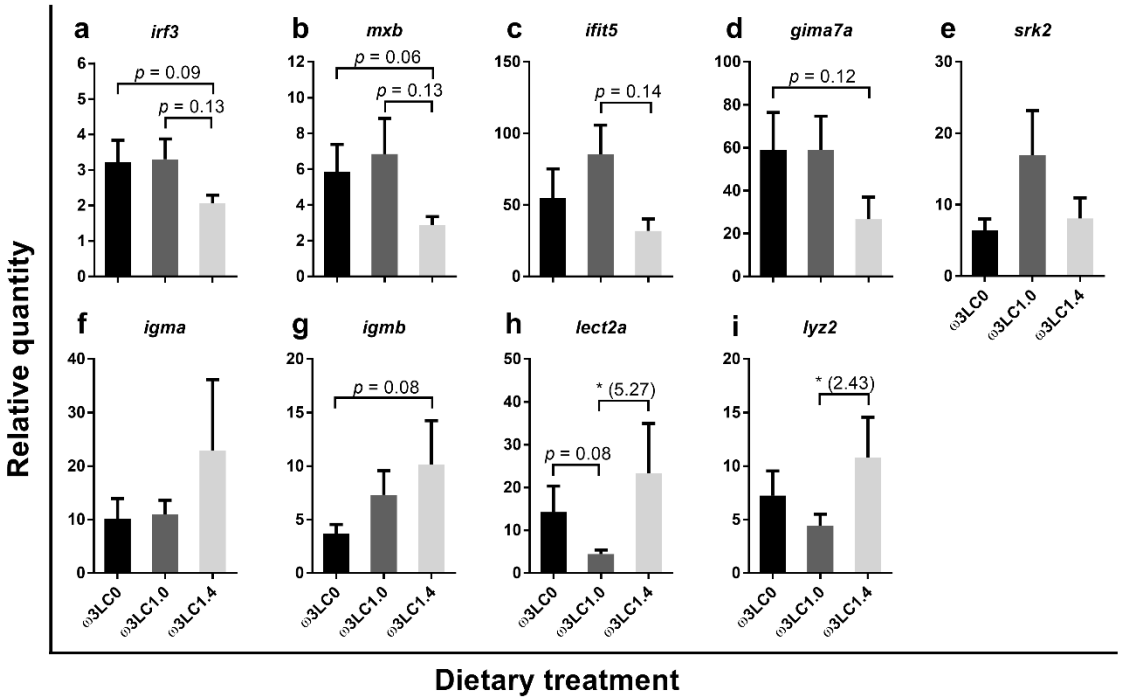

Figure 2.4. qPCR analysis of transcripts with putative roles in immune function (**a-i**) in the liver of salmon fed diets contain different levels of ω3 LC-PUFA. Columns and error bars represent mean relative quantity (RQ) values and SE, respectively. Significant difference by dietary treatment is indicated with asterisks (Student's *t*-test: *, $p < 0.05$). Fold-change is shown in brackets next to the asterisks.

with ω3LC1.4 (**Figure 2.3c**). There were no significant differences in the transcript expression levels of *gpx4a*, *rdh3a* and *gfer* among dietary treatments; furthermore, the qPCR results did not agree with the microarray results for *rdh3a* and *gfer* in direction of change (**Figure 2.3a, d and e**).

Expression levels of three well-known antiviral transcripts (*irf3*, *mxb* and *ifit5*), as well as *gima7a*, all trended lower (*p*-values ranging from 0.06 to 0.14) in fish fed ω3LC1.4 compared with fish fed ω3LC1.0 and/or ω3LC0 diets (**Figure 2.4a-d**). There were no significant differences in *srk2* and *igma* transcript expression levels among dietary groups (**Figure 2.4e and f**); however, *igmb* levels trended higher ($p = 0.08$) in the liver of salmon fed ω3LC1.4 diet compared with ω3LC0 (**Figure 2.4g**). Fish fed ω3LC1.4 diet also significantly up-regulated *lect2a* and *lyz2* transcript expression compared with ω3LC1.0 diet (**Figure 2.4h and i**).

2.4.4 Correlations between transcript expression levels and liver fatty acids

In hierarchical clustering analyses, transcripts involved in the interferon pathway (e.g. *mxb*, *irf3*, and *ifit5*) grouped with most of the lipid metabolism-related transcripts (e.g. *srebp1*, *fadsd6a*, and *fasb*) in Cluster I (**Figure 2.5**). Cluster II consisted of *igmb* and *mgst1*; while the antibacterial transcripts (*lyz2* and *lect2a*) were segregated in Cluster III. Interestingly, *elovl2* and *pdk2a* were grouped together in Cluster IV, separate from other lipid metabolism transcripts. Liver FA levels and ratios were segregated into three major groups by clustering analysis (**Figure 2.5**). All of the ω6 fatty acids including ARA (20:4ω6) except 20:2ω6, as well as MUFA, were grouped together (Cluster I), while most

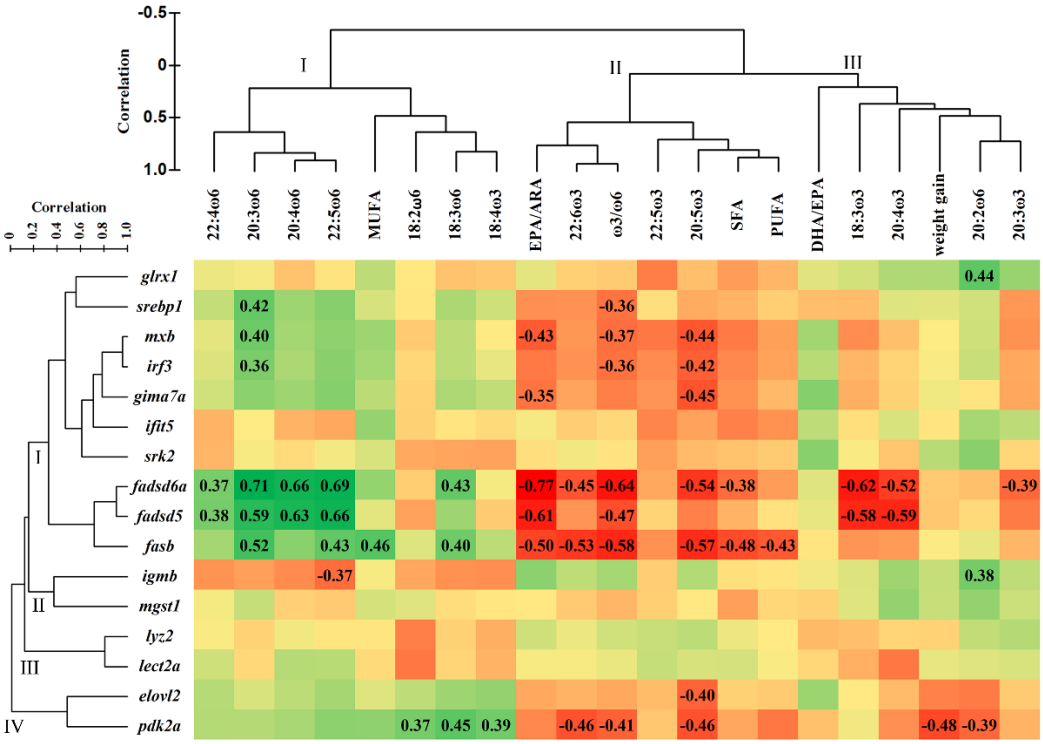

Figure 2.5. Matrix representing Pearson's correlation coefficients between RQs (log_2-transformed) of the qPCR-analyzed transcripts (rows) and the different lipid composition parameters (columns) in the liver of salmon fed the experimental diets. Transcriptomic and phenotypic data were arranged based on hierarchical clustering analyses performed using Pearson correlation resemblance matrices (PRIMER, Version 6.1.15, Ivybridge, UK). Pearson's correlation coefficients with significant regressions ($p < 0.05$) are shown. EPA: eicosapentaenoic acid (20:5ω3); ARA: arachidonic acid (20:4ω6); SFA: saturated fatty acids; PUFA: polyunsaturated fatty acid; DHA: docosahexaenoic acid (22:6ω3); MUFA: monounsaturated fatty acids.

of the ω3 fatty acids were grouped in Clusters II and III. Cluster II comprised DHA (22:6ω3), EPA (20:5ω3), 22:5ω3, the sum of SFA, and the sum of PUFA, as well as two important fatty acids ratios (EPA/ARA and ω3/ω6). DHA/EPA, weight gain, and 20:2ω6, as well as ω3 LC-PUFA precursors (18:3ω3, 20:3ω3, and 20:4ω3), were grouped in Cluster III.

Fatty acid synthesis-related transcript expression levels (namely *fadsd6a*, *fadsd5*, and/or *fasb*) exhibited major significant correlations with different fatty acid parameters according to the linear regression analysis (**Figure 2.5**). Among these transcripts, there were a total of 13 significantly positive correlations found with five ω6 fatty acids (22:4ω6, 20:3ω6, ARA, 22:5ω6, 18:2ω6) and the sum of MUFA, and a total of 18 negative correlations found with five ω3 fatty acids (DHA, EPA, 18:3ω3, 20:4ω3, 20:3ω3), the sums of SFA and PUFA, and fatty acid ratios (EPA/ARA and ω3/ω6). Levels of *srebp1*, *mxb*, and *irf3* were positively and negatively correlated with 20:3ω6 and ω3/ω6, respectively. In addition, levels of *mxb*, *irf3*, and *gima7a* were negatively correlated with EPA; while *mxb* and *gima7a* also showed negative correlations with EPA/ARA. Levels of *glrx1* showed a positive correlation with 20:2ω6. Levels of *pdk2a* showed positive correlations with 18:2ω6, 18:3ω6, and 18:4ω3, and negative correlations with DHA, EPA, 20:2ω6, ω3/ω6, and weight gain. Surprisingly, levels of *elovl2* were only negatively correlated with EPA. No significant correlation was found between levels of *ifit5*, *srk2*, *mgst1* and of two antibacterial transcripts (*lyz2* and *lect2a*) with hepatic lipid composition parameters.

2.4.5 Treatment comparisons by multivariate statistical analyses

PCoA was able to segregate the three dietary groups, and confirmed the associations between the transcriptomic (i.e. transcription of qPCR-analyzed genes) and phenotypic (i.e. liver fatty acid composition) parameters (**Figure 2.6a**). The ω6 fatty acid family (e.g. 20:3ω6, 22:5ω6, ARA) and ω3 fatty acid family (e.g. EPA and DHA), as well as ratios of EPA/ARA and ω3/ω6, had the greatest influence on PCO1. PCO1 accounted for 36.8% of the variation among samples (**Figure 2.6a**). PCO2 explained 17.1% of the variability, and was most strongly influenced by 22:5ω3, *srk2*, *ifit5*, *glrx1*, and *mgst1*. PERMANOVA was conducted in order to quantitatively compare differences among samples from fish fed different levels of DHA+EPA in fatty acid composition and transcript expression. The results showed that all pair-wise comparisons between diets were highly significant (**Figure 2.6b**). SIMPER was further conducted to explore the major drivers that differentiated dietary treatments. The comparison of the liver fatty acid profile and transcript expression between fish fed ω3LC1.4 and ω3LC0 diets was the most dissimilar (average dissimilarity = 27.99%), with 8 fatty acids and/or ratios (e.g. 18:3ω6, 22:5ω6, EPA/ARA) and 4 lipid metabolism-related transcripts (e.g. *fadsd5*, *fasb*, *srebp1*) as the top 50% contributing variables to this dissimilarity (**Figure 2.6b**). The comparison of the liver fatty acid profile and transcript levels between fish fed ω3LC1.0 and ω3LC0 diets was less dissimilar (average dissimilarity = 24.87%), with 6 fatty acids (e.g. 18:3ω6, 22:5ω6, ARA) and 7 transcripts (e.g. *fadsd5*, *elovl2*, *mxb*) as the top 50% contributing variables to this dissimilarity. The comparison of the liver fatty acid profile and transcript

a

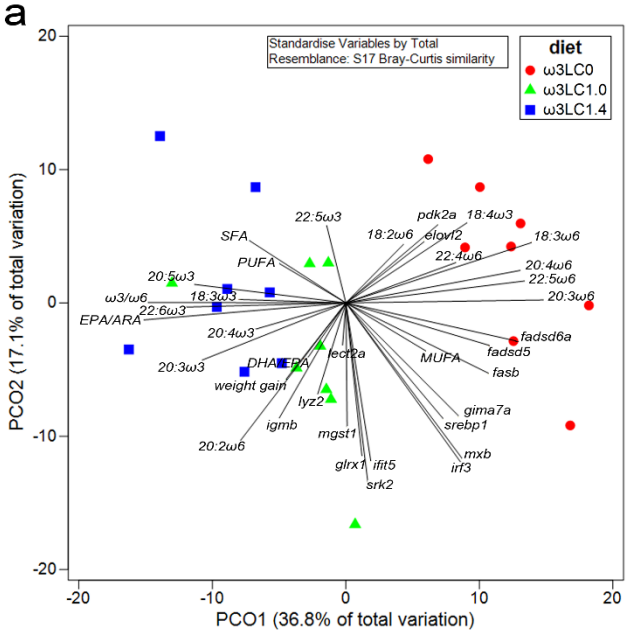

b

	ω3LC1.0 vs ω3LC0	ω3LC1.4 vs ω3LC0	ω3LC1.4 vs ω3LC1.0
p (perm)	0.0002	0.0003	0.0045
Average dissimilartity (%)	24.87	27.99	20.23
Contributing variables (top 50%)	18:3ω6	18:3ω6	*mgst1*
	22:5ω6	22:5ω6	*mxb*
	20:3ω3	20:3ω3	*igmb*
	fadsd5	*fadsd5*	*irf3*
	22:4ω6	EPA/ARA	20:3ω3
	elovl2	*fasb*	*lect2a*
	fadsd6a	20:3ω6	*srk2*
	igmb	*fadsd6a*	*lyz2*
	20:4ω6	22:4ω6	*srebp1*
	mxb	ω3/ω6	*fadsd5*
	irf3	20:4ω6	*elovl2*
	mgst1	*srebp1*	
	18:4ω3		

Figure 2.6. (**a**) Principal coordinate analysis (PCoA), (**b**) permutational multivariate ANOVA (PERMANOVA) and similarity of percentages analysis (SIMPER), of analyzed transcripts (log_2 RQ values) and the different lipid composition parameters in the liver of salmon fed the experimental diets. *p* (perm) is the statistical significance value obtained from PERMANOVA. The pair-wise comparisons were conducted with 9999 permutations. Average dissimilarity and contributing variables (top 50%) were obtained through SIMPER.

levels between fish fed ω3LC1.4 and ω3LC1.0 diets was the least dissimilar (average dissimilarity = 20.23%), with only 1 fatty acid (20:3ω3) and 10 transcripts (e.g. *mgst1*, *mxb*, *lect2a*, and *srebp1*) as the top 50% contributing variables to this dissimilarity.

2.5 Discussion

2.5.1 Effects of dietary ω3 LC-PUFA on the growth performance of Atlantic salmon

The goal of the current study was to evaluate the influence of graded levels of dietary DHA and EPA (0, 1.0 and 1.4% of the diet, as formulated; 0.75, 3.57 and 4.74% of total fatty acids, as fed), in the presence of high levels of LA, on Atlantic salmon performance and hepatic transcript expression. High levels of LA in diets primarily resulted from the inclusion of rapeseed oil as the main oil source. The relatively low DHA+EPA (< 2%) and high lipid content (> 27%) in the current experimental diets may be regarded as practical for modern salmon farming (Rosenlund et al., 2016; Eslamloo et al., 2017). In contrast to the growth data presented by Foroutani et al. (2018) which involved 7 dietary treatments, data reanalysis including only the 3 diets relevant to the present study showed that Atlantic salmon post-smolts performed better on ω3LC1.0 and ω3LC1.4 diets compared with fish fed ω3LC0 diet based on the growth parameter assessment. Similarly, Rosenlund et al. (2016) used VO mix (rapeseed, palm, and linseed oils) to substitute FO in order to manipulate dietary levels of ω3 LC-PUFA and showed that Atlantic salmon have a specific requirement for DHA+EPA at 2.7 to 4.4% of total fatty acids (approximately 1.0 to 1.5% of diet) based on long-term growth performance data. Another study on salmon smolts also showed better growth when fed with 1.0% DHA supplemented with 1.0% EPA

(as fed) compared to fish fed only DHA supplemented diets (Glencross et al., 2014). Collectively, these results support the hypothesis that approximately 1.0% of dietary ω3 LC-PUFA (mainly EPA and DHA) is needed for optimal growth of Atlantic salmon. However, the impact of low level of dietary ω3 LC-PUFA in the presence of high level of LA on salmon metabolism, physiology and immune function is less well understood.

2.5.2 Effects of dietary ω3 LC-PUFA on nutrient metabolism of Atlantic salmon

In the current microarray experiment, two genes directly involved in glycolysis, *gck* (not significant in the qPCR analysis, but agreeing in direction of change) and *glyceraldehyde-3-phosphate dehydrogenase*, showed decreased expression in fish fed ω3LC1.0 and ω3LC1.4 diets compared with fish fed ω3LC0 diet, suggesting possible decreased hepatic glycolysis in Atlantic salmon fed ω3LC1.0 and ω3LC1.4 diets. Gck phosphorylates glucose to produce glucose-6-phosphate, the first step in most glucose metabolism pathways, in the liver of fish and other vertebrates (Wilson, 1994). Similarly, in mammals, higher contents of PUFAs including DHA and EPA are known to suppress hepatic glycolysis through the inhibition of genes involved in glucose utilization (Dentin et al., 2005).

Gck activity supplies the oxidative branch of the pentose phosphate pathway (PPP) with glucose-6-phosphate (Wamelink et al., 2008). *G6pda* encodes an enzyme that mediates this pathway and was microarray-detected in the current study as down-regulated by ω3LC1.0 diet. qPCR analyses of *g6pda* support the trend (although not significant) observed in the microarray results, which showed down-regulation in fish fed ω3LC1.0 and ω3LC1.4 diets compared with fish fed ω3LC0 diet. G6pd reduces $NADP^+$ to NADPH

while oxidizing glucose-6-phosphate (Wamelink et al., 2008). The production of NADPH is needed for fatty acid biosynthesis and the maintenance of the redox state of hepatocytes in fish and other vertebrates (Hemre et al., 2002). G6pd activity was previously found to be inhibited by both DHA and EPA in a rainbow trout hepatocyte study (Alvarez et al., 2000). Therefore, the down-regulation trends of genes involved in the PPP in fish fed ω3LC1.0 diet may reflect the lower demand of NADPH for fatty acid biosynthesis in these fish.

Pdk2a encodes an enzyme that directly inhibits pyruvate dehydrogenase activity, and thereby inhibits the formation of acetyl-coA from pyruvate (i.e. end product of glycolysis). The current qPCR analysis confirmed significant up-regulation of *pdk2a* transcript in fish fed ω3LC0 diet compared with the ω3LC1.0 group. As previously discussed, fish fed the ω3LC0 diet might have increased glycolysis, which provides substrates and energy for fatty acid synthesis. The up-regulation of *pdk2a* in fish fed ω3LC0 diet may represent a negative feedback mechanism in restricting the conversion of glucose into fatty acids. Hemre et al. (2002) suggested that carbohydrate in fish diets is needed to stimulate lipid biosynthesis not so much through the delivery of carbon backbones (i.e. acetyl-coA), but instead via increased availability of reducing equivalents (i.e. NADPH). Nevertheless, the present study also showed that the expression level of *pdk2a* was negatively correlated with several lipid composition parameters in the liver including EPA, DHA, and ω3/ω6 ratio, suggesting roles in fatty acid metabolism. In sum, further research is needed on the molecular mechanisms controlling conversions of glucose

for fatty acid/lipid synthesis in the liver of Atlantic salmon, especially under a limited supply of dietary ω3 LC-PUFA.

In the current study, the expression levels of transcripts involved in the LC-PUFA biosynthesis pathway (i.e. *fadsd5* and *fadsd6a*) and in the formation of LC-FA from acetyl-CoA and malonyl-CoA (i.e. *fasb*) were down-regulated in salmon fed ω3LC1.0 and/or ω3LC1.4 diets. In a previous study in Atlantic salmon, the macrophage-like SHK-1 cell line showed decreased transcript expression of genes involved in fatty acid biosynthesis (*fas*, *fadsd5* and *fadsd6a*) in response to EPA/DHA supplementation, and these genes were thought to be targets of *srebp1* (Minghetti et al., 2011). The transcript expression of *srebp1* in the present qPCR study was reduced (although not significantly) in fish fed ω3LC1.4 diet, which was also observed previously (Betancor et al., 2014; Hixson et al., 2017). Collectively, these results confirm that *srebp1* plays a key role in regulating fatty acid synthesis including LC-PUFA biosynthesis. The current linear regression analyses showed that fatty acid biosynthesis-related genes except *elovl2* were positively correlated with ω6 fatty acids, and negatively correlated with ω3 fatty acids and two important fatty acid ratios (i.e. EPA/ARA and ω3/ω6). These findings further confirmed that the ω3 LC-PUFA synthesis pathway can be activated when dietary EPA and DHA levels are low. In addition, as suggested by Katan et al. (2019), the positive correlation identified between fatty acid biosynthesis-related transcripts and some of the ω6 fatty acids found in the current study may indicate an activated ω6 LC-PUFA biosynthesis pathway in fish fed ω3LC0 diet.

The elongase-encoding transcript *elovl2* was less affected (i.e. no significant changes) by dietary DHA and EPA compared with desaturase-encoding transcripts;

however, the *elovl2* transcript level did correlate negatively with the liver EPA level. The transcript expression response of *elovl2* to dietary ω3 LC-PUFA level in Atlantic salmon, usually resulting from replacing FO with different VOs, varies greatly across different studies and experimental settings (Morais et al., 2009; Xue et al., 2015; Hixson et al., 2017). The regulatory mechanism for elongase-encoding genes including *elovl2* in Atlantic salmon warrants further investigation.

According to the microarray analyses, *csad* (both a and b), encoding key enzymes in taurine synthesis, were up-regulated (not significant in the qPCR analyses, but agreeing in direction of change) in fish fed ω3LC1.0 compared with fish fed ω3LC0 diet. Taurine is a sulfonic acid/free amino acid found in high concentrations in the tissues of animals including mammals, birds, fish and aquatic invertebrates (Salze and Davis, 2015). In mammals, taurine is involved in a variety of functions including bile salt conjugation, osmoregulation, antioxidation, immunomodulation, and neuroprotection (Salze and Davis, 2015). A previous study examined the effect of taurine supplementation on antioxidant status of totoaba (*Totoaba macdonaldi*), and showed a significant reduction of liver lipid peroxidation (Bañuelos-Vargas et al., 2014). It is important to note that the taurine levels (although not measured) were expected to be the same across the three experimental diets since the feed ingredients (e.g. FM and poultry by-product meals) that contain taurine were not changed across diet formulations. I hypothesize that the increased expression (although not significant) of *csad* in fish fed ω3LC1.0 diet may be a response to increased lipid peroxidation as suggested by the expression of two redox homeostasis relevant genes (*mgst1* and *glrx1*; see discussion below).

2.5.3 Effects of dietary ω3 LC-PUFA on redox homeostasis of Atlantic salmon

The qPCR analysis of *mgst1* and *glrx1* transcript expression confirmed their up-regulation by the ω3LC1.0 diet compared with the ω3LC0 diet. Mgst1, a membrane bound glutathione transferase, has been shown to be able to neutralize lipid peroxides and conjugate other reactive intermediates to glutathione (reviewed by Schaffert, 2011). Rabbits fed high DHA diets showed increased expression of *MGST1*, coinciding with enhanced lipid peroxidation in the liver (Gladine et al., 2012). Similarly, Betancor et al. (2015) found that zebrafish fed DHA-rich diet had considerably increased lipid peroxidation. Glrx1, a small thiol transferase, protects against oxidative stress by reducing disulfides in targeted proteins. It relies on the reducing power of glutathione to maintain and regulate the cellular redox state (reviewed by Lillig et al., 2008). The transcript expression of *glrx1* was increased in manila clam (*Venerupis philippinarum*) after chemical stress and bacterial challenge (Mu et al., 2012). It is worth noting that only one significantly positive correlation (i.e. 20:2ω6 with *glrx1*) was found between liver fatty acids and the transcript levels of these two redox relevant genes. Collectively, Atlantic salmon fed 1.0% of DHA+EPA diet may exhibit higher oxidative stress; however, such an effect was diminished in fish fed ω3LC1.4 diet. The mechanism for the decrease in oxidative stress in the liver of Atlantic salmon fed ω3LC1.4 diet remains unknown.

2.5.4 Effects of dietary ω3 LC-PUFA on the hepatic immune-relevant gene expression of Atlantic salmon

Fatty acids, particularly LC-PUFA, play an important role in innate immune responses (Calder, 2013; Eslamloo et al., 2017). According to the current qPCR results, the

mRNA levels of three well-known antiviral genes (*irf3*, *mxb* and *ifit5*) as well as *gima7a* showed consistent down-regulation trends (i.e. not significant) in fish fed ω3LC1.4 compared with fish fed both ω3LC0 and ω3LC1.0 diets. This trend could also be interpreted as up-regulated expression in fish fed the lower DHA+EPA diets (i.e. ω3LC0 and ω3LC1.0) relative to those fish fed the higher DHA+EPA diet. The constitutive transcript expression of *mx* in gilthead sea bream liver was elevated in fish fed a VO diet compared with FO control group (Montero et al., 2008). Furthermore, in a separate liver transcriptome study, Caballero-Solares et al. (2018) reported that a high vegetable diet (VEG; involving both fish meal and FO replacements) up-regulated the basal expression of antiviral transcripts (i.e., *mxa*, *mxb*, and *ifit5*). Alongside this study, Eslamloo et al. (2017) utilized an *ex vivo* model to study the effects of ω3LC1.0 and ω3LC1.4 diets on transcriptome profile of antiviral immune response in Atlantic salmon macrophages; however, the constitutive expression and viral mimic (i.e. polyriboinosinic polyribocytidylic acid) induction of *mxb* did not change in macrophages of Atlantic salmon fed different levels of dietary DHA+EPA (i.e. 1.0% *vs* 1.4%). Therefore, the *mxb* transcript responses seen in present and previous studies suggest that the influence of dietary EPA+DHA on antiviral gene expression of Atlantic salmon may be cell- and/or tissue-dependent.

The current linear regression analyses showed that the transcript expression of antiviral genes and/or *gima7a* correlated negatively with hepatic ω3/ω6 and EPA/ARA ratios, and EPA, and positively with 20:3ω6. This suggests that the expression changes in antiviral genes may be a function of ω3/ω6 and EPA/ARA ratios in the liver tissue rather

than being directly caused by different levels of dietary DHA and EPA. It is important to note that the dietary ARA content in ω3LC0 diet was actually lower compared with the other two feeds (Table 2.1); however, ARA level in the liver of fish fed this diet was significantly higher than fish fed other two diets (Foroutani, 2017). This is likely due to the higher expression of genes related to LC-PUFA biosynthesis in the fish fed ω3LC0 diet since these genes work on both ω3 and ω6 LC-PUFA synthesis pathways. Higher amounts of liver ARA in fish fed ω3LC0 diet may enhance the synthesis of ARA-derived eicosanoids, which promote stronger inflammation than those synthesized from EPA (Calder, 2013). In the present microarray experiment, no suggestion of changes in hepatic eicosanoid metabolism was found. However, Eslamloo et al. (2017) reported an increased transcript level of *fabp4* (*fatty acid-binding protein, adipocyte*) in macrophages of Atlantic salmon fed ω3LC1.0 compared to ω3LC1.4, and this gene plays putative roles in positive regulation of inflammatory cytokine production. Further experiments are needed to elucidate the effect of different dietary DHA+EPA levels, and ω3/ω6 and EPA/ARA ratios, on interferon pathway activity, eicosanoid metabolism and ultimately immunity against viral infection in Atlantic salmon.

Immunoglobulins (Igs), including IgM, are mediators of both innate and adaptive immunity in fish and other vertebrates (Ye et al., 2013; Makesh et al., 2015). In the present microarray experiment, the transcript levels of immunoglobulin genes including *igm* (represented by 7 probes) were higher (although not significant in the qPCR analyses) in fish fed ω3LC1.4 diet compared with ω3LC0 group. Similarly, the transcript level of *igm* was higher in the pyloric caeca of Atlantic salmon fry fed with FO diet compared with VO

diet fed fish based on RNA-seq analysis (Jalili et al., 2019). Moldal et al. (2014) also reported that Atlantic salmon fed a high soybean oil diet had significantly lower expression of both *igm* and *igt* in the distal intestine compared with FO control diet, agreeing with the higher transcript level of *igm* in ω3LC1.4 group from the present work. This suggests that higher level of DHA+EPA in the diet of Atlantic salmon may be associated with higher abundance of genes involved in adaptive immune responses.

In contrast to antiviral transcript expression (i.e. *irf3*, *mxb* and *ifit5*), several key genes of the innate immune systems for defense against bacterial infection including *lect2a*, *lyz2*, *pleiotrophic factor-alpha-2 precursor* and *CD59 glycoprotein*, were shown by microarray and/or qPCR analyses to be more highly expressed in the liver of Atlantic salmon fed ω3LC1.4 diet compared with ω3LC1.0 group. Lect2 acts as a chemotactic factor to activate neutrophils, and its transcript expression was shown to be induced in various tissues in *Vibrio alginolyticus*-infected croceine croaker (*Pseudosciaena crocea*) (Li et al., 2008), and in *Vibrio harveyi*-infected Asian seabass (*Lates calcarifer*) (Fu et al., 2014). The transcript expression of *lect2* was also found to be influenced by diet in previous FO replacement studies in Atlantic salmon, and it was significantly up-regulated in the liver of salmon fed FO/high ω3 LC-PUFA diets (Morais et al., 2012; Xue et al., 2015). *Lyz2* encodes an antimicrobial enzyme that plays a key role in the innate immune system (Gao et al., 2012). Lysozyme enzymatic activity in serum was significantly increased in large yellow croaker fed high ω3 LC-PUFA diets (Zuo et al., 2012). Similarly, in gilthead sea bream, the serum lysozyme activity showed a trend toward higher levels in fish fed FO diets compared with soybean and linseed oil replacement diets (Montero et al., 2010).

However, other studies on the inclusion of dietary VO in fish including Atlantic salmon showed no impact on serum lysozyme activity (Bell et al., 2006; Betancor et al., 2016). Cheng et al. (2015) reported that transgenic zebrafish (with enhanced liver-specific expression of *fadsd6* and *elovl5a*) had significantly higher tissue DHA and EPA, and higher survival after challenging with *Vibrio vulnificus*, compared with the wild type controls. Collectively, my data and the results of others suggest that a higher dietary level of DHA+EPA (1.4%) in Atlantic salmon may be associated with stronger expression of antibacterial genes.

Finally, it is worth noting that in a recent study Atlantic salmon fed 0.2 and 1.0% of DHA+EPA diets in the presence of high amounts of LA in a commercial sea cage setting showed a significant decrease in survival after delousing at high water temperature compared with fish fed 1.7% DHA+EPA diet (Bou et al., 2017b). This study suggested that 1.0% of dietary DHA+EPA in Atlantic salmon diet may be too low to maintain fish health or robustness under stressful conditions. Together with the current microarray and qPCR results related to immune-relevant genes, it is reasonable to hypothesize that Atlantic salmon fed 1.4% DHA+EPA of diet (i.e., ω3LC1.4) may have increased resistance to bacterial infection compared with fish fed 0% and 1.0% of DHA+EPA in diets in the presence of high dietary LA.

2.5.5 Overall differences in fatty acid composition and transcript expression among fish fed different DHA+EPA levels

Multivariate analyses including PCoA, PERMANOVA and SIMPER were conducted to explore overall differences in fatty acid composition and transcript expression

among samples from fish fed different levels of DHA+EPA. The loadings in the PCoA plot related to diet-driven changes. The ω6 fatty acid family and fatty acid biosynthesis-related transcripts were associated with the ω3LC0 diet (right side of the plot), while ω3 LC-PUFA loadings and fatty acid ratios appeared on the left side of the plot with the ω3LC1.4 diet. It is not surprising to see the fatty acid biosynthesis-related transcripts were more correlated with the ω6 fatty acid family since these diets contain higher amounts of short chain ω6 fatty acids (e.g. LA) compared with short chain ω3 fatty acids (e.g. ALA). Overall, the PCoA validated the correlations between the transcriptomic and phenotypic parameters observed in the linear regression and hierarchical clustering analyses.

As expected, there were marked differences in liver fatty acid composition and transcript expression of the qPCR-analyzed genes across dietary treatment as shown by PERMANOVA. The ω6 fatty acid family and fatty acid biosynthesis-related transcripts were the major drivers in the dissimilarity observed between fish fed ω3LC1.0 and ω3LC1.4 diets and those fed ω3LC0 diet. Interestingly, the majority of the top 50% variables contributing to the dissimilarity in the ω3LC1.4 and ω3LC1.0 diet comparison were the qPCR-analyzed genes including those with redox-relevant (*mgst1*), antiviral (*mxb* and *irf3*), antibacterial (*lect2a* and *lyz2*), and fatty acid biosynthesis-related (*srebp1*, *fadsd5*, and *elovl2*) functional annotations. This further indicates that fish fed ω3LC1.4 and ω3LC1.0 diets had similar hepatic fatty acid profiles, but contrasting transcript expression profiles. Since the increase in dietary DHA+EPA (from 1.0 to 1.4%) significantly modulated hepatic transcript expression of genes involved in several important pathways,

1.0% of dietary ω3 LC-PUFA (i.e. DHA+EPA) may not be the optimal level for Atlantic salmon under current diet formulations, especially with high inclusion of LA.

2.6 Conclusions

The present study demonstrates the use of functional genomic tools and techniques to identify and validate hepatic molecular biomarkers of Atlantic salmon response to different levels of dietary DHA+EPA in the presence of high LA. Overall, my results indicate that the experimental diets modulated the transcript expression of genes involved in carbohydrate metabolism, fatty acid synthesis, redox homeostasis, and immunity. Fish fed the 0% DHA+EPA diet (i.e. ω3LC0) seemed to be able to increase fatty acid synthesis capacity including LC-PUFA synthesis. Based on growth performance alone, 1.0% of ω3 LC-PUFA (as formulated) seems to be a minimum requirement for Atlantic salmon. However, the transcript expression data showed modulation of molecular biomarkers involved in redox homeostasis (*mgst1* and *glrx1*) and innate immune responses (*irf3*, *mxb*, *lect2a*, and *lyz2*) between ω3LC1.0 and ω3LC1.4 dietary treatments. In addition, there were significant correlations between some of these immune biomarkers (e.g. *mxb* and *irf3*) and liver fatty acid composition (e.g. EPA/ARA ratio and EPA). Therefore, the hepatic transcript expression changes may be a function of ω3/ω6 and EPA/ARA ratios in the tissue rather than being directly caused by different levels of dietary DHA and EPA. Finally, it is important to stress that future experiments such as environmental/pathogen challenges (e.g. virus *vs* bacteria) are needed to further assess the potential effects of dietary DHA and EPA on fish physiology and health. Also, the interaction between levels of DHA+EPA, shorter

chain precursors (ALA and LA) and fatty acid ratios (e.g. EPA/ARA and ω3/ω6) in the context of VO inclusion on Atlantic salmon health warrants further investigation.

2.7 Supplemental materials

The Supplemental Table and Figure for this chapter can be found in the supplemental materials of Xue et al. (2020) [available at: (https://doi.org/10.1007/s10126-020-09950-x)]. These files (as listed below) have also been supplied in a zipped folder that accompanies this thesis.

Supplemental Table S2.1. Complete list of microarray identified ω3 LC-PUFA responsive genes that were differentially expressed in the liver of Atlantic salmon (Rank Products analyses; PFP < 10%).

Supplemental Figure S2.1. Scatterplot of gene expression fold-change values between diets calculated from the microarray $\log_2$ ratios and qPCR relative quantity (RQ) ratios. Each dot represents the fold-change of dietary comparison (ω3LC1.0 *vs* ω3LC0, ω3LC1.4*vs* ω3LC0, or ω3LC1.4 *vs* ω3LC1.0) for a given gene.

2.8 References

Alvarez, M., Diez, A., Lopez-Bote, C., Gallego, M., Bautista, J., 2000. Short-term modulation of lipogenesis by macronutrients in rainbow trout (*Oncorhynchus mykiss*) hepatocytes. Br. J. Nutr. 84, 619-628.

Anderson, M.J., 2014. Permutational multivariate analysis of variance (PERMANOVA). In Wiley Statsref: Statistics Reference Online (eds N. Balakrishnan, T. Colton, B. Everitt, W. Piegorsch, F. Ruggeri and J.L. Teugels).

Bañuelos-Vargas, I., López, L.M., Pérez-Jiménez, A., Peres, H., 2014. Effect of fishmeal replacement by soy protein concentrate with taurine supplementation on hepatic

intermediary metabolism and antioxidant status of totoaba juveniles (*Totoaba macdonaldi*). Comp. Biochem. Physiol. B: Biochem. Mol. Biol. 170, 18-25.

Beheshti Foroutani, M.B., 2017. Minimizing marine resource utilization in diets of farmed Atlantic salmon (*Salmo salar*): effects on growth performance and muscle, liver, and head kidney chemical composition. M.Sc. Thesis. Memorial University of Newfoundland, St. John's, NL, Canada.

Beheshti Foroutani, M.B., Parrish, C.C., Wells, J., Taylor, R.G., Rise, M.L., Shahidi, F., 2018. Minimizing marine ingredients in diets of farmed Atlantic salmon (*Salmo salar*): Effects on growth performance and muscle lipid and fatty acid composition. PLoS ONE 13, e0198538.

Bell, J.G., McEvoy, J., Tocher, D.R., McGhee, F., Campbell, P.J., Sargent, J.R., 2001. Replacement of fish oil with rapeseed oil in diets of Atlantic salmon (*Salmo salar*) affects tissue lipid compositions and hepatocyte fatty acid metabolism. J. Nutr. 131, 1535-1543.

Bell, J.G., Pratoomyot, J., Strachan, F., Henderson, R.J., Fontanillas, R., Hebard, A., Guy, D.R., Hunter, D., Tocher, D.R., 2010. Growth, flesh adiposity and fatty acid composition of Atlantic salmon (*Salmo salar*) families with contrasting flesh adiposity: Effects of replacement of dietary fish oil with vegetable oils. Aquaculture 306, 225-232.

Bell, J.G., Strachan, F., Good, J.E., Tocher, D.R., 2006. Effect of dietary echium oil on growth, fatty acid composition and metabolism, gill prostaglandin production and macrophage activity in Atlantic cod (*Gadus morhua* L.). Aquacult. Res. 37, 606-617.

Betancor, M., Almaida-Pagán, P., Hernandez, A., Tocher, D.R., 2015. Effects of dietary fatty acids on mitochondrial phospholipid compositions, oxidative status and mitochondrial gene expression of zebrafish at different ages. Fish Physiol. Biochem. 41, 1187-1204.

Betancor, M.B., Howarth, F.J., Glencross, B.D., Tocher, D.R., 2014. Influence of dietary docosahexaenoic acid in combination with other long-chain polyunsaturated fatty acids on expression of biosynthesis genes and phospholipid fatty acid compositions in tissues of post-smolt Atlantic salmon (*Salmo salar*). Comp Biochem Physiol B Biochem Mol Biol 172-173, 74-89.

Betancor, M.B., Sprague, M., Sayanova, O., Usher, S., Metochis, C., Campbell, P.J., Napier, J.A., Tocher, D.R., 2016. Nutritional evaluation of an EPA-DHA oil from transgenic *Camelina sativa* in feeds for post-smolt Atlantic salmon (*Salmo salar* L.). PLoS ONE 11, e0159934.

Bo, T.H., Dysvik, B., Jonassen, I., 2004. LSimpute: accurate estimation of missing values in microarray data with least squares methods. Nucleic Acids Res. 32, e34.

Booman, M., Borza, T., Feng, C.Y., Hori, T.S., Higgins, B., Culf, A., Leger, D., Chute, I.C., Belkaid, A., Rise, M., Gamperl, A.K., Hubert, S., Kimball, J., Ouellette, R.J., Johnson, S.C., Bowman, S., Rise, M.L., 2011. Development and experimental validation of a 20K Atlantic cod (*Gadus morhua*) oligonucleotide microarray based on a collection of over 150,000 ESTs. Mar. Biotechnol. 13, 733-750.

Bou, M., Berge, G.M., Baeverfjord, G., Sigholt, T., Østbye, T.-K., Romarheim, O.H., Hatlen, B., Leeuwis, R., Venegas, C., Ruyter, B., 2017a. Requirements of n-3 very long-chain PUFA in Atlantic salmon (*Salmo salar* L): effects of different dietary levels of EPA and DHA on fish performance and tissue composition and integrity. Br. J. Nutr. 117, 30-47.

Bou, M., Berge, G.M., Baeverfjord, G., Sigholt, T., Østbye, T.-K., Ruyter, B., 2017b. Low levels of very-long-chain n-3 PUFA in Atlantic salmon (*Salmo salar*) diet reduce fish robustness under challenging conditions in sea cages. J Nutr Sci 6, E32.

Breitling, R., Armengaud, P., Amtmann, A., Herzyk, P., 2004. Rank products: a simple, yet powerful, new method to detect differentially regulated genes in replicated microarray experiments. FEBS Lett. 573, 83-92.

Brown, T.D., Hori, T.S., Xue, X., Ye, C.L., Anderson, D.M., Rise, M.L., 2016. Functional genomic analysis of the impact of camelina (*Camelina sativa*) meal on Atlantic salmon (*Salmo salar*) distal intestine gene expression and physiology. Mar. Biotechnol. 18, 418-435.

Caballero-Solares, A., Hall, J.R., Xue, X., Eslamloo, K., Taylor, R.G., Parrish, C.C., Rise, M.L., 2017. The dietary replacement of marine ingredients by terrestrial animal and plant alternatives modulates the antiviral immune response of Atlantic salmon (*Salmo salar*). Fish Shellfish Immunol. 64, 24-38.

Caballero-Solares, A., Xue, X., Parrish, C.C., Foroutani, M.B., Taylor, R.G., Rise, M.L., 2018. Changes in the liver transcriptome of farmed Atlantic salmon (*Salmo salar*) fed experimental diets based on terrestrial alternatives to fish meal and fish oil. BMC Genomics 19, 796.

Calder, P.C., 2013. n-3 fatty acids, inflammation and immunity: new mechanisms to explain old actions. Proc. Nutr. Soc. 72, 326-336.

Calder, P.C., 2015. Marine omega-3 fatty acids and inflammatory processes: effects, mechanisms and clinical relevance. Biochim. Biophys. Acta, Mol. Cell. Biol. Lipids 1851, 469-484.

Celton, M., Malpertuy, A., Lelandais, G., de Brevern, A.G., 2010. Comparative analysis of missing value imputation methods to improve clustering and interpretation of microarray experiments. BMC Genomics 11, 15.

Cheng, C.L., Huang, S.J., Wu, C.L., Gong, H.Y., Ken, C.F., Hu, S.Y., Wu, J.L., 2015. Transgenic expression of omega-3 PUFA synthesis genes improves zebrafish survival during *Vibrio vulnificus* infection. J. Biomed. Sci. 22, 103.

Clarke, K.R., 1993. Non-parametric multivariate analyses of changes in community structure. Austral. Ecol. 18, 117-143.

Conesa, A., Götz, S., García-Gómez, J.M., Terol, J., Talón, M., Robles, M., 2005. Blast2GO: a universal tool for annotation, visualization and analysis in functional genomics research. Bioinformatics 21, 3674-3676.

Dentin, R., Benhamed, F., Pégorier, J.-P., Foufelle, F., Viollet, B., Vaulont, S., Girard, J., Postic, C., 2005. Polyunsaturated fatty acids suppress glycolytic and lipogenic genes through the inhibition of ChREBP nuclear protein translocation. J Clin Invest 115, 2843-2854.

Eslamloo, K., Xue, X., Hall, J.R., Smith, N.C., Caballero-Solares, A., Parrish, C.C., Taylor, R.G., Rise, M.L., 2017. Transcriptome profiling of antiviral immune and dietary fatty acid dependent responses of Atlantic salmon macrophage-like cells. BMC Genomics 18, 706.

Foroutani, M.B., Parrish, C.C., Wells, J., Taylor, R.G., Rise, M.L., 2020. Minimizing marine ingredients in diets of farmed Atlantic salmon (*Salmo salar*): effects on liver and head kidney lipid class and fatty acid composition. Fish Physiol. Biochem. 46, 2331-2353.

Fu, G.H., Bai, Z.Y., Xia, J.H., Liu, X.J., Liu, F., Wan, Z.Y., Yue, G.H., 2014. Characterization of the LECT2 gene and its associations with resistance to the big belly disease in Asian seabass. Fish Shellfish Immunol. 37, 131-138.

Gao, F., Qu, L., Yu, S., Ye, X., Tian, Y., Zhang, L., Bai, J., Lu, M., 2012. Identification and expression analysis of three c-type lysozymes in *Oreochromis aureus*. Fish Shellfish Immunol. 32, 779-788.

Gladine, C., Roy, N.C., Rigaudiere, J.-P., Laillet, B., Da Silva, G., Joly, C., Pujos-Guillot, E., Morio, B., Feillet-Coudray, C., McNabb, W.C., 2012. Increasing intake of long-chain n-3 PUFA enhances lipoperoxidation and modulates hepatic gene expression in a dose-dependent manner. Br. J. Nutr. 107, 1254-1273.

Glencross, B.D., 2009. Exploring the nutritional demand for essential fatty acids by aquaculture species. Rev. Aquac. 1, 71-124.

Glencross, B.D., Tocher, D.R., Matthew, C., Bell, J.G., 2014. Interactions between dietary docosahexaenoic acid and other long-chain polyunsaturated fatty acids on performance and fatty acid retention in post-smolt Atlantic salmon (*Salmo salar*). Fish Physiol. Biochem. 40, 1213-1227.

Gower, J.C., 2014. Principal Coordinates Analysis. In Wiley Statsref: Statistics Reference Online (eds N. Balakrishnan, T. Colton, B. Everitt, W. Piegorsch, F. Ruggeri and J.L. Teugels).

Hemre, G.I., Mommsen, T.P., Krogdahl, A., 2002. Carbohydrates in fish nutrition: effects on growth, glucose metabolism and hepatic enzymes. Aquacult. Nutr. 8, 175-194.

Hixson, S.M., Parrish, C.C., Anderson, D.M., 2014. Full substitution of fish oil with camelina (*Camelina sativa*) oil, with partial substitution of fish meal with camelina meal, in diets for farmed Atlantic salmon (*Salmo salar*) and its effect on tissue lipids and sensory quality. Food Chem. 157, 51-61.

Hixson, S.M., Parrish, C.C., Xue, X., Wells, J.S., Collins, S.A., Anderson, D.M., Rise, M.L., 2017. Growth performance, tissue composition, and gene expression responses in Atlantic salmon (*Salmo salar*) fed varying levels of different lipid sources. Aquaculture 467, 76-88.

Hong, F., Breitling, R., McEntee, C.W., Wittner, B.S., Nemhauser, J.L., Chory, J., 2006. RankProd: a bioconductor package for detecting differentially expressed genes in meta-analysis. Bioinformatics 22, 2825-2827.

Hori, T.S., Gamperl, A.K., Booman, M., Nash, G.W., Rise, M.L., 2012. A moderate increase in ambient temperature modulates the Atlantic cod (*Gadus morhua*) spleen transcriptome response to intraperitoneal viral mimic injection. BMC Genomics 13, 431.

Jalili, M., Jin, Y., Bones, A.M., Olsen, Y., Vadstein, O., Østensen, M.-A., Buonocore, F., Gerdol, M., Pallavicini, A., Scapigliati, G., 2019. Dietary fatty acid source has little effect on the development of the immune system in the pyloric caeca of Atlantic salmon fry. Sci Rep. 9, 27.

Jantzen, S.G., Sanderson, D.S., von Schalburg, K.R., Yasuike, M., Marass, F., Koop, B.F., 2011. A 44K microarray dataset of the changing transcriptome in developing Atlantic salmon (*Salmo salar* L.). BMC Res. Notes 4, 88.

Jeffery, I.B., Higgins, D.G., Culhane, A.C., 2006. Comparison and evaluation of methods for generating differentially expressed gene lists from microarray data. BMC Bioinf. 7, 359.

Katan, T., Caballero-Solares, A., Taylor, R.G., Rise, M.L., Parrish, C.C., 2019. Effect of plant-based diets with varying ratios of ω6 to ω3 fatty acids on growth performance, tissue composition, fatty acid biosynthesis and lipid-related gene expression in Atlantic salmon (*Salmo salar*). Comp. Biochem. Physiol. D: Genomics Proteomics 30, 290-304.

Leaver, M.J., Bautista, J.M., Björnsson, B.T., Jönsson, E., Krey, G., Tocher, D.R., Torstensen, B.E., 2008. Towards fish lipid nutrigenomics: current state and prospects for fin-fish aquaculture. Rev. Fish. Sci. 16, 73-94.

Li, M.Y., Chen, J., Shi, Y.H., 2008. Molecular cloning of leucocyte cell-derived chemotaxin-2 gene in croceine croaker (*Pseudosciaena crocea*). Fish Shellfish Immunol. 24, 252-256.

Lillig, C.H., Berndt, C., Holmgren, A., 2008. Glutaredoxin systems. Biochim. Biophys. Acta, Gen. Subj. 1780, 1304-1317.

Makesh, M., Sudheesh, P.S., Cain, K.D., 2015. Systemic and mucosal immune response of rainbow trout to immunization with an attenuated *Flavobacterium psychrophilum* vaccine strain by different routes. Fish Shellfish Immunol. 44, 156-163.

Minghetti, M., Leaver, M.J., Tocher, D.R., 2011. Transcriptional control mechanisms of genes of lipid and fatty acid metabolism in the Atlantic salmon (*Salmo salar* L.) established cell line, SHK-1. Biochim. Biophys. Acta, Mol. Cell. Biol. Lipids 1811, 194-202.

Moldal, T., Løkka, G., Wiik-Nielsen, J., Austbø, L., Torstensen, B.E., Rosenlund, G., Dale, O.B., Kaldhusdal, M., Koppang, E.O., 2014. Substitution of dietary fish oil with plant oils is associated with shortened mid intestinal folds in Atlantic salmon (*Salmo salar*). BMC Vet. Res. 10, 60.

Montero, D., Grasso, V., Izquierdo, M., Ganga, R., Real, F., Tort, L., Caballero, M., Acosta, F., 2008. Total substitution of fish oil by vegetable oils in gilthead sea bream (*Sparus aurata*) diets: effects on hepatic mx expression and some immune parameters. Fish Shellfish Immunol. 24, 147-155.

Montero, D., Kalinowski, T., Obach, A., Robaina, L., Tort, L., Caballero, M.J., Izquierdo, M.S., 2003. Vegetable lipid sources for gilthead seabream (*Sparus aurata*): effects on fish health. Aquaculture 225, 353-370.

Montero, D., Mathlouthi, F., Tort, L., Afonso, J.M., Torrecillas, S., Fernández-Vaquero, A., Negrin, D., Izquierdo, M.S., 2010. Replacement of dietary fish oil by vegetable

oils affects humoral immunity and expression of pro-inflammatory cytokines genes in gilthead sea bream *Sparus aurata*. Fish Shellfish Immunol. 29, 1073-1081.
Morais, S., Monroig, O., Zheng, X., Leaver, M.J., Tocher, D.R., 2009. Highly unsaturated fatty acid synthesis in Atlantic salmon: characterization of ELOVL5- and ELOVL2-like elongases. Mar. Biotechnol. 11, 627-639.
Morais, S., Pratoomyot, J., Taggart, J.B., Bron, J.E., Guy, D.R., Bell, J.G., Tocher, D.R., 2011. Genotype-specific responses in Atlantic salmon (*Salmo salar*) subject to dietary fish oil replacement by vegetable oil: a liver transcriptomic analysis. BMC Genomics 12, 255.
Morais, S., Taggart, J.B., Guy, D.R., Bell, J.G., Tocher, D.R., 2012. Hepatic transcriptome analysis of inter-family variability in flesh n-3 long-chain polyunsaturated fatty acid content in Atlantic salmon. BMC Genomics 13, 410.
Mourente, G., Good, J.E., Bell, J.G., 2005. Partial substitution of fish oil with rapeseed, linseed and olive oils in diets for European sea bass (*Dicentrarchus labrax* L.): effects on flesh fatty acid composition, plasma prostaglandins E_2 and $F_{2\alpha}$, immune function and effectiveness of a fish oil finishing diet. Aquacult. Nutr. 11, 25-40.
Mu, C., Wang, Q., Yuan, Z., Zhang, Z., Wang, C., 2012. Identification of glutaredoxin 1 and glutaredoxin 2 genes from *Venerupis philippinarum* and their responses to benzo [a] pyrene and bacterial challenge. Fish Shellfish Immunol. 32, 482-488.
Panserat, S., Hortopan, G.A., Plagnes-Juan, E., Kolditz, C., Lansard, M., Skiba-Cassy, S., Esquerré, D., Geurden, I., Médale, F., Kaushik, S., Corraze, G., 2009. Differential gene expression after total replacement of dietary fish meal and fish oil by plant products in rainbow trout (*Oncorhynchus mykiss*) liver. Aquaculture 294, 123-131.
Patterson, E., Wall, R., Fitzgerald, G., Ross, R., Stanton, C., 2012. Health implications of high dietary omega-6 polyunsaturated fatty acids. J Nutr Metab 2012, 539426.
Pfaffl, M., 2001. A new mathematical model for relative quantification in real-time RT-PCR. Nucleic Acids Res. 29, e45.
Rosenlund, G., Torstensen, B.E., Stubhaug, I., Usman, N., Sissener, N.H., 2016. Atlantic salmon require long-chain n-3 fatty acids for optimal growth throughout the seawater period. J Nutr Sci 5, e19.
Ruyter, B., Rosjo, C., Einen, O., Thomassen, M., 2000. Essential fatty acids in Atlantic salmon: effects of increasing dietary doses of n-6 and n-3 fatty acids on growth, survival and fatty acid composition of liver, blood and carcass. Aquac. Nutr. 6, 119-127.
Sahlmann, C., Sutherland, B.J.G., Kortner, T.M., Koop, B.F., Krogdahl, Å., Bakke, A.M., 2013. Early response of gene expression in the distal intestine of Atlantic salmon (*Salmo salar* L.) during the development of soybean meal induced enteritis. Fish Shellfish Immunol. 34, 599-609.
Salze, G.P., Davis, D.A., 2015. Taurine: a critical nutrient for future fish feeds. Aquaculture 437, 215-229.
Schaffert, C.S., 2011. Role of MGST1 in reactive intermediate-induced injury. World J Gastroenterol 17, 2552.
Sissener, N., Waagbø, R., Rosenlund, G., Tvenning, L., Susort, S., Lea, T., Oaland, Ø., Chen, L., Breck, O., 2016. Reduced n-3 long chain fatty acid levels in feed for

Atlantic salmon (*Salmo salar* L.) do not reduce growth, robustness or product quality through an entire full scale commercial production cycle in seawater. Aquaculture 464, 236-245.

Torstensen, B.E., Bell, J.G., Rosenlund, G., Henderson, R.J., Graff, I.E., Tocher, D.R., Lie, O., Sargent, J.R., 2005. Tailoring of Atlantic salmon (*Salmo salar* L.) flesh lipid composition and sensory quality by replacing fish oil with a vegetable oil blend. J. Agric. Food Chem. 53, 10166-10178.

Torstensen, B.E., Espe, M., Sanden, M., Stubhaug, I., Waagbø, R., Hemre, G.-I., Fontanillas, R., Nordgarden, U., Hevrøy, E.M., Olsvik, P., Berntssen, M.H.G., 2008. Novel production of Atlantic salmon (*Salmo salar*) protein based on combined replacement of fish meal and fish oil with plant meal and vegetable oil blends. Aquaculture 285, 193-200.

Tusher, V.G., Tibshirani, R., Chu, G., 2001. Significance analysis of microarrays applied to the ionizing radiation response. Proc. Natl. Acad. Sci. U.S.A. 98, 5116-5121.

Vandesompele, J., De Preter, K., Pattyn, F., Poppe, B., Van Roy, N., De Paepe, A., Speleman, F., 2002. Accurate normalization of real-time quantitative RT-PCR data by geometric averaging of multiple internal control genes. Genome Biol 3, RESEARCH0034.

Vilhelmsson, O.T., Martin, S.A.M., Médale, F., Kaushik, S.J., Houlihan, D.F., 2004. Dietary plant-protein substitution affects hepatic metabolism in rainbow trout (*Oncorhynchus mykiss*). Br. J. Nutr. 92, 71-80.

Wamelink, M., Struys, E., Jakobs, C., 2008. The biochemistry, metabolism and inherited defects of the pentose phosphate pathway: a review. J. Inherit. Metab. Dis. 31, 703-717.

Wilson, R., 1994. Utilization of dietary carbohydrate by fish. Aquaculture 124, 67-80.

Xu, Q., Feng, C.Y., Hori, T.S., Plouffe, D.A., Buchanan, J.T., Rise, M.L., 2013. Family-specific differences in growth rate and hepatic gene expression in juvenile triploid growth hormone (GH) transgenic Atlantic salmon (*Salmo salar*). Comp Biochem Physiol, Part D: Genomics Proteomics 8, 317-333.

Xue, X., Hall, J.R., Caballero-Solares, A., Eslamloo, K., Taylor, R.G., Parrish, C.C., Rise, M.L., 2020. Liver transcriptome profiling reveals that dietary DHA and EPA levels influence suites of genes involved in metabolism, redox homeostasis, and immune function in Atlantic salmon (*Salmo salar*). Mar. Biotechnol., 1-22.

Xue, X., Hixson, S.M., Hori, T.S., Booman, M., Parrish, C.C., Anderson, D.M., Rise, M.L., 2015. Atlantic salmon (*Salmo salar*) liver transcriptome response to diets containing *Camelina sativa* products. Comp. Biochem. Physiol. D: Genomics Proteomics 14, 1-15.

Ye, J., Kaattari, I.M., Ma, C., Kaattari, S., 2013. The teleost humoral immune response. Fish Shellfish Immunol. 35, 1719-1728.

Zuo, R., Ai, Q., Mai, K., Xu, W., Wang, J., Xu, H., Liufu, Z., Zhang, Y., 2012. Effects of dietary n-3 highly unsaturated fatty acids on growth, nonspecific immunity, expression of some immune related genes and disease resistance of large yellow croaker (*Larmichthys crocea*) following natural infestation of parasites (*Cryptocaryon irritans*). Fish Shellfish Immunol. 32, 249-258.

CHAPTER 3: Transcriptome profiling of Atlantic salmon (*Salmo salar*) parr with higher and lower pathogen loads following *Piscirickettsia salmonis* infection

The research described in **Chapter 3** has been published in the journal Frontiers in Immunology as: Xue, X., Caballero-Solares, A., Hall, J.R., Umasuthan, N., Kumar, S., Jakob, E., Skugor, S., Hawes, C., Santander, J., Taylor, R.G., Rise, M.L., 2021. Transcriptome profiling of Atlantic salmon (*Salmo salar*) parr with higher and lower pathogen loads following *Piscirickettsia salmonis* infection. Front. Immunol. 12, 789465.

3.1 Abstract

Salmonid rickettsial septicemia (SRS), caused by *Piscirickettsia salmonis*, is one of the most devastating diseases of salmonids. However, the transcriptomic responses of Atlantic salmon (*Salmon salar*) in freshwater to an EM-90-like isolate (highly prevalent across Chilean salmon farms) have not been explored. Here, Atlantic salmon parr were infected with an EM-90-like isolate and time-course qPCR analyses of pathogen load and four biomarkers (*campb*, *hampa*, *il8a*, *tlr5a*) of innate immunity were conducted on the head kidney samples. Transcript expression of three of these genes (except *hampa*), as well as pathogen level, peaked at 21 days post-injection (DPI). Multivariate analyses of infected individuals at 21 DPI revealed two infection phenotypes [lower (L-SRS) and higher (H-SRS) infection level]. Five fish from each group (Control, L-SRS, and H-SRS) were selected for transcriptome profiling using a 44K salmonid microarray platform. I identified 1,636 and 3,076 differentially expressed probes (DEPs) in the L-SRS and H-SRS groups compared with the control group, respectively (FDR = 1%). Gene ontology term enrichment analyses of SRS-responsive genes revealed the activation of a large number of innate (e.g. “phagocytosis”, “defense response to bacterium”, “inflammatory response”) and adaptive (e.g. “regulation of T cell activation”, “antigen processing and presentation of exogenous antigen”) immune processes, while a small number of general physiological processes (e.g. “apoptotic process”, development and metabolism relevant) was enriched. Transcriptome results were confirmed by qPCR analyses of 42 microarray-identified transcripts. Furthermore, the comparison of individuals with differing levels of infection (H-SRS *vs* L-SRS) generated insights into the biological processes possibly involved in

disease resistance or susceptibility. This study demonstrated a low mortality (~30%) EM-90-like infection model and broadened the current understanding of molecular pathways underlying *P. salmonis*-triggered responses of Atlantic salmon, identifying biomarkers that should aid in diagnosis and other methods to combat this pathogen.

3.2 Introduction

There is an excellent potential for the aquaculture industry to expand to fulfill the worldwide seafood demand for human consumption (FAO, 2018). Atlantic salmon (*Salmo salar*) is one of the most economically important species currently farmed in the marine finfish aquaculture sector (Kiron, 2012). However, infectious diseases have resulted in substantial mortality and losses for Atlantic salmon aquaculture worldwide, affecting the growth and sustainability of the industry. Piscirickettsiosis or salmonid rickettsial septicemia (SRS) caused by the intracellular Gram-negative bacterial pathogen, *Piscirickettsia salmonis*, constitutes one of the main infectious diseases in salmonid aquaculture (Rise et al., 2004; Hernandez et al., 2016). For example, in Chile, it was estimated by the National Fisheries and Aquaculture Service that about 50% of disease-causing mortalities in Atlantic salmon were attributed to piscirickettsiosis in 2020 (Sernapesca, 2021). The economic losses caused by piscirickettsiosis to the Chilean aquaculture industry were approximately USD 700 million yearly (Maisey et al., 2017; Meza et al., 2019b). Occurrences of this pathogen have also been reported in farmed salmonids in Norway, Scotland, Ireland and Canada (Meza et al., 2019b; Jones et al., 2020). *P. salmonis* causes systemic, chronic septicemia in fish, which is characterized by a variety of clinical signs, including a discoloured and swollen head kidney, anemia, enlarged spleen, and skin and liver lesions (Rise et al., 2004; Maisey et al., 2017; Nourdin-Galindo et al., 2017). Although research progress has been made in several *in vitro* and *in vivo* models, the molecular mechanisms involved in *P. salmonis* pathogenesis are not entirely known (Maisey et al., 2017; Nourdin-Galindo et al., 2017). Attempts to control this disease

thus far have been unsuccessful due to the low efficacy of existing vaccines and antibiotic treatments (Rise et al., 2004; Nourdin-Galindo et al., 2017).

Previous transcriptomic analyses of Atlantic salmon challenged with live *P. salmonis* showed up-regulation of genes involved in oxidative and inflammatory pathways (Rise et al., 2004; Tacchi et al., 2011) as well as up-regulation of genes related to cellular iron metabolism (Rise et al., 2004; Pulgar et al., 2015). These studies revealed the activation of numerous immune responses upon *P. salmonis* infection. However, it remains unclear which of these immune responses are protective and what role is played by the host iron withholding response (also known as nutritional immunity), which aims to limit the access of bacteria to iron and heme, by promoting intracellular storage away from invading pathogens (Cherayil, 2011; Díaz et al., 2021). The key iron regulator Hepcidin exerted a protective effect against the extracellular *Flavobacterium columnare* in grass carp (*Ctenopharyngodon idella*) (Wei et al., 2018), while suppression of *hepcidin* was associated with protection in Atlantic salmon challenged by the facultative intracellular *Aeromonas salmonicida* bacterium (Škugor et al., 2009). In contrast, a previous study with an iron chelator that successfully reduced the amount of available iron, had induction of *hepcidin-1* in multiple organs of Atlantic salmon undergoing *P. salmonis* infection that coincided with improved survival compared with the groups supplemented with iron (Valenzuela-Muñoz et al., 2020). The study of Díaz et al. (2021) also showed positive effects of the iron chelator deferoxamine mesylate in *P. salmonis* infected salmon SHK-1 cells which coincided with an increase in *hepcidin* expression. Possible host-pathogen interactions, such as the suppression of genes encoding pro-apoptotic proteins and

induction of cell proliferation-related genes were also suggested in early studies (Rise et al., 2004; Tacchi et al., 2011). The modulation of these host pathways may represent a mechanism used by *P. salmonis* to ensure the maintenance of host cells and to allow them to survive and replicate within host cells (Tacchi et al., 2011). In addition, this pathogen may inhibit the adaptive immune response in infected fish as a mechanism to evade host defenses and promote replication and survival (Rise et al., 2004; Tacchi et al., 2011; Rozas-Serri et al., 2018b).

In Chile, the existence of two distinct *P. salmonis* genogroups, LF-89-like and EM-90-like strains, has been reported (Nourdin-Galindo et al., 2017; Saavedra et al., 2017; Meza et al., 2019b). Saavedra et al. (2017) found that EM-90-like isolates, similar to LF-89-like ones, are highly prevalent and disseminated across Chilean marine farms. Studies revealed differences between these two genogroups in relation to geographic distribution, antibiotic susceptibility and host specificity (Saavedra et al., 2017). For example, *P. salmonis* field isolates showed a marked host preference with EM-90-like isolates exclusively recovered from farmed Atlantic salmon (Saavedra et al., 2017). Comparative pan-genome analysis of LF-89 and EM-90 strains has identified strain-specific virulence factors linked to adherence, colonization, invasion factors, and endotoxins (Nourdin-Galindo et al., 2017). These genomic divergences may directly be associated with inter-genogroup differences in pathogenesis and host-pathogen interactions (Nourdin-Galindo et al., 2017; Rozas-Serri et al., 2017; Rozas-Serri et al., 2018a; Rozas-Serri et al., 2018b). As a result, there has been a growing interest in studying the piscirickettsiosis resulting from EM-90-like isolates (Rozas-Serri et al., 2017; Rozas-Serri et al., 2018a; Rozas-Serri

et al., 2018b; Meza et al., 2019a; Meza et al., 2019b). Rozas-Serri et al. (2018b) evaluated the transcriptomic changes of post-smolt Atlantic salmon challenged with an EM-90-like *P. salmonis* via cohabitation in seawater. Fish infected with EM-90-like isolate showed extremely high mortality (100% in Trojans and 94.9% in cohabitant fish) (Rozas-Serri et al., 2017; Rozas-Serri et al., 2018a; Rozas-Serri et al., 2018b). However, relatively small numbers of differentially expressed genes (298 in Trojans and 170 in cohabitant fish) were identified. Meza et al. (2019a) also analyzed the disease development of salmon after being challenged with an EM-90-like strain in seawater and resulted in 100% mortality in both Trojan and cohabitant fish. The transcriptomic responses of Atlantic salmon parr in freshwater to an EM-90-like isolate have not been explored. Although piscirickettsiosis has often been reported in seawater-reared salmonids, previous reports have documented the disease in coho salmon (*Oncorhynchus kisutch*) and rainbow trout (*O. mykiss*) farmed in freshwater (Bravo, 1994; Gaggero et al., 1995), and experimental infection trials have been successfully demonstrated in freshwater reared coho salmon, Atlantic salmon and rainbow trout (Almendras et al., 1997; House et al., 1999; Smith et al., 1999).

The present study aimed to explore the head kidney transcriptomic responses of the Atlantic salmon parr from a low mortality EM-90-like *P. salmonis* infection trial. Fish head kidney is one of the major organs of the immune system and is the functional homolog of the bone marrow (i.e. main site of haematopoiesis) in higher vertebrates (Zapata et al., 2006). A low mortality infection model is needed to fill the gaps in the current knowledge regarding piscirickettsiosis outbreaks involving EM-90-like strains; this model can also be beneficial in evaluating the performance of novel functional feeds designed to improve fish

health and mitigating/reducing disease incidence in aquaculture. Samples collected from multiple time points post-infection (up to 42 days) were included to study the temporal patterns of pathogen level and host immune responses. All exposed fish in the present study received the same dose of *P. salmonis*; however, two infection phenotypes (higher and lower infection levels) at 21 days post-injection (DPI) were detected by multivariate analyses of pathogen load and levels of 4 antibacterial transcript biomarkers. A number of previous disease challenge studies in Atlantic salmon have shown that pathogen load can be used as a good indicator of disease resistance (Jørgensen et al., 2008; Timmerhaus et al., 2012; Dettleff et al., 2015; Pulgar et al., 2015). Dettleff et al. (2015) found that the bacterial load of fish infected with *P. salmonis* was significantly lower in resistant individuals when compared with the susceptible ones; the resistant fish had increased expression of *c-type lysozyme* in the head kidney, while the susceptible fish demonstrated an exaggerated innate immune response. Therefore, a specific focus on the transcriptional differences between lower and higher infection individuals (i.e. L-SRS *vs* H-SRS) was also attempted using the consortium for Genomic Research on All Salmonids Project (cGRASP)-designed Agilent 44K salmonid oligonucleotide microarray (Jantzen et al., 2011). This particular microarray platform has proven to be a useful and robust tool in detecting differentially expressed transcripts in several immune-related studies in Atlantic salmon and rainbow trout (Sutherland et al., 2014a; Sutherland et al., 2014b; Müller et al., 2015; Eslamloo et al., 2017; Eslamloo et al., 2020a; Eslamloo et al., 2020b; Umasuthan et al., 2020). I hypothesize that the exploration into transcriptomic differences between high and low infection individuals may provide insight into the molecular mechanisms

associated with the ability to evade or clear *P. salmonis* infection as well as the dysregulations leading to susceptibility and more adverse outcomes. Finally, this study revealed candidate biomarker genes that should be valuable for future SRS-related research.

3.3 Materials and methods

3.3.1 Experimental animals

The *P. salmonis* disease challenge trial was conducted at the Cargill Innovation Center (Colaco, Chile). Atlantic salmon parr (64.2 ± 10.4 g mean initial weight ± SD) were randomly distributed into 10 challenge tanks (200 L) with 125 fish/tank. Prior to the study, 30 fish were screened for *Flavobacterium psychrophilum, P. salmonis*, *Renibacterium salmoninarum*, infectious pancreatic necrosis virus (IPNV) and infectious salmon anemia virus (ISAV) using real-time quantitative polymerase chain reaction (qPCR), and were negative for all of these pathogens (data not shown). Fish were kept in a flow-through freshwater system (~15.2°C and 24 h light). Oxygen in the tank was maintained at 92.3 ± 7.3% (mean ± SD) of saturation. Fish were held for 14 days prior to the start of the infection trial to acclimate to tank conditions. A standard EWOS commercial diet (EWOS Micro 50) was supplied using automatic feeders over a period of 18 h per day (from 2:00 pm to 8:00 am) and fed to satiation. Fish were fasted 12 h before and after all experimental procedures (e.g. injection and sampling).

An EM90-like strain of *P. salmonis* was purchased from Fundacion Fraunhofer Chile Research (Puerto Montt, Chile). The bacteria were cultured in CHSE-214 cells

according to standard operating procedures of Fundacion Fraunhofer Chile Research, and the inoculum with the desired infectious titer was prepared and transferred under chilled conditions within 1 h to the Cargill Innovation Center challenge facility on the day of the infection. The inoculum (i.e. suspension of CHSE-214 cells infected with *P. salmonis*) was checked for contaminations (i.e. IPNV, ISAV, *Piscine reovirus*, *R. salmoninarum*, *Flavobacterium sp.*, *Aeromonas salmonicida*) using qPCR. The titer of the inoculum [i.e. median tissue culture infective dose ($TCID_{50}$)] was determined on CHSE-214 cells using an endpoint dilution assay. All fish from the challenge group (7 tanks) were anesthetized using benzocaine (150 µL L^{-1} BZ-20®, Veterquímica S.A., Maipú, Santiago, Chile) and intraperitoneally (IP) injected with 0.1 mL of bacterial inoculum with a titer of $10^{0.83}$ $TCID_{50}$/mL. The target titer of 10^{1} $TCID_{50}$/mL (real titer $10^{0.83}$ $TCID_{50}$/mL) was chosen based on results from previously conducted dose dilution trials (10^{1}-10^{4} $TCID_{50}$/mL) with the same bacterial isolate at the Cargill Innovation Center. The aim of this trial was to achieve a slow onset of mortality and to reach about 30-40% accumulative mortality over the duration of the trial to evaluate the pathological changes over time. Fish from the mock-injection control group (3 tanks) were anesthetized as above, and IP injected with 0.1 mL of the medium that was used to prepare the bacterial inoculum (i.e. minimum essential medium, MEM) (**Figure 3.1A,B**). Ten fish per tank [3 tanks from the challenge group (i.e. *P. salmonis*-injected) and 3 tanks from the control group (CON)] were euthanized using an overdose of benzocaine (300 µL L^{-1} BZ-20®) and dissected on the day before injection (PRE) of the remaining fish, as well as 2, 7, 13, 21 and 42 DPI. Head kidney samples were

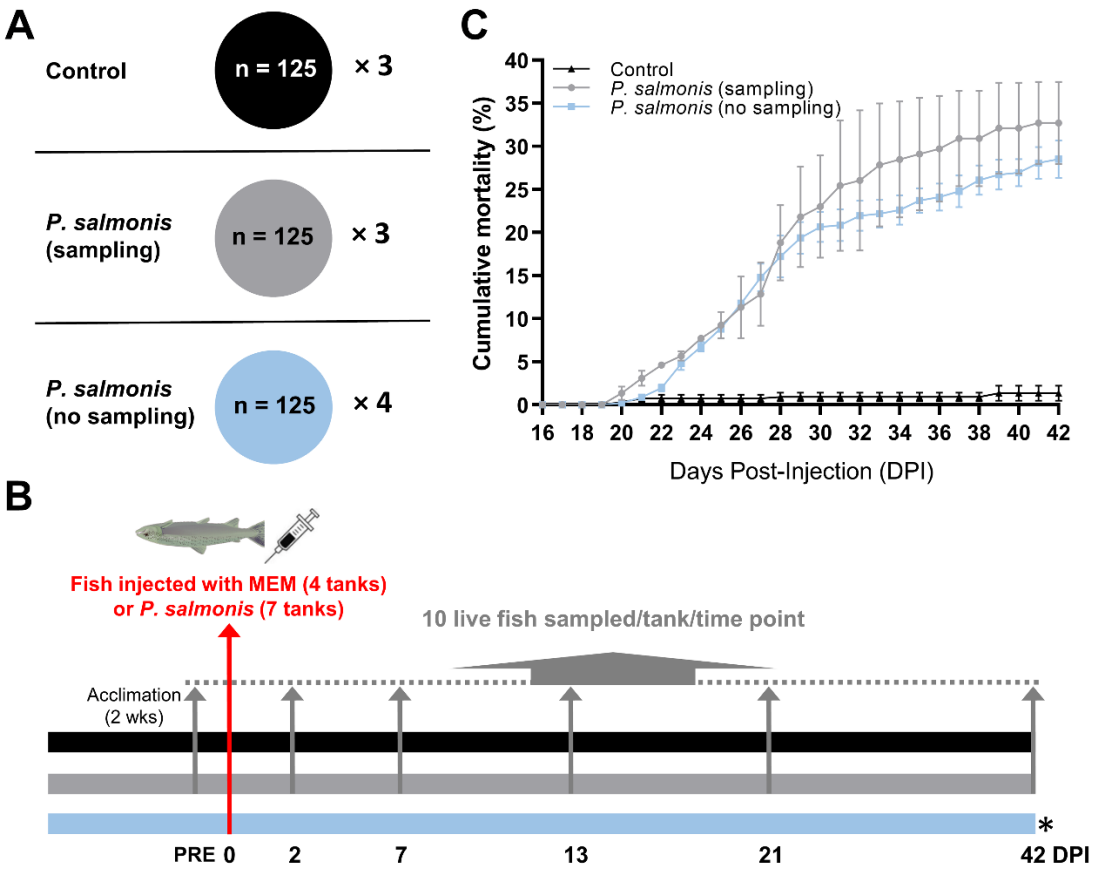

Figure 3.1. Overview of the infection trial, sampling and cumulative mortality. (**A**) The tank allocation and the number of fish for each treatment group [Control (MEM media injected), *P. salmonis*-injected (sampling), *P. salmonis*-injected (no sampling)]. (**B**) Timeline of the overall study with sampling regime showing the number of days post-infection (DPI). Four out of 7 tanks in the challenge group [i.e. *P. salmonis*-injected (no sampling)] were left untouched in order to monitor mortality. (**C**) Cumulative mortality in each treatment group. No significant difference was found in the cumulative mortality by the end of the infection trial between *P. salmonis*-injected (sampling) and *P. salmonis*-injected (no sampling) groups ($p = 0.42$; Student's t test).

collected and stored in RNAlater (Ambion/Life Technologies, Austin, TX, USA) for 48 h at 4°C and transferred to -80°C until RNA extraction. Four out of 7 tanks in the challenge group were left untouched in order to monitor mortality (**Figures 3.1A,B**). All procedures in this study were conducted following the guidelines of the Canadian Council on Animal Care (CCAC, 2005).

3.3.2 RNA extraction, DNase treatment, and column purification

RNAlater was removed prior to RNA extraction. All samples were lysed in TRIzol reagent (Invitrogen/Life Technologies, Carlsbad, CA, USA) using a tissue homogenizer (Precellys 24, Bertin Instruments, Montigny-le-Bretonneux, France), and subjected to RNA extraction according to manufacturer instructions. Forty micrograms of each total RNA sample were treated with 6.8 Kunitz units of DNase I (QIAGEN, Mississauga, ON, Canada) to degrade residual genomic DNA, and then purified using the RNeasy Mini Kit (QIAGEN) following manufacturer protocols. RNA integrity was verified by 1% agarose gel electrophoresis, and RNA purity was assessed by A260/280 and A260/230 ratios using NanoDrop spectrophotometry (Thermo Fisher, Mississauga, ON, Canada).

3.3.3 qPCR analysis of pathogen load and candidate host immune biomarkers

For pathogen load assessment, specific primers and probe for the *P. salmonis 16S-23S ribosomal RNA internal transcribed spacer* (*ITS*; in-house developed by Cargill Innovation) were used for pathogen load detection, with Atlantic salmon *elongation factor 1 alpha 1* (*ef1a1*) (Lockhart et al., 2007) levels analyzed as an internal control (i.e. reference gene). Primer and probe sequences for these genes can be found in **Supplemental**

Table S3.1. Pathogen load was assessed across all available samples (n = 337) in technical duplicates using a probe-based detection (i.e. TaqMan) kit AGPATH-ID ONE-STEP RT-PCR (Ambion/Life Technologies) and the ViiA7 Real-Time PCR system (Applied Biosystems/Life Technologies). The reaction mix contained 6.5 µL of 2X RT-PCR Buffer, 0.52 µL of 25X RT-PCR Enzyme Mix, 0.88 µL detection enhancer, 900 nM of forward primer, 600 nM of reverse primer, 225 nM of probe, 50 ng of RNA template, and DEPC-treated water to reach a final volume of 13 µL. The real-time PCR thermal cycling profile consisted of the reverse transcription step at 45°C for 10 min, the reverse transcriptase inactivation/initial denaturation step at 95°C for 10 min, and the amplification step of 45 cycles of 95°C for 15 s and 60°C for 45 s. Prior to pathogen load assessment, head kidney RNA templates from three infected animals were selected to test the performance and amplification efficiencies of primers, and determine the optimal input RNA quantity. Amplification efficiencies (Pfaffl, 2001) of *ITS* and *ef1a1* for pathogen load assessment were determined from three standard curves performed using a 5-point 1:3 dilution series starting with 150 ng of input total RNA. The reported efficiencies are an average of the three values. The infection level assays for each sample were then measured using 50 ng of input RNA in each reaction. No-template and positive (RNAs from three highly infected fish) controls were included in each plate run. The relative quantity (RQ) of *P. salmonis ITS* was determined using the ViiA 7 Software Relative Quantification Study Application (Version 1.2.3) (Applied Biosystems/Life Technologies), with normalization to *ef1a1* transcript levels, and with amplification efficiencies incorporated. The sample with the

lowest detectable expression level was set as the calibrator sample (i.e. assigned an RQ value = 1.0).

Following the bacterial screening, smaller sample sizes of the control fish (i.e. PRE and time-match controls) together with all available fish from the *P. salmonis*-injected group (except for 2 DPI) (total $n = 192$) were further subjected to qPCR analyses of 4 well-known antibacterial biomarkers [*campb* (Bridle et al., 2011; Rozas-Serri et al., 2018b; Eslamloo et al., 2020b; Soto-Dávila et al., 2020; Zanuzzo et al., 2020), *hampa* (Pulgar et al., 2015; Eslamloo et al., 2020a; Zanuzzo et al., 2020), *il8a* (Tacchi et al., 2011; Rozas-Serri et al., 2018a; Zanuzzo et al., 2020), and *tlr5a* (Rozas-Serri et al., 2018a; Eslamloo et al., 2020b)] to assess the infection and host immune response dynamics. The qPCR analysis for these genes was conducted on a ViiA7 384 well platform (Applied Biosystems/Life Technologies), and the methods (e.g. cDNA synthesis, primer quality control, and PCR program) for these assays are described in Section 2.5. Transcript levels of these four biomarkers were normalized to transcript levels of two endogenous control genes. To select these control genes, the expression of 6 candidate normalizers [i.e. *60S ribosomal protein 32* (*rpl32*; BT043656), *β-actin* (*actb*; BG933897), *ef1a1* (AF321836), *ef1a2* (BT058669), *eukaryotic translation initiation factor 3 subunit D* (*eif3d*; GE777139), and *polyadenylate-binding protein 1* (*pabpc1*; EG908498)] was measured in 48 out of 192 individuals (i.e. 25%) involved in this screen step and then analyzed using *geNorm* (Vandesompele et al., 2002). Using this software, *eif3d* (*geNorm* M = 0.217) and *rpl32* (*geNorm* M = 0.211) were determined to be the most stable across infection levels and time points. The expression levels (RQ) of these genes were analyzed using a two-way ANOVA test, followed by Sidak

multiple comparisons post hoc test in order to identify significant differences between *P. salmonis* injected and control groups at each time point, and within one treatment group at multiple time points. The normality of the qPCR data (i.e., RQ values) was analyzed using the Shapiro-Wilk and Kolmogorov-Smirnov normality tests. All of the statistical tests above were performed using Prism v7.0 (GraphPad Software Inc., La Jolla, CA, USA). Differences were considered statistically significant when $p < 0.05$.

3.3.4 Transcriptome profiling by 44K microarray

3.3.4.1 Selection of time point and individuals

The RQ of *P. salmonis ITS* across the infection course peaked at 21 DPI, with all exposed fish testing positive (**Figure 3.2A,B**). Complete results of *P. salmonis ITS* expression levels in all samples can be seen in **Supplemental Table S3.2**. Similar to *P. salmonis ITS* levels, the transcript expression of *campb*, *il8a* and *tlr5a* also peaked at 21 DPI and was significantly higher compared with the time-matched control fish (**Figure 3.2**). Therefore, I decided to study the transcriptomic responses of Atlantic salmon to *P. salmonis* at the peak of infection and presumed peak of most immune activities (i.e. 21 DPI). In addition, multivariate statistical analyses (i.e. principal component analysis and hierarchical clustering) were performed using PRIMER (Version 6.1.15; PRIMER-E Ltd., Ivybridge, UK) to identify different infection phenotypes. Within infected fish, there were two infection level phenotypes identified at 21 DPI (except fish #C7-8): one group of fish with higher transcript levels of *P. salmonis ITS* and the antibacterial biomarkers (H-SRS)

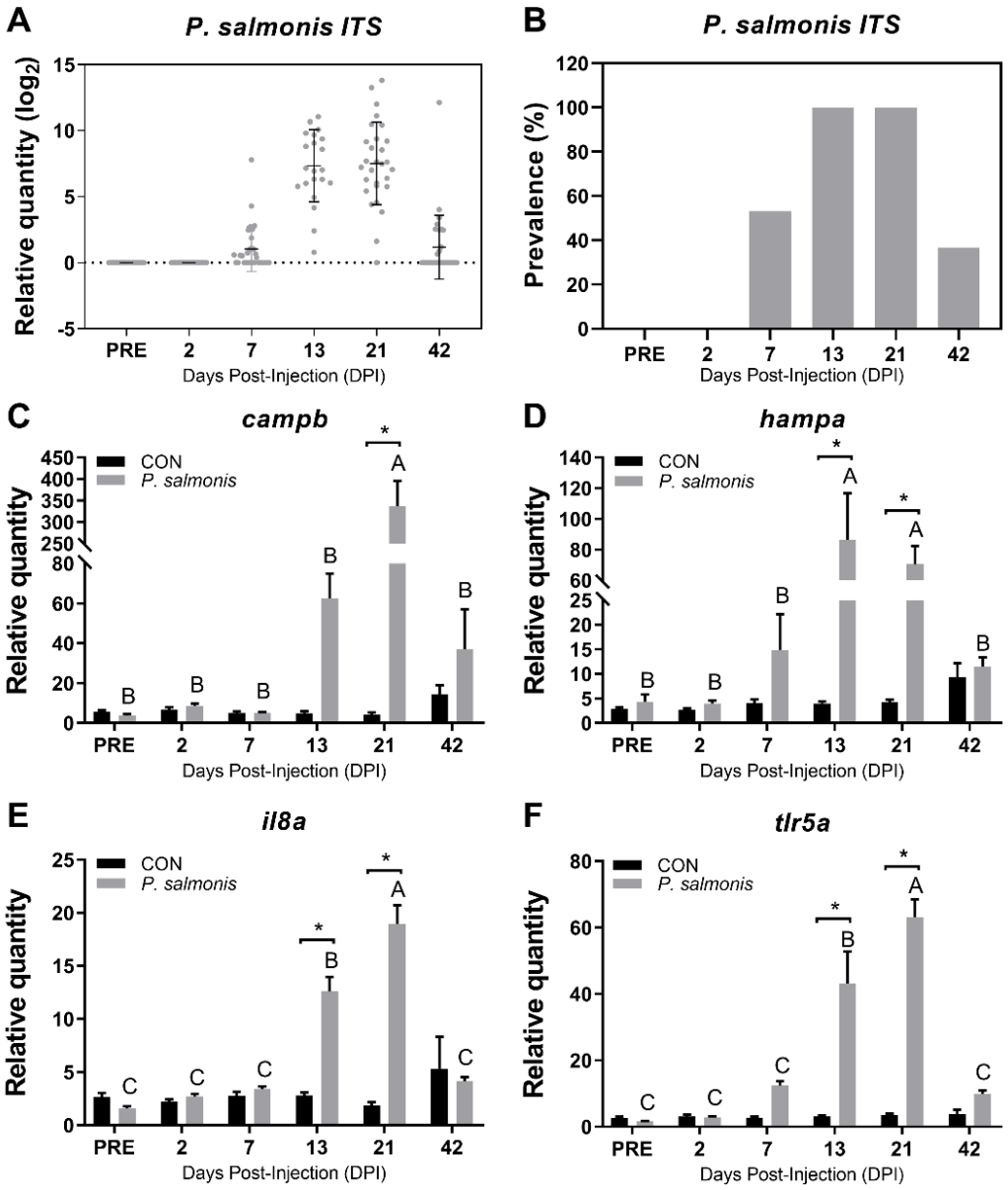
A
P. salmonis ITS
Relative quantity (log2)
15
10
5
0
-5
PRE
2
7
13
21
42
Days Post-Injection (DPI)
B
P. salmonis ITS
Prevalence (%)
120
100
80
60
40
20
0
PRE
2
7
13
21
42
Days Post-Injection (DPI)
C
campb
CON
P. salmonis
Relative quantity
450
400
350
300
250
80
60
40
20
0
B
B
B
B
*
A
B
PRE
2
7
13
21
42
Days Post-Injection (DPI)
D
hampa
CON
P. salmonis
Relative quantity
140
120
100
80
60
25
20
15
10
5
0
B
B
B
*
A
*
A
B
PRE
2
7
13
21
42
Days Post-Injection (DPI)
E
il8a
CON
P. salmonis
Relative quantity
25
20
15
10
5
0
C
C
C
*
B
*
A
C
PRE
2
7
13
21
42
Days Post-Injection (DPI)
F
tlr5a
CON
P. salmonis
Relative quantity
80
60
40
20
0
C
C
C
*
B
*
A
C
PRE
2
7
13
21
42
Days Post-Injection (DPI)

Figure 3.2. Detection of *P. salmonis* transcript and evaluation of candidate immune biomarkers in the head kidney of Atlantic salmon across different time points. (**A**) Transcript levels (i.e. relative quantity) of *P. salmonis 16S-23S ribosomal RNA internal transcribed spacer* (*ITS*) in the head kidney of Atlantic salmon injected with the same dose of bacterial inoculum, as determined by TaqMan assays across all sampling time points. (**B**) The relative prevalence of *P. salmonis* positive (i.e. detection of *P. salmonis ITS*) in fish that were injected with bacterial inoculum. (**C-F**) qPCR analysis of host immune biomarkers (*campb*, *hampa*, *il8a*, *tlr5a*) in both control (CON) and *P. salmonis* injected fish. Data are mean ± SE. The expression levels of these genes were analyzed using a two-way ANOVA test, followed by Sidak multiple comparisons post hoc test. An asterisk indicates a significant difference between time-matched *P. salmonis* injected and control groups. Different letters represent the significant differences within an injection group over time. All data presented in the Figure are provided in **Supplemental Table S3.2**.

and another group of fish with lower transcript levels of *P. salmonis ITS* and the antibacterial biomarkers (L-SRS) (**Supplemental Figure S3.1A,B**). The level of *P. salmonis ITS* in fish classified as H-SRS was significantly higher (19.1-fold) than that of L-SRS fish (**Supplemental Figure S3.1C**). Five individual fish from each infection phenotype (L-SRS or H-SRS) that were more closely clustered based on multivariate analysis were included in the microarray analysis along with five fish from the control group (i.e. CON) (**Supplemental Figure S3.1D**).

3.3.4.2 Microarray hybridization and data acquisition

The cGRASP-designed Agilent 4×44K salmonid oligonucleotide microarray (Jantzen et al., 2011; Xue et al., 2015; Eslamloo et al., 2017) was used to evaluate the impact of *P. salmonis* infection on the Atlantic salmon head kidney transcriptome at 21 DPI. With a common reference design, 15 arrays were used in this study, with one array per individual fish. The microarray experiment was performed as previously described (Xue et al., 2015; Eslamloo et al., 2020a; Umasuthan et al., 2020; Xue et al., 2020). Briefly, anti-sense amplified RNA (aRNA) was *in vitro* transcribed from 1 µg of each RNA template using the Amino Allyl MessageAmp II aRNA Amplification kit (Ambion/Life Technologies), following the manufacturer's instructions. For each fish, 20 µg of aRNA were precipitated overnight following standard molecular biology procedures and re-suspended in 9 µl of the manufacturer's coupling buffer. To generate the common reference pool, 5 µg of aRNA from each of the fifteen samples were pooled, and divided into 20 µg aliquots, which were precipitated and re-suspended as above. Resulting aRNA was labelled with either Cy3 (for the common reference) or Cy5 (for the experimental individuals) fluor

(GE HealthCare, Mississauga, ON, Canada) through a dye-coupling reaction, following the manufacturer's instructions. Equal quantities (825 ng) of each labelled aRNA from one experimental sample and the common reference were pooled, fragmented following the manufacturer's instructions and co-hybridized to a cGRASP-designed Agilent 44K salmonid oligonucleotide microarray (GEO accession # GPL11299) (Jantzen et al., 2011) as per the manufacturer's instructions (Agilent, Mississauga, ON, Canada). The arrays were hybridized at 65°C for 17 h with 10 rpm rotation in an Agilent hybridization oven. The array slides were washed immediately following hybridization as per the manufacturer's instructions. Slides were dried by centrifuging at 200 × g for 5 min at room temperature prior to scanning.

Each microarray was scanned at 5 µm resolution and 90% of laser power using a ScanArray Gx Plus scanner and ScanArray Express software (v4.0; Perkin Elmer, Woodbridge, ON, Canada) with photomultiplier tube (PMT) set to balance fluorescence signal between channels. The resulting TIFF images containing raw microarray data were extracted using Imagene (v9.0; BioDiscovery Inc., El Segundo, CA). Background correction, data transformation ($\log_2$), print-tip Loess normalization, and removal of low-quality/flagged spots were performed using R and the Bioconductor package *mArray* (Booman et al., 2011; Xue et al., 2015; Xue et al., 2020). After spot quality filtering, probes absent in more than 25% of the arrays (i.e. 4 arrays out of 15) were discarded, resulting in a final list of 20,701 probes for statistical analyses. All microarray data have been submitted to Gene Expression Omnibus (GEO) under the accession GSE178327.

3.3.4.3 Differential expression analysis and probe annotation

Prior to statistical analyses, missing data points for the 20,701 probes were imputed using the EM_array method from LSimpute (Bo et al., 2004; Celton et al., 2010). The differentially expressed probes (DEPs) among groups (i.e. L-SRS *vs* CON; H-SRS *vs* CON; H-SRS *vs* L-SRS) were determined using Significance Analysis of Microarrays (SAM) (Tusher et al., 2001). SAM was conducted at a false discovery rate (FDR) cutoff of 1% to focus on the most significant DEPs, using the Bioconductor package *siggenes* (Schwender et al., 2006). The resulting gene lists were annotated using the probe sequences (60mer) for gene identification by BLASTn against the NCBI nr/nt databases for both Atlantic salmon and rainbow trout. Stringent filtering criteria (only 2 allowed mismatches with un-gapped alignment option) were applied for the 60mer probe BLASTn hits. The contiguous sequences (contigs) from which the microarray probes were designed were also used for gene identification by BLASTx against the NCBI Swiss-Prot database (April 2019 version). If there were no or non-informative BLASTn results for a given probe, then the best BLASTx hit that had an Expect (E) value $<10^{-5}$ and an informatively named protein hit was reported. The gene symbols for probes were assigned from HUGO Gene Nomenclature Committee (HGNC; https://www.genenames.org/) and/or GeneCards (https://www.genecards.org/) databases. Using R and *gplots* package, a hierarchically clustered heat map was constructed with microarray normalized $\log_2$ ratios (Cy5/Cy3 ratios) of all identified DEPs using Euclidean distance and Ward's agglomerative linkage method (ward.D2).

3.3.4.4 GO term enrichment test and visualization of GO term networks

GO term enrichment tests were performed on lists of DEPs (i.e. 166 L-SRS responsive only, 1470 overlap, and 1606 H-SRS responsive only) using ClueGO (Bindea et al., 2009) and CluePedia plugins in Cytoscape (v3.7.0) (Shannon et al., 2003). The biological process (BP) GO database (20.12.2019) was used. The enrichment analysis was performed using a right-sided hypergeometric test after its adjustment by the Bonferroni-Hochberg procedure with a p-value set at 0.01 (i.e. FDR = 1%). GO term fusion strategy and a Kappa-statistics score of 0.5 were employed to integrate GO categories, minimize the complexity, and create a functionally organized GO cluster network. For each cluster (reflected by a different colour), a GO term with the lowest p-value was selected as the leading term in each functional group (i.e. highly connected terms within the GO network). As previously described in Eslamloo et al. (2020a), the enriched GO terms were classified using Gene Ontology Browser (http://www.informatics.jax.org) into 6 functional themes: (1) "adaptive immune response"; (2) "immune response"; (3) "response to stress"; (4) "development"; (5) "metabolic process"; and (6) "cellular process, localisation, and structure". The enriched GO terms for DEPs responsive to L-SRS only were classified into three themes ("adaptive immune response", "immune response", and "cellular process, localization, and structure"). The GO terms were classified based on the biological process to which they were related and/or their parent terms (especially for highly specific terms). Finally, a hierarchically clustered heat map was constructed based on probes having the associated GO term “adaptive immune response” using Genesis (Sturn et al., 2002); all data were median-centred and clustered using Pearson correlation and complete linkage hierarchical clustering as in Rise et al. (2015).

3.3.5 qPCR confirmation of microarray-identified DEPs

In total, 42 candidate *P. salmonis*-responsive biomarkers were selected for qPCR analysis. In addition to samples chosen for the microarray study, the remaining samples from both infection level groups (see **Section 3.3.4.1** and **Supplemental Figure S3.1** for sample classification) at 21 DPI (total $n = 37$; 11 L-SRS, 17 H-SRS, and 9 CON) were also included in the qPCR experiment.

First-strand cDNA templates for qPCR were synthesized in 20 µL reactions from 1 µg of DNaseI-treated, column-purified total RNA using random primers (250 ng; Invitrogen/Life Technologies), dNTPs (0.5 mM final concentration; Invitrogen/ Life Technologies) and M-MLV reverse transcriptase (200 U; Invitrogen/Life Technologies) with the manufacturer's first strand buffer (1× final concentration) and DTT (10 mM final concentration) at 37°C for 50 min. PCR amplifications were performed in 13 µL reactions using 1× Power SYBR Green PCR Master Mix (Applied Biosystems/Life Technologies), 50 nM of both the forward and reverse primers, and the indicated cDNA quantity (see below). The real-time analysis program consisted of 1 cycle of 50°C for 2 min, 1 cycle of 95°C for 10 min and 40 cycles of 95°C for 15 sec and 60°C for 1 min, with fluorescence detection at the end of each 60°C step.

The sequences of all primer pairs used in qPCR analyses are presented in **Supplemental Table S3.1**. Each primer pair was quality tested using the QuantStudio 6 Flex Real-Time PCR System (384-well format) (Applied Biosystems/Life Technologies). Quality testing ensured that a single product was amplified (dissociation curve analysis) and that there was no primer-dimer present in the no-template control. Amplification

efficiencies (Pfaffl, 2001) were calculated using two cDNA templates that were pooled post-cDNA synthesis: one pool of 5 CON samples and one pool of 5 H-SRS samples. Standard curves were generated using a 5-point 1:3 dilution series starting with cDNA representing 10 ng of input total RNA. The reported efficiencies (**Supplemental Table S3.1**) are an average of the two values.

After completing the primer quality control tests, qPCR analyses of transcript expression levels of the target genes were performed using the QuantStudio 6 Flex Real-Time PCR System (Applied Biosystems/Life Technologies). Diluted cDNAs corresponding to 5 ng of input RNA were used as templates in the PCR reactions. The C_T values of the GOIs and references genes were determined using the QuantStudio Real Time PCR Software Relative Quantification Study Application (Version 1.3) (Applied Biosystems/ Life Technologies). The RQ of each transcript was determined using a qBase relative quantification framework (Hellemans et al., 2007; Xue et al., 2019), with normalization to both *rpl32* and *eif3d* (see **Section 3.3.3** for normalizer gene testing), and with amplification efficiencies incorporated. The RQs of each transcript were calibrated against the control group.

All qPCR data (i.e. RQ values) were subjected to the Grubbs' test to identify potential outliers, and $\log_2$-transformed to meet the normality assumption. The normality of the qPCR data (i.e., $\log_2$ RQ values) was analyzed using the Shapiro-Wilk and Kolmogorov-Smirnov normality tests. In total, 19 RQ values were determined to be statistical outliers in the entire dataset (i.e., out of 1554 RQ values), and were excluded from the study. Fold-change values derived from microarray and qPCR were $\log_2$-

transformed and analyzed for correlation via linear regression as performed in previous studies (Caballero-Solares et al., 2018; Umasuthan et al., 2020; Xue et al., 2020). A significant correlation ($p < 0.05$) between both datasets was considered as confirmation of the microarray results. Transcript expression differences between groups were analyzed using a one-way ANOVA followed by Tukey's post hoc test for multiple comparisons at the 5% level of significance. Furthermore, the relationships between the expression of qPCR-studied transcripts and *P. salmonis* infection level were assessed using linear correlation analysis. Control fish were excluded from this analysis as all of these fish tested negative for *P. salmonis* (i.e. no RQ available). All of the statistical tests above were performed using Prism v7.0 (GraphPad Software Inc., La Jolla, CA, USA).

3.4 Results

3.4.1 Cumulative mortality

The cumulative mortality of fish infected with an EM-90-like isolate (sampling and non-sampling groups), as well as non-infected controls, are shown in **Figure 3.1C**. The mortality rate in the sampling group does not consider fish that were removed for sample collection. The first mortalities in both *P. salmonis*-injected groups were registered at 20 DPI. The cumulative mortality of the *P. salmonis*-injected (sampling) group by the end of the infection trial reached 32.7%, which was not significantly different from the *P. salmonis*-injected (no sampling) group (i.e. 28.5%).

3.4.2 qPCR analysis of pathogen load and candidate host immune biomarkers

The *P. salmonis ITS* transcript level was assessed using a Taqman assay. All head kidney samples for the PRE and 2 DPI were negative for the *ITS* transcript (**Figure 3.2A,B**). The infection prevalence of *P. salmonis* (detectable pathogen *ITS*) reached 100% at both 13 and 21 DPI, and the mean *ITS* expression level peaked at 21 DPI based on all available samples tested.

Four well-known antibacterial biomarker transcripts (*campb*, *hampa*, *il8a* and *tlr5a*) were analyzed via qPCR to assess the infection and host immune response dynamics (**Figures 3.2C-F**). The highest expression level of *campb*, *il8a* and *tlr5a* in response to *P. salmonis* infection was observed at 21 DPI, while the expression of *hampa* in the *P. salmonis*-injected group peaked at 13 DPI. All four genes assayed in the current study were significantly up-regulated in the *P. salmonis*-injected group at both 13 and 21 DPIs compared with time-matched mock-injection controls, except for *campb*, which was only significant at 21 DPI. Further multivariate statistical analyses of the infection level and the expression of 4 antibacterial biomarkers of individuals collected at 21 DPI revealed infection and immune response phenotypes (i.e. L-SRS and H-SRS), with the exception of fish C7-8 which did not group with either phenotype (**Supplemental Figure S3.1A,B**). Complete qPCR results for *P. salmonis ITS* level and these four antibacterial biomarkers can be found in **Supplemental Table S3.2**.

3.4.3 Global transcriptomic expression in salmon head kidney

In this study, I used the cGRASP-designed Agilent 44K microarray platform (Jantzen et al., 2011) to explore the transcriptomic response of Atlantic salmon head kidney

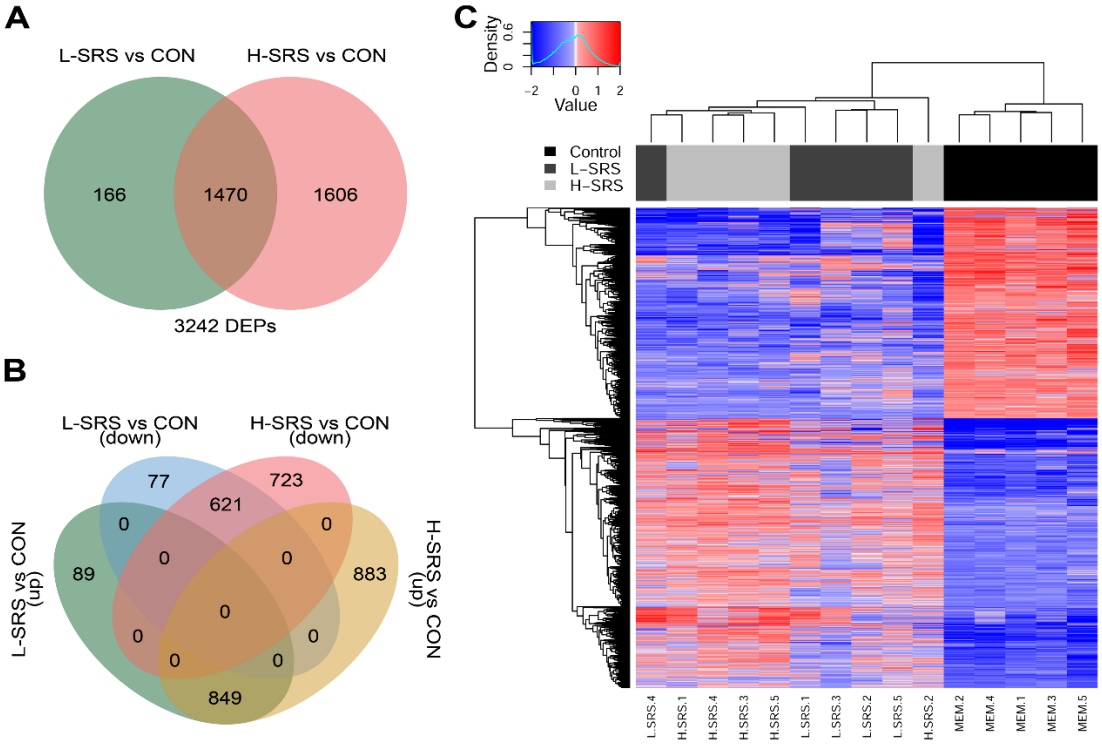

Figure 3.3. Overview of the head kidney transcriptomic responses of Atlantic salmon with higher (H-SRS) and lower (L-SRS) levels of *P. salmonis* compared with the control group at 21 days post-injection (DPI). Differentially expressed probes (DEP) were identified by Significance Analysis of Microarray (FDR = 1%). (**A**) Venn diagram illustrates the total number of DEPs in L-SRS or H-SRS groups in comparison to the control fish (CON). (**B**) Venn diagram shows the corresponding number of DEPs that were up- or down-regulated in L-SRS or H-SRS groups in comparison to the control fish (CON). (**C**) Hierarchical clustering analyses of samples based on all *P. salmonis* responsive probes (n = 3242).

to *P. salmonis* at 21 DPI. Fish showing a lower (L-SRS) or a higher (H-SRS) level of the *P. salmonis* infection were selected for comparison of their transcriptome profiles with the mock-injection control group (CON). The overall results of the microarray study, including the number of genes identified in each comparison, are summarised in **Figure 3.3A,B**. In total, 3242 significantly differentially expressed probes (DEPs) were identified in the *P. salmonis*-injected groups using SAM analyses (FDR = 1%) compared to the control (CON). However, SAM analysis failed to detect any significant DEPs when comparing H-SRS and L-SRS groups directly. The complete gene lists, including gene names and symbols, are shown in **Supplemental Table S3.3**. As illustrated by the Venn diagrams (**Figure 3.3A,B**), the two significant comparisons in the present study shared 1470 DEPs (849 up- and 621 down-regulated). Among these DEPs, the direction of gene expression regulation by *P. salmonis* infection was all the same among H-SRS and L-SRS when compared with the control group; however, they often differed in the degree of regulation (i.e. fold-change) with the H-SRS group generally showing higher fold-changes (**Figure 3.3C**). In addition, there was a larger number of SRS-responsive probes in the H-SRS group compared with the L-SRS group (i.e. 3076 *vs* 1636), suggesting a higher level of *P. salmonis* infection was associated with a more pronounced gene expression response. Using all identified DEPs in hierarchical analyses, all mock-injection control samples clustered in a separate branch from all infected samples; however, within each infected group (i.e. L-SRS or H-SRS), only 4 out of 5 samples were clustered together (**Figure 3.3C**).

3.4.4 Insight into biological pathways regulated by *P. salmonis* (L-SRS *vs* H-SRS)

To identify host molecular pathways regulated by *P. salmonis* infection, I compared the GO Biological Process (BP) term compositions of SRS-responsive transcript lists to that of the whole array using a Fisher's exact test in ClueGO (FDR = 1%). First, I identified 292 BP terms enriched in SRS-responsive transcripts (1,470 DEPs) overlapping both infection groups (L-SRS and H-SRS) (**Figure 3.4**; **Supplemental Table S3.4**). The BP terms enriched by SRS (**Figure 3.4**) were associated with adaptive immune response (38.0%), immune response (36.3%), cellular process, localisation, and structure (10.3%), development (5.8%), metabolic process (5.1%), and response to stress (4.5%). A large number of BP terms involved in adaptive immunity were enriched by *P. salmonis* infection in Atlantic salmon. These included many terms related to lymphocyte differentiation and activation (e.g. "B cell activation", "regulation of T cell activation", "lymphocyte proliferation", "immunoglobulin mediated immune response", "response to interferon-gamma"), and some terms related to antigen presentation processes (e.g. "antigen processing and presentation of exogenous antigen") (**Figure 3.4**; **Supplemental Table S3.4**). A total of 81 DEPs contributing to the enriched GO term, "adaptive immune response", were used in constructing a heatmap to reveal the transcript profile of adaptive immunity-related genes (**Supplemental Figure S3.2**). Among these genes, 66 DEPs (e.g. *tap1*, *tap2*, *ifng*, *irf1*, *cd209a*, *bcl10*, *ada*) were up-regulated and 15 DEPs (e.g. *il7r*, *cd5*, *foxp3*) were down-regulated by *P. salmonis* infection (**Supplemental Figure S3.2**). A diverse and large group of BP terms related to the innate immune response (e.g.

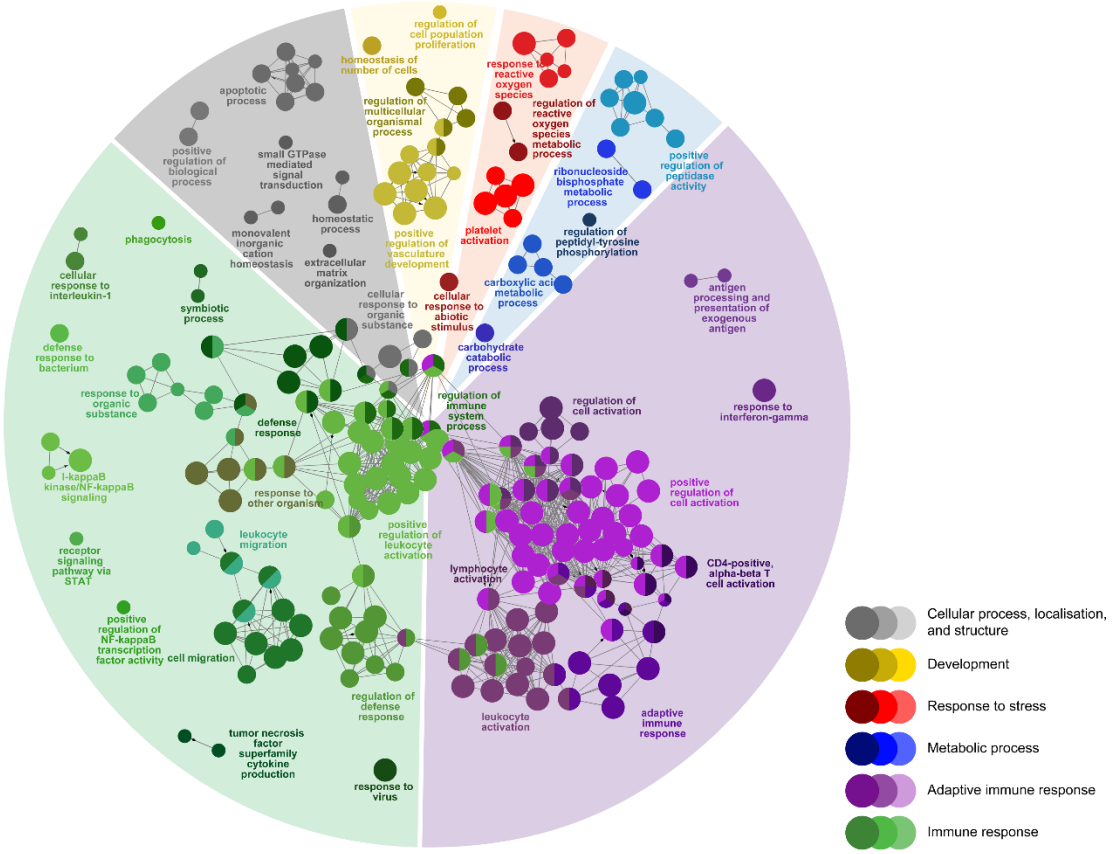

Figure 3.4. Enriched biological processes GO term networks of SRS-responsive probes (n = 1470) in the head kidney of Atlantic salmon at 21 days post-injection (DPI) shared by both H-SRS and L-SRS groups. Nodes represent significantly enriched GO terms [right-sided hypergeometric test, p-values ($p < 0.01$) corrected by Benjamini-Hochberg]. GO terms are grouped by functional theme and arranged to fit the sectors of a pie chart representing the proportion of GO terms in each functional theme. Nodes are coloured according to the functional theme to which they were assigned. Grey lines in between GO terms indicate high connectivity (kappa coefficient > 0.5). Lines with arrows indicate the direction of positive regulation between GO terms, and lines with diamonds indicate the direction of regulation between GO terms.

"phagocytosis", "defense response to bacterium", "response to interleukin-1", "response to virus", "chemotaxis", "leukocyte migration", "inflammatory response") and regulation of immune response (e.g. "regulation of I-kappaB kinase/NF-kappaB signalling", "regulation of defense response", "regulation of leukocyte migration") were activated in response to SRS infection. In addition, pathways related to various cellular processes (e.g. "positive regulation of programmed cell death", "positive regulation of peptidase activity", "homeostatic process") were regulated in *P. salmonis*-infected salmon (**Figure 3.4**; **Supplemental Table S3.4**). Lastly, SRS affected head kidney genes related to development (e.g. "positive regulation of vasculature development"), metabolic process (e.g. "carboxylic acid metabolic process"), and response to stress (e.g. "regulation of reactive oxygen species metabolic process") (**Figure 3.4**; **Supplemental Table S3.4**).

There were 166 DEPs only identified in the L-SRS group (L-SRS *vs* Control) associated with several immune-related BP terms (73.6%), including "response to type I interferon", "regulation of cytokine-mediated signaling pathway", and "alpha-beta T cell activation". In addition, many of these DEPs were involved in cellular process, localisation, and structure (26.3%), such as "regulation of muscle cell apoptotic process" and "actin filament-based movement" (**Figure 3.5A**; **Supplemental Table S3.5**). A much larger set of DEPs (n = 1606) was identified only in the H-SRS group (H-SRS *vs* Control), and their over-represented BP terms (n = 269; **Figure 3.5B**; **Supplemental Table S3.6**) were similar in number and diversity to the enriched terms associated with the overlapping SRS-responsive DEPs. Briefly, 37.5% of the enriched BP terms were linked with the adaptive

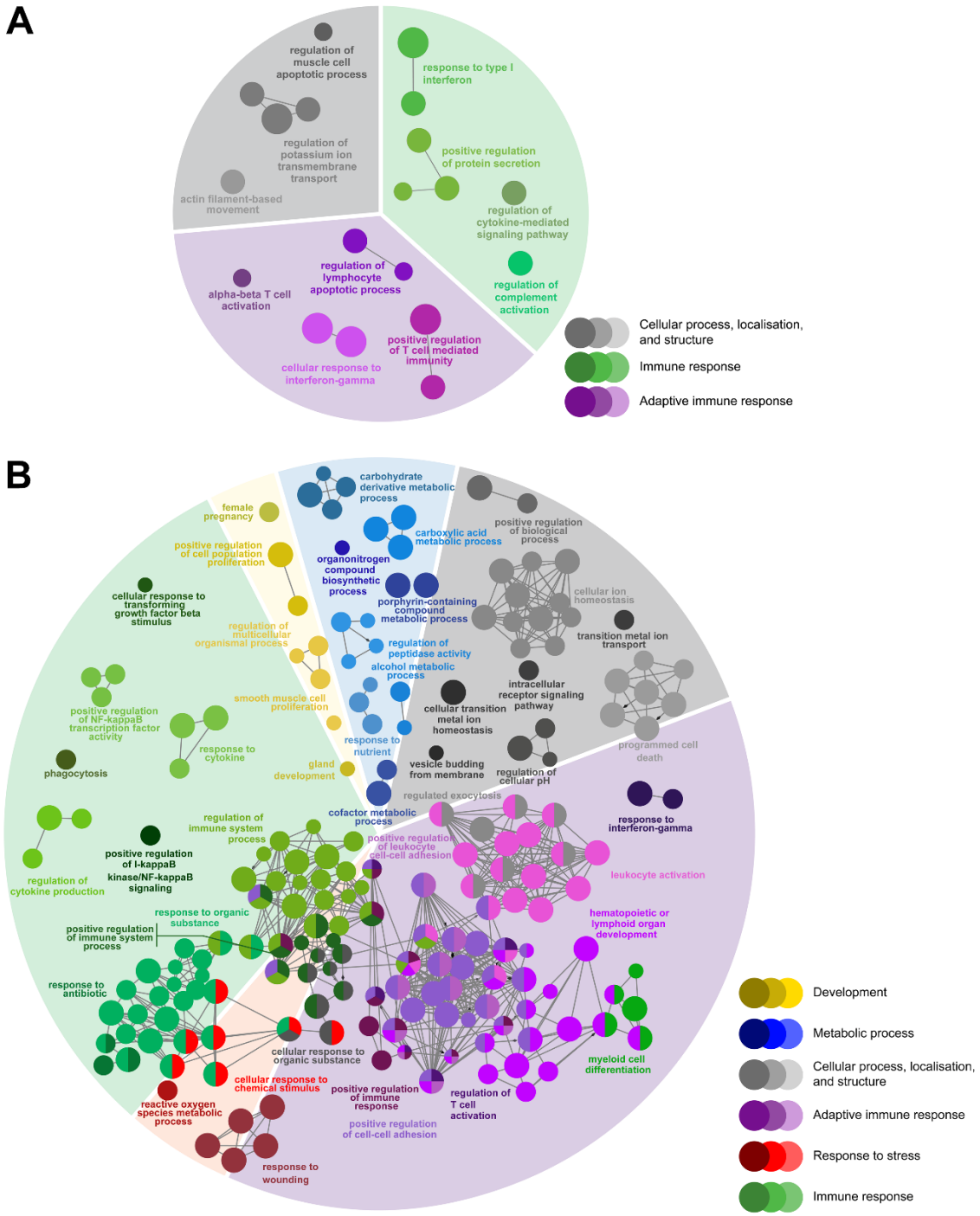
A
regulation of muscle cell apoptotic process
regulation of potassium ion transmembrane transport
actin filament-based movement
response to type I interferon
positive regulation of protein secretion
regulation of cytokine-mediated signaling pathway
regulation of complement activation
regulation of lymphocyte apoptotic process
alpha-beta T cell activation
positive regulation of T cell mediated immunity
cellular response to interferon-gamma
Cellular process, localisation, and structure
Immune response
Adaptive immune response
B
carbohydrate derivative metabolic process
carboxylic acid metabolic process
positive regulation of biological process
female pregnancy
positive regulation of cell population proliferation
organonitrogen compound biosynthetic process
porphyrin-containing compound metabolic process
cellular ion homeostasis
transition metal ion transport
cellular response to transforming growth factor beta stimulus
regulation of multicellular organismal process
regulation of peptidase activity
alcohol metabolic process
intracellular receptor signaling pathway
cellular transition metal ion homeostasis
positive regulation of NF-kappaB transcription factor activity
smooth muscle cell proliferation
response to cytokine
response to nutrient
programmed cell death
phagocytosis
gland development
vesicle budding from membrane
regulation of cellular pH
regulated exocytosis
cofactor metabolic process
response to interferon-gamma
regulation of immune system process
positive regulation of leukocyte cell-cell adhesion
positive regulation of I-kappaB kinase/NF-kappaB signaling
leukocyte activation
regulation of cytokine production
response to organic substance
positive regulation of immune system process
hematopoietic or lymphoid organ development
response to antibiotic
cellular response to organic substance
myeloid cell differentiation
cellular response to chemical stimulus
positive regulation of immune response
regulation of T cell activation
reactive oxygen species metabolic process
positive regulation of cell-cell adhesion
response to wounding
Development
Metabolic process
Cellular process, localisation, and structure
Adaptive immune response
Response to stress
Immune response

Figure 3.5. Enriched biological processes GO term networks of (**A**) SRS-responsive probes only identified in L-SRS group (n = 166) and (**B**) SRS-responsive probes only identified in H-SRS group (n = 1606) in the head kidney of Atlantic salmon at 21 days post-injection (DPI). Nodes represent significantly enriched GO terms [right-sided hypergeometric test, p-values corrected by Benjamini-Hochberg of 0.01 (i.e. FDR = 1%)]. GO terms are grouped by functional theme and arranged to fit the sectors of a pie chart representing the proportion of GO terms in each functional theme. Nodes are coloured according to the functional theme to which they were assigned. Grey lines in between GO terms indicate high connectivity (kappa coefficient > 0.5). Lines with arrows indicate the direction of positive regulation between GO terms, and lines with diamonds indicate the direction of regulation between GO terms.

immune response (e.g. “regulation of T cell activation”, “response to interferon-gamma”, “B cell differentiation”, “hematopoietic or lymphoid organ development”), and 31.2% were associated with the immune response (e.g. “myeloid cell differentiation”, “regulation of cytokine production”) (**Figure 3.5B**; **Supplemental Table S3.6**). The enriched BPs in the transcript list only identified in the H-SRS group also included terms related to cellular process, localisation, and structure (15.6%; e.g. “cellular transition metal ion homeostasis”, “programmed cell death”, “vesicle budding from membrane”), metabolic process (7.8%; e.g. “carbohydrate derivative metabolic process”), response to stress (4.8%; e.g. “reactive oxygen species metabolic process”), and development (3.0%; e.g. “regulation of multicellular organismal process”) (**Figure 3.5B**; **Supplemental Table S3.6**).

3.4.5 qPCR confirmation

Forty-two transcripts representing various molecular pathways [innate immune response (i.e. antibacterial response, inflammatory response, immune lipid mediators, antiviral response), cellular immunity (i.e. leukocyte activation and migration, antigen presentation and recognition), and other physiological processes (i.e. oxidative stress response, iron metabolism, apoptosis)] based on GO term enrichment analyses were selected for qPCR confirmation using a complete set of biological replicates collected at 21 DPI (total n = 37; 11 L-SRS, 17 H-SRS, and 9 CON). All of the transcripts evaluated for qPCR confirmation, except for *frrs1b*, agreed with the microarray results in the direction of change (i.e. up- or down-regulation) (**Figures 3.6-3.8**). In addition, the $\log_2$ fold-change values calculated from microarray and qPCR data showed a highly significant

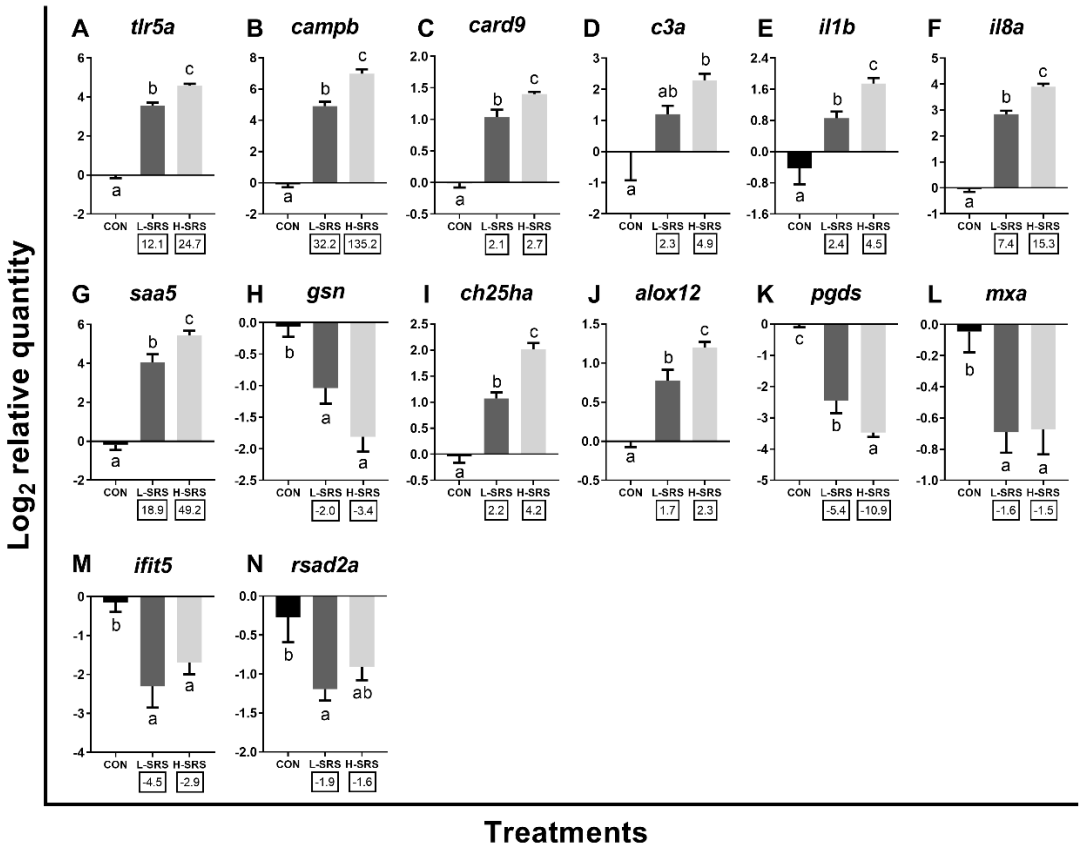

Figure 3.6. qPCR analyses of *P. salmonis*-responsive genes involved in the innate immune response. Fish with lower (L-SRS; n = 11) and higher (H-SRS; n = 17) level of *P. salmonis* infection at 21 days post-injection (DPI) as well as time-matched control (CON; n = 9) were used for qPCR confirmation. Average $\log_2$ RQs with SE bars are plotted. Different letters represent the significant differences among treatments ($p < 0.05$) with fold-change relative to control indicated below the x-axis. For qPCR fold-change calculation, overall fold up-regulation was calculated as 2^{A-B}, where A is the mean of $\log_2$ RQ from the L-SRS or H-SRS groups, and B is the mean of $\log_2$ RQ from the CON group. For down-regulated transcripts, fold-change values were further inverted (-1/fold-change). (**A**) *toll-like receptor 5a*; (**B**) *cathelicidin antimicrobial peptide b*; (**C**) *caspase recruitment domain-containing protein 9*; (**D**) *complement c3a*; (**E**) *interleukin 1 beta*; (**F**) *interleukin 8a* (alias *C-X-C motif chemokine ligand 8a*); (**G**) *serum amyloid A-5 protein*; (**H**) *gelsolin precursor*; (**I**) *cholesterol 25-hydroxylase a*; (**J**) *arachidonate 12-lipoxygenase, 12S-type*; (K) *lipocalin-type prostaglandin D synthase*; (**L**) *interferon-induced GTP-binding protein Mx a*; (**M**) *interferon-induced protein with tetratricopeptide repeats 5*; (**N**) *radical S-adenosyl methionine domain-containing protein 2a*.

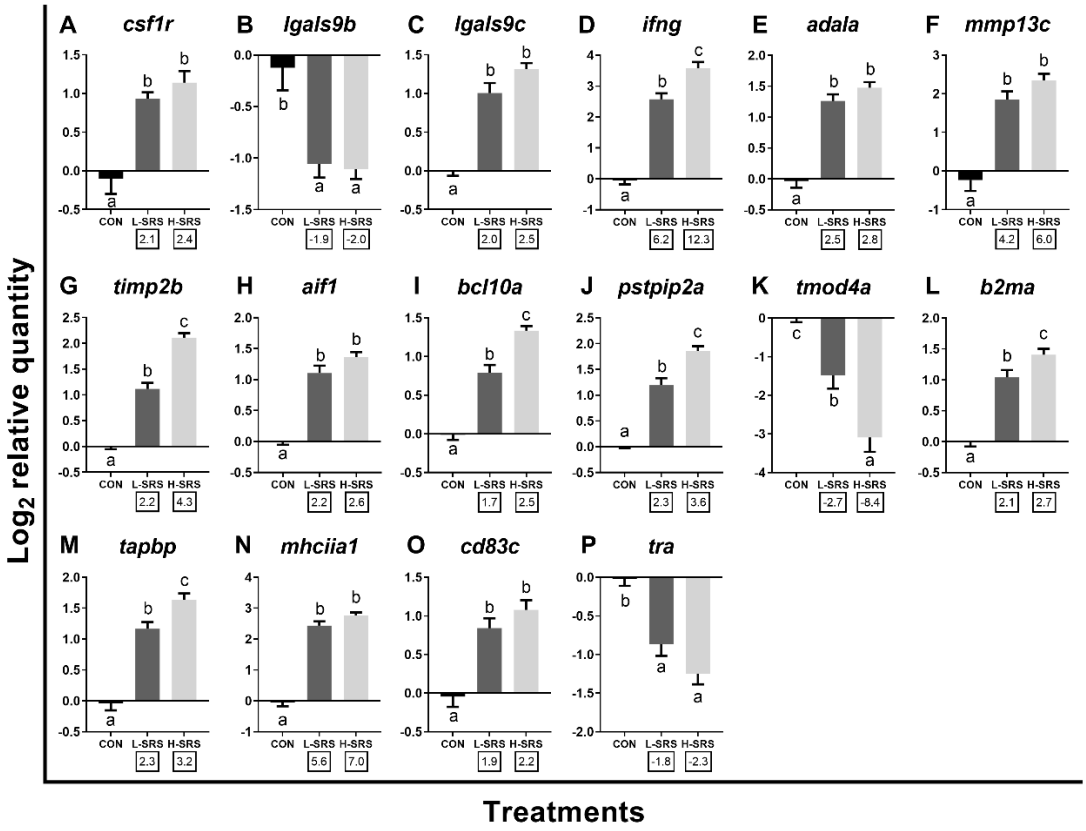

Figure 3.7. qPCR analysis of *P. salmonis*-responsive genes involved in cellular immunity (e.g. leukocyte activation and function). Fish with lower (L-SRS; n = 11) and higher (H-SRS; n = 17) level of *P. salmonis* infection at 21 days post-injection (DPI) as well as time-matched control (CON; n = 9) were used for qPCR confirmation. Average $\log_2$ RQs with SE bars are plotted. Different letters represent the significant differences among treatments ($p < 0.05$) with fold-change relative to control indicated below the x-axis. For qPCR fold-change calculation, overall fold up-regulation was calculated as 2^{A-B}, where A is the mean of $\log_2$ RQ from the L-SRS or H-SRS groups, and B is the mean of $\log_2$ RQ from the CON group. For down-regulated transcripts, fold-change values were further inverted (-1/fold-change). (**A**) *macrophage colony-stimulating factor 1 receptor*; (**B**) *galectin 9b*; (**C**) *galectin 9c*; (**D**) *interferon gamma;* (**E**) *adenosine deaminase-like a*; (**F**) *matrix metalloproteinase 13c*; (**G**) *metalloproteinase inhibitor 2b* (alias: *tissue inhibitor of metalloproteinase 2b*); (**H**) *allograft inflammatory factor 1*; (**I**) *B-cell lymphoma/leukemia 10a*; (**J**) *proline-serine-threonine phosphatase-interacting protein 2a*; (**K**) *tropomodulin-4a*; (**L**) *beta-2-microglobulin precursor a*; (**M**) *tapasin*; (**N**) *MHC class II antigen alpha chain 1*; (**O**) *cd83 antigen c*; (**P**) *T cell receptor alpha*.

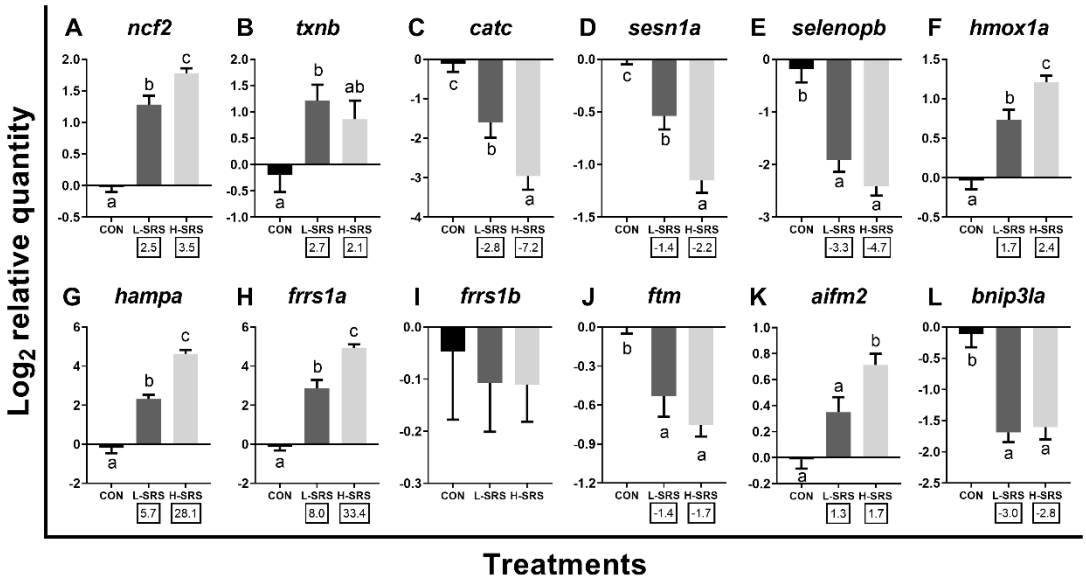

Figure 3.8. qPCR analysis of *P. salmonis*-responsive genes involved in redox homeostasis and other cellular processes. Fish with lower (L-SRS; n = 10) and higher (H-SRS; n = 16) level of *P. salmonis* infection at 21 days post-injection (DPI) as well as time-matched control (CON; n = 8) were used for qPCR confirmation. Average $\log_2$ RQs with SE bars are plotted. Different letters represent the significant differences among treatments ($p < 0.05$) with fold-change relative to control indicated below the x-axis. For qPCR fold-change calculation, overall fold up-regulation was calculated as 2^{A-B}, where A is the mean of $\log_2$ RQ from the L-SRS or H-SRS groups, and B is the mean of $\log_2$ RQ from the CON group. For down-regulated transcripts, fold-change values were further inverted (-1/fold-change). (**A**) *neutrophil cytosol factor 2*; (**B**) *thioredoxin b*; (**C**) *catalase c*; (**D**) *sestrin-1a*; (**E**) *selenoprotein p b*; (**F**) *heme oxygenase 1a*; (**G**) *hepcidin a*; (**H**) *ferric-chelate reductase 1a*; (**I**) *ferric-chelate reductase 1b*; (**J**) *ferritin, middle subunit*; (**K**) *apoptosis inducing factor mitochondria associated 2*; (**L**) *BCL2/adenovirus E1B 19 KDa protein-interacting protein 3-like a*.

correlation (R^2 = 0.8653; p < 0.0001), showing excellent overall confirmation of the microarray results by qPCR (**Supplemental Figure S3.3**).

qPCR results for 14 transcripts involved in the innate immune response are shown in Figure 6. Expression levels of *tlr5a*, *campb*, *card9*, *il1b*, *il8a*, *saa5*, *ch25ha* and *alox12* were significantly induced by *P. salmonis* infection in both H-SRS and L-SRS groups (**Figure 3.6A-C,E-G,I,J**). On the contrary, SRS-induced expression of *c3a* was only significant in the H-SRS group (**Figure 3.7D**). The expression levels of *gsn*, *pgds*, and three well-known antiviral genes (*rsad2a*, *ifit5*, *mxa*) were repressed by *P. salmonis* infection in both the H-SRS and L-SRS groups except for *rsad2a*, which only showed a significant difference between L-SRS and the control (**Figure 3.6H,K-N**). All genes in this category, except for the three antiviral genes, exhibited infection level-dependent up-regulation (e.g. *tlr5a*, *campb*, *il8a*, *il1b*, *saa5*, *c3a*) or down-regulation (i.e. *gsn*, *pgds*). Sixteen transcripts playing roles in the leukocyte activation and function were subjected to qPCR analysis in the current study (**Figure 3.7**). Genes related to leukocyte activation, differentiation and migration (i.e. *csf1r*, *lgals9c*, *ifng*, *adala*, *mmp13c*, *timp2b*, *aif1*, *bcl10a*, *pstip2a*) were induced in both L-SRS and H-SRS groups, whereas the expression of two other genes (*lgals9b* and *tmod4a*) were repressed compared with the control fish (**Figure 3.7A-K**). *P. salmonis* infection significantly induced four genes related to antigen presentation (*mhciia1*, *tapbp*, *cd83c*, *b2ma*); however, it suppressed the expression of *tra* (encoding T cell receptor alpha, which is involved in antigen recognition) in both L-SRS and H-SRS groups (**Figure 3.7L-P**). Overall, in this category, 6 genes showed infection

level-dependent up-regulation (*ifng*, *timp2b*, *bcl10a*, *pstpip2a*, *b2ma*, *tapbp*), and 1 gene showed infection level-dependent down-regulation (*tmod4a*).

Expression levels of 12 transcripts encoding proteins related to other physiological processes (i.e. redox homeostasis, iron metabolism, and apoptosis) were also evaluated (**Figure 3.8**). Among the 5 genes related to the oxidative stress response, 2 of them (*ncf2*, *txnb*) had increased expression in fish infected with *P. salmonis* (with *txnb* only significant for L-SRS group), while the other three transcripts (*catc*, *sesn1a*, *selenopb*) showed the opposite regulation (**Figure 3.8A-E**). Considering iron metabolism-related transcripts, expression levels of *hmox1a*, *hampa,* and *frrs1a* were significantly higher in fish infected with *P. salmonis,* whereas the level of *frrs1b* was not affected (**Figure 3.8F-I**). In addition, SRS suppressed the transcript expression of *ftm* (**Figure 3.8J**). Considering apoptotic relevant genes, the expression levels of *aifm2* and *bnip3la* were higher (only for H-SRS) and lower in fish infected with *P. salmonis* compared with the control, respectively (**Figure 3.8K,L**). Overall, 4 genes (*ncf2*, *hmox1a*, *hampa*, *frrs1a*) exhibited infection level-dependent up-regulation, and 2 genes (*catc*, *sesn1a*) showed infection level-dependent down-regulation among all genes in this category.

3.4.6 Correlation analyses for the expression of qPCR-assessed transcripts with the level of *P. salmonis* infection

Of the 42 qPCR-analyzed transcripts, 25 showed a significant correlation with the level of *P. salmonis* infection (**Table 3.1**). The RQ values of *hampa*, *frrs1a*, *il8a*, *timp2b*, *campb*, *tlr5a*, *ifng*, *ch25ha*, *il1b*, *pstpip2a*, *bcl10a*, *saa5*, *tapbp*, *card9*, *ncf2*, *hmox1a*,

Table 3.1. Correlation analyses for the expression of qPCR-studied transcripts with the level of *P. salmonis* infection.

Transcript[1]	Direction of change[2]	Pearson r	*p*-value	Theme	Putative Function
Significant positive correlation					
hampa	Up-regulation	0.841	<0.001	Other physiological processes	Iron metabolism
frrs1a	Up-regulation	0.777	<0.001	Other physiological processes	Iron metabolism
il8a	Up-regulation	0.775	<0.001	Innate immune response	Inflammatory response
timp2b	Up-regulation	0.760	<0.001	Cellular immunity	Leukocyte migration
campb	Up-regulation	0.750	<0.001	Innate immune response	Antibacterial response
tlr5a	Up-regulation	0.703	<0.001	Innate immune response	Antibacterial response
ifng	Up-regulation	0.689	<0.001	Cellular immunity	Leukocyte activation
ch25ha	Up-regulation	0.681	<0.001	Innate immune response	Immune lipid mediators
il1b	Up-regulation	0.676	<0.001	Innate immune response	Inflammatory response
pstpip2a	Up-regulation	0.646	<0.001	Cellular immunity	Leukocyte migration
bcl10a	Up-regulation	0.577	0.001	Cellular immunity	Leukocyte migration
saa5	Up-regulation	0.569	0.002	Innate immune response	Inflammatory response
tapbp	Up-regulation	0.496	0.007	Cellular immunity	Antigen presentation and recognition
card9	Up-regulation	0.467	0.012	Innate immune response	Inflammatory response
ncf2	Up-regulation	0.450	0.016	Other physiological processes	Oxidative stress response
hmox1a	Up-regulation	0.421	0.026	Other physiological processes	Iron metabolism
alox12	Up-regulation	0.413	0.029	Innate immune response	Immune lipid mediators
aifm2	Up-regulation	0.385	0.043	Other physiological processes	Apoptosis
c3a	Up-regulation	0.378	0.047	Innate immune response	Antibacterial response
Significant negative correlation					
sesn1a	Down-regulation	-0.796	<0.001	Other physiological processes	Oxidative stress response
pgds	Down-regulation	-0.640	<0.001	Innate immune response	Immune lipid mediators
selenopb	Down-regulation	-0.552	0.002	Other physiological processes	Oxidative stress response
gsn	Down-regulation	-0.521	0.004	Innate immune response	Inflammatory response
ftm	Down-regulation	-0.441	0.019	Other physiological processes	Iron metabolism
tra	Down-regulation	-0.419	0.026	Cellular immunity	Antigen presentation and recognition
Non-significant correlation					
tmod4a	Down-regulation	-0.351	0.067	Cellular immunity	Leukocyte migration
catc	Down-regulation	-0.342	0.075	Other physiological processes	Oxidative stress response
mhciia1	Up-regulation	0.298	0.124	Cellular immunity	Antigen presentation and recognition
lgals9c	Up-regulation	0.269	0.167	Cellular immunity	Leukocyte activation
aif1	Up-regulation	0.249	0.201	Cellular immunity	Leukocyte migration
b2ma	Up-regulation	0.244	0.211	Cellular immunity	Antigen presentation and recognition
adala	Up-regulation	0.225	0.250	Cellular immunity	Leukocyte activation
mmp13c	Up-regulation	0.196	0.318	Cellular immunity	Leukocyte migration
lgals9b	Down-regulation	-0.156	0.427	Cellular immunity	Leukocyte activation
csf1r	Up-regulation	-0.097	0.624	Cellular immunity	Leukocyte activation
txnb	Up-regulation	-0.096	0.627	Other physiological processes	Oxidative stress response
frrs1b	-	0.090	0.647	Other physiological processes	Iron metabolism
mxa	Down-regulation	-0.069	0.727	Innate immune response	Antiviral response
cd83c	Up-regulation	0.063	0.751	Cellular immunity	Antigen presentation and recognition
ifit5	Down-regulation	-0.040	0.839	Innate immune response	Antiviral response
bnip3la	Down-regulation	-0.037	0.850	Other physiological processes	Apoptosis
rsad2a	Down-regulation	0.033	0.869	Innate immune response	Antiviral response

[1]Control fish were excluded from the current analysis. [2]Direction of transcript expression change as compared to the control groups. *hampa*, *hepcidin a*; *frrs1a*, *ferric-chelate reductase 1a*; *il8a*, *interleukin 8a*; *timp2b*, *metalloproteinase inhibitor 2b* (alias: *tissue inhibitor of metalloproteinase 2b*); *campb*, *cathelicidin antimicrobial peptide b*; *tlr5a*, *toll-like receptor 5a*; *ifng*, *interferon gamma*; *ch25ha*, *cholesterol 25-*

hydroxylase a; *il1b*, *interleukin 1 beta*; *pstpip2a*, *proline-serine-threonine phosphatase-interacting protein 2a*; *bcl10a*, *B-cell lymphoma/leukemia 10a*; *saa5*, *serum amyloid A-5 protein*; *tapbp*, *tapasin*; *card9*, *caspase recruitment domain-containing protein 9*; *ncf2*, *neutrophil cytosol factor 2*; *hmox1a*, *heme oxygenase 1a*; *alox12*, *arachidonate 12-lipoxygenase, 12S-type*; *aifm2*, *apoptosis inducing factor mitochondria associated 2*; *c3a*, *complement c3a*; *sesn1a*, *sestrin-1a*; *pgds*, *lipocalin-type prostaglandin D synthase*; *selenopb*, *selenoprotein p b*; *gsn*, *gelsolin precursor*; *ftm*, *ferritin, middle subunit*; *tra*, *T cell receptor alpha*; *tmod4a*, *tropomodulin-4a*; *catc*, *catalase c*; *mhciia1*, *MHC class II antigen alpha chain 1*; *lgals9c*, *galectin 9c*; *aif1*, *allograft inflammatory factor 1*; *b2ma*, *beta-2-microglobulin precursor a*; *adala*, *adenosine deaminase-like a*; *mmp13c*, *matrix metalloproteinase 13c*; *lgals9b*, *galectin 9b*; *csf1r*, *macrophage colony-stimulating factor 1 receptor*; *txnb*, *thioredoxin b*; *frrs1b*, *ferric-chelate reductase 1b*; *mxa*, *interferon-induced GTP-binding protein Mx a*; *cd83c*, *cd83 antigen c*; *ifit5*, *interferon-induced protein with tetratricopeptide repeats 5*; *bnip3la*, *BCL2/adenovirus E1B 19 KDa protein-interacting protein 3-like a*; *rsad2a*, *radical S-adenosyl methionine domain-containing protein 2a*.

alox12, *aifm2* and *c3a* were positively correlated with the infection level, whereas *sesn1a*, *pgds*, *selenopb*, *gsn*, *ftm* and *tra* showed significant negative correlations with the expression level of *P. salmonis ITS*. Interestingly, 13 out of the remaining 17 transcripts (*mhciia1*, *lgals9c*, *aif1*, *adala*, *mmp13c*, *lgals9b*, *csf1r*, *txnb*, *mxa*, *cd83c*, *ifit5*, *bnip3la*, *rsad2a*) that did not have significant correlations with the level of *P. salmonis* infection, still exhibited either an increase or decrease in their expression in infected groups compared with control fish; their expression did not differ between L-SRS and H-SRS groups (**Figures 3.6-3.8; Table 3.1**).

3.5 Discussion

3.5.1 A low mortality model of piscirickettsiosis in Atlantic salmon parr involving an EM-90-like strain but with a strong transcriptomic response in head kidney

Improved understanding of the molecular mechanisms involved in the host response to *P. salmonis* will accelerate the development of effective diagnostics, vaccines, therapeutics, and nutritional solutions to combat SRS. The present study used a robust microarray platform, the cGRASP-designed Agilent 44K salmonid oligonucleotide microarray (Jantzen et al., 2011), to explore the transcriptomic response of the Atlantic salmon head kidney from a low mortality *P. salmonis* EM-90-like strain infection in freshwater. EM-90-like strains represent an epidemiologically relevant group in the current situation of piscirickettsiosis (e.g. in Chilean salmon aquaculture) (Saavedra et al., 2017); however, it has received fewer research efforts compared with that of LF-89-like isolates. Piscirickettsiosis has often been reported in seawater-reared salmonids; the disease in coho

salmon and rainbow trout farmed in freshwater has also been documented previously (Bravo, 1994; Gaggero et al., 1995; Rozas and Enríquez, 2014). The lower incidence of SRS outbreaks in freshwater may be related to the instability of the bacterium in this environment (Rozas and Enríquez, 2014). Nevertheless, experimental infection trials have been successfully demonstrated in freshwater reared coho salmon, Atlantic salmon and rainbow trout with up to 98% mortalities (Almendras et al., 1997; House et al., 1999; Smith et al., 1999).

Two recent studies on the development of challenge models involving *P. salmonis* EM-90-like isolates in Atlantic salmon post-smolts showed extremely high mortalities (>95%) in both Trojan and cohabitant groups (Rozas-Serri et al., 2017; Meza et al., 2019a). In contrast, much lower mortalities (28.5-32.7%) were observed in fish injected with an EM-90-like strain in the present study. Although the life stages of salmon in the current study differed from previous challenge models, the lower mortality rate observed here is likely due to the lower amount/concentration of bacterial inoculum given to the fish. A low mortality EM-90-like *P. salmonis* infection model is needed to fill in the gaps in the current knowledge on piscirickettsiosis, and it can be an essential tool to develop and test future preventive measures (e.g. functional feed) against the disease.

The infection prevalence of *P. salmonis* in all fish analyzed was 100% at both 13 and 21 DPI, with the highest transcript level of *P. salmonis ITS* detected at 21 DPI (**Figure 3.2A,B**). Congruently, the screening of four well-known antibacterial biomarkers (*campb*, *hampa*, *il8a* and *tlr5a*) in salmon head kidney also showed similar immune response dynamics. Although different challenge models (IP *vs* cohabitation) were used, the current

results agree well with a previous study by Rozas-Serri et al. (2018a), where they found that the expression of many mediators of innate immunity (e.g. *il1b*, *il8*) correlated positively with the bacterial load in the head kidney of Atlantic salmon infected with an EM-90-like isolate. Based on the current assessment of immune biomarker gene expression and pathogen levels across all sampling time points, I focused my efforts on profiling the transcriptome response of Atlantic salmon head kidney to *P. salmonis* infection at 21 DPI, a time point that is likely to reveal the highest transcriptome modulation. In addition, all fish in the current study were infected with the same dose of *P. salmonis* inoculum; however, multivariate statistical analyses (i.e. PCA and clustering analysis) of infected fish at 21 DPI revealed two infection level phenotypes: a lower *P. salmonis* level with lower expression of antibacterial biomarkers (L-SRS); and a higher *P. salmonis* level with higher expression of antibacterial biomarkers (H-SRS) (**Supplemental Figure S3.1**). These two phenotypes observed in the current study are likely indicative of SRS resistance with H-SRS being more susceptible and L-SRS being less susceptible to *P. salmonis*.

Although several transcriptomic studies have examined the impact of *P. salmonis* infection in Atlantic salmon (Rise et al., 2004; Tacchi et al., 2011; Pulgar et al., 2015; Rozas-Serri et al., 2018b; Moraleda et al., 2021), only one study, carried out by Rozas-Serri et al. (2018b), focused on an EM-90-like isolate in post-smolts. Despite a relatively low mortality rate observed in the present study, I have identified a much larger set of *P. salmonis*-responsive molecular biomarkers (a total of 3,242 DEPs) in the head kidney of Atlantic salmon compared with the results (298 DEGs in the IP injection model) of Rozas-Serri et al. (2018b). Although the salmon's life stage differed between studies, the smaller

number of transcripts identified therein may be attributed to the difference in response to the studied time points (5 *vs* 21 days). There is a high variation in the transcriptomic response (i.e. total numbers of differentially expressed probes/genes) to infection in Atlantic salmon among studies involving other strains of *P. salmonis* (e.g. LF-89). For instance, the first transcriptome study using a 3.5K GRASP cDNA microarray identified 69 transcripts differentially expressed in response to *P. salmonis* in Atlantic salmon head kidney, following 14 days of infection (Rise et al., 2004). Pulgar et al. (2015) used the same time point (14 DPI) and a 32K cGRASP cDNA microarray, identified approximately 2,500 DEPs between infected and non-infected fish among Atlantic salmon families with varying levels of susceptibility to the infection. In contrast, only 207 *P. salmonis*-responsive transcripts in the head kidney of Atlantic salmon were detected two days post-infection using a different version of the 44K oligo microarray compared with the present study (Tacchi et al., 2011). As discussed earlier, this is likely due to a mild transcriptomic modulation during an early stage of *P. salmonis* infection.

To confirm the microarray results, 42 transcripts representing various molecular pathways [innate immune response (e.g. antibacterial response, inflammatory response), cellular immunity (e.g. leukocyte activation and migration), and other physiological processes (e.g. oxidative stress response, iron metabolism)] were subjected to qPCR analyses using larger numbers of biological replicates in addition to those that were included in the microarray study. All of the qPCR-analyzed transcripts, except for *frrs1b*, agreed with microarray results in the direction of change and statistical significance in at least one of the comparisons (i.e. L-SRS *vs* control or H-SRS *vs* control). A highly

significant correlation ($R^2 = 0.8653$; $p < 0.0001$) was also obtained between microarray and qPCR data, suggesting an excellent overall confirmation of microarray results by qPCR.

3.5.2 *P. salmonis* infection affects host innate immunity

In the present study, I examined the global gene expression response in both lower and higher *P. salmonis* level individuals compared with the time-matched control fish; the identified pathways overlapping between lower and higher infection level groups (L-SRS and H-SRS) may represent the core defense response in Atlantic salmon. The pathway enrichment analysis of SRS-responsive transcripts overlapping between both infection groups (1,470 DEPs) showed a large number of BPs (36.3%) associated with innate immune responses were regulated in response to *P. salmonis* infection (**Figure 3.4**; **Supplemental Table S3.4**). Enriched BP terms related to immune response include "positive regulation of NF-kappaB transcription factor activity", "defense response to bacterium", "regulation of inflammatory response", "response to interleukin-1", and "response to virus and chemotaxis". Similar to the current study, previous transcriptomic analyses of head kidneys in Atlantic salmon infected with *P. salmonis* revealed an activated innate immune defense response mechanism (Rise et al., 2004; Tacchi et al., 2011; Pulgar et al., 2015; Rozas-Serri et al., 2018b).

In the current study, 14 genes directly involved in the innate immune response were analyzed by qPCR (**Figure 3.6**). *P. salmonis* infection showed up-regulation of *tlr5a*, *campb*, *card9* and *c3a* in both L-SRS and H-SRS groups compared with the control, except for *c3a*, which was only significant in H-SRS group. The flagellin-dependent activation of

Tlr5, a pattern-recognition receptor (PRR), has been well recognized in mammals and a similar mechanism has been reported in some teleosts [e.g. rainbow trout and Japanese flounder (*Paralichthys olivaceus*)] (Zhang et al., 2014). However, some recent studies on non-motile bacterial infection models in Atlantic salmon (e.g. *P. salmonis* and *R. salmoninarum*) (Rozas-Serri et al., 2018b; Eslamloo et al., 2020a), as well as the current research, suggest that the induction of *tlr5a* in Atlantic salmon may not be flagellin-dependent. Transcripts *campb* and *c3a* encode an antimicrobial peptide and a complement protein, respectively; they are both essential members of humoral components of innate immunity against a large array of pathogens (Ellis, 2001). In agreement with my results, the transcript expression of Atlantic salmon *camp* and *c3* was induced in fish infected with EM-90-like *P. salmonis* isolate (Rozas-Serri et al., 2018b). Card9 is an adaptor protein that mediates signals from PRRs to activate inflammatory cytokines, playing a key role in the innate immune response to several intracellular pathogens in humans (Hsu et al., 2007). The increased expression of *campb*, *c3a*, and *card9* in fish infected with *P. salmonis* in the present study indicate stimulation of innate immune response.

The innate immune pathways activated by *P. salmonis* infection modulated the expression of *il1b*, *il8a*, *saa5*, and *gsn*, which are associated with inflammation and acute phase response. Il1b is one of the earliest expressed pro-inflammatory cytokines after activation of host PRRs (Zou and Secombes, 2016), and enables organisms to respond promptly to an infection by inducing a cascade of reactions leading to inflammation (Seppola et al., 2008). A member of the CXC chemokine family, Il8/Cxcl8, regulated by Il1b, functions as a chemotactic factor by recruiting specific subsets of leukocytes to sites

of inflammation and infection (Seppola et al., 2008). As in my study, Rozas-Serri et al. (2018a) observed up-regulation of both *il1b* and *il8* in the head kidney of Atlantic salmon challenged by LF-89-like and EM-90-like isolates. Saa5 plays a significant role in the acute phase response in animals suffering from infection or injury, and its transcript levels increased dramatically in rainbow trout with *Yersinia ruckeri* infection (Raida and Buchmann, 2009). In mammals, GSN is a crucial regulator of actin filament assembly and disassembly; however, recent evidence from mammals suggests that GSN inhibits the inflammatory and cytokine response induced by LPS and overexpression of GSN decreases inflammation and apoptosis in experimental allergic encephalomyelitis animals (Cheng et al., 2017; Gao et al., 2017). Moreover, in agreement with the current results, Eslamloo et al. (2020a) also showed the decreased expression of *gsn* in Atlantic salmon infected with *R. salmoninarum*. The suppressed *gsn* expression may enhance the overall inflammatory response in the *P. salmonis* infected Atlantic salmon.

The present study showed that *P. salmonis* infection modulated transcripts encoding lipid mediators (i.e. *ch25ha*, *alox12*, and *pgds*), which play vital roles in the innate immune response. Ch25h converts cholesterol to oxysterol 25-hydroxycholesterol to maintain cholesterol homeostasis (Abrams et al., 2020). Studies in mammals and fish suggested that Ch25h has additional functions in immunomodulation (e.g. antiviral and antibacterial activities) and can positively and negatively regulate the inflammatory responses (Zhang et al., 2019; Abrams et al., 2020; Zhao et al., 2020). Similar to my study, *R. salmoninarum* induced the expression of *ch25ha* in Atlantic salmon head kidney (Eslamloo et al., 2020a). Transcripts *alox12* and *pgds* encode enzymes that act on different

polyunsaturated fatty acid substrates to generate bioactive lipid mediators (e.g. eicosanoids) and mediate inflammatory response (Gómez-Abellán and Sepulcre, 2016; Zheng et al., 2020). The observed down-regulation of *pgds* in the head kidney of Atlantic salmon infected with *P. salmonis* in this study agrees well with previous Atlantic salmon infection and immune challenge models (Rise et al., 2004; Caballero-Solares et al., 2017; Eslamloo et al., 2020a). These data confirm that lipid mediators could be playing important roles in different infectious diseases in Atlantic salmon.

Three well-known antiviral (or viral-induced) biomarkers studied by qPCR (i.e. *mxa*, *ifit5*, and *rsad2a*) had decreased mRNA expression in fish infected with *P. salmonis* in the present study. Previous studies on sea lice infection models in Atlantic salmon showed similar down-regulation of several antiviral effector genes, including those that were regulated by the interferon pathway (Krasnov et al., 2012; Umasuthan et al., 2020). Further, sea lice-infected Atlantic salmon that had lower expression of antiviral genes showed higher infectious salmon anemia viral load and mortality (Barker et al., 2019). It is worth noting that the current microarray analyses also revealed increased expression of additional *mx* paralogues and other transcripts known to be involved in antiviral response (e.g. *interferon-induced protein 44*, *guanylate-binding protein 1*) (Power et al., 2015; Li et al., 2016) upon *P. salmonis* infection (**Supplemental Table S3.3**). Therefore, it is possible that some aspects of antiviral immunity were altered, which could influence their susceptibility to viral infection.

3.5.3 *P. salmonis* infection affects host cellular immunity

The present study showed that SRS influenced molecular pathways (e.g. "leukocyte migration", "leukocyte activation", "CD4-positive alpha-beta T cell activation", "antigen processing and presentation of exogenous antigen") involved in both innate and adaptive cellular immunity. More than one-third of over-represented BPs from the overlapping SRS-responsive transcript list (1,470 DEPs) were related to adaptive immunity. In contrast, relatively low numbers of *P. salmonis*-responsive transcripts associated with adaptive immune response were identified by other relevant studies (Rise et al., 2004; Tacchi et al., 2011; Pulgar et al., 2015; Rozas-Serri et al., 2018b). Nevertheless, Atlantic salmon infected with live *Renibacterium salmoninarum* (an intracellular Gram-positive bacterial pathogen, causative agent of Bacterial Kidney Disease) also revealed an extensive amount of adaptive immune processes being regulated (Eslamloo et al., 2020a).

Sixteen transcripts studied by qPCR in the current investigation play essential roles in leukocyte activation, migration, and function, and their mRNA levels in Atlantic salmon head kidney were significantly modulated by *P. salmonis* infection (**Figure 3.7**). For instance, *P. salmonis* induced four transcripts (i.e. *csf1r*, *lgals9c*, *ifng*, *adala*) and suppressed one transcript (i.e. *lgals9b*) that play putative roles in macrophage and/or lymphocyte activation. Csf1r acts as the receptor for colony stimulating factor 1, which regulates the production, differentiation, and function of monocytes/macrophages (Rojo et al., 2019). In grass carp (*Ctenopharyngodon idellus*), Csf1r was identified as a specific surface marker of monocytes/macrophages, and its transcript level in various tissues was elevated in fish infected with *Aeromonas hydrophila* (Chen et al., 2015). Mammalian

LGALS9 induces antibacterial activity in macrophages infected with *Mycobacterium tuberculosis* through macrophage activation and IL1B secretion (Sada-Ovalle et al., 2012), consistent with the up-regulation of one *lgals9* paralogue (i.e. *lgals9c*) in salmon infected with *P. salmonis* found in the present study. The opposite transcript expression change of *lgals9b* observed here suggests that these paralogues have undergone regulatory and potentially functional divergence. IFNG or type II interferon is a cytokine that exerts regulatory roles in both innate and adaptive immunity, including activating macrophages, enhancing antigen presentation and promoting T cell differentiation and activation (Tacchi et al., 2011; Wang and Secombes, 2013; Zou and Secombes, 2016; Eslamloo et al., 2020a). Adal, an enzyme involved in the salvage of purine nucleotides, also plays an important role in regulating T cell activation and differentiation (Dong et al., 1996; Martinez‐Navio et al., 2011).

The present qPCR study showed that *P. salmonis* infection modulated transcripts that play key roles in immune cell migration and actin/cytoskeleton reorganization (*mmp13c*, *timp2b*, *aif1*, *bcl10a*, *pstpip2a*, *tmod4a*) (**Figure 3.7**). Matrix metalloproteinases (MMPs) are a family of zinc-containing proteolytic enzymes that exert multiple roles in the immune response to infection, including facilitating leucocyte recruitment and migration, modulating cytokine and chemokine activity, and extracellular matrix remodelling (Elkington et al., 2005). In the zebrafish heart regeneration model, the inhibition of both Mmp9 and Mmp13 resulted in impaired tissue regeneration and leukocyte recruitment (Xu et al., 2018). However, excess Mmp activity following infection may lead to immunopathology favouring the pathogen, agreeing with the up-regulation of

transcript encoding Timp2b, a regulatory inhibitor of Mmps, in *P. salmonis*-infected salmon. The cytoskeleton and its components (e.g. different actins), well known for their roles in cell division, shape and movement, have essential functions in innate immunity and cellular self-defense (Mostowy and Shenoy, 2015; Rozas-Serri et al., 2018b; Moraleda et al., 2021). In mammals, transcripts encoding AIF1, PSTPIP2, and BCL10 positively regulate actin polymerization and/or filopodia formation, while Tmod4 prevents actin filaments from elongation (Chitu et al., 2005; Kelemen and Autieri, 2005; Rueda et al., 2007; Yamashiro et al., 2012; Zhao et al., 2013; Sikora et al., 2020). The activated actin polymerization is likely to contribute to the promotion of immune cell mobility and migration in *P. salmonis* infected animals (Pulgar et al., 2015). The transcript expression of *tmod4* in Atlantic salmon was also suppressed by *R. salmoninarum* (Eslamloo et al., 2020a). Future studies are needed to better understand the function of cytoskeletal remodelling during piscirickettsiosis. Part of the observed responses could contribute to phagocytosis, which may eliminate *P. salmonis* bacteria. At the same time, intracellular bacterial pathogens such as *P. salmonis* and *R. salmoninarum* likely need to modulate cytoskeleton rearrangements to favour their replication in host cells (Ramirez et al., 2015; Moraleda et al., 2021).

The activation of cytotoxic T lymphocytes by recognition of antigenic peptides presented on major histocompatibility complex (MHC) molecules associated with antigen-presenting cells (APCs) is a critical process in the adaptive immunity of vertebrates (Jørgensen et al., 2007; Grimholt, 2016). As shown by the current qPCR analyses, transcripts involved in antigen processing, presentation, and recognition (i.e. *b2ma*, *tapbp*,

mhciia1, *cd83c*, *tra*) were modulated by *P. salmonis* infection (**Figure 3.7**). B2m is a component of MHC class I molecules, which bind and present endogenously derived peptides to $CD8^+$ T-cells (Grimholt, 2016). Tapbp is an MHC class I antigen-processing molecule present in the endoplasmic reticulum that helps the stabilization of a multimeric peptide-loading complex (Jørgensen et al., 2007). Unlike MHC class I, the MHC class II molecules primarily reside on the surface of professional APCs such as dendritic cells which present the antigens derived from extracellular proteins to $CD4^+$ T-cells (Grimholt, 2016; Yamaguchi and Dijkstra, 2019). In mammals, CD83 is a member of the immunoglobulin (Ig) superfamily and a surface marker on mature dendritic cells (Li et al., 2019). In addition to the roles that CD83 plays in lymphocyte development, a previous study revealed that CD83 influences cell-surface MHC class II expression on B cells and other APCs in mice, therefore affecting antigen presentation (Kuwano et al., 2007). The increased transcript expression of genes involved in both MHC class I and II in the present study suggests the importance of antigen processing and presentation pathways in the Atlantic salmon response to SRS. Interestingly, the current microarray study showed lower transcript levels of T-cell receptors [represented by 63 probes for T-cell receptor alpha (*tra*) and 6 probes for T-cell receptor beta] in fish infected with *P. salmonis* (**Supplemental Table S3.3**) with the lower transcript level of *tra* confirmed by qPCR in both L-SRS and H-SRS fish. Tra is a protein complex found on the surface of T-cells responsible for recognizing fragments of antigen presented by MHC molecules (Castro et al., 2011). In agreement with the current results, previous studies also reported the lower level of *tra* in *P. salmonis*-infected Atlantic salmon head kidney (Rise et al., 2004; Tacchi et al., 2011).

CD274 could also play a role in the suspected suppression of T-cell activity/recruitment in the current study. This inhibitory receptor ligand, induced in both L-SRS and H-SRS fish (**Supplemental Table S3.3**), binds to the receptor PD-1, commonly expressed on T-cells, thereby blocking T-cell activation (Han et al., 2020).

3.5.4 *P. salmonis* infection affects other physiological processes

Apart from the regulation of immune pathways and processes, the current microarray data also showed genes involved in other physiological processes [e.g. "response to reactive oxygen species" (**Figure 3.4**), "transition metal ion transport" and "programmed cell death" (**Figure 3.5B**)] were affected in *P. salmonis*-infected Atlantic salmon. I selected 12 microarray-identified genes related to these processes for qPCR confirmation (**Figure 3.8**). It is well-known that reactive oxygen species (ROS) play a dual role in pathogenic infections (Pohanka, 2013). ROS (i.e. free radicals) can protect the host from invading pathogens. However, their overproduction can cause oxidative stress, resulting in tissue damage. The up-regulation of *ncf2*, part of the NADPH oxidase components (de Oliveira-Junior et al., 2011), suggests the elevated production of free radicals in response to *P. salmonis* infection. This result is consistent with the up-regulation of NADPH oxidase in the liver of Atlantic salmon infected with *P. salmonis* found in a previous study (Tacchi et al., 2011). Interestingly, the transcript encoding for the protein Txn, a critical antioxidant enzyme, was up-regulated only in L-SRS group. The up-regulation of *txnb* in L-SRS group may be a protective response to oxidative stress resulting from *P. salmonis* infection. In the current study, *P. salmonis* infection also suppressed transcripts encoding enzymes that are important in the antioxidant defense system (e.g.

catc, *sesn1a*, and *selenopb*). Similar results for *selenopb* transcript expression was reported in a previous study on Atlantic salmon head kidney infected with *P. salmonis* (Rise et al., 2004). Moreover, Rozas-Serri et al. (2018b) found that more than 10 genes associated with the anti-oxidative response were down-regulated in the head kidney of *P. salmonis* infected Atlantic salmon. These results suggest that *P. salmonis* infection modulates the host antioxidant system, which may result in severe tissue damage.

Iron is a crucial nutrient for the survival of bacteria and a key regulator of the host-pathogen interaction (Doherty, 2007). Of the iron metabolism relevant genes studied by qPCR, the current results showed that *P. salmonis* infection up-regulated the expression of *hampa*, *frrs1a* and *hmox1a*, and down-regulated the expression of *ftm* in both the L-SRS and H-SRS groups. It is well-known that HAMP exhibits antimicrobial activity against bacteria and fungi (Park et al., 2001). It also plays a key role in the maintenance of iron homeostasis and the negative regulation of iron efflux in macrophages (Nemeth et al., 2004; Michels et al., 2015). FRRS1 (also referred to as SDR2) reduces ferric to ferrous iron before its transport from the endosome to the cytoplasm (Vargas et al., 2003). Iron withholding response or nutritional immunity is a process initiated by infection-induced inflammation that aims to deprive invading pathogens from circulating iron; the host sequesters iron within intracellular pools which is thought to starve pathogens of this essential nutrient further limiting disease progression (Cherayil, 2011; Díaz et al., 2021). The activation of nutritional immunity was evidenced by the up-regulation of *hampa*, *frrs1a*, *haptoglobin* and *hemopexin* (microarray-identified; **Supplemental Table S3.3**) that increase iron intracellular storage, while the slight down-regulation of *ftm* suggests that the

response needs to be finely tuned. Pulgar et al. (2015) found that significant up-regulation of *hamp* was only shown in Atlantic salmon families with high susceptibility to *P. salmonis* but not in the low susceptibility families. Given that *P. salmonis* is a facultative intracellular bacterium, iron withholding response may be more detrimental for the host and more beneficial to *P. salmonis* once established inside the cells. Recently, several groups have successfully treated *P. salmonis* infection with iron chelators (Valenzuela-Muñoz et al., 2020; Díaz et al., 2021) – induction of the nutritional immunity (iron withholding response) and limiting access of iron to bacteria under this condition appears to be a viable disease control strategy. The lack of sufficient amounts of extracellular iron resulted from iron withholding response likely had adverse consequences for the differentiation of red blood cells in the head kidney, which is considered to be the primary site of erythropoiesis in teleost fish (Witeska, 2013). This was evidenced by the decrease in the expression of erythrocyte-specific genes (e.g. *spectrin beta chain* and *hemoglobin*) (Liem, 2016), and a gene governing erythropoiesis (*erythropoietin receptor*) (Watowich, 2011) in *P. salmonis* infected fish as shown by the current microarray analyses (**Supplemental Table S3.3**). The increased transcript expression of *hmox1*, an essential enzyme in the breakdown of heme originating from degraded senescent erythrocytes and heme-proteins, producing equal amounts of iron, carbon monoxide and biliverdin (Cassat and Skaar, 2013), suggested that the heme metabolism was also affected by SRS.

My results suggest that *P. salmonis* infection affects the host redox status, which may influence cell death and necrosis. Previous studies have shown that *P. salmonis* modulates cellular apoptosis to enable their replication and survival within the host cells

(Rise et al., 2004; Tacchi et al., 2011; Rozas-Serri et al., 2018b; Moraleda et al., 2021). Of the apoptosis-related genes studied by qPCR, the current results revealed that *P. salmonis* infection up-regulated the expression of *aifm2* in H-SRS and down-regulated the expression of *bnip3la* in both the L-SRS and H-SRS groups. Human AIFM2 (also referred to as AMID) has a pro-apoptotic function and is a p53 target to promote caspase-independent cell death (Gong et al., 2007). Bnip3 is another pro-apoptotic gene that belongs to the Bcl-2 protein family (Burton and Gibson, 2009). Moraleda et al. (2021) also showed that *bnip3* was down-regulated in Atlantic salmon during SRS infection, and it was positively correlated with resistance to SRS. Taken together, these results suggest that the host apoptotic pathways might be modulated by *P. salmonis* infection.

3.5.5 Genes and their expression that might be associated with SRS resistance

As mentioned earlier, the present study also aimed to explore the transcriptomic differences between individuals having higher and lower pathogen loads (L-SRS *vs* H-SRS), which could potentially provide insight into disease resistance mechanisms (11, 27, 28). At the pathway level (i.e. GO term enrichment), I analyzed two groups of DEPs between infected and non-infected fish. The first group included 166 probes that were significantly modulated only in the L-SRS group, and the second group had 1606 probes that were significantly modulated only in the H-SRS group. Although a relatively small number of DEPs were exclusive to the L-SRS group, the enriched GO terms were primarily associated with the immune response (36.8%; e.g. “response to type I interferon”, “regulation of complement activation”) and the adaptive immune response (36.8%; e.g. “alpha-beta T cell activation” and “cellular response to interferon-gamma”), suggesting the

importance of these pathways (e.g. IFN-mediated) for the positive outcome of *P. salmonis* infection. The enriched GO terms associated with 1606 DEPs responsive only in the H-SRS group were similar to the enriched terms related to the overlapping SRS-responsive genes in terms of number and diversity. It included not only pathways related to immune responses but also pathways representing more general physiological processes such as development, metabolic process, and response to stress. This observation suggests that the transcriptional response to *P. salmonis* in the H-SRS group was more pronounced compared with the L-SRS group. In a previous *P. salmonis* challenge study in Atlantic salmon, resistant individuals had lower levels of bacterial load and higher expression of *c-type lysozyme* in head kidney, while susceptible fish presented with higher levels of bacterial load and higher expression of pro-inflammatory genes and genes involved in acute phase response (Dettleff et al., 2015). As indicated by several studies of bacterial (Škugor et al., 2009; Braden et al., 2019) and viral diseases (Jørgensen et al., 2008; Timmerhaus et al., 2012; Martinez-Rubio et al., 2014) in salmonids, exaggerated innate immune responses are often linked to increase in pathology and other adverse outcomes.

At the gene level, I correlated the levels of qPCR-analyzed transcripts with the *P. salmonis* level. Among them, 19 transcripts had a significant positive correlation with the *P. salmonis* level, and many of them are related to iron metabolism (e.g. *hampa*, *frrs1a*), inflammatory response (e.g. *il8a*, *saa5*), antibacterial response (e.g. *campb*, *c3a*) and leukocyte function (e.g. *ifng*, *bcl10a*). There were 6 transcripts that had a significantly negative correlation with the *P. salmonis* level; these included genes involved in oxidative stress response (i.e. *sesn1a*, *selenopb*). As discussed earlier, some of these infection level-

dependent responses (e.g. antibacterial response) are beneficial in eliminating the pathogen, while others (e.g. inflammatory response, iron withholding response) may be detrimental to the host. The significant correlations of these transcripts with the infection level suggest they could be suitable biomarkers for the assessment of infection level-dependent SRS responses in Atlantic salmon. It is worth mentioning that 13 qPCR-analyzed transcripts had a similar magnitude of increase or decrease in expression between the L-SRS and H-SRS groups. Among these were genes involved in cellular immunity [leukocyte function (e.g. *lgals9b*, *lgals9c*, *aif1*, *adala*, *mmp13c*, *csf1r*), antigen presentation and recognition (e.g. *mhciia1*, *cd83c*)], antiviral response (e.g. *mxa*, *ifit5*, *rsad2a*), apoptosis (*bnip3la*), and oxidative stress response (*txnb*). These results suggest that the L-SRS fish can effectively modulate those important immune pathways, which may be key for SRS resistance.

3.6 Conclusion

The time-course analyses of pathogen load and four biomarkers of innate immunity in the head kidney of Atlantic salmon parr challenged with EM-90-like *P. salmonis* bacterium revealed two groups of fish with different infection levels at 21 DPI. Although the challenge resulted in a relatively low mortality rate, transcriptome profiling of infected fish revealed that piscirickettsiosis affected a great number of genes and pathways, particularly in the high infection group (i.e. H-SRS). High expression levels of genes involved in innate and adaptive immune processes were observed, while a relatively mild regulation of genes governing general physiological processes (e.g. development and metabolism) was seen in response to the *P. salmonis* infection. Furthermore, the

comparison of individuals with differing levels of infection (H-SRS *vs* L-SRS) generated insights into the biological processes possibly involved in natural resistance. A more pronounced immune response against infection at a late stage observed in H-SRS fish suggests that at least part of these responses was exaggerated and not protective. It is however also possible that the H-SRS fish need to maintain a stronger immune response in order to deal with the high pathogen load and prevent further bacterial growth. To help fully elucidate mechanisms responsible for different infection phenotypes (L-SRS and H-SRS) and protection against *P. salmonis* infection, examination of earlier time points (e.g. 2 DPI) and other relevant tissues (e.g. spleen and liver) are necessary. It should be noted that aspects such as route of infection, infection level, and patterns of disease spread during natural SRS outbreaks may differ from the IP injection model. Finally, this study demonstrated a low mortality EM-90-like *P. salmonis* infection model and qPCR-validated many SRS-responsive molecular biomarkers, which are valuable tools for future research (e.g. evaluation of novel functional feeds that often require low mortality outcomes) aimed at improving farmed Atlantic salmon resistance to SRS.

3.7 Supplemental materials

The Supplemental Tables and Figures for this chapter can be found in the supplemental materials of Xue et al. (2021) [available at: (https://www.frontiersin.org/articles/10.3389/fimmu.2021.789465/full#supplementary-material)]. These files (as listed below) have also been supplied in a zipped folder that accompanies this thesis.

Supplemental Table S3.1. Primers for pathogen load assessment and qPCR validation.

Supplemental Table S3.2. Sample inventory, RNA purity information, and pathogen load and antibacterial biomarker screening results.

Supplemental Table S3.3. Complete list of microarray identified SRS-responsive gene that were differentially expressed in the head kidney of Atlantic salmon (Significant Analysis of Microarray; FDR < 1%).

Supplemental Table S3.4. List of Biological Process GO terms enriched in SRS-responsive transcripts shared by both SRS groups (L-SRS and H-SRS) (1,470 DEPs). An additional table below shows the contribution (%) of each functional theme to the total number of over-represented GO terms.

Supplemental Table S3.5. List of Biological Process GO terms enriched in SRS-responsive transcripts identified only in L-SRS group (166 DEPs). An additional table below shows the contribution (%) of each functional theme to the total number of over-represented GO terms.

Supplemental Table S3.6. List of Biological Process GO terms enriched in SRS-responsive transcripts identified only in H-SRS group (1606 DEPs). An additional table

below shows the contribution (%) of each functional theme to the total number of over-represented GO terms.

Supplemental Figure S3.1. Classification of infection level phenotypes by multivariate statistical analyses and microarray experimental design. (**A**) principal component analysis (PCA) and (**B**) hierarchical clustering of the expression levels of *P. salmonis* ITS and antibacterial biomarkers (*campb*, *hampa*, *il8a* and *tlr5a*) of 21 DPI individuals. Hierarchical clustering analyses performed using Pearson's correlation resemblance matrices (PRIMER, Version 6.1.15, Ivybridge, UK). Two infection level phenotypes were identified except fish C7-8: one group of fish with higher levels of the *P. salmonis* ITS and the antibacterial biomarkers (H-SRS) and another group of fish with lower levels of the *P. salmonis* ITS and the antibacterial biomarkers (L-SRS). (**C**) Levels of *P. salmonis* ITS in fish classified as L-SRS and H-SRS compared to the control fish (CON). (**D**) microarray experimental design. Five fish from each group were selected and used for the transcriptome analyses.

Supplemental Figure S3.2. Hierarchical clustering analysis for a subset of SRS-responsive genes involved in adaptive immunity. All microarray analyzed samples were clustered based on probes having the associated GO term "adaptive immune response".

Supplemental Figure S3.3. Scatterplot of gene expression fold-change values (log_2) between treatments calculated from the microarray log_2 ratios and qPCR relative quantity

(RQ) values. Each dot represents the fold-change of treatment comparison (L-SRS *vs* control or H-SRS *vs* control) for a given gene.

3.8 Reference

Abrams, M.E., Johnson, K.A., Perelman, S.S., Zhang, L.-s., Endapally, S., Mar, K.B., Thompson, B.M., McDonald, J.G., Schoggins, J.W., Radhakrishnan, A., 2020. Oxysterols provide innate immunity to bacterial infection by mobilizing cell surface accessible cholesterol. Nat. Microbiol. 5, 929-942.

Almendras, F., Fuentealba, I., Jones, S., Markham, F., Spangler, E., 1997. Experimental infection and horizontal transmission of *Piscirickettsia salmonis* in freshwater - raised Atlantic salmon, *Salmo salar* L. J. Fish Dis. 20, 409-418.

Barker, S.E., Bricknell, I.R., Covello, J., Purcell, S., Fast, M.D., Wolters, W., Bouchard, D.A., 2019. Sea lice, *Lepeophtheirus salmonis* (Krøyer 1837), infected Atlantic salmon (*Salmo salar* L.) are more susceptible to infectious salmon anemia virus. PLoS One 14, e0209178.

Bindea, G., Mlecnik, B., Hackl, H., Charoentong, P., Tosolini, M., Kirilovsky, A., Fridman, W.-H., Pagès, F., Trajanoski, Z., Galon, J., 2009. ClueGO: a Cytoscape plug-in to decipher functionally grouped gene ontology and pathway annotation networks. Bioinformatics 25, 1091-1093.

Bo, T.H., Dysvik, B., Jonassen, I., 2004. LSimpute: accurate estimation of missing values in microarray data with least squares methods. Nucleic Acids Res. 32, e34.

Booman, M., Borza, T., Feng, C.Y., Hori, T.S., Higgins, B., Culf, A., Léger, D., Chute, I.C., Belkaid, A., Rise, M., Gamperl, A.K., Hubert, S., Kimball, J., Ouellette, R.J., Johnson, S.C., Bowman, S., Rise, M.L., 2011. Development and experimental validation of a 20K Atlantic cod (*Gadus morhua*) oligonucleotide microarray based on a collection of over 150,000 ESTs. Mar. Biotechnol. 13, 733-750.

Braden, L.M., Whyte, S.K., Brown, A.B., Vaniderstine, C., Letendre, C., Groman, D., Lewis, J., Purcell, S., Hori, T., Fast, M.D., 2019. Vaccine-induced protection against furunculosis involves pre-emptive priming of humoral immunity in Arctic charr. Front. Immunol. 10, 120.

Bravo, S., 1994. Piscirickettsiosis in freshwater. Bull. Eur. Assoc. Fish Pathol. 14, 137-138.

Bridle, A., Nosworthy, E., Polinski, M., Nowak, B., 2011. Evidence of an antimicrobial-immunomodulatory role of Atlantic salmon cathelicidins during infection with *Yersinia ruckeri*. PLoS One 6, e23417.

Burton, T.R., Gibson, S.B., 2009. The role of Bcl-2 family member BNIP3 in cell death and disease: NIPping at the heels of cell death. Cell Death Differ. 16, 515-523.

Caballero-Solares, A., Hall, J.R., Xue, X., Eslamloo, K., Taylor, R.G., Parrish, C.C., Rise, M.L., 2017. The dietary replacement of marine ingredients by terrestrial animal and plant alternatives modulates the antiviral immune response of Atlantic salmon (*Salmo salar*). Fish Shellfish Immunol. 64, 24-38.

Caballero-Solares, A., Xue, X., Parrish, C.C., Foroutani, M.B., Taylor, R.G., Rise, M.L., 2018. Changes in the liver transcriptome of farmed Atlantic salmon (*Salmo salar*) fed experimental diets based on terrestrial alternatives to fish meal and fish oil. BMC Genomics 19, 796.

Cassat, J.E., Skaar, E.P., 2013. Iron in infection and immunity. Cell Host & Microbe 13, 509-519.

Castro, R., Bernard, D., Lefranc, M., Six, A., Benmansour, A., Boudinot, P., 2011. T cell diversity and TcR repertoires in teleost fish. Fish Shellfish Immunol. 31, 644-654.

CCAC, 2005. Guidelines on: the care and use of fish in research, teaching and testing. Canadian Council on Animal Care.

Celton, M., Malpertuy, A., Lelandais, G., de Brevern, A.G., 2010. Comparative analysis of missing value imputation methods to improve clustering and interpretation of microarray experiments. BMC Genomics 11, 15.

Chen, Q., Lu, X.-J., Chen, J., 2015. Identification and functional characterization of the CSF1R gene from grass carp *Ctenopharyngodon idellus* and its use as a marker of monocytes/macrophages. Fish Shellfish Immunol. 45, 386-398.

Cheng, Y., Hu, X., Liu, C., Chen, M., Wang, J., Wang, M., Gao, F., Han, J., Sun, D., Zhang, C., 2017. Gelsolin inhibits the inflammatory process induced by LPS. Cell. Physiol. Biochem. 41, 205-212.

Cherayil, B.J., 2011. The role of iron in the immune response to bacterial infection. Immunol. Res. 50, 1-9.

Chitu, V., Pixley, F.J., Macaluso, F., Larson, D.R., Condeelis, J., Yeung, Y.G., Stanley, E.R., 2005. The PCH family member MAYP/PSTPIP2 directly regulates F-actin bundling and enhances filopodia formation and motility in macrophages. Mol. Biol. Cell 16, 2947-2959.

de Oliveira-Junior, E., Bustamante, J., Newburger, P.E., Condino‐Neto, A., 2011. The human NADPH oxidase: primary and secondary defects impairing the respiratory burst function and the microbicidal ability of phagocytes. Scand. J. Immunol. 73, 420-427.

Dettleff, P., Bravo, C., Patel, A., Martinez, V., 2015. Patterns of *Piscirickettsia salmonis* load in susceptible and resistant families of *Salmo salar*. Fish Shellfish Immunol. 45, 67-71.

Díaz, R., Troncoso, J., Jakob, E., Skugor, S., 2021. Limiting access to iron decreases infection of Atlantic salmon SHK-1 cells with bacterium *Piscirickettsia salmonis*. BMC Vet. Res. 17, 155.

Doherty, C.P., 2007. Host-pathogen interactions: the role of iron. J. Nutr. 137, 1341-1344.

Dong, R.-P., Kameoka, J., Hegen, M., Tanaka, T., Xu, Y., Schlossman, S.F., Morimoto, C., 1996. Characterization of adenosine deaminase binding to human CD26 on T cells and its biologic role in immune response. J. Immunol. 156, 1349-1355.

Elkington, P., O'kane, C., Friedland, J., 2005. The paradox of matrix metalloproteinases in infectious disease. Clin. Exp. Immunol. 142, 12-20.

Ellis, A., 2001. Innate host defense mechanisms of fish against viruses and bacteria. Dev. Comp. Immunol. 25, 827-839.

Eslamloo, K., Caballero-Solares, A., Inkpen, S.M., Emam, M., Kumar, S., Bouniot, C., Avendaño-Herrera, R., Jakob, E., Rise, M.L., 2020a. Transcriptomic profiling of the adaptive and innate immune responses of Atlantic salmon to *Renibacterium salmoninarum* infection. Front. Immunol. 11, 2487.

Eslamloo, K., Kumar, S., Caballero-Solares, A., Gnanagobal, H., Santander, J., Rise, M.L., 2020b. Profiling the transcriptome response of Atlantic salmon head kidney to formalin-killed *Renibacterium salmoninarum*. Fish Shellfish Immunol. 98, 937-949.

Eslamloo, K., Xue, X., Hall, J.R., Smith, N.C., Caballero-Solares, A., Parrish, C.C., Taylor, R.G., Rise, M.L., 2017. Transcriptome profiling of antiviral immune and dietary fatty acid dependent responses of Atlantic salmon macrophage-like cells. BMC Genomics 18, 706.

FAO, 2018. The state of world fisheries and aquaculture 2018. Food and Agriculture Organization of the United Nations, Rome.

Gaggero, A., Castro, H., Sandino, A., 1995. First isolation of Piscirickettsia salmonis from coho salmon, *Oncorhynchus kisutch* (Walbaum), and rainbow trout, *Oncorhynchus mykiss* (Walbaum), during the freshwater stage of their life cycle. J. Fish Dis. 18, 277-279.

Gao, J., Qin, Z., Guan, X., Guo, J., Wang, H., Liu, S., 2017. Overexpression of GSN could decrease inflammation and apoptosis in EAE and may enhance vitamin D therapy on EAE/MS. Sci. Rep. 7, 604.

Gómez-Abellán, V., Sepulcre, M.P., 2016. The role of prostaglandins in the regulation of fish immunity. Mol. Immunol. 69, 139-145.

Gong, M., Hay, S., Marshall, K.R., Munro, A.W., Scrutton, N.S., 2007. DNA binding suppresses human AIF-M2 activity and provides a connection between redox chemistry, reactive oxygen species, and apoptosis. J. Biol. Chem. 282, 30331-30340.

Grimholt, U., 2016. MHC and evolution in teleosts. Biology 5, 6.

Han, Y., Liu, D., Li, L., 2020. PD-1/PD-L1 pathway: current researches in cancer. Am. J. Cancer Res. 10, 727.

Hellemans, J., Mortier, G., De Paepe, A., Speleman, F., Vandesompele, J., 2007. qBase relative quantification framework and software for management and automated analysis of real-time quantitative PCR data. Genome Biol. 8, R19.

Hernandez, A.J., Romero, A., Gonzalez-Stegmaier, R., Dantagnan, P., 2016. The effects of supplemented diets with a phytopharmaceutical preparation from herbal and macroalgal origin on disease resistance in rainbow trout against *Piscirickettsia salmonis*. Aquaculture 454, 109-117.

House, M., Bartholomew, J., Winton, J., Fryer, J., 1999. Relative virulence of three isolates of *Piscirickettsia salmonis* for coho salmon *Oncorhynchus kisutch*. Dis. Aquat. Org. 35, 107-113.

Hsu, Y.-M.S., Zhang, Y., You, Y., Wang, D., Li, H., Duramad, O., Qin, X.-F., Dong, C., Lin, X., 2007. The adaptor protein CARD9 is required for innate immune responses to intracellular pathogens. Nat. Immunol. 8, 198-205.

Jantzen, S.G., Sanderson, D.S., von Schalburg, K.R., Yasuike, M., Marass, F., Koop, B.F., 2011. A 44K microarray dataset of the changing transcriptome in developing Atlantic salmon (*Salmo salar* L.). BMC Res Notes 4, 88.

Jones, S.R., Long, A., MacWilliams, C., Polinski, M., Garver, K., 2020. Factors associated with severity of naturally occurring piscirickettsiosis in netpen‐and tank‐reared juvenile Atlantic salmon at a research aquarium in western Canada. J. Fish Dis. 43, 49-55.

Jørgensen, S.M., Afanasyev, S., Krasnov, A., 2008. Gene expression analyses in Atlantic salmon challenged with infectious salmon anemia virus reveal differences between individuals with early, intermediate and late mortality. BMC Genomics 9, 179.

Jørgensen, S.M., Grimholt, U., Gjøen, T., 2007. Cloning and expression analysis of an Atlantic salmon (*Salmo salar* L.) tapasin gene. Dev. Comp. Immunol. 31, 708-719.

Kelemen, S.E., Autieri, M.V., 2005. Expression of allograft inflammatory factor-1 in T lymphocytes: a role in T-lymphocyte activation and proliferative arteriopathies. Am. J. Pathol. 167, 619-626.

Kiron, V., 2012. Fish immune system and its nutritional modulation for preventive health care. Anim. Feed Sci. Technol. 173, 111 - 133.

Krasnov, A., Skugor, S., Todorcevic, M., Glover, K.A., Nilsen, F., 2012. Gene expression in Atlantic salmon skin in response to infection with the parasitic copepod *Lepeophtheirus salmonis*, cortisol implant, and their combination. BMC Genomics 13, 130.

Kuwano, Y., Prazma, C.M., Yazawa, N., Watanabe, R., Ishiura, N., Kumanogoh, A., Okochi, H., Tamaki, K., Fujimoto, M., Tedder, T.F., 2007. CD83 influences cell-surface MHC class II expression on B cells and other antigen-presenting cells. Int. Immunol. 19, 977-992.

Li, L.-F., Yu, J., Li, Y., Wang, J., Li, S., Zhang, L., Xia, S.-L., Yang, Q., Wang, X., Yu, S., 2016. Guanylate-binding protein 1, an interferon-induced GTPase, exerts an antiviral activity against classical swine fever virus depending on its GTPase activity. J. Virol. 90, 4412-4426.

Li, Z., Ju, X., Silveira, P.A., Abadir, E., Hsu, W.-H., Hart, D.N., Clark, G.J., 2019. CD83: Activation marker for antigen presenting cells and its therapeutic potential. Front. Immunol. 10, 1312.

Liem, R.K., 2016. Cytoskeletal integrators: the spectrin superfamily. Cold Spring Harb. Perspect. Biol. 8, a018259.

Lockhart, K., McBeath, A., Collet, B., Snow, M., Ellis, A., 2007. Expression of Mx mRNA following infection with IPNV is greater in IPN-susceptible Atlantic salmon post-smolts than in IPN-resistant Atlantic salmon parr. Fish Shellfish Immunol. 22, 151-156.

Maisey, K., Montero, R., Christodoulides, M., 2017. Vaccines for piscirickettsiosis (salmonid rickettsial septicaemia, SRS): the Chile perspective. Expert Rev. Vaccines 16, 215-228.

Martinez-Rubio, L., Evensen, Ø., Krasnov, A., Jørgensen, S.M., Wadsworth, S., Ruohonen, K., Vecino, J.L., Tocher, D.R., 2014. Effects of functional feeds on the lipid composition, transcriptomic responses and pathology in heart of Atlantic

salmon (*Salmo salar* L.) before and after experimental challenge with Piscine Myocarditis Virus (PMCV). BMC Genomics 15, 462.

Martinez‐Navio, J.M., Casanova, V., Pacheco, R., Naval‐Macabuhay, I., Climent, N., Garcia, F., Gatell, J.M., Mallol, J., Gallart, T., Lluis, C., 2011. Adenosine deaminase potentiates the generation of effector, memory, and regulatory CD4+ T cells. J. Leukoc. Biol. 89, 127-136.

Meza, K., Inami, M., Dalum, A.S., Bjelland, A.M., Sørum, H., Løvoll, M., 2019a. Development of piscirickettsiosis in Atlantic salmon (*Salmo salar* L.) smolts after intraperitoneal and cohabitant challenge using an EM90‐like isolate: A comparative study. J. Fish Dis. 42, 1001-1011.

Meza, K., Inami, M., Dalum, A.S., Lund, H., Bjelland, A.M., Sørum, H., Løvoll, M., 2019b. Comparative evaluation of experimental challenge by intraperitoneal injection and cohabitation of Atlantic salmon (*Salmo salar* L) after vaccination against *Piscirickettsia salmonis* (EM90‐like). J. Fish Dis. 42, 1713-1730.

Michels, K., Nemeth, E., Ganz, T., Mehrad, B., 2015. Hepcidin and host defense against infectious diseases. PLoS Pathog 11, e1004998.

Moraleda, C.P., Robledo, D., Gutiérrez, A.P., Del-Pozo, J., Yáñez, J.M., Houston, R.D., 2021. Investigating mechanisms underlying genetic resistance to Salmon Rickettsial Syndrome in Atlantic salmon using RNA sequencing. BMC Genomics 22, 156.

Mostowy, S., Shenoy, A.R., 2015. The cytoskeleton in cell-autonomous immunity: structural determinants of host defence. Nat. Rev. Immunol. 15, 559-573.

Müller, A., Sutherland, B.J., Koop, B.F., Johnson, S.C., Garver, K.A., 2015. Infectious hematopoietic necrosis virus (IHNV) persistence in Sockeye Salmon: influence on brain transcriptome and subsequent response to the viral mimic poly (I:C). BMC Genomics 16, 634.

Nemeth, E., Tuttle, M.S., Powelson, J., Vaughn, M.B., Donovan, A., Ward, D.M., Ganz, T., Kaplan, J., 2004. Hepcidin regulates cellular iron efflux by binding to ferroportin and inducing its internalization. science 306, 2090-2093.

Nourdin-Galindo, G., Sánchez, P., Molina, C.F., Espinoza-Rojas, D.A., Oliver, C., Ruiz, P., Vargas-Chacoff, L., Cárcamo, J.G., Figueroa, J.E., Mancilla, M., 2017. Comparative pan-genome analysis of *Piscirickettsia salmonis* reveals genomic divergences within genogroups. Front. Cell. Infect. Microbiol. 7, 459.

Park, C.H., Valore, E.V., Waring, A.J., Ganz, T., 2001. Hepcidin, a urinary antimicrobial peptide synthesized in the liver. J. Biol. Chem. 276, 7806-7810.

Pfaffl, M.W., 2001. A new mathematical model for relative quantification in real-time RT-PCR. Nucleic Acids Res. 29, e45.

Pohanka, M., 2013. Role of oxidative stress in infectious diseases. A review. Folia Microbiol. 58, 503-513.

Power, D., Santoso, N., Dieringer, M., Yu, J., Huang, H., Simpson, S., Seth, I., Miao, H., Zhu, J., 2015. IFI44 suppresses HIV-1 LTR promoter activity and facilitates its latency. Virology 481, 142-150.

Pulgar, R., Hodar, C., Travisany, D., Zuniga, A., Dominguez, C., Maass, A., Gonzalez, M., Cambiazo, V., 2015. Transcriptional response of Atlantic salmon families to *Piscirickettsia salmonis* infection highlights the relevance of the iron-deprivation defence system. BMC Genomics 16, 495.

Raida, M.K., Buchmann, K., 2009. Innate immune response in rainbow trout (*Oncorhynchus mykiss*) against primary and secondary infections with *Yersinia ruckeri* O1. Dev. Comp. Immunol. 33, 35-45.

Ramirez, R., Gomez, F.A., Marshall, S.H., 2015. The infection process of *Piscirickettsia salmonis* in fish macrophages is dependent upon interaction with host-cell clathrin and actin. FEMS Microbiol. Lett. 362.

Rise, M.L., Hall, J.R., Nash, G.W., Xue, X., Booman, M., Katan, T., Gamperl, A.K., 2015. Transcriptome profiling reveals that feeding wild zooplankton to larval Atlantic cod (*Gadus morhua*) influences suites of genes involved in oxidation-reduction, mitosis, and selenium homeostasis. BMC Genomics 16, 1016.

Rise, M.L., Jones, S.R.M., Brown, G.D., von Schalburg, K.R., Davidson, W.S., Koop, B.F., 2004. Microarray analyses identify molecular biomarkers of Atlantic salmon macrophage and hematopoietic kidney responses to *Piscirickettsia salmonis* infection. Physiol. Genomics 20, 21 - 35.

Rojo, R., Raper, A., Ozdemir, D.D., Lefevre, L., Grabert, K., Wollscheid-Lengeling, E., Bradford, B., Caruso, M., Gazova, I., Sánchez, A., 2019. Deletion of a Csf1r enhancer selectively impacts CSF1R expression and development of tissue macrophage populations. Nat. Commun. 10, 1-17.

Rozas-Serri, M., Ildefonso, R., Peña, A., Enríquez, R., Barrientos, S., Maldonado, L., 2017. Comparative pathogenesis of piscirickettsiosis in Atlantic salmon (*Salmo salar* L.) post‐smolt experimentally challenged with LF‐89‐like and EM‐90‐like *Piscirickettsia salmonis* isolates. J. Fish Dis. 40, 1451-1472.

Rozas-Serri, M., Peña, A., Arriagada, G., Enríquez, R., Maldonado, L., 2018a. Comparison of gene expression in post‐smolt Atlantic salmon challenged by LF‐89‐like and EM‐90‐like *Piscirickettsia salmonis* isolates reveals differences in the immune response associated with pathogenicity. J. Fish Dis. 41, 539-552.

Rozas-Serri, M., Peña, A., Maldonado, L., 2018b. Transcriptomic profiles of post-smolt Atlantic salmon challenged with *Piscirickettsia salmonis* reveal a strategy to evade the adaptive immune response and modify cell-autonomous immunity. Dev. Comp. Immunol. 81, 348-362.

Rozas, M., Enríquez, R., 2014. Piscirickettsiosis and *Piscirickettsia salmonis* in fish: a review. J. Fish Dis. 37, 163-188.

Rueda, D., Gaide, O., Ho, L., Lewkowicz, E., Niedergang, F., Hailfinger, S., Rebeaud, F., Guzzardi, M., Conne, B., Thelen, M., 2007. Bcl10 controls TCR-and FcγR-induced actin polymerization. J. Immunol. 178, 4373-4384.

Saavedra, J., Hernandez, N., Osses, A., Castillo, A., Cancino, A., Grothusen, H., Navas, E., Henriquez, P., Bohle, H., Bustamante, F., 2017. Prevalence, geographic distribution and phenotypic differences of *Piscirickettsia salmonis* EM‐90‐like isolates. J. Fish Dis. 40, 1055-1063.

Sada-Ovalle, I., Chávez-Galán, L., Torre-Bouscoulet, L., Nava-Gamiño, L., Barrera, L., Jayaraman, P., Torres-Rojas, M., Salazar-Lezama, M.A., Behar, S.M., 2012. The Tim3–galectin 9 pathway induces antibacterial activity in human macrophages infected with *Mycobacterium tuberculosis*. J. Immunol. 189, 5896-5902.

Schwender, H., Krause, A., Ickstadt, K., 2006. Identifying interesting genes with siggenes. RNews 6, 45 - 50.

Seppola, M., Larsen, A.N., Steiro, K., Robertsen, B., Jensen, I., 2008. Characterisation and expression analysis of the interleukin genes, IL-1β, IL-8 and IL-10, in Atlantic cod (*Gadus morhua* L.). Mol. Immunol. 45, 887-897.

Sernapesca, 2021. Informe Sanitario de Salmonicultura en Centros Marinos 2020. Servicio Nacional de Pesca y Acuicultura.

Shannon, P., Markiel, A., Ozier, O., Baliga, N.S., Wang, J.T., Ramage, D., Amin, N., Schwikowski, B., Ideker, T., 2003. Cytoscape: a software environment for integrated models of biomolecular interaction networks. Genome Res. 13, 2498-2504.

Sikora, M., Kopeć, B., Piotrowska, K., Pawlik, A., 2020. Role of allograft inflammatory factor-1 in pathogenesis of diseases. Immunol. Lett. 218, 1-4.

Škugor, S., Jørgensen, S.M., Gjerde, B., Krasnov, A., 2009. Hepatic gene expression profiling reveals protective responses in Atlantic salmon vaccinated against furunculosis. BMC Genomics 10, 503.

Smith, P., Pizarro, P., Ojeda, P., Contreras, J., Oyanedel, S., Larenas, J., 1999. Routes of entry of Piscirickettsia salmonis in rainbow trout *Oncorhynchus mykiss*. Dis. Aquat. Org. 37, 165-172.

Soto-Dávila, M., Valderrama, K., Inkpen, S.M., Hall, J.R., Rise, M.L., Santander, J., 2020. Effects of vitamin D2 (Ergocalciferol) and D3 (Cholecalciferol) on Atlantic salmon (*Salmo salar*) primary macrophage immune response to *Aeromonas salmonicida* subsp. *salmonicida* infection. Front. Immunol. 10, 3011.

Sturn, A., Quackenbush, J., Trajanoski, Z., 2002. Genesis: cluster analysis of microarray data. Bioinformatics 18, 207 - 208.

Sutherland, B.J., Hanson, K.C., Jantzen, J.R., Koop, B.F., Smith, C.T., 2014a. Divergent immunity and energetic programs in the gills of migratory and resident *Oncorhynchus mykiss*. Mol. Ecol. 23, 1952-1964.

Sutherland, B.J., Koczka, K.W., Yasuike, M., Jantzen, S.G., Yazawa, R., Koop, B.F., Jones, S.R., 2014b. Comparative transcriptomics of Atlantic *Salmo salar*, chum *Oncorhynchus keta* and pink salmon *O. gorbuscha* during infections with salmon lice *Lepeophtheirus salmonis*. BMC Genomics 15, 200.

Tacchi, L., Bron, J.E., Taggart, J.B., Secombes, C.J., Bickerdike, R., Adler, M.A., Takle, H., Martin, S.A., 2011. Multiple tissue transcriptomic responses to *Piscirickettsia salmonis* in Atlantic salmon (*Salmo salar*). Physiol. Genomics 43, 1241-1254.

Timmerhaus, G., Krasnov, A., Takle, H., Afanasyev, S., Nilsen, P., Rode, M., Jørgensen, S.M., 2012. Comparison of Atlantic salmon individuals with different outcomes of cardiomyopathy syndrome (CMS). BMC Genomics 13, 205.

Tusher, V.G., Tibshirani, R., Chu, G., 2001. Significance analysis of microarrays applied to the ionizing radiation response. Proc. Natl. Acad. Sci. U.S.A. 98, 5116-5121.

Umasuthan, N., Xue, X., Caballero-Solares, A., Kumar, S., Westcott, J.D., Chen, Z., Fast, M.D., Skugor, S., Nowak, B.F., Taylor, R.G., Rise, M.L., 2020. Transcriptomic profiling in fins of Atlantic salmon parasitized with sea lice: evidence for an early imbalance between chalimus-induced immunomodulation and the host's defense response. Int. J. Mol. Sci. 21, 2417.

Valenzuela-Muñoz, V., Valenzuela-Miranda, D., Gonçalves, A., Novoa, B., Figueras, A., Gallardo-Escárate, C., 2020. Induced-iron overdose modulate the immune response in Atlantic salmon increasing the susceptibility to *Piscirickettsia salmonis* infection. Aquaculture 521, 735058.

Vandesompele, J., De Preter, K., Pattyn, F., Poppe, B., Van Roy, N., De Paepe, A., Speleman, F., 2002. Accurate normalization of real-time quantitative RT-PCR data by geometric averaging of multiple internal control genes. Genome Biol 3, research0034.0031.

Vargas, J., Herpers, B., McKie, A., Gledhill, S., McDonnell, J., Van Den Heuvel, M., Davies, K., Ponting, C., 2003. Stromal cell-derived receptor 2 and cytochrome b561 are functional ferric reductases. Biochim. Biophys. Acta, Proteins Proteomics 1651, 116-123.

Wang, T., Secombes, C.J., 2013. The cytokine networks of adaptive immunity in fish. Fish Shellfish Immunol. 35, 1703-1718.

Watowich, S.S., 2011. The erythropoietin receptor: molecular structure and hematopoietic signaling pathways. J. Investig. Med. 59, 1067-1072.

Wei, X., Babu, V.S., Lin, L., Hu, Y., Zhang, Y., Liu, X., Su, J., Li, J., Zhao, L., Yuan, G., 2018. Hepcidin protects grass carp (*Ctenopharyngodon idellus*) against *Flavobacterium columnare* infection via regulating iron distribution and immune gene expression. Fish Shellfish Immunol. 75, 274-283.

Witeska, M., 2013. Erythrocytes in teleost fishes: a review. Zool. Ecol. 23, 275-281.

Xu, S., Webb, S.E., Lau, T.C.K., Cheng, S.H., 2018. Matrix metalloproteinases (MMPs) mediate leukocyte recruitment during the inflammatory phase of zebrafish heart regeneration. Sci. Rep. 8, 7199.

Xue, X., Caballero-Solares, A., Hall, J.R., Umasuthan, N., Kumar, S., Jakob, E., Skugor, S., Hawes, C., Santander, J., Taylor, R.G., Rise, M.L., 2021. Transcriptome Profiling of Atlantic Salmon (*Salmo salar*) Parr With Higher and Lower Pathogen Loads Following Piscirickettsia salmonis Infection. Front. Immunol. 12.

Xue, X., Hall, J.R., Caballero-Solares, A., Eslamloo, K., Taylor, R.G., Parrish, C.C., Rise, M.L., 2020. Liver transcriptome profiling reveals that dietary DHA and EPA levels influence suites of genes involved in metabolism, redox homeostasis, and immune function in Atlantic salmon (*Salmo salar*). Mar. Biotechnol. 22, 263-284.

Xue, X., Hixson, S.M., Hori, T.S., Booman, M., Parrish, C.C., Anderson, D.M., Rise, M.L., 2015. Atlantic salmon (*Salmo salar*) liver transcriptome response to diets containing *Camelina sativa* products. Comp. Biochem. Physiol. D: Genomics Proteomics 14, 1-15.

Xue, X., Woldemariam, N.T., Caballero-Solares, A., Umasuthan, N., Fast, M.D., Taylor, R.G., Rise, M.L., Andreassen, R., 2019. Dietary immunostimulant CpG modulates

microRNA biomarkers associated with immune responses in Atlantic salmon (*Salmo salar*). Cells 8, 1592.
Yamaguchi, T., Dijkstra, J.M., 2019. Major histocompatibility complex (MHC) genes and disease resistance in fish. Cells 8, 378.
Yamashiro, S., Gokhin, D.S., Kimura, S., Nowak, R.B., Fowler, V.M., 2012. Tropomodulins: pointed ‐ end capping proteins that regulate actin filament architecture in diverse cell types. Cytoskeleton 69, 337-370.
Zanuzzo, F.S., Beemelmanns, A., Hall, J.R., Rise, M.L., Gamperl, A.K., 2020. The innate immune response of Atlantic salmon (*Salmo salar*) is not negatively affected by high temperature and moderate hypoxia. Front. Immunol. 11, 1009.
Zapata, A., Diez, B., Cejalvo, T., Gutierrez-de Frias, C., Cortes, A., 2006. Ontogeny of the immune system of fish. Fish Shellfish Immunol. 20, 126-136.
Zhang, J., Kong, X., Zhou, C., Li, L., Nie, G., Li, X., 2014. Toll-like receptor recognition of bacteria in fish: ligand specificity and signal pathways. Fish Shellfish Immunol. 41, 380-388.
Zhang, Y., Wang, L., Huang, X., Wang, S., Huang, Y., Qin, Q., 2019. Fish cholesterol 25-hydroxylase inhibits virus replication via regulating interferon immune response or affecting virus entry. Front. Immunol. 10, 322.
Zhao, J., Chen, J., Li, M., Chen, M., Sun, C., 2020. Multifaceted functions of CH25H and 25HC to modulate the lipid metabolism, immune responses, and broadly antiviral activities. Viruses 12, 727.
Zhao, Y.Y., Yan, D.J., Chen, Z.W., 2013. Role of AIF-1 in the regulation of inflammatory activation and diverse disease processes. Cell. Immunol. 284, 75-83.
Zheng, Z., Li, Y., Jin, G., Huang, T., Zou, M., Duan, S., 2020. The biological role of arachidonic acid 12-lipoxygenase (ALOX12) in various human diseases. Biomed. Pharmacother. 129, 110354.
Zou, J., Secombes, C.J., 2016. The function of fish cytokines. Biology 5, 23.

CHAPTER 4: Dietary immunostimulant CpG modulates microRNA biomarkers associated with immune responses in Atlantic salmon (*Salmo salar*)

The research described in **Chapter 4** has been published in the journal Cells as: Xue, X., Woldemariam, N.T., Caballero-Solares, A., Umasuthan, N., Fast, M.D., Taylor, R.G., Rise, M.L., Andreassen, R., 2019. Dietary immunostimulant CpG modulates microRNA biomarkers associated with immune responses in Atlantic salmon (*Salmo salar*). Cells 8, 1592. doi:10.3390/cells8121592

4.1 Abstract

MicroRNAs (miRNAs) are key regulators in fish immune responses. However, no study has previously characterized the impact of polyriboinosinic polyribocytidylic acid (pIC) and formalin-killed typical *Aeromonas salmonicida* bacterin on miRNA expression in Atlantic salmon fed a commercial diet with and without immunostimulant CpG (cytosine-phosphate-guanosine). To this end, first, small RNA deep sequencing and qPCR analyses were performed to identify and confirm pIC- and/or bacterin-responsive miRNAs in the head kidney of salmon fed a control diet. DESeq2 analyses identified 12 and 18 miRNAs differentially expressed in pIC and bacterin groups, respectively, compared to the controls. Fifteen of these miRNAs were studied by qPCR; nine remained significant by qPCR. Five miRNAs (miR-27d-1-2-5p, miR-29b-2-5p, miR-146a-5p, miR-146a-1-2-3p, miR-221-5p) were shown by qPCR to be significantly induced by both pIC and bacterin. Second, the effect of CpG-containing functional feed on miRNA expression was investigated by qPCR. In pre-injection samples, 6 of 15 miRNAs (e.g., miR-181a-5-3p, miR-462a-3p, miR-722-3p) had significantly lower expression in fish fed CpG diet than control diet. In contrast, several miRNAs (e.g., miR-146a-1-2-3p, miR-192a-5p, miR-194a-5p) in the PBS- and bacterin-injected groups had significantly higher expression in CpG-fed fish. Multivariate statistical analyses confirmed that the CpG diet had a greater impact on miRNA expression in bacterin-injected compared with pIC-injected fish. This study identified immune-relevant miRNA biomarkers that will be valuable in the development of diets to combat infectious diseases of salmon.

4.2 Introduction

Worldwide demand for seafood for human consumption, including a growing contribution from aquaculture (~50% in 2016), continues to climb because of a flat or decreasing global wild fisheries production in the face of rising human population (Agaba et al., 2005; Tocher et al., 2006; FAO, 2018). Consequently, there is great potential for the aquaculture industry to expand. With a variety of species being farmed, Atlantic salmon (*Salmo salar*) is one of the most economically important species in aquaculture (Kiron, 2012). Infectious diseases have resulted in substantial mortality and losses to Atlantic salmon aquaculture worldwide, affecting the growth and sustainability of the industry (Caballero-Solares et al., 2017). Several well-known viruses that cause severe diseases in Atlantic salmon are RNA viruses (Lang et al., 2009). These include viruses with single-stranded RNA genomes (e.g., salmonid alphavirus (SAV), infectious salmon anemia virus (ISAV) and viral hemorrhagic septicemia virus (VHSV)) and double-stranded RNA genomes (e.g., infectious pancreatic necrosis virus (IPNV)) (Lang et al., 2009). Bacterial pathogens that have a severe impact on salmonid aquaculture include *Piscirickettsia salmonis* (which causes piscirickettsiosis or salmonid rickettsial septicaemia) (Rise et al., 2004), *Aeromonas salmonicida* (the cause of furunculosis) (Ewart et al., 2005), *Renibacterium salmoninarum* (the cause of bacterial kidney disease) (Murray et al., 2012), and *Moritella viscosa* (the cause of winter ulcer disease) (Løvoll et al., 2009).

Microbial cell components (e.g., lipopolysaccharide, peptidoglycan, RNAs, and DNAs), recognized by animal immune cells as pathogen-associated molecular patterns (PAMPs), can elicit host immune responses to fight the invading pathogen (Vallejos-Vidal

et al., 2016). The detection of PAMPs by specific pattern-recognition receptors (PRRs) on or within the host immune cells triggers intracellular signaling cascades that increase the expression of soluble mediators (e.g., both pro-inflammatory and anti-inflammatory cytokines), which can lead to increased phagocytosis, bactericidal activity, respiratory burst, antiviral and complement activities (Secombes and Wang, 2012). Taking advantage of this mechanism, researchers have used polyriboinosinic polyribocytidylic acid (pIC), a PAMP-like synthetic double-stranded RNA (dsRNA) analogue, to elicit antiviral responses (Akira et al., 2006; Robertsen, 2006; Eslamloo et al., 2016; Caballero-Solares et al., 2017), and formalin-killed *Aeromonas salmonicida*, a PAMP-containing bacterin, to elicit antibacterial responses (Feng et al., 2009; Hori et al., 2013).

Immune response-mediated gene expression can be regulated through small non-coding RNAs (ncRNAs) including microRNAs (miRNAs) (Andreassen and Høyheim, 2017; Andreassen et al., 2017; Eslamloo et al., 2018; Herkenhoff et al., 2018). miRNAs are important regulators of gene expression at the post-transcriptional level (Andreassen and Høyheim, 2017; Woldemariam et al., 2019). The primary miRNA transcripts (pri-miRNAs) are cleaved by ribonuclease enzyme Drosha into shorter miRNA precursors (pre-miRNAs). Thereafter, pre-miRNAs are exported out of the nucleus and further processed by endoribonuclease Dicer to produce two small mature miRNAs (i.e., 5p and 3p) that are usually 20–24 nt in length (Woldemariam et al., 2019). Typically, one of the mature miRNAs is then assembled into the miRNA-induced silencing complex (miRISC), which can exercise its gene-silencing function by binding mainly to the 3′ untranslated region (UTR) of target mRNA (Herkenhoff et al., 2018).

Recent advances in high-throughput sequencing technology (e.g., small RNA deep sequencing) and bioinformatics tools have led to the detection of virus/bacteria-responsive miRNAs in teleosts (Andreassen et al., 2017; Valenzuela-Miranda et al., 2017; Eslamloo et al., 2018; Cao et al., 2019). For instance, twenty differentially expressed miRNAs were identified in Atlantic salmon challenged with SAV; the majority of the predicted mRNA targets were involved in promoting the inflammatory response (Andreassen et al., 2017). Analyses of Atlantic salmon tissues infected with *P. salmonis* revealed 84 and 25 differentially expressed miRNAs in head kidney and spleen, respectively; functional annotation of predicted mRNA targets of *P. salmonis*-responsive miRNAs showed involvement in the immune response, such as genes related to chemokine-mediated signaling pathway and neutrophil chemotaxis (Valenzuela-Miranda et al., 2017). Such studies have improved the current understanding of miRNAs involved in immune responses in teleosts (Andreassen and Høyheim, 2017). However, the impact of pIC-triggered antiviral and *A. salmonicida* bacterin-triggered antibacterial immune responses on the miRNA expression in Atlantic salmon were previously uncharacterized.

Over recent decades the development of aquafeeds has continued to progress with diets being more specifically designed to meet the nutritional needs of species, stage of the life cycle, and health status of the fish (Tacchi et al., 2011). Functional feeds are diets designed to have positive effects on both the health and growth of the animals ingesting them by supplying additional functional ingredients beyond the basic nutritional requirements of the animal (Martin and Król, 2017). Components that act as immunostimulants are often added to the feeds, and can generally increase resistance to

disease by enhancing the non-specific immune system (Tacchi et al., 2011; Martin and Król, 2017). For example, algal and plant extracts as dietary immunostimulants have been tested in different fish species; other dietary supplements containing PAMPs as immunostimulants also showed promising results in mitigating fish diseases (Vallejos-Vidal et al., 2016).

A type of PAMP commonly used as an immunostimulant is unmethylated DNA, which contains cytosine–phosphate–guanine oligodeoxynucleotide motifs (CpG ODN) (Covello et al., 2012). Bacterial genomes, some viral genomes and invertebrate genomes differ structurally from vertebrate genomes, which exhibit CpG suppression and methylation (Carrington and Secombes, 2006; Covello et al., 2012). Unmethylated DNA, containing CpG motifs, acts as a danger signal to the vertebrate host and triggers an immune response (Covello et al., 2012). The immune response induced by CpG is mediated through Toll-like receptor 9 (TLR9), a PRR present on the cell surface or within endosomal compartments of B cells, dendritic cells, and macrophages (Cuesta et al., 2008; Liu et al., 2010). Based on the backbone structure and oligonucleotide sequences, synthetic CpG ODNs are divided into three classes (i.e., A-, B-, and C-classes) with distinct immunomodulating properties (Carrington and Secombes, 2006). B-class CpG ODNs primarily stimulate the proliferation of B cells (Cárdenas-Reyna et al., 2016). For example, CpG ODN 205 (i.e., B-class) stimulated the immune system of turbot (*Scophthalmus maximus*), and induced protection against bacterial challenge (Liu et al., 2010). Another B-class ODN, CpG ODN 1668, was shown to activate immune responses against iridovirus infection in rock bream (*Oplegnathus fasciatus*) (Jung and Jung, 2017), and *Vibrio*

parahaemolitycus challenge in Pacific red snapper (*Lutjanus peru*) (Cárdenas-Reyna et al., 2016). In addition, protection against sea lice (*Lepeophtheirus salmonis*) infection in Atlantic salmon by orally administered CpG ODN 1668 (10–20 mg kg^{-1} feed) has been reported (Covello et al., 2012; Purcell et al., 2013). Nevertheless, the impact of dietary CpG on the expression of miRNAs associated with antiviral and antibacterial responses in fish including Atlantic salmon was previously unknown.

In the present study, I investigated the host miRNA expression responses to viral mimic pIC and *A. salmonicida* bacterin stimulations in the head kidney of Atlantic salmon fed a control diet by a deep sequencing approach. Head kidney was chosen as the target tissue as it plays an important role in the specific and non-specific defense mechanisms in teleost fish, and its role in hematopoiesis is equivalent to bone marrow in higher vertebrates (Press and Evensen, 1999; Chen et al., 2012; Kiron, 2012). Putative antiviral and antibacterial responsive miRNAs identified through sequencing were also studied by qPCR in fish fed a functional feed (control diet top-coated with CpG ODN 1668). The expression of these candidate miRNAs was measured before and 24 h after immunogen injection. This study allowed us to identify miRNAs that are valuable biomarkers for responses to pIC and bacterin stimulations in the head kidney of Atlantic salmon, and to study the influence of this CpG-containing functional feed on the expression of immune-relevant miRNAs.

4.3 Materials and methods

4.3.1 Feed production

EWOS Dynamic S feed (5 mm; 27% fat, 46% protein) was used in this experiment as the control diet and base feed for the functional diet (referred as CpG diet). The CpG diet was produced by dissolving CpG ODN 1668 (Integrated DNA Technologies, Coralville, IA, USA) components in distilled water and spraying onto the pellets. Then, coated pellets were brought under −0.9 bar of vacuum for 10 min, followed by a drying step at 60°C for 30 min to remove excess water, to obtain a final concentration of 10 mg kg^{-1} of feed. The CpG coating procedures were carried out at the Chute Animal Nutrition Centre of Dalhousie University Agricultural Campus (Truro, NS, Canada).

4.3.2 Feeding trial, immune challenge, and fish sampling

The Atlantic salmon feeding trial was conducted at the Dr. Joe Brown Aquatic Research Building [JBARB, Ocean Sciences Centre (OSC), Memorial University of Newfoundland, St. John's, NL, Canada]. Salmon smolts were obtained from Northern Harvest Sea Farms (Stephenville, NL, Canada), transported to the JBARB and held in 3800 L tanks. After arrival, salmon were PIT (passive integrated transponder)-tagged and fed with the control diet before the start of the feeding trial. Atlantic salmon (post-smolts; 232 ± 52 g mean initial weight ± SD; n = 67) were randomly distributed among four 620 L tanks (16–17 fish per tank). After 7 weeks acclimation, salmon from 2 tanks were switched from the control diet to the CpG diet while the other two tanks remained on the control diet for another 7 weeks. Fish were kept in a flow-through seawater system (~10–11°C,

dissolved oxygen ≥ 10 mg L^{-1}) under a 24 h light photoperiod. Fish were fed to apparent satiation using automatic feeders (AVF6 Vibratory Feeder; Pentair Aquatic Eco-Systems, Inc., Nanaimo, BC, Canada), which were set to vibrate for 3 s hourly from 5 pm to 3 am. The daily ration was set at 1% of the average body weight (BW) of the salmon in each tank, which was estimated using their initial weight (for each tank, individually) and assuming an exponential growth of 1% BW/day. Satiation was assessed by monitoring the amount of uneaten pellets the next morning. An overview of the experimental design, including the feeding trial, immune challenges and subsequent molecular analyses (discussed below), is illustrated in **Figure 4.1**.

At the end of the feeding trial, both dietary groups were subjected to immune challenge by an intraperitoneal (IP) injection (25 gauge needle) of immunogens: *A. salmonicida* bacterin or viral mimic pIC. Fish were starved for 24 h, after which 4 fish per tank (8 per treatment) were euthanized with an overdose of MS-222 (400 mg L^{-1}, Syndel Laboratories, Vancouver, BC, Canada) and dissected for time 0 (i.e., pre-injection) head kidney samples. Formalin-killed typical *A. salmonicida* bacterin was obtained in the form of a vaccine [Furogen Dip, Elanco (formerly Novartis), Charlottetown, PE, Canada]. The bacterin solution was prepared as in Hori et al. (2013), while the pIC (Catalogue # P0913; Sigma-Aldrich, Oakville, ON, Canada) was diluted in sterile phosphate-buffered saline (PBS; Gibco, Carlsbad, CA, USA) at 2 μg μL^{-1} for injection. Then, 4–5 salmon per tank (i.e., 8–9 per treatment) were lightly anesthetized (50 mg L^{-1} of MS-222) and injected with 1 μL of pIC, bacterin or PBS per g of wet mass. Fish were then sampled 24 h post-injection as described above. Body weight, fork length, and liver weight of fish were measured. Head

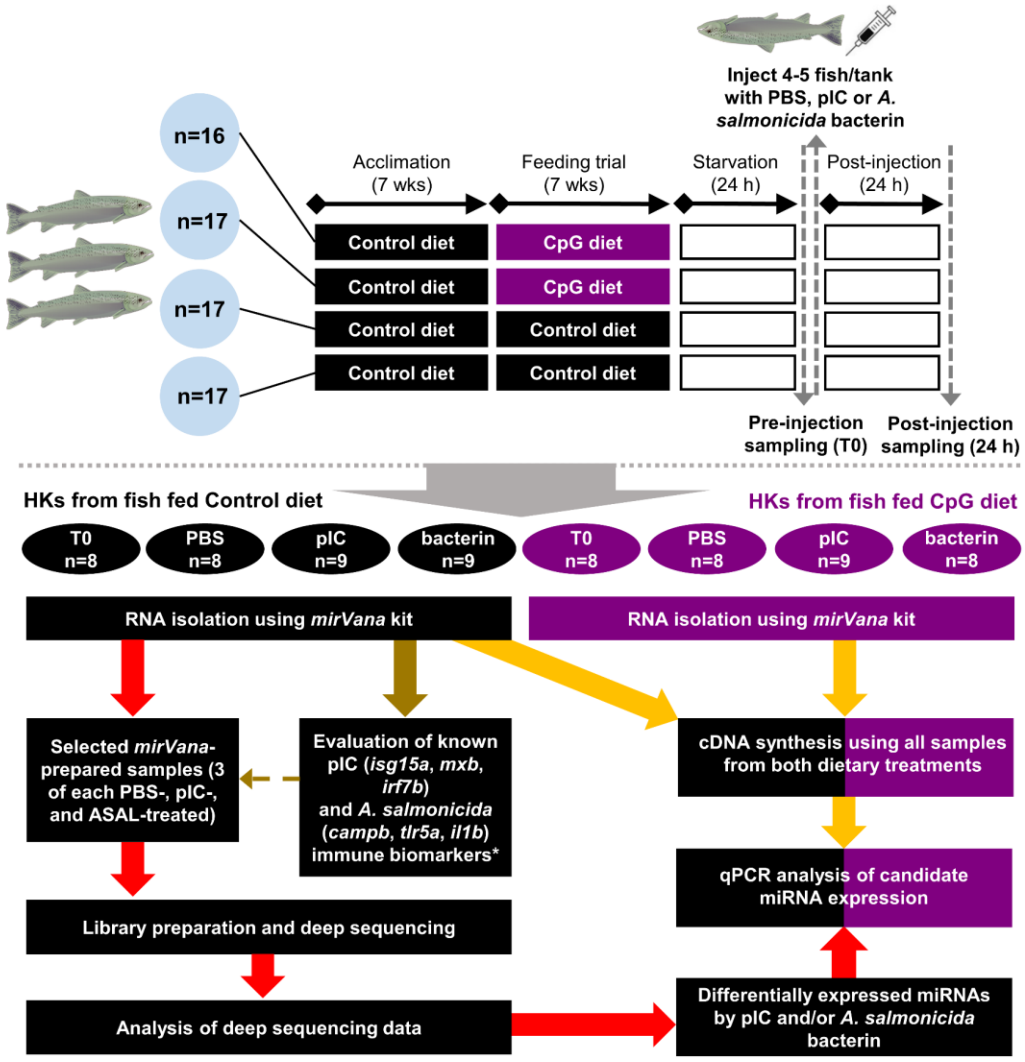

Figure 4.1. Overview of experimental design. Following the 7 week feeding trial, fish fed both diets were subjected to immune challenge by an intraperitoneal (IP) injection of sterile phosphate-buffered saline (PBS), formalin-killed typical *Aeromonas salmonicida* bacterin, or viral mimic polyriboinosinic polyribocytidylic acid (pIC). *mirVana*-prepared head kidney (HK) templates from three of each PBS-, pIC-, and bacterin-injected fish (control diet only) were selected for deep sequencing based on the qPCR assessed expression of known pIC (i.e., *isg15a*, *mxb*, *irf7b*) and *A. salmonicida* (i.e., *campb*, *tlr5a*, *il1b*) immune biomarker transcripts. Selected pIC- and/or bacterin-responsive miRNAs were studied by qPCR using all samples from both dietary groups. *mRNA qPCR analyses were conducted using DNase-treated and column-purified total RNA.

kidney samples (50–100 mg) were collected, flash-frozen in liquid nitrogen, and stored at −80°C until RNA extraction. This study was carried out in accordance with animal care protocol 17-77-MR, approved by the Institutional Animal Care Committee of Memorial University of Newfoundland.

4.3.3 RNA isolation

Total RNAs of all collected head kidney samples were extracted using the *mirVana* miRNA isolation kit (Ambion/Life Technologies, Carlsbad, CA, USA) according to manufacturer instructions. The RNA integrity was verified by 1% agarose gel electrophoresis, and RNA purity was assessed by A260/280 and A260/230 using NanoDrop spectrophotometry (Thermo Fisher, Mississauga, ON, Canada). All RNA samples used in this study showed tight 18S and 28S ribosomal RNA bands and A260/230 ratios greater than 2. Also, A260/280 ratios of most of the samples were higher than 1.9; 3 out of 67 samples had A260/280 ratios between 1.7 and 1.9.

4.3.4 Library preparation and deep sequencing

Prior to the selection of the samples for deep sequencing, aliquots of *mirVana*-prepared total RNAs from all fish fed control diet were subjected to DNase treatment and column purification (Caballero-Solares et al., 2018). These RNAs were subjected to qPCR analyses of known *A. salmonicida* bacterin- [i.e., *cathelicidin antimicrobial peptide b* (*campb*), *tlr5a*, *interleukin-1 beta* (*il1b*)] (Caballero-Solares et al. manuscript in preparation) and pIC- [i.e., *interferon stimulated gene 15a* (*isg15a*), *interferon-induced GTP-binding protein b* (alias *myxovirus resistance b*, *mxb*), *interferon regulatory factor 7b*

(*irf7b*)] (Caballero-Solares et al., 2017) responsive immune biomarker transcripts, to ensure the efficacy of the immune challenges and to select representative individuals for deep sequencing. The qPCR analyses of these immune biomarkers were conducted as described in Caballero-Solares et al. (2018). Details on the methods and results for immune biomarker mRNA qPCR are provided in **Supplemental Table S4.1**. The *mirVana*-prepared total RNAs from three of each PBS-, bacterin-, and pIC-injected individuals fed control diet were selected for miRNA sequencing analyses (see **Supplemental Table S4.1** for qPCR-based sample selection). Small RNA library construction and sequencing were performed at the Norwegian Genomics Consortium (NGC)'s Genomics Core Facility. All sequencing libraries were generated using the NEBNext Small RNA Library Prep Set for Illumina (New England Biolabs, Ipswich, MA, USA) with 1 µg of total RNA input, following manufacturer instructions. In brief, *mirVana*-prepared total RNAs were ligated with 3′ and 5′ RNA adapters, followed by reverse transcription (RT) and PCR enrichment using barcoded RT-primers. The resulting cDNA products were purified using 6% polyacrylamide gels, and size selection of fragments (approximately 145–160 bp) was carried out to enrich small RNAs. The sequencing was performed on a NextSeq 500 instrument (Illumina, Inc, San Diego, CA, USA), producing 75 bp single-end reads.

4.3.5 Analysis of deep sequencing data

The quality of raw sequencing reads (fastq files) was assessed using FastQC toolkit (v.0.11.5; http://www.bioinformatics.babraham.ac.uk/projects/fastqc), to ensure that the quality was satisfactory before adaptor sequences were removed using cutadapt (v.1.13) (Martin, 2011). The trimmed sequence reads were size-filtered to discard reads that were

outside the expected size range of mature miRNAs (18–25 nt). The quality of the trimmed and size-filtered reads was checked by a second FastQC analysis. All deep sequencing reads have been submitted to the NCBI Sequence Read Archive (SRA) database (BioProject PRJNA555179).

The clean sequence reads were aligned to a reference index consisting of all known mature miRNAs in Atlantic salmon (Woldemariam et al., 2019), using STAR aligner software (v.2.5.2b) (Dobin et al., 2013). The alignment files (BAM format) were further processed in R using the *featureCounts* function from the *Rsubread* package to produce count matrices (Liao et al., 2013). These count tables were used as input to test for differential expression of miRNAs using the R package DESeq2 (Love et al., 2014). Differentially expressed miRNAs were identified by comparing the bacterin or pIC groups to the PBS group (control) (n = 3 from each experimental condition). miRNAs were considered to be differentially expressed if they had Benjamini-Hochberg adjusted p-value of $\leqslant$ 0.10.

4.3.6 Prediction of target Genes and their functional annotations

The miRNA target prediction tool RNAhybrid (Rehmsmeier et al., 2004) was applied to identify the putative target genes of the pIC- and/or bacterin-responsive miRNAs identified by the DESeq2 analyses. The mature miRNA sequences were tested against 3′UTRs from all Atlantic salmon transcripts in the NCBI Reference Sequence database (Refseq; https://www.ncbi.nlm.nih.gov/refseq/). The following parameters were applied in the RNA hybrid analysis: helix constraint 2–8, no G:U in seed, and a minimum free energy threshold of −18 kcal/mol. Gene ontology (GO) terms of the predicted target genes from

Atlantic salmon were obtained from UniProt Knowledgebase (http://www.uniprot.org/). Based on the GO term annotations and published studies, a subset of predicted target genes with functions associated with immune response were identified. Cross-reference links from the UniProt database were further used to retrieve organism-specific pathway annotations from the online resource Kyoto Encyclopedia of Genes and Genomes (KEGG) pathway database (https://www.genome.jp/kegg/pathway.html).

4.3.7 qPCR analysis of miRNA expression

The expression of 15 miRNAs (5 pIC-responsive, 7 bacterin-responsive, 3 commonly responsive to both pIC and bacterin) (see **Supplemental Table S4.2** for qPCR primers), selected from the DESeq2 analyses, was quantified by qPCR using samples from all individuals (i.e., 8–9 samples per treatment). In addition to fish fed control diet, the qPCR experiment also included head kidney samples from fish fed CpG containing diet and subjected to the immune stimulations.

cDNA templates for qPCR were synthesized in 20-µL reactions from 400 ng of *mirVana* extracted total RNA using miScript II RT Kit (Qiagen, Hilden, Germany) as recommended by the manufacturer's instructions. The cDNAs were diluted by adding 180 µL of RNase-free water (Qiagen) for use in the qPCR assays. PCR amplifications were performed in duplicate using 12.5 µL of 2× QuantiTect SYBR Green PCR Master Mix, 2.5 µL of 10× miScript Universal Primer, 2.5 µL specific forward primer (10 µM), 5 µL RNase-free water (Qiagen), and 2.5 µL of diluted cDNA template representing 5 ng of input total RNA. All qPCR assays were conducted in an AriaMx Real-time PCR System (Agilent Technologies, Santa Clara, CA, USA) using 96-well plates. The real-time analysis program

consisted of 1 cycle of 95°C for 15 min, and 40 cycles of 94°C for 15 s, 55°C for 30 s and 70°C for 30 s, followed by a final melting point analysis.

All forward primers were designed based on the mature sequences of miRNAs of interest (**Table 4.1**), while a universal primer, provided by the miScript SYBR Green PCR Kit (Qiagen), was used as a reverse primer in each qPCR assay. Quality testing ensured that a single product was amplified (dissociation curve analysis) and that there was no primer-dimer present in the no-template control except for miR-181a-5-3p. Amplification efficiencies (Pfaffl, 2001) were calculated using cDNA synthesized from head kidney RNA samples (n = 6; 2 of each PBS-, bacterin-, and pIC-injected) that had been pooled post-cDNA synthesis. Standard curves were generated using a 4-5-point 1:3 dilution series. Two miRNAs (miR-25-3p and miR-17-5p), suggested as the most suitable normalizers for miRNA expression in Atlantic salmon (Johansen and Andreassen, 2014), were used as normalizers in the current study. These normalizers were expressed stably in the current qPCR study (i.e., the geometric mean of normalizers' C_T less than 0.3 cycles different for injection-matched groups or diet-matched groups) (see **Supplemental Table S4.3** for normalizer C_T values). Agilent AriaMx software v1.5 was applied to obtain C_T (or Cq) values. The relative quantity (RQ) of each miRNA was determined using a qBase relative quantification framework (Hellemans et al., 2007; Booman et al., 2014), with normalization to both miR-25-3p and miR-17-5p, and with amplification efficiencies incorporated. For pre-injection samples (i.e., T0 samples), the RQs of each miRNA were calibrated against fish fed the control diet, while for IP-injected groups, the RQs of each miRNA were calibrated against PBS-injected fish fed the control diet.

Table 4.1. Overview of the deep sequencing results from the head kidney of fish fed the control diet.

Sample ID [1]	Total Number of Raw Reads [2]	Trimmed and Filtered Reads [3]	Reads Mapped to miRNAs (%) [4]	Accession Number [5]
1-PBS-T30-2	9,609,300	4,800,941	89.1	SRR9709006
2-PBS-T30-3	15,384,722	9,966,411	90.4	SRR9709007
3-PBS-T33-3	12,674,361	8,124,580	89.9	SRR9709008
4-bacterin-T33-1	11,715,675	7,190,332	89.4	SRR9709009
5-bacterin-T30-4	14,028,188	9,134,360	89.7	SRR9709002
6-bacterin-T33-3	34,491,682	8,654,401	91.3	SRR9709003
7-pIC-T33-2	18,600,224	8,519,434	80.6	SRR9709004
8-pIC-T30-3	13,957,705	9,864,824	93.4	SRR9709005
9-pIC-T33-3	16,877,729	5,453,442	68.2	SRR9709010

[1] The *mirVana*-prepared total RNAs from three of each PBS-, bacterin-, and pIC-injected individuals fed the control diet were selected for miRNA sequencing analyses. [2] The total number of reads in raw fastq file for each sample. [3] Total number of reads after removing adapters and filtering reads by size (18–25 nt). [4] Percent of trimmed and filtered reads mapped to the reference miRNAome (i.e., all known mature miRNAs of Atlantic salmon) (Woldemariam et al., 2019). [5] The accession number of sequencing results for each sample submitted to the NCBI Sequence Read Archive (SRA) database (http://www.ncbi.nlm.nih.gov/sra). All data were deposited under the BioProject PRJNA555179.

4.3.8 Statistical analyses

All qPCR data (i.e., RQs) were subjected to Grubbs' test to identify potential outliers and then $\log_2$-transformation to meet the normality assumption. Grubbs' test can determine if the most extreme value in a univariate dataset is a significant outlier from the rest, and is based on the assumption of normality (Grubbs, 1969). In total, 19 RQ values were identified as statistical outliers in the entire dataset (i.e., out of 765 RQ values), and excluded from the study. Each miRNA of interest had a minimum of 7 samples per treatment. For pre-injection samples, miRNA expression differences between diet groups were determined using a Student's *t*-test ($p < 0.05$). For IP-injected groups, miRNA expression differences between treatments and diets were determined using two-way analysis of variance (ANOVA), followed by a Dunnett's test to assess the effect of immunogens within each dietary group (i.e., pIC/bacterin *vs* PBS), and a Student's *t*-test to assess the dietary effect within treatment groups ($p < 0.05$). All of the statistical tests above were performed in Prism v7.0 (GraphPad Software Inc., La Jolla, CA, USA).

Principal coordinates analysis (PCoA), permutational multivariate ANOVA (PERMANOVA), and similarity of percentages analysis (SIMPER) were performed using PRIMER (Version 6.1.15; PRIMER-E Ltd, Ivybridge, UK) to explore the differences in qPCR-analyzed miRNA expression among samples from fish fed different diets (control *vs* CpG) and in different treatment groups (pre-injection, PBS-, pIC- and bacterin-injected).

4.4 Results

4.4.1 Deep sequencing and identification of differentially expressed miRNAs

A deep sequencing approach was used to discover pIC- or bacterin-responsive miRNAs in the head kidney of salmon fed the control diet. **Table 4.1** provides an overview of the read numbers obtained from the deep sequencing of the samples used in the present study. The total number of raw reads obtained from sequencing for all samples ranged from 9.6 to 34.5 million. After trimming and filtering, the number of clean reads for all samples ranged from 4.8 to 10.0 million reads. More than 68% of clean reads (i.e., after trimming and size filtering) were mapped to a recent update of Atlantic salmon reference miRNAome (i.e., all known mature miRNAs) (Woldemariam et al., 2019). The sequencing results of all samples are available in the SRA database of NCBI under the BioProject PRJNA555179 (**Table 4.1**).

DESeq2 analyses (adjusted p-value < 0.10) were applied to identify miRNAs that were pIC- or bacterin-responsive in the head kidney of Atlantic salmon. This revealed 12 mature miRNAs that were significantly up-regulated in the pIC group when compared to the PBS-injected control group; the expression of these miRNAs was 1.6- to 14.0-fold higher in the pIC group (**Table 4.2**). Only one miRNA (miR-106a-3p) showed decreased expression (-1.9-fold) in the pIC group (**Table 4.2**). The comparison of the bacterin group against the PBS-injected control group revealed 16 significantly up-regulated miRNAs; the expression of these miRNAs was 1.5- to 17.2-fold higher in the bacterin group (**Table 4.3**). Two miRNAs (miR-722-3p and miR-727a-3p) had decreased expression (-2.1-fold and

Table 4.2. pIC-responsive miRNAs in the head kidney of fish fed the control diet identified by DESeq2 (n = 3) and confirmed by qPCR (n = 8–9).

miRNAs [1]	**Base Mean** [2]	**Fold-change** [3]	**Adjusted *p*-values** [4]	**qPCR Fold-change** [5]
		Up-regulated by pIC		
miR-27d-1-5p [6]	868.11	2.17	0.049	2.69
miR-27d-2-5p [6]	861.10	2.17	0.049	2.69
miR-30e-1-2-3p	404.73	2.16	0.049	2.57
miR-135bd-5p	52.80	14.03	0.036	1.54
miR-146a-5p	152066.51	1.71	0.028	1.62
miR-146a-1-2-3p	6322.03	7.94	3.85×10^{-4}	7.89
miR-181a-5-3p	11080.58	1.59	0.051	1.97
miR-221-5p	221.52	4.44	0.036	7.55
miR-462a-3p	1554.09	2.69	0.098	5.72
miR-462b-3p	941.82	5.46	8.0×10^{-12}	N/A
miR-8159-5p	97.72	9.92	0.055	N/A
		Down-regulated by pIC		
miR-106a-3p	960.11	−1.93	0.036	N/A

[1] miRNAs with bold font are differentially expressed in both pIC and *A. salmonicida* bacterin groups when compared to the PBS-injected control group. The mature sequences and miRBase identities of each miRNA are given in Supplemental Table S4.4. [2] The mean of normalized read counts for all of the samples included in the comparison. [3] Fold-change (pIC/PBS) was converted from the $\log_2$ fold-change (given by DESeq2 analyses). For the down-regulated miRNA, the fold-change value was inverted (−1/fold-change). [4] Adjusted p-values as determined by DESeq2 analyses. [5] For qPCR fold-change calculation (fish fed the control diet), overall fold up-regulation was calculated as 2^{A-B} as in Xue et al. (2015), where A was the mean of $\log_2$ RQ from the pIC group, and B was the mean of $\log_2$ RQ from PBS group. Underlined qPCR fold-change values indicate statistical significance ($p < 0.05$). miRNAs noted with N/A (i.e. not applicable) were not subjected to qPCR analysis. [6] miR-27d-2-5p and miR-27d-1-5p are identical except the length difference (24 *vs* 23 nt). Therefore, the qPCR assay was generic to both miRNAs.

Table 4.3. *A. salmonicida* bacterin-responsive miRNAs in the head kidney of fish fed the control diet identified by DESeq2 (n = 3) and confirmed by qPCR (n = 8–9).

miRNAs [1]	**Base Mean** [2]	**Fold-change** [3]	**Adjusted *p*-values** [4]	**qPCR Fold-change** [5]
		Up-regulated by bacterin		
miR-21a-1-3p	267.99	1.52	0.099	N/A
miR-29b-2-5p	516.80	1.55	0.091	1.47
miR-146a-5p	202688.90	2.01	8.9×10^{-6}	1.89
miR-146a-1-2-3p	8503.53	9.06	9.06×10^{-37}	5.87
miR-146a-3-3p	12146.14	3.43	2.62×10^{-11}	N/A
miR-146d-1-3p	421.43	2.60	2.45×10^{-4}	N/A
miR-183-1-3-3p	19.55	4.17	0.018	N/A
miR-183-2-3p	19.24	4.08	0.021	N/A
miR-192a-5p	391.09	6.68	0.016	1.64
miR-194a-5p	82.25	6.68	0.016	1.37
miR-200b-3p	275.30	8.00	0.009	N/A
miR-221-5p	141.35	1.92	0.018	2.23
miR-429ab-3p	11.34	8.40	0.071	N/A
miR-725-5p	26.55	17.15	2.27×10^{-6}	1.55
miR-725-3p	163.89	4.63	6.75×10^{-6}	N/A
miR-novel-16-5p	1066.67	2.01	1.81×10^{-4}	1.09
		Down-regulated by bacterin		
miR-722-3p	410.45	−2.08	0.021	−1.64
miR-727a-3p	886.63	−1.82	0.085	−1.94

[1] miRNAs with bold font were differentially expressed in both pIC and *A. salmonicida* bacterin groups when compared to the PBS-injected control group. The mature sequences and miRBase identities of each miRNA are given in Supplemental Table S4.4. [2] The mean of normalized read counts for all of the samples included in the comparison. [3] Fold-change (bacterin/PBS) was converted from the $\log_2$ fold-change (given by DESeq2 analyses). For down-regulated miRNAs, fold-change values were inverted (−1/fold-change). [4] Adjusted *p*-values as determined by DESeq2 analyses. [5] For qPCR fold-change calculation (fish fed the control diet), overall fold up-regulation was calculated as 2^{A-B} as in Xue et al. (2015), where A was the mean of $\log_2$ RQ from the bacterin group, and B was the mean of $\log_2$ RQ from the PBS group. Underlined qPCR fold-change values indicate statistical significance ($p < 0.05$). miRNAs noted with N/A (i.e. not applicable) were not subjected to qPCR analysis.

-1.8-fold) in the bacterin group (**Table 4.3**). In addition, 3 miRNAs (miR-146a-1-2-3p, miR-221-5p, miR-146-5p) were up-regulated in both pIC and bacterin groups compared with the PBS controls (**Tables 4.2 and 4.3**). The mature sequences and miRBase identities of all pIC- and/or bacterin-responsive miRNAs are given in **Supplemental Table S4.4**.

The predicted target genes of the pIC- and/or bacterin-responsive miRNAs from the DESeq2 analysis were identified by *in silico* analysis against the 3′ UTRs from the Atlantic salmon transcriptome (i.e., mRNA Refseq database). A total of 1591 genes was identified as putative targets of pIC- and/or bacterin-responsive miRNAs (**Supplemental Table S4.5**). The gene ontology annotations of these genes (retrieved from the UniProt database if available) revealed 130 of them have immune-relevant functions (**Supplemental Tables S4.6 and S4.7**). Within these 130 immune-relevant predicted target genes, 24 and 54 were unique targets associated with pIC- and bacterin-responsive miRNAs, respectively; 52 target genes were in common (**Supplemental Tables S4.6 and S4.7**). Among the immune-relevant predicted targets of pIC-responsive miRNAs, 27 could be mapped to species-specific KEGG pathways; while 35 could be mapped for predicted targets of bacterin-responsive miRNAs. These KEGG pathways included NOD-like receptor signaling pathway, cytokine–cytokine receptor interaction, necroptosis, Toll-like receptor signaling pathway, apoptosis, C-type lectin receptor signaling pathway, RIG-I-like receptor signaling pathway, and cell adhesion molecules (CAMs) (**Table 4.4**). The two KEGG pathways that had the most target genes assigned in both putative target gene lists were NOD-like receptor signaling pathway and cytokine–cytokine receptor interaction (**Table 4.4**).

Table 4.4. Kyoto Encyclopedia of Genes and Genomes (KEGG) pathways of immune-relevant predicted target genes of pIC- and/or *A. salmonicida* bacterin-responsive miRNAs.

Pathway	Name	Assigned Target Genes of pIC-responsive miRNAs [1]	Assigned Target Genes of bacterin-responsive miRNAs [2]
sasa04621	NOD-like receptor signaling pathway	8	12
sasa04060	Cytokine-cytokine receptor interaction	7	13
sasa04217	Necroptosis	7	11
sasa04620	Toll-like receptor signaling pathway	6	10
sasa04210	Apoptosis	6	7
sasa04625	C-type lectin receptor signaling pathway	5	5
sasa04622	RIG-I-like receptor signaling pathway	4	7
sasa04514	Cell adhesion molecules (CAMs)	4	2

[1] Complete list of immune-relevant predicted target genes of pIC-responsive miRNAs is given in Supplemental Table S4.6. [2] Complete list of immune-relevant predicted target genes of bacterin-responsive miRNAs is given in Supplemental Table S4.7.

4.4.2 qPCR validation of DESeq2-identified pIC- and/or *A. salmonicida* bacterin-responsive miRNAs

Fifteen miRNAs (5 pIC-responsive, 7 bacterin-responsive, three commonly responsive to both pIC and bacterin) identified as differentially expressed by DESeq2 were successfully subjected to qPCR analyses to confirm the sequencing results using larger numbers of biological replicates (n = 8–9) than were included in the sequencing study (**Tables 4.2 and 4.3**). qPCR analyses on miRNA expression of fish fed the control diet are discussed below. Fold-change values and significance are summarized in **Tables 4.2 and 4.3**. Among deep sequencing-identified pIC-responsive miRNAs, the results from qPCR analyses agreed well (i.e., statistically significant) with the results from DESeq2 analyses for 7 of the 8 miRNAs tested; while not statistically significant, qPCR for miR-135bd-5p revealed the same direction of change as shown by deep sequencing (**Table 4.2**). Among the 10 deep sequencing-identified bacterin-responsive miRNAs subjected to qPCR analyses, 5 of these (50%), namely miR-29b-2-5p, miR-146a-5p, miR-146a-1-2-3p, miR-221-5p and miR-727a-3p, were confirmed (i.e., statistically significant) by qPCR; 4 of the remaining miRNAs showed the same direction of change (i.e., up- or down-regulation) as the sequencing results (**Table 4.3**).

In addition to 3 DESeq2-identified miRNAs (miR-146a-1-2-3p, miR-146a-5p, miR-221-5p) that were commonly responsive to both pIC and bacterin stimulations, the qPCR results also showed that miR-27d-1-2-5p and miR-29b-2-5p were significantly up-regulated by both stimulations when compared with the PBS-injected salmon fed the control diet (**Tables 4.2 and 4.3**; **Figure 4.2A,B**). Among these 5 miRNAs, the expression

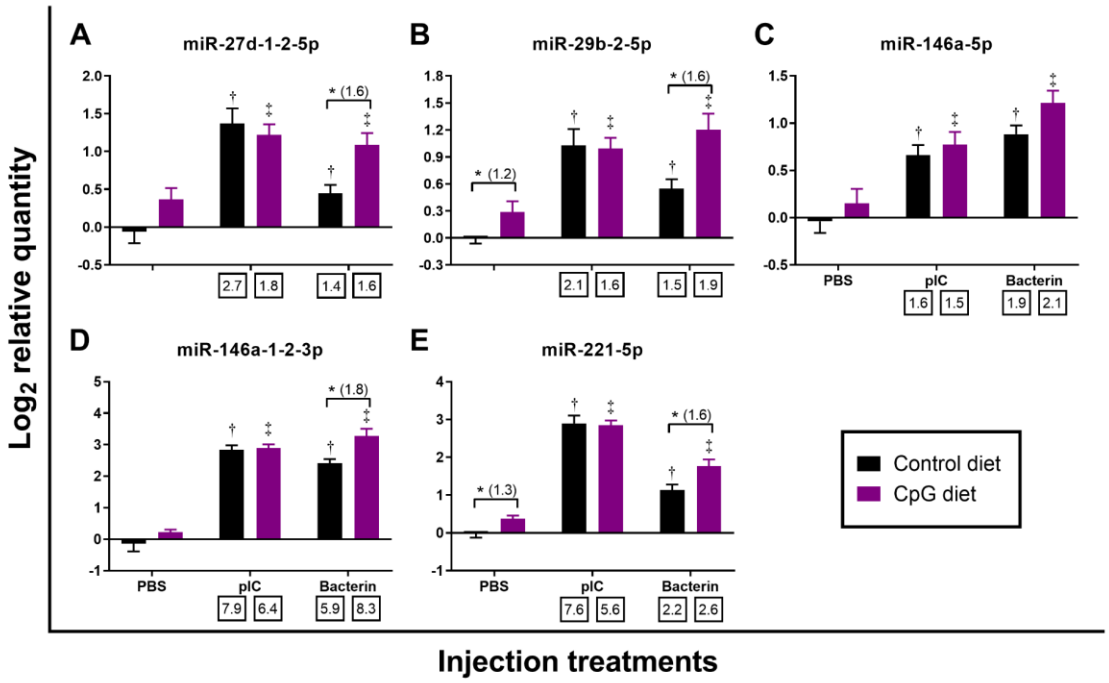

Figure 4.2. qPCR analyses of miRNAs identified by deep sequencing as being responsive to both pIC and *A. salmonicida* bacterin injections (n = 8–9). Average $\log_2$ RQs with SE bars are plotted. An asterisk (*) represents a significant difference between diets in each injection treatment ($p < 0.05$) with fold-change given in brackets. A dagger (†) or diesis (‡) represents a significant difference between immunogen-injected salmon and the diet-matched PBS-injected control ($p < 0.05$) with fold-change indicated below the x-axis. For qPCR fold-change calculation, overall fold up-regulation was calculated as 2^{A-B} as in Xue et al. (2015), where A is the mean of $\log_2$ RQ from the pIC or bacterin groups, and B is the mean of $\log_2$ RQ from the diet-matched PBS group. (**A**) miR-27d-1-2-5p; (**B**) miR-29b-2-5p; (**C**) miR-146a-5p; (**D**) miR-146a-1-2-3p; (**E**) miR-221-5p.

of miR-146a-1-2-3p and miR-221-5p was more strongly induced by pIC stimulation (up to 7.9-fold) than miR-27d-1-2-5p, miR-29b-2-5p, and miR-146a-5p (up to 2.7-fold) (**Tables 4.2 and 4.3**; **Figure 4.2**). The bacterin induction of miR-146a-1-2-3p (5.9-fold) was stronger than that of miR-27d-1-2-5p, miR-29b-2-5p, miR-146a-5p, and miR-221-5p (~2-fold) (**Tables 4.2 and 4.3**; **Figure 4.2**). Among the miRNAs that were only responsive to pIC stimulation, the induction of miR-462a-3p (5.7-fold) was higher than miR-30e-1-2-3p (2.7-fold) and miR-181a-5-3p (2.2-fold) (**Table 4.2**; **Figure 4.3A,C,D**). For deep sequencing-identified miRNAs that were only responsive to bacterin, miR-727a-3p was shown by qPCR to be significantly down-regulated in bacterin-injected salmon compared with PBS control (**Table 4.3**; **Figure 4.4F**). It is worth noting that miR-725-5p was significantly up-regulated (2.3-fold) by pIC stimulation in fish fed the control diet (**Figure 4.4C**).

4.4.3 Impact of diets on the expression of pIC- and/or *A. salmonicida* bacterin-responsive miRNAs

The putative pro-immune impact of the diet containing functional ingredient CpG ODN 1668 *vs* the control feed was investigated in pre-injection head kidney samples (i.e., basal expression) by analyzing the gene expression of the 15 pIC- and/or bacterin-responsive miRNAs. This comparison revealed that 6 out of these miRNAs (i.e., miR-181a-5-3p, miR-192a-5p, miR-194a-5p, miR-462a-3p, miR722-3p, and miR-novel-16-5p) showed significant down-regulation by the CpG diet (-1.4, -1.4, -1.5, -1.5, -1.6, and -1.2-fold, respectively; **Figure 4.5G-I, K, L, and O**). The remaining miRNAs assayed by qPCR

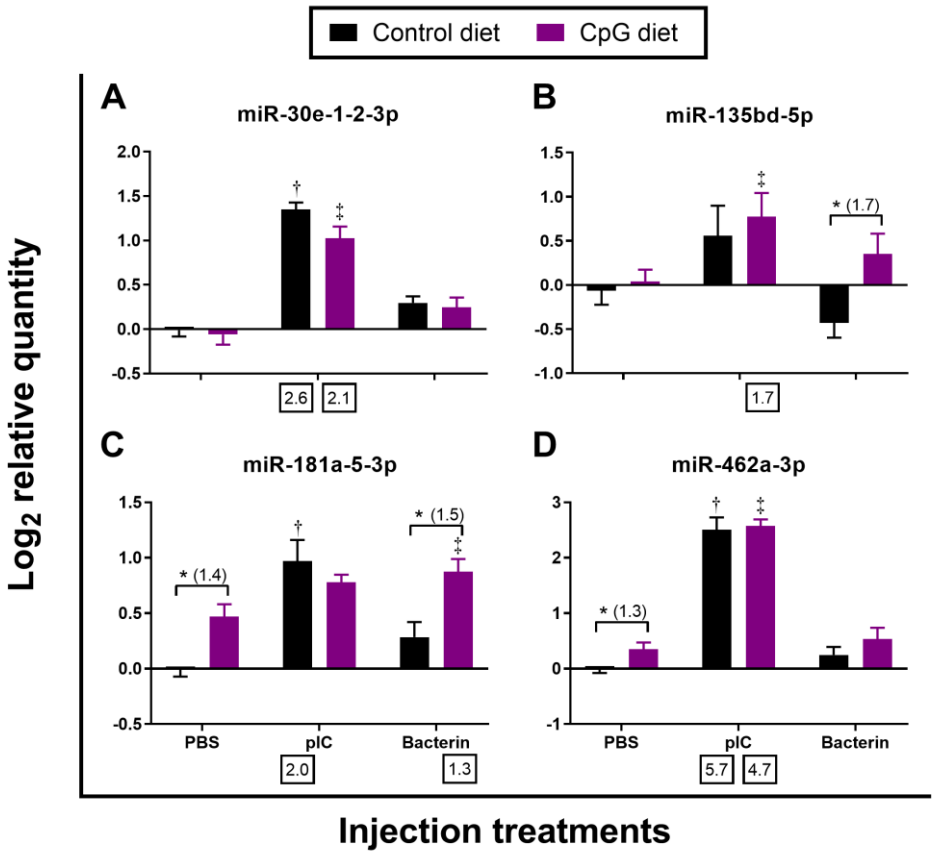

Figure 4.3. qPCR analyses of miRNAs identified by deep sequencing as being responsive to pIC alone (n = 8–9). Average $\log_2$ RQs with SE bars are plotted. An asterisk (*) represents a significant difference between diets in each injection treatment ($p < 0.05$) with fold-change given in brackets. A dagger (†) or diesis (‡) represents a significant difference between the pIC/*A. salmonicida* bacterin-injected salmon and the diet-matched PBS-injected control ($p < 0.05$) with fold-change indicated below the x-axis. For qPCR fold-change calculation, overall fold up-regulation was calculated as 2^{A-B} as in Xue et al. (2015), where A is the mean of $\log_2$ RQ from the pIC or bacterin groups, and B is the mean of $\log_2$ RQ from the diet-matched PBS group. (**A**) miR-30e-1-2-3p; (**B**) miR-135bd-5p; (**C**) miR-181a-5-3p; (**D**) miR-462a-3p.

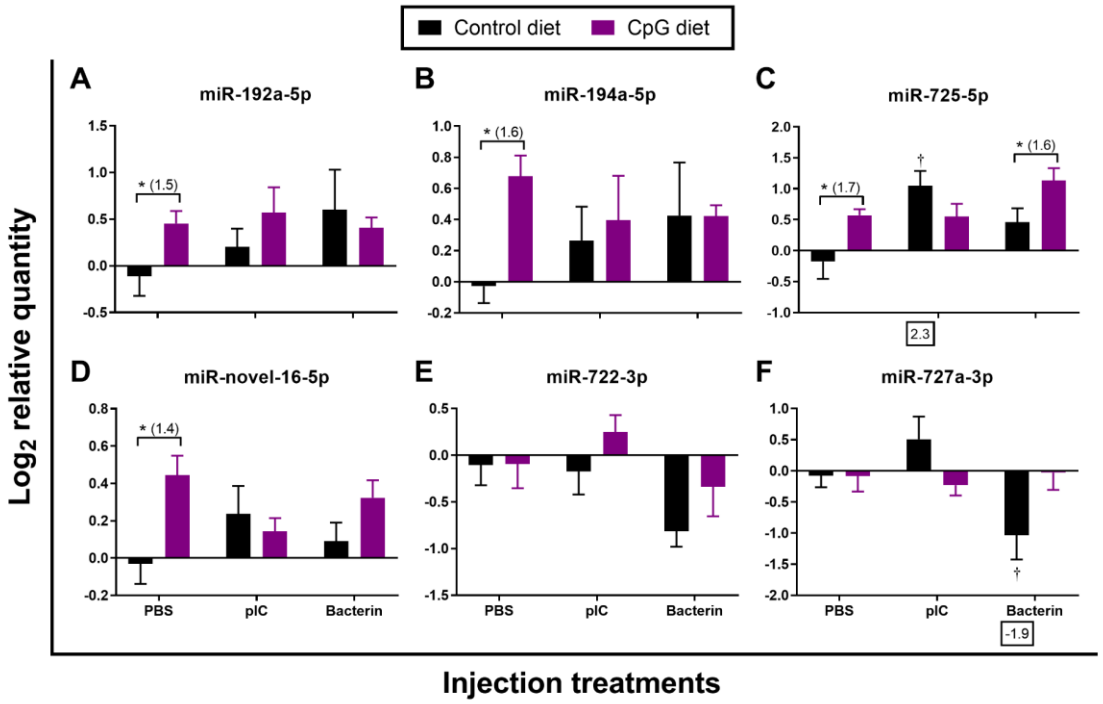

Figure 4.4. qPCR analyses of miRNAs identified by deep sequencing as being responsive to *A. salmonicida* bacterin alone (n = 8–9). Average $\log_2$ RQs with SE bars are plotted. An asterisk (*) represents a significant difference between diets in each injection treatment ($p < 0.05$) with fold-change given in brackets. A dagger (†) represents a significant difference between immunogen-injected salmon and the diet-matched PBS-injected control ($p < 0.05$) with fold-change indicated below the x-axis. For qPCR fold-change calculation, overall fold up-regulation was calculated as 2^{A-B} as in Xue et al. (2015), where A is the mean of $\log_2$ RQ from the pIC or bacterin groups, and B is the mean of $\log_2$ RQ from the diet-matched PBS group. For down-regulated miRNAs, fold-change values were inverted (−1/fold-change). (**A**) miR-192a-5p; (**B**) miR-194a-5p; (**C**) miR-725-5p; (**D**) miR-novel-16-5p; (**E**) miR-722-3p; (**F**) miR-727a-3p.

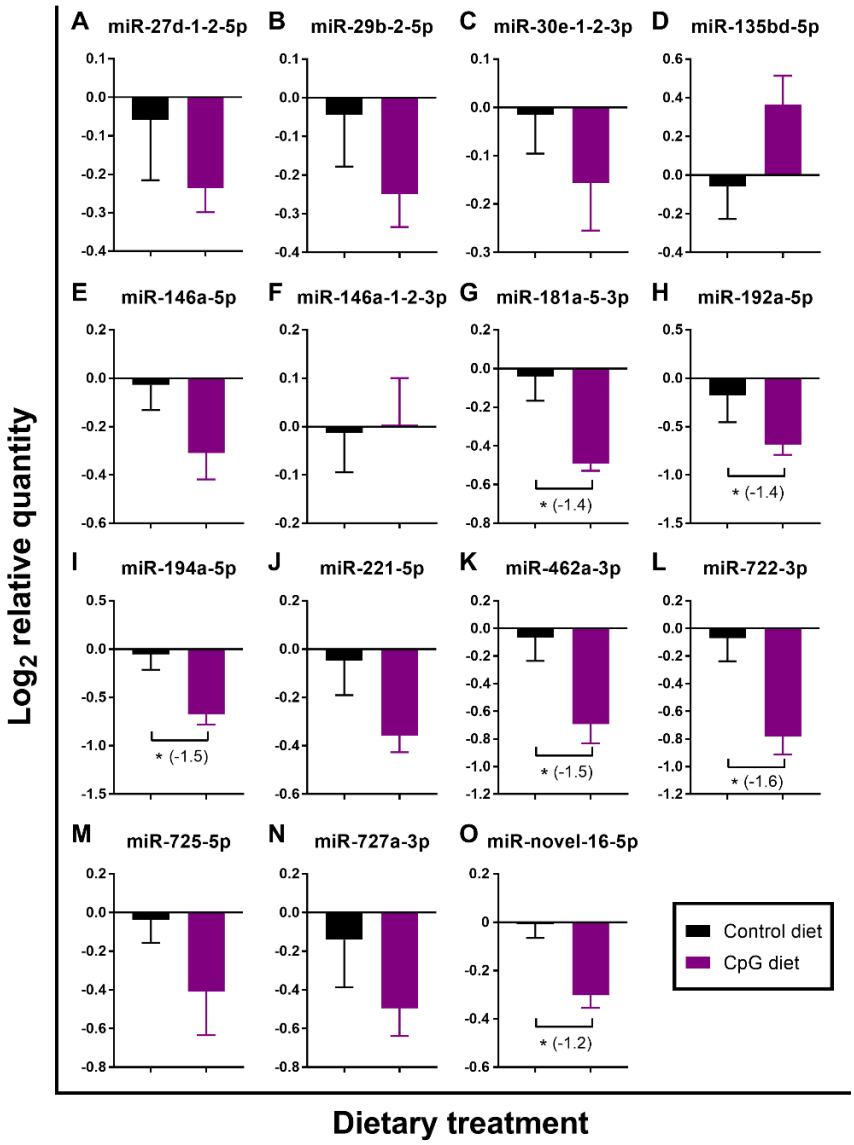

Figure 4.5. qPCR analyses of basal expression (pre-injection samples) of candidate pIC- and/or *A. salmonicida* bacterin-responsive miRNAs identified by deep sequencing ($n = 8$). Average $\log_2$ RQs with SE bars are plotted. An asterisk (*) indicates a significant difference between diets for a given miRNA ($p < 0.05$) with fold-change given in brackets. For qPCR fold-change calculation, overall fold up-regulation was calculated as 2^{A-B} as in Xue et al. (2015), where A is the mean of $\log_2$ RQ from the CpG group, and B is the mean of $\log_2$ RQ from the control group. For down-regulated miRNAs, fold-change values were inverted (−1/fold-change). (**A**) miR-27d-1-2-5p; (**B**) miR-29b-2-5p; (**C**) miR-30e-1-2-3p; (**D**) miR-135bd-5p; (**E**) miR-146a-5p; (**F**) miR-146a-1-2-3p; (**G**) miR-181a-5-3p; (**H**) miR-192a-5p; (**I**) miR-194a-5p; (**J**) miR-221-5p; (**K**) miR-462a-3p; (**L**) miR-722-3p; (**M**) miR-725-5p; (**N**) miR-727a-3p; (**O**) miR-novel-16-5p.

except miR-135bd-5p and miR-146a-1-2-3p showed trends of lower expression in salmon fed the CpG diet compared to the controls (**Figure 4.5**).

In contrast to the pre-injection samples, several miRNAs in the PBS- and bacterin-injected groups, had higher expression in fish fed CpG diet compared to the controls (**Figures 4.2–4.4**). In PBS-treated salmon, fish fed CpG diet showed significantly higher expression of the 8 miRNAs: miR-29b-2-5p, miR-221-5p, miR-181a-5-3p, miR-462a-3p, miR-192a-5p, miR-194a-5p, miR-725-5p, and miR-novel-16-5p (1.2-, 1.3-, 1.4-, 1.3-, 1.5-, 1.6-, 1.7-, and 1.4-fold, respectively) than those fed the control diet (**Figure 4.2B,E**; **Figure 4.3C,D**; **Figure 4.4A–D**). In bacterin-treated salmon, 7 miRNAs, namely miR-27d-1-2-5p, miR-29b-2-5p, miR-146a-1-2-3p, miR-221-5p, miR-135bd-5p, miR-181a-5-3p, and miR-725-5p, had significantly higher expression (1.6-, 1.6-, 1.8-, 1.6-, 1.7-, 1.5- and 1.6-fold, respectively) in fish fed the CpG diet compared to the fish fed the control diet (**Figure 4.2A,B,D,E**; **Figure 4.3B,C**; **Figure 4.4C**). Given the effect of the CpG diet in PBS and bacterin injected groups, it was an unexpected finding that no miRNA was significantly modulated by the CpG diet when compared to the control diet in the pIC-treated salmon (**Figures 4.2–4.4**).

4.4.4 Multivariate statistical analyses

For the pre-injection samples, the PCoA was able to segregate the two dietary groups (**Figure 4.6A**). miR-146a-5p, miR-27d-1-2-5p, and miR-181a-5-3p had the greatest influence on PCO1, which accounted for 47% of the variation among samples. PCO2 only explained 17.5% of the variability and was most strongly influenced by miR-727a-3p,

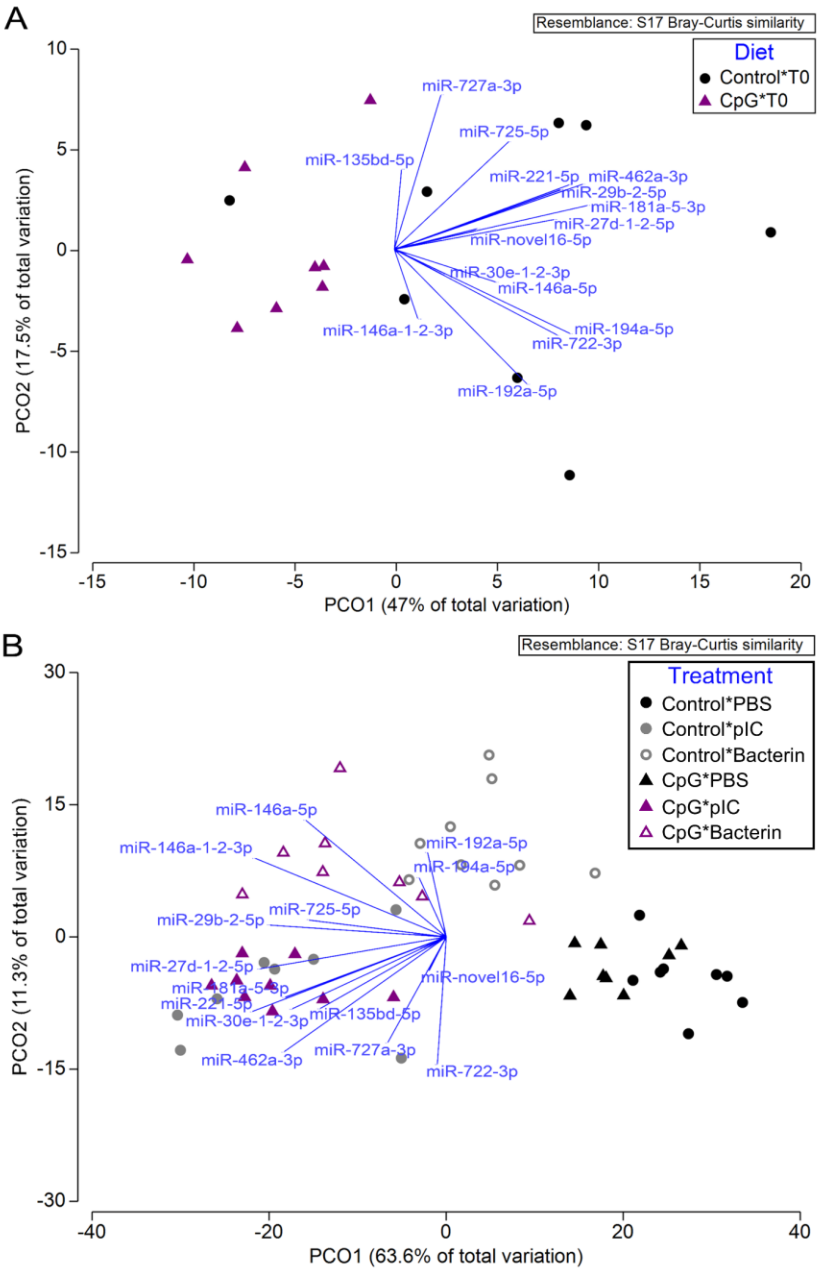

Figure 4.6. Principal coordinate analyses (PCoA) of qPCR analyzed miRNA genes (RQ values) in pre-injection samples (i.e., T0 samples; **A**) and 24 h post-injection head kidney samples (**B**).

miR-135bd-5p, and miR-146a-1-2-3p. For the post-injection groups, the PCoA was able to segregate different injection treatments and dietary groups within PBS- or bacterin-injected groups (**Figure 4.6B**). The top three miRNAs that influenced the PCO1 were miR-725-5p, miR-29b-2-5p, and miR-27d-1-2-5p, while PCO2 was mostly influenced by miR-192a-5p, miR-194a-5p, and miR-722-3p. PCO1 and PCO2 accounted for 63.6% and 11.3% of the variation among post-injected groups, respectively. PERMANOVA was conducted in order to quantify the differences among samples from fish fed different diets before and after stimulations. The results showed that the comparisons between diets within pre-injection and two of the post-injected groups (i.e., PBS and bacterin) were highly significant based on the expression of the 15 qPCR analyzed miRNAs (**Table 4.5**). SIMPER was conducted to explore the major drivers that differentiated dietary treatments. The comparison of miRNA expression between fish fed control and CpG diets within the bacterin treatment group was the most dissimilar (average dissimilarity = 26.8%), with 7 miRNAs (e.g., miR-146a-1-2-3p, miR-192a-5p, miR-221-5p, miR-29b-2-5p) as the top 70% contributing variables to this dissimilarity (**Table 4.5**). In the pre-injection and PBS-treated groups, the dissimilarities between diets were 17.5% and 19.0%, respectively. miR-194a-5p, miR-727a-3p, miR-725-5p, miR-722-3p, miR-192a-5p, and miR-181a-5-3p were the common contributing variables to both dissimilarities (**Table 4.5**).

4.5 Discussion

4.5.1 Deep sequencing and identification of differentially expressed miRNAs

Table 4.5. Permutational multivariate ANOVA (PERMANOVA) and similarity of percentages analysis (SIMPER) of analyzed transcripts (RQ values).

	Control *vs* CpG [3]			
	Pre-injection	**PBS**	**pIC**	**Bacterin**
p (perm) [1]	0.0015	0.0041	0.4461	0.0015
Average dissimilarity (%) [2]	17.5	19.0	-	26.8
Contributing variables (top 70%)	miR-722-3p	miR-194a-5p	-	miR-146a-1-2-3p
	miR-192a-5p	miR-725-5p	-	miR-192a-5p
	miR-462a-3p	miR-192a-5p	-	miR-221-5p
	miR-727a-3p	miR-722-3p	-	miR-725-5p
	miR-194a-5p	miR-27d-1-2-5p	-	miR-29b-2-5p
	miR-725-5p	miR-727a-3p	-	miR-194a-5p
	miR-181a-5-3p	miR-146a-1-2-3p	-	miR-27d-1-2-5p
	miR-135bd-5p	miR-novel-16-5p	-	-
	-	miR-181a-5-3p	-	-

[1] *p* (perm) is the statistical significance value obtained from PERMANOVA with 9999 permutations. [2] Average dissimilarity and contributing variables (top 70%) were obtained through SIMPER. [3] Dietary effects were evaluated within each injection treatment.

Small RNA deep sequencing was used to discover miRNAs potentially involved in the antiviral and antibacterial immune responses in Atlantic salmon. The DESeq2 analyses of the head kidney from fish fed the control diet identified 12 and 18 miRNAs differentially expressed in pIC and bacterin groups, respectively, compared to PBS controls. It is well established that PAMPs can be detected by specific PRRs on or within the host cells, triggering immune responses (Secombes and Wang, 2012). In fish, pIC and bacterin have been used as models to study differentially expressed mRNAs associated with antiviral responses (Akira et al., 2006; Robertsen, 2006; Eslamloo et al., 2016; Caballero-Solares et al., 2017) and antibacterial responses (Feng et al., 2009; Hori et al., 2013), respectively. Similarly, various PAMPs (e.g., lipopolysaccharide, peptidoglycan, pIC) have been shown to modulate immune–relevant miRNA expression in teleosts (Gong et al., 2015; Chu et al., 2017a; Chu et al., 2017b; Eslamloo et al., 2018). Here, I demonstrated that pIC and bacterin can lead to changes in expression of many miRNAs known to be involved in host responses to infection.

The predicted target gene analyses of pIC- and/or bacterin-responsive miRNAs revealed that each of the miRNAs could regulate from 2 to 21 genes that have immune-relevant functions (**Supplementary Tables S4.6 and S4.7**). Some of these predicted target genes were mapped to KEGG pathways (e.g., NOD-like receptor signaling pathway, Toll-like receptor signaling pathway, RIG-I-like receptor signaling pathway or cytokine–cytokine receptor interaction pathway; see **Table 4.4**) that are important to host immune responses to viral and/or bacterial infection. This further confirms that the pIC- and/or

bacterin-responsive miRNAs identified herein are relevant to the host-pathogen immune response.

The DESeq2 analyses of deep sequencing results were performed with a relatively small number of biological replicates (n = 3); therefore, there was a risk of false positives as well as false negatives. To avoid false positives, fifteen miRNAs identified as differentially expressed by DESeq2 were selected for qPCR confirmation using larger numbers of biological replicates (n = 8–9) than were included in the sequencing study. Among deep sequencing-identified pIC-responsive miRNAs subjected to qPCR analyses, only 1 miRNA (out of 8) did not confirm the DESeq2 results. For deep sequencing-identified bacterin-responsive miRNAs, 5 out of 10 were confirmed (i.e., statistically significant) by qPCR analyses. The library preparations of all samples involved in this study utilized identical chemistry and yielded similar percentages of high-quality reads. Therefore, the relative lower validation level of bacterin-responsive miRNA markers is unlikely to have been caused by the chemistry and/or sequencing-related factors. Rather, it is likely attributed to the difference in the sample sizes between sequencing and qPCR (i.e., 3 biological replicates in sequencing *vs* 8–9 biological replicates in qPCR). In order to decrease the likelihood of false negatives, future miRNA deep sequencing studies could employ higher numbers of biological replicates. For the remainder of the discussion, I will focus on the qPCR-confirmed miRNAs that were associated with antiviral and antibacterial immune responses.

4.5.2 miRNAs associated with both antiviral and antibacterial immune responses in Atlantic salmon head kidney

The qPCR results showed that 5 miRNAs (miR-27d-1-2-5p, miR-29b-2-5p, miR-146a-5p, miR-146a-1-2-3p, and miR-221-5p) were significantly up-regulated by both pIC and bacterin stimulations when compared with the PBS-injection controls. The expression of miR-27d-1-2-5p in Atlantic salmon fry was recently shown to be decreased in fish challenged with IPNV at both 7 and 20 days post-infections (Woldemariam et al., 2020). In mice, miR-27 was reported to be down-regulated in multiple mouse cell lines and primary macrophages by cytomegalovirus (i.e., a DNA virus) infection; however, upon overexpression it exerted an antiviral function (Buck et al., 2010). Compared with the pIC-induced miR-27d-1-2-5p in the present study, the opposite regulation of miR-27 by cytomegalovirus in mouse cells may be influenced by the virus–host interaction and/or difference in viral or PAMP nucleic acid (DNA virus *vs* RNA pIC). In Asian seabass (*Lates calcarifer*), the up-regulation of miR-27 in the spleen was associated with LPS-induced inflammatory immune response (Xia et al., 2011). In agreement with my findings, miR-29b was shown to be up-regulated in zebrafish embryos infected with *Salmonella typhimurium*, and in adult zebrafish infected with *Mycobacterium marinum* (Ordas et al., 2013). In contrast, the expression of miR-29 in Nile tilapia (*Oreochromis niloticus*) was down-regulated in fish challenged with *Streptococcus agalactiae* at early infection stages (i.e., 72 h) (Wang et al., 2016). Interestingly, in mice, miR-29 was shown to suppress the interferon-gamma (IFN-γ) production by targeting IFN-γ mRNA directly, and miR-29 knockdown mice initiated more potent innate and type 1 helper T cell adaptive responses

to intracellular bacterial infection (Ma et al., 2011). Recently miR-29b-2-5p was also shown to respond to IPNV challenge in Atlantic salmon (Woldemariam et al., 2020). However, the functions of miR-27d-1-2-5p and miR-29b-2-5p in the antiviral and antibacterial responses in teleost fish including Atlantic salmon are yet to be determined.

In mammals, miR-146 was shown to regulate inflammatory responses following TLR-dependent pathogen recognition (Pedersen and David, 2008). A study in human monocytes revealed that miR-146 attenuated TLR and cytokine signaling via a negative feedback loop involving the suppression of IL-1 receptor-associated kinase 1 and TNF receptor-associated factor 6 (Taganov et al., 2006). In fish, the expression of miR-146 increased in olive flounder (*Paralichthys olivaceus*) infected with VHSV (Najib et al., 2016), in Atlantic salmon infected with SAV (Andreassen et al., 2017), and in half-smooth tongue sole (*Cynoglossus semilaevis*) infected with *Vibrio anguillarum* (Sha et al., 2014). In humans, studies have revealed that the expression of miR-221 is up-regulated in several types of cancers and was related to cancer cell proliferation (Lu et al., 2009; Galardi et al., 2011; Li et al., 2011). Yan et al. (2016) evaluated the expression of miR-221 in half-smooth tongue sole after challenge with *V. anguillarum*, and a head kidney cell line stimulated with different PAMPs. Similar to my study, the expression of miR-221 was increased in the liver and spleen of the infected sole, and the in vitro study indicated that both LPS and pIC up-regulated the expression of miR-221 at 6 h post-stimulation (Yan et al., 2016). The expression of miR-221-5p was also evaluated in olive flounder in response to VHSV infection, showing increased level 24 h post-injection (Najib et al., 2016). In olive flounder, miR-221-5p was predicted to target important immune genes (i.e., *cd18* and *irf5*) (Najib et

al., 2016). Recently, it was also shown to respond to IPNV infection in Atlantic salmon (Woldemariam et al., 2020). Taken together with the current results, it appears that miR-146 and miR-221 are involved in both antiviral and antibacterial immune responses and may play critical immune regulatory roles in Atlantic salmon.

4.5.3 miRNAs only associated with antiviral immune response in Atlantic salmon head kidney

Of the 4 miRNAs identified by deep sequencing as being responsive only to pIC, 3 (i.e., miR-30e-1-2-3p, miR-181a-5-3p, and miR-462a-3p) were qPCR confirmed as being significantly up-regulated in fish fed the control diet. Although there have been no studies to date reporting the association of miR-30e with antiviral immune response in Atlantic salmon, a previous study in Atlantic salmon infected with the intracellular bacterium *P. salmonis* did show increased miR-30e expression in both spleen and head kidney (Valenzuela-Miranda et al., 2017). miR-181 and miR-462 were classified as evolutionarily conserved miRNAs associated with immune response in teleosts following viral challenges (Andreassen and Høyheim, 2017). The expression of miR-181a was increased in response to red-spotted grouper nervous necrosis virus in a head kidney cell line of half-smooth tongue sole (Gong et al., 2015). Similarly, Andreassen et al. (2017) showed that SAV infection in Atlantic salmon caused the up-regulation of miR-181c-5p. The predicted target mRNAs of miR-181c-5p in Atlantic salmon included a number of immune-relevant genes such as neutrophil cytosolic factor 1 (*ncf1*), *irf3*, and inhibitor of nuclear factor kappa-B kinase subunit alpha-like (*ikbka*; alias: *chuk*) (Andreassen et al., 2017). In mammals, it is suggested that the miR-181 family plays a central role in vascular inflammation by

controlling critical signaling pathways (e.g., NF-κB signaling) and targets relevant to immune cell activation and homeostasis (Sun et al., 2014). Similar to my findings, miR-462 was shown to be up-regulated in the spleen of flounder challenged with megalocytivirus (a DNA virus) infection (Zhang et al., 2014), RTL-W1 (i.e., rainbow trout liver cell line) and Atlantic cod macrophages stimulated with pIC (Schyth et al., 2015; Eslamloo et al., 2018), and Atlantic salmon challenged with SAV (Andreassen et al., 2017). Atlantic salmon miR-462a-3p was predicted to target macrosialin/CD68, a SAV-responsive gene (Andreassen et al., 2017). Collectively, these results support the hypothesis that miR-30e-1-2-3p, miR-181a-5-3p, and miR-462a-3p have immune-related functions and possibly play important roles in the antiviral immune response in Atlantic salmon.

4.5.4 miRNAs only associated with antibacterial immune response in Atlantic salmon head kidney

Among the 6 miRNAs identified by deep sequencing as being responsive only to bacterin, miR-727a-3p was qPCR confirmed as being significantly down-regulated compared with PBS control in fish fed the control diet. Similarly, the expression of miR-727-3p was reduced in the LPS-stimulated blunt snout bream (*Megalobrama amblycephala*) (Yuhong et al., 2016). It should be noted that miR-727 is likely a teleost-specific miRNA (Zhu et al., 2012), and the role of miR-727a-3p in the antibacterial immune response in fish is yet to be determined. Taken together, it seems that the 9 qPCR-confirmed miRNAs identified as pIC- and/or bacterin-responsive in the current study have

some conserved immune-related functions and may play important regulatory roles in the antiviral and/or antibacterial immune responses in Atlantic salmon.

4.5.5 CpG supplement modulated the expression of immune-relevant miRNAs in *A. salmonicida* bacterin-treated Atlantic salmon

Unmethylated DNAs containing CpG motifs are PAMPs that are commonly used as immunostimulants in fish (Carrington and Secombes, 2006; Cuesta et al., 2008; Liu et al., 2010; Kang and Kim, 2012; Purcell et al., 2013; Cárdenas-Reyna et al., 2016; Jung and Jung, 2017). The immune response induced by CpG is mediated through TLR9, a PRR present on the cell surface or within endosomal compartments of immune cells (Cuesta et al., 2008). Three different classes of CpG ODNs (A-, B-, and C-classes) have been characterized based on the backbone structure and sequence composition (Carrington and Secombes, 2006; Kang and Kim, 2012). In humans, A-class CpG ODNs are known to activate type I IFN response, while B-class CpG ODNs (e.g., CpG ODN 1668, used in the current study) are more potent in B cell stimulation (Kerkmann et al., 2003). Similarly, Strandskog et al. (2007) showed that A- and C-class CpG-ODNs induced strong IFN α/β activity, while B- and C-class CpG ODNs stimulated proliferation of leukocytes in Atlantic salmon. However, the impact of CpG as a functional feed ingredient on the modulation of immune-relevant miRNA expression in fish including Atlantic salmon had not been explored prior to this study.

To further investigate the immune-modulating property of the CpG-containing diet in Atlantic salmon, I analyzed 15 DESeq2-identified miRNAs associated with immune response on the pre- and post-immune stimulation head kidney samples. The current qPCR

analyses of candidate antiviral and antibacterial miRNAs showed that CpG supplementation generally suppressed basal expression of many miRNAs studied (i.e., in pre-injection samples). This may lead to the higher basal expression of genes targeted by these miRNAs. In post-injection groups (i.e., PBS and bacterin), however, many of these miRNAs were up-regulated in fish fed the CpG diet compared with fish fed the control diet. As shown by multivariate statistical analyses, dietary CpG had the most significant impact on the miRNA expression in the bacterin treated fish compared with other injection treatments, while the overall dietary CpG impact on candidate miRNAs expression in the pIC-injected fish was not significant (p (perm) = 0.446). Seven miRNAs (e.g., miR-146a-1-2-3p, miR-192a-5p, miR-221-5p, and miR-29b-2-5p) were the most significant contributing variables to the dissimilarity between the bacterin-treated fish. As discussed above, many of these miRNAs, as shown in previous studies, are involved in immune responses of teleost fish.

Studies involving CpG administration via IP-injection showed that CpG ODN 1668 enhanced the immune responses of Pacific red snapper against *Vibrio parahaemolitycus* exposure and rock bream against iridovirus (a DNA virus) infection (Cárdenas-Reyna et al., 2016; Jung and Jung, 2017). In contrast, studies in olive flounder revealed that CpG ODN 1668 conferred no protection against VHSV challenge and did not modulate the expression of well-known antiviral genes (i.e., *mx* and *isg15*), but elicited strong protection and immune response in fish challenged with a unicellular marine eukaryotic parasite *Miamiensis avidus* (Kang and Kim, 2012). In the current study, dietary CpG seemed to have no impact on the expression of candidate miRNAs in pIC-treated individuals, while

inducing several miRNAs in the PBS- and bacterin-treated fish. This suggests that CpG ODN 1668 may modulate *A. salmonicida* bacterin-stimulated antibacterial immune response rather than the pIC stimulated antiviral immune response based on candidate miRNA expression profiles. The selection of a CpG ODN appropriate to the characteristics of a specific pathogen (e.g., bacteria, virus or parasite) may be key to designing diets to improve defense against that pathogen. Finally, although the physiological and health-related consequences of the observed miRNA expression changes caused by the CpG diet remain unclear and require further study, it seems that selections of these miRNAs are suitable as immune-system associated biomarkers.

4.6 Conclusions

The present study identified and qPCR-confirmed 9 miRNA biomarkers of Atlantic salmon response to pIC and/or *A. salmonicida* bacterin immune stimulations. Many of the miRNAs identified herein are involved in immune responses, as shown in many similar teleost immune/pathogen challenge studies (discussed above). Regarding the immune-modulating properties of CpG diet on Atlantic salmon, I applied candidate miRNA biomarkers associated with immune response (identified in the current study) and evaluated the expression changes in pre- and post-stimulation individuals. CpG ODN 1668-containing diet may be useful in modulating the *A. salmonicida* bacterin-triggered antibacterial immune response but not the pIC-triggered antiviral immune response of Atlantic salmon. Since the current study utilized pIC and bacterin rather than live pathogens, in the future it would be important to determine if dietary immunostimulant CpG ODN 1668 could have a protective effect in live bacterial pathogen challenges in

Atlantic salmon. Finally, I anticipate that the molecular biomarkers identified herein will also be useful in the future development of functional feeds involving immunostimulants.

4.7 Supplementary materials

The Supplemental Tables and Figures for this chapter can be found in the supplemental materials of Xue et al. (2019) [available at: (http://www.mdpi.com/2073-4409/8/12/1592/s1)]. These files (as listed below) have also been supplied in a zipped folder that accompanies this thesis.

Supplemental Table S4.1. qPCR analyses of known *A. salmonicida* bacterin and pIC immune biomarker transcripts in the head kidney of fish fed the control diet.

Supplemental Table S4.2. miRNA qPCR primers.

Supplemental Table S4.3. C_T values of normalizers (miR-25-3p and miR-17-5p) in all analyzed samples.

Supplemental Table S4.4. Mature sequences and miRBase identities of pIC- and/or *A. salmonicida* bacterin-responsive miRNAs (identified by DESeq2 analyses).

Supplemental Table S4.5. Predicted target genes of pIC- and/or *A. salmonicida* bacterin-responsive miRNAs from the DESeq2 analyses.

Supplemental Table S4.6. Immune-relevant predicted target genes of pIC-responsive miRNAs from the DESeq2 analysis.

Supplemental Table S4.7. Immune-relevant predicted target genes of *A. salmonicida* bacterin-responsive miRNAs from the DESeq2 analysis.

4.8 References

Agaba, M.K., Tocher, D.R., Zheng, X., Dickson, C.A., Dick, J.R., Teale, A.J., 2005. Cloning and functional characterisation of polyunsaturated fatty acid elongases of marine and freshwater teleost fish. Comp. Biochem. Physiol. Part B Biochem. Mol. Biol. 142, 342-352.

Akira, S., Uematsu, S., Takeuchi, O., 2006. Pathogen recognition and innate immunity. Cell 124, 783-801.

Andreassen, R., Høyheim, B., 2017. miRNAs associated with immune response in teleost fish. Dev. Comp. Immunol. 75, 77-85.

Andreassen, R., Woldemariam, N.T., Egeland, I.Ø., Agafonov, O., Sindre, H., Høyheim, B., 2017. Identification of differentially expressed Atlantic salmon miRNAs responding to salmonid alphavirus (SAV) infection. BMC Genomics 18, 349.

Booman, M., Xu, Q.H., Rise, M.L., 2014. Evaluation of the impact of camelina oil-containing diets on the expression of genes involved in the innate anti-viral immune response in Atlantic cod (*Gadus morhua*). Fish Shellfish Immunol. 41, 52-63.

Buck, A.H., Perot, J., Chisholm, M.A., Kumar, D.S., Tuddenham, L., Cognat, V., Marcinowski, L., Dölken, L., Pfeffer, S., 2010. Post-transcriptional regulation of miR-27 in murine cytomegalovirus infection. RNA 16, 307-315.

Caballero-Solares, A., Hall, J.R., Xue, X., Eslamloo, K., Taylor, R.G., Parrish, C.C., Rise, M.L., 2017. The dietary replacement of marine ingredients by terrestrial animal and plant alternatives modulates the antiviral immune response of Atlantic salmon (*Salmo salar*). Fish Shellfish Immunol. 64, 24-38.

Caballero-Solares, A., Xue, X., Parrish, C.C., Foroutani, M.B., Taylor, R.G., Rise, M.L., 2018. Changes in the liver transcriptome of farmed Atlantic salmon (*Salmo salar*) fed experimental diets based on terrestrial alternatives to fish meal and fish oil. BMC Genomics 19, 796.

Cao, Y., Wang, D., Li, S., Zhao, J., Xu, L., Liu, H., Lu, T., Mou, Z., 2019. A transcriptome analysis focusing on splenic immune-related mciroRNAs of rainbow trout upon *Aeromonas salmonicida* subsp. *salmonicida* infection. Fish Shellfish Immunol. 91, 350-357.

Cárdenas-Reyna, T., Angulo, C., Hori-Oshima, S., Velázquez-Lizárraga, E., Reyes-Becerril, M., 2016. B-cell activating CpG ODN 1668 enhance the immune response

of Pacific red snapper (*Lutjanus peru*) exposed to *Vibrio parahaemolitycus*. Dev. Comp. Immunol. 62, 72-81.
Carrington, A.C., Secombes, C.J., 2006. A review of CpGs and their relevance to aquaculture. Vet. Immunol. Immunopathol. 112, 87-101.
Chen, J., Li, C., Huang, R., Du, F., Liao, L., Zhu, Z., Wang, Y., 2012. Transcriptome analysis of head kidney in grass carp and discovery of immune-related genes. BMC Vet. Res. 8, 108.
Chu, Q., Sun, Y., Bi, D., Cui, J., Xu, T., 2017a. Up-regulated of miR-8159-5p and miR-217-5p by LPS stimulation negatively co-regulate TLR1 in miiuy croaker. Dev. Comp. Immunol. 67, 117-125.
Chu, Q., Sun, Y., Cui, J., Xu, T., 2017b. MicroRNA-3570 modulates the NF-κB pathway in teleost fish by targeting MyD88. J. Immunol. 198, 3274-3282.
Covello, J.M., Friend, S.E., Purcell, S.L., Burka, J.F., Markham, R.J.F., Donkin, A.W., Groman, D.B., Fast, M.D., 2012. Effects of orally administered immunostimulants on inflammatory gene expression and sea lice (*Lepeophtheirus salmonis*) burdens on Atlantic salmon (*Salmo salar*). Aquaculture 366, 9-16.
Cuesta, A., Esteban, M.A., Meseguer, J., 2008. The expression profile of TLR9 mRNA and CpG ODNs immunostimulatory actions in the teleost gilthead seabream points to a major role of lymphocytes. Cell. Mol. Life Sci. 65, 2091-2104.
Dobin, A., Davis, C.A., Schlesinger, F., Drenkow, J., Zaleski, C., Jha, S., Batut, P., Chaisson, M., Gingeras, T.R., 2013. STAR: ultrafast universal RNA-seq aligner. Bioinformatics 29, 15-21.
Eslamloo, K., Inkpen, S.M., Rise, M.L., Andreassen, R., 2018. Discovery of microRNAs associated with the antiviral immune response of Atlantic cod macrophages. Mol. Immunol. 93, 152-161.
Eslamloo, K., Xue, X., Booman, M., Smith, N.C., Rise, M.L., 2016. Transcriptome profiling of the antiviral immune response in Atlantic cod macrophages. Dev. Comp. Immunol. 63, 187-205.
Ewart, K.V., Belanger, J.C., Williams, J., Karakach, T., Penny, S., Tsoi, S.C., Richards, R.C., Douglas, S.E., 2005. Identification of genes differentially expressed in Atlantic salmon (*Salmo salar*) in response to infection by *Aeromonas salmonicida* using cDNA microarray technology. Dev. Comp. Immunol. 29, 333-347.
FAO, 2018. The state of world fisheries and aquaculture 2018. Food and Agriculture Organization of the United Nations, Rome.
Feng, C.Y., Johnson, S.C., Hori, T.S., Rise, M., Hall, J.R., Gamperl, A.K., Hubert, S., Kimball, J., Bowman, S., Rise, M.L., 2009. Identification and analysis of differentially expressed genes in immune tissues of Atlantic cod stimulated with formalin-killed, atypical *Aeromonas salmonicida*. Physiol. Genomics 37, 149-163.
Galardi, S., Mercatelli, N., Farace, M.G., Ciafre, S.A., 2011. NF-kB and c-Jun induce the expression of the oncogenic miR-221 and miR-222 in prostate carcinoma and glioblastoma cells. Nucleic Acids Res. 39, 3892-3902.
Gong, G., Sha, Z., Chen, S., Li, C., Yan, H., Chen, Y., Wang, T., 2015. Expression profiling analysis of the microRNA response of *Cynoglossus semilaevis* to *Vibrio anguillarum* and other stimuli. Mar. Biotechnol. 17, 338-352.

Grubbs, F.E., 1969. Procedures for detecting outlying observations in samples, Technometrics, 11(1), 1-21.

Hellemans, J., Mortier, G., De Paepe, A., Speleman, F., Vandesompele, J., 2007. qBase relative quantification framework and software for management and automated analysis of real-time quantitative PCR data. Genome Biol. 8, R19.

Herkenhoff, M.E., Oliveira, A.C., Nachtigall, P.G., Costa, J.M., Campos, V.F., Hilsdorf, A.W., Pinhal, D., 2018. Fishing into the MicroRNA transcriptome. Front. Genet. 9, 88.

Hori, T.S., Gamperl, A.K., Nash, G., Booman, M., Barat, A., Rise, M.L., 2013. The impact of a moderate chronic temperature increase on spleen immune-relevant gene transcription depends on whether Atlantic cod (*Gadus morhua*) are stimulated with bacterial versus viral antigens. Genome 56, 567-576.

Johansen, I., Andreassen, R., 2014. Validation of miRNA genes suitable as reference genes in qPCR analyses of miRNA gene expression in Atlantic salmon (*Salmo salar*). BMC Res Notes 8.

Jung, M.-H., Jung, S.-J., 2017. CpG ODN 1668 induce innate and adaptive immune responses in rock bream (*Oplegnathus fasciatus*) against rock bream iridovirus (RBIV) infection. Fish Shellfish Immunol. 69, 247-257.

Kang, Y.J., Kim, K.H., 2012. Effect of CpG-ODNs belonging to different classes on resistance of olive flounder (*Paralichthys olivaceus*) against viral hemorrhagic septicemia virus (VHSV) and *Miamiensis avidus* (Ciliata; Scuticociliatia) infections. Aquaculture 324-325, 39-43.

Kerkmann, M., Rothenfusser, S., Hornung, V., Towarowski, A., Wagner, M., Sarris, A., Giese, T., Endres, S., Hartmann, G., 2003. Activation with CpG-A and CpG-B oligonucleotides reveals two distinct regulatory pathways of type I IFN synthesis in human plasmacytoid dendritic cells. J. Immunol. 170, 4465-4474.

Kiron, V., 2012. Fish immune system and its nutritional modulation for preventive health care. Anim. Feed Sci. Technol. 173, 111 - 133.

Lang, A.S., Rise, M.L., Culley, A.I., Steward, G.F., 2009. RNA viruses in the sea. FEMS Microbiol. Rev. 33, 295-323.

Li, J., Wang, Y., Yu, W., Chen, J., Luo, J., 2011. Expression of serum miR-221 in human hepatocellular carcinoma and its prognostic significance. Biochem. Biophys. Res. Commun. 406, 70-73.

Liao, Y., Smyth, G.K., Shi, W., 2013. featureCounts: an efficient general purpose program for assigning sequence reads to genomic features. Bioinformatics 30, 923-930.

Liu, C.-S., Sun, Y., Hu, Y.-H., Sun, L., 2010. Identification and analysis of a CpG motif that protects turbot (*Scophthalmus maximus*) against bacterial challenge and enhances vaccine-induced specific immunity. Vaccine 28, 4153-4161.

Love, M.I., Huber, W., Anders, S., 2014. Moderated estimation of fold change and dispersion for RNA-seq data with DESeq2. Genome Biol. 15, 550.

Løvoll, M., Wiik-Nielsen, C.R., Tunsjø, H.S., Colquhoun, D., Lunder, T., Sørum, H., Grove, S., 2009. Atlantic salmon bath challenged with *Moritella viscosa* – Pathogen invasion and host response. Fish Shellfish Immunol. 26, 877-884.

Lu, X., Zhao, P., Zhang, C., Fu, Z., Chen, Y., Lu, A., Liu, N., You, Y., Pu, P., Kang, C., 2009. Analysis of miR-221 and p27 expression in human gliomas. Mol. Med. Rep. 2, 651-656.

Ma, F., Xu, S., Liu, X., Zhang, Q., Xu, X., Liu, M., Hua, M., Li, N., Yao, H., Cao, X., 2011. The microRNA miR-29 controls innate and adaptive immune responses to intracellular bacterial infection by targeting interferon-γ. Nat. Immunol. 12, 861.

Martin, M., 2011. Cutadapt removes adapter sequences from high-throughput sequencing reads. EMBnet.journal 17, 10-12.

Martin, S.A.M., Król, E., 2017. Nutrigenomics and immune function in fish: new insights from omics technologies. Dev. Comp. Immunol. 75, 86-98.

Murray, A.G., Munro, L.A., Wallace, I.S., Allan, C.E.T., Peeler, E.J., Thrush, M.A., 2012. Epidemiology of *Renibacterium salmoninarum* in Scotland and the potential for compartmentalised management of salmon and trout farming areas. Aquaculture 324-325, 1-13.

Najib, A., Kim, M.S., Choi, S.H., Kang, Y.J., Kim, K.H., 2016. Changes in microRNAs expression profile of olive flounder (*Paralichthys olivaceus*) in response to viral hemorrhagic septicemia virus (VHSV) infection. Fish Shellfish Immunol. 51.

Ordas, A., Kanwal, Z., Lindenberg, V., Rougeot, J., Mink, M., Spaink, H.P., Meijer, A.H., 2013. MicroRNA-146 function in the innate immune transcriptome response of zebrafish embryos to *Salmonella typhimurium* infection. BMC Genomics 14, 696.

Pedersen, I., David, M., 2008. MicroRNAs in the immune response. Cytokine 43, 391-394.

Pfaffl, M., 2001. A new mathematical model for relative quantification in real-time RT-PCR. Nucleic Acids Res. 29, e45.

Press, C.M., Evensen, Ø., 1999. The morphology of the immune system in teleost fishes. Fish Shellfish Immunol. 9, 309-318.

Purcell, S.L., Friend, S.E., Covello, J.M., Donkin, A., Groman, D.B., Poley, J., Fast, M.D., 2013. CpG inclusion in feed reduces sea lice, *Lepeophtheirus salmonis*, numbers following re‐infection. J. Fish Dis. 36, 229-240.

Rehmsmeier, M., Steffen, P., Höchsmann, M., Giegerich, R., 2004. Fast and effective prediction of microRNA/target duplexes. RNA 10, 1507-1517.

Rise, M.L., Jones, S.R.M., Brown, G.D., von Schalburg, K.R., Davidson, W.S., Koop, B.F., 2004. Microarray analyses identify molecular biomarkers of Atlantic salmon macrophage and hematopoietic kidney responses to *Piscirickettsia salmonis* infection. Physiol. Genomics 20, 21 - 35.

Robertsen, B., 2006. The interferon system of teleost fish. Fish Shellfish Immunol. 20, 172-191.

Schyth, B.D., Bela-ong, D.B., Jalali, S.A.H., Kristensen, L.B.J., Einer-Jensen, K., Pedersen, F.S., Lorenzen, N., 2015. Two virus-induced MicroRNAs known only from teleost fishes are orthologues of MicroRNAs involved in cell cycle control in humans. PLoS One 10, e0132434.

Secombes, C.J., Wang, T., 2012. The innate and adaptive immune system of fish, in: Austin, B. (Ed.), Infectious Disease in Aquaculture. Woodhead Publishing, pp. 3-68.

Sha, Z., Gong, G., Wang, S., Lu, Y., Wang, L., Wang, Q., Chen, S., 2014. Identification and characterization of *Cynoglossus semilaevis* microRNA response to *Vibrio anguillarum* infection through high-throughput sequencing. Dev. Comp. Immunol. 44, 59-69.

Strandskog, G., Ellingsen, T., Jørgensen, J.B., 2007. Characterization of three distinct CpG oligonucleotide classes which differ in ability to induce IFN α/β activity and cell proliferation in Atlantic salmon (*Salmo salar* L.) leukocytes. Dev. Comp. Immunol. 31, 39-51.

Sun, X., Sit, A., Feinberg, M.W., 2014. Role of miR-181 family in regulating vascular inflammation and immunity. Trends Cardiovascul. Med. 24, 105-112.

Tacchi, L., Bickerdike, R., Douglas, A., Secombes, C.J., Martin, S.A.M., 2011. Transcriptomic responses to functional feeds in Atlantic salmon (*Salmo salar*). Fish Shellfish Immunol. 31, 704-715.

Taganov, K.D., Boldin, M.P., Chang, K.-J., Baltimore, D., 2006. NF-κB-dependent induction of microRNA miR-146, an inhibitor targeted to signaling proteins of innate immune responses. Proc. Natl. Acad. Sci. U. S. A. 103, 12481-12486.

Tocher, D.R., Zheng, X., Schlechtriem, C., Hastings, N., Dick, J.R., Teale, A.J., 2006. Highly unsaturated fatty acid synthesis in marine fish: Cloning, functional characterization, and nutritional regulation of fatty acyl Δ6 desaturase of Atlantic cod (*Gadus morhua* L.). Lipids 41, 1003-1016.

Valenzuela-Miranda, D., Valenzuela-Muñoz, V., Farlora, R., Gallardo-Escárate, C., 2017. MicroRNA-based transcriptomic responses of Atlantic salmon during infection by the intracellular bacterium *Piscirickettsia salmonis*. Dev. Comp. Immunol. 77, 287-296.

Vallejos-Vidal, E., Reyes-López, F., Teles, M., MacKenzie, S., 2016. The response of fish to immunostimulant diets. Fish Shellfish Immunol. 56, 34-69.

Wang, B., Gan, Z., Cai, S., Wang, Z., Yu, D., Lin, Z., Lu, Y., Wu, Z., Jian, J., 2016. Comprehensive identification and profiling of Nile tilapia (*Oreochromis niloticus*) microRNAs response to *Streptococcus agalactiae* infection through high-throughput sequencing. Fish Shellfish Immunol. 54, 93-106.

Woldemariam, N.T., Agafonov, O., Høyheim, B., Houston, R.D., Taggart, J.B., Andreassen, R., 2019. Expanding the miRNA repertoire in Atlantic salmon; discovery of isomiRs and miRNAs highly expressed in different tissues and developmental stages. Cells 8, 42.

Woldemariam, N.T., Agafonov, O., Sindre, H., Høyheim, B., Houston, R.D., Robledo, D., Bron, J.E., Andreassen, R., 2020. miRNAs Predicted to Regulate Host Anti-viral Gene Pathways in IPNV-Challenged Atlantic Salmon Fry Are Affected by Viral Load, and Associated With the Major IPN Resistance QTL Genotypes in Late Infection. Front. Immunol. 11, 2113.

Xia, J.H., He, X.P., Bai, Z.Y., Yue, G.H., 2011. Identification and characterization of 63 MicroRNAs in the Asian seabass *Lates calcarifer*. PLoS One 6, e17537.

Xue, X., Hixson, S.M., Hori, T.S., Booman, M., Parrish, C.C., Anderson, D.M., Rise, M.L., 2015. Atlantic salmon (*Salmo salar*) liver transcriptome response to diets

containing *Camelina sativa* products. Comp. Biochem. Physiol. Part D Genomics Proteomics 14.

Xue, X., Woldemariam, N.T., Caballero-Solares, A., Umasuthan, N., Fast, M.D., Taylor, R.G., Rise, M.L., Andreassen, R., 2019. Dietary immunostimulant CpG modulates microRNA biomarkers associated with immune responses in Atlantic salmon (*Salmo salar*). Cells 8, 1592.

Yan, H., Chen, Y., Zhou, S., Li, C., Gong, G., Chen, X., Wang, T., Chen, S., Sha, Z., 2016. Expression profile analysis of miR-221 and miR-222 in different tissues and head kidney cells of *Cynoglossus semilaevis*, following pathogen infection. Mar. Biotechnol. 18, 37-48.

Yuhong, J., Leilei, T., Fuyun, Z., Hongyang, J., Xiaowen, L., Liying, Y., Lei, Z., Jingrong, M., Jinpeng, Y., 2016. Identification and characterization of immune-related microRNAs in blunt snout bream, *Megalobrama amblycephala*. Fish Shellfish Immunol. 49, 470-492.

Zhang, B.-C., Zhang, J., Sun, L., 2014. In-depth profiling and analysis of host and viral microRNAs in Japanese flounder (*Paralichthys olivaceus*) infected with megalocytivirus reveal involvement of microRNAs in host-virus interaction in teleost fish. BMC Genomics 15, 878.

Zhu, Y.-P., Xue, W., Wang, J.-T., Wan, Y.-M., Wang, S.-L., Xu, P., Zhang, Y., Li, J.-T., Sun, X.-W., 2012. Identification of common carp (*Cyprinus carpio*) microRNAs and microRNA-related SNPs. BMC Genomics 13, 413.

CHAPTER 5: Characterization of the impact of dietary immunostimulant CpG on the expression of mRNA biomarkers involved in the immune responses in Atlantic salmon (*Salmo salar*)

The research described in **Chapter 5** is being prepared for submission to the journal Fish & Shellfish Immunology as: Xue, X., Eslamloo, K., Caballero-Solares, A., Katan T, Umasuthan N, Taylor, R.G., Fast, M.D., Andreassen R, Rise, M.L. Characterization of the impact of dietary immunostimulant CpG on the expression of mRNA biomarkers involved in the immune responses in Atlantic salmon (*Salmo salar*).

5.1 Abstract

Infectious diseases have significantly impacted Atlantic salmon aquaculture worldwide. Boosting fish immunity with immunostimulant-containing functional feeds is one of the most effective strategies in mitigating disease problems. Previously, I characterized the impact of polyriboinosinic polyribocytidylic acid (pIC) and formalin-killed typical *Aeromonas salmonicida* bacterin on miRNA expression in Atlantic salmon fed a commercial diet with and without immunostimulant CpG, and identified a set of miRNA biomarkers of Atlantic salmon response to pIC and/or bacterin immune stimulations. Herein, I report a complementary qPCR study that investigated the impact of the pIC, bacterin and dietary CpG on the expression of immune-relevant mRNAs (n = 31) using the same samples as were previously used in the miRNA study (Xue et al., 2019). Twenty-three of these genes were predicted target transcripts of the pIC- and/or bacterin-responsive miRNAs in Atlantic salmon identified in the earlier study. The current qPCR data showed that pIC and/or bacterin stimulations significantly modulated the majority of the predicted target genes involved in various immune pathways. Some genes responded to both stimulations (e.g. *tnfa*, *il10rb*, *ifng*, *irf9*, *cxcr3*, *campb*) while others appeared to be stimulation specific [e.g. *irf3*, *irf7a*, *il1r1*, *mxa*, *mapk3* (pIC only); *clra* (bacterin only)]. *A. salmonicida* bacterin stimulation produced a stronger inflammatory response (e.g. higher expression of *il1b*, *il8a* and *tnfa*) compared with pIC-treated group, while salmon stimulated with pIC showed stronger interferon responses (both type I and II). Furthermore, the current data indicated significant down-regulation of immune-relevant transcripts (e.g. *tlr9*, *irf5*, *il1r1*, *hsp90ab1*, *itgb2*) by dietary immunostimulant CpG, especially among pre-

injection and PBS-injected fish. I also attempted to explore connections between the changes in mRNA and miRNA expression, and identified some significant correlations that represented putative miRNA-target pairs, providing further insights into how miRNAs might fine-tune the expression of immune-relevant mRNAs.

5.2 Introduction

Infectious diseases have resulted in substantial mortality and losses to Atlantic salmon (*Salmo salar*) aquaculture worldwide, affecting the growth and sustainability of the industry (Caballero-Solares et al., 2017). Several well-known viruses that cause severe diseases in Atlantic salmon include salmonid alphavirus (SAV), infectious salmon anemia virus (ISAV), viral hemorrhagic septicemia virus (VHSV), and infectious pancreatic necrosis virus (IPNV) (Lang et al., 2009). Bacterial pathogens that have a severe impact on salmonid aquaculture include Gram negative bacteria such as *Piscirickettsia salmonis* (Rozas and Enríquez, 2014), *Aeromonas salmonicida* (Ewart et al., 2005), *Moritella viscosa* (Løvoll et al., 2009), and Gram positive bacteria such as *Renibacterium salmoninarum* (Murray et al., 2012). For instance, in Chile, the National Fisheries and Aquaculture Service estimated that about 50% of disease-causing mortalities in Atlantic salmon were attributed to piscirickettsiosis (a disease caused by *P. salmonis*) in 2020 (Sernapesca, 2021). The annual direct and indirect losses in the Chilean aquaculture industry due to piscirickettsiosis were approximately USD 700 million (Maisey et al., 2017; Meza et al., 2019).

One important strategy to fight disease problems in intensive culture systems is to enhance immune responses of cultured fish using immunostimulant-containing functional feeds (Martin and Król, 2017; Tacchi et al., 2011a). Immunostimulants may include intact microbes (e.g. probiotic organisms) and microbial cell components (e.g. lipopolysaccharide). These substances generally have repeat structures, often referred to as pattern associated molecular patterns (PAMPs), and can be recognized by specific

receptors within the host immune cells, triggering the host immune responses (Vallejos-Vidal et al., 2016). Unmethylated DNA containing cytosine-phosphate-guanine oligodeoxynucleotides motifs (CpG ODNs), often found in bacterial genomes as well as in some viral and invertebrate genomes, are essential immunomodulators that can induce or enhance host Toll-like receptor 9 (TLR9)-mediated immune responses (Cuesta et al., 2008; Liu et al., 2010). Synthetic CpG ODNs are divided into three classes (i.e., A-, B- and C-classes) with distinct immunomodulating properties based on the backbone structure and sequences (Carrington and Secombes, 2006). For example, CpG ODN 1668 (i.e., B-class), was shown to activate immune responses against iridovirus infection in rock bream (*Oplegnathus fasciatus*) (Jung and Jung, 2017), and *Vibrio parahaemolyticus* infection in Pacific red snapper (*Lutjanus peru*) (Cárdenas-Reyna et al., 2016). In addition, previous studies showed protection against sea lice (*Lepeophtheirus salmonis*) infection in Atlantic salmon by orally administered CpG ODN 1668 (Covello et al., 2012; Purcell et al., 2013).

miRNAs are a group of small (usually 20-24 nucleotides), non-coding RNAs that inhibit gene expression at the post-transcriptional level by binding to partially complementary sequences in their target mRNAs (Andreassen and Høyheim, 2017; Herkenhoff et al., 2018; Woldemariam et al., 2019). A growing body of literature indicates that miRNAs play critical roles in diverse biological processes such as development, tissue differentiation and regeneration, growth, reproduction and responses to environmental stimuli (Andreassen and Høyheim, 2017). In addition, the potential regulatory role of miRNAs in fish immune response has been reported in a number of species by identifying the miRNAs that are differentially expressed between the control and challenged animals

(Guo et al., 2015; Zhang et al., 2016a; Andreassen et al., 2017; Eslamloo et al., 2018; Xu et al., 2018; Xue et al., 2019; Woldemariam et al., 2020). For example, my previous study (**Chapter 4**; Xue et al., 2019) showed that the analyses of head kidneys from Atlantic salmon injected with immunogens [polyriboinosinic polyribocytidylic acid (pIC, a PAMP-like synthetic dsRNA analogue or viral mimic) or formalin-killed typical *Aeromonas salmonicida* (a PAMP-containing bacterin)] revealed 12 and 18 miRNAs differentially expressed in pIC and bacterin groups, respectively, compared to the controls. Further, the functional annotations of predicted target genes of the pIC- and/or bacterin-responsive miRNAs revealed 130 immune-relevant target genes (Xue et al., 2019). The pathways mapped to these target genes include NOD-like receptor signaling pathway, cytokine–cytokine receptor interaction, necroptosis, Toll-like receptor signaling pathway, apoptosis, C-type lectin receptor signaling pathway, RIG-I-like receptor signaling pathway, and cell adhesion molecules (CAMs) (**Chapter 4**; Xue et al., 2019). The impact of dietary CpG ODN 1668 on the expression of miRNAs associated with antiviral and antibacterial responses in Atlantic salmon was also evaluated; the expression of several miRNAs (e.g., miR-146a-1-2-3p, miR-192a-5p, miR-194a-5p) was modulated by dietary CpG (Chapter 4; Xue et al., 2019).

There was previously no information on the impact of pIC and *A. salmonicida* bacterin on immune-relevant mRNAs that are predicted targets of the pIC- and/or bacterin-responsive miRNAs in Atlantic salmon. In the present study, I investigated the expression response of immune-relevant mRNA biomarkers [e.g. predicted target genes of pIC- and/or *A. salmonicida* bacterin-responsive miRNAs from the previous research (**Chapter 4**; Xue

et al., 2019)] to viral mimic pIC and *A. salmonicida* bacterin stimulations in the head kidney of Atlantic salmon. I also studied these predicted target mRNAs in fish fed diets with and without immunostimulant CpG. Finally, I explored connections between the changes in mRNA and miRNA expression.

5.3 Materials and methods

5.3.1 Feed production, feeding trial, immune challenge and fish sampling

The production of feeds used in the current study was described previously (Xue et al., 2019). Briefly, EWOS Dynamic S feed (5 mm; 27% fat, 46% protein) was used in this experiment as the control diet and base feed for the functional diet (referred to as CpG diet). The CpG diet was top-coated with 10 mg kg^{-1} of CpG ODN 1668 (Integrated DNA Technologies, Coralville, IA, USA).

The detailed information and procedures related to the feeding trial, immune challenge and fish sampling were described in the previous investigation (Xue et al., 2019). Briefly, PIT (passive integrated transponder)-tagged Atlantic salmon smolts (232 ± 52 g mean initial weight ± SD; n=67) were allocated to four 620 L tanks (16-17 fish per tank) connected to a flow-through seawater system (~10-11°C, dissolved oxygen ≥ 10 mg L^{-1}) under a 24 h light photoperiod in the Dr. Joe Brown Aquatic Research Building [JBARB, Ocean Sciences Centre (OSC), Memorial University of Newfoundland, St. John's, NL, Canada]. After acclimation, each dietary treatment was randomly assigned to 2 replicate tanks. Fish were fed to apparent satiation using automatic feeders for seven weeks.

At the end of the feeding trial, both dietary groups were subjected to immune challenge by an intraperitoneal (IP) injection of *A. salmonicida* bacterin, viral mimic pIC or phosphate-buffered saline (PBS). The detailed methodology on immunogen preparation, injection procedures, and injection dosage was described previously (Xue et al., 2019). Briefly, four fish were euthanized with an overdose of MS-222 (400 mg L^{-1}, Syndel Laboratories, Vancouver, BC, Canada) and dissected for pre-injection (i.e., Time 0) head kidney samples. Formalin-killed typical *A. salmonicida* bacterin was obtained in the form of a vaccine (Furogen Dip, Elanco (formerly Novartis), Charlottetown, PE, Canada). The *A. salmonicida* bacterin solution was prepared as in Hori et al. (2013), while the pIC (Catalogue # P0913; Sigma-Aldrich, Oakville, ON, Canada) was diluted in sterile phosphate-buffered saline (PBS; Gibco, Carlsbad, CA, USA) at 2 μg μL^{-1} for injection. Then, 4-5 fish from each tank were anesthetized (50 mg L^{-1} of MS-222) and injected with 1 μL of pIC, bacterin or PBS per g of body weight. Fish were then sampled 24 h post-injection as described above, and head kidney samples (50-100 mg) were collected, flash-frozen in liquid nitrogen, and stored at −80°C until RNA extraction. This study was carried out in accordance with animal care protocol 17-77-MR, approved by the Institutional Animal Care Committee of Memorial University of Newfoundland.

5.3.2 RNA isolation

Total RNAs of all collected head kidney samples were previously extracted using the *mirVana* miRNA isolation kit (Ambion/Life Technologies, Carlsbad, CA, USA) according to manufacturer instructions (Xue et al., 2019). Aliquots of *mirVana*-prepared total RNAs (40 μg) were further treated with DNase I (Qiagen) to degrade residual genomic

DNA and then purified using the RNeasy Mini Kit (Qiagen) following the manufacturer's protocols. The RNA integrity was verified by 1% agarose gel electrophoresis, and RNA purity was assessed by A260/280 and A260/230 using NanoDrop spectrophotometry (Thermo Fisher, Mississauga, ON, Canada). All RNA samples used in this study showed high integrity (i.e., tight 18S and 28S ribosomal RNA bands) and purity (i.e., A260/230 ratios > 1.8 and A260/280 ratios > 2.0).

5.3.3 Candidate gene selection

In the previous investigation, I performed small RNA deep sequencing to identify pIC- and/or *A. salmonicida* bacterin-responsive miRNAs in the head kidney of Atlantic salmon fed the control diet (**Chapter 4**; Xue et al., 2019). DESeq2 analyses identified 12 and 18 miRNAs differentially expressed in pIC and bacterin groups compared with the controls, respectively; further, the putative target genes of the pIC- and/or bacterin-responsive miRNAs were predicted and described (**Chapter 4**; Xue et al., 2019). Briefly, the mature miRNA sequences were tested against 3' UTRs from all Atlantic salmon transcripts in the NCBI Reference Sequence database (Refseq; https://www.ncbi.nlm.nih.gov/refseq/) using a miRNA target prediction tool RNAhybrid (Rehmsmeier et al., 2004). A subset of predicted target genes with functions associated with immune response identified based on the Gene Ontology (GO) term annotations and published studies are available in Supplemental Tables S6 and S7 of Xue et al. (2019). In total, 23 predicted target genes (i.e. mRNAs) of the pIC- and/or bacterin-responsive miRNAs known to play roles in the immune response of fish were selected for qPCR analysis (**Table 5.1**). Finally, eight additional candidate immune biomarkers (*tlr5a*, *tlr7*,

Table 5.1. 23 predicted target mRNAs of pIC- and/or bacterin-responsive miRNAs and 8 other candidate immune biomarkers analyzed by qPCR.

Candidate genes	GenBank accession number	Functional annotation[1]	pIC-responsive miRNA[2]	Bacterin-responsive miRNA[2]
Transcripts encoding pattern recognition receptors (PRRs) or involved in PRR signaling pathways				
toll-like receptor 5a (*tlr5a*)[3]	AY628755	Toll-like receptor signaling pathway; defense response to bacterium	N/A	N/A
toll-like receptor 7 (*tlr7*)[3]	HF970585	Toll-like receptor signaling pathway; defense response to virus	N/A	N/A
toll-like receptor 9 (*tlr9*)[3]	NM_001123653	Toll-like receptor signaling pathway; unmethylated CpG binding	N/A	N/A
C type lectin receptor A (*clra*)[4]	NM_001123579	PRR recognizing carbohydrate patterns present on the surface of microorganisms (Zhang et al., 2000)	miR-135bd-5p	N/A
MYD88 innate immune signal transduction adaptor (*myd88*)[3]	NM_001136545	MyD88-dependent Toll-like receptor signaling pathway	N/A	N/A
interferon regulatory factor 3 (*irf3*)[4]	BT059292	type I interferon signaling pathway	miR-8159-5p	miR-725-5p
interferon regulatory factor 5 (*irf5*)[4]	NM_001139852	positive regulation of type I interferon production	miR-135bd-5p miR-462a-3p miR-462b-3p	N/A
interferon regulatory factor 7a (*irf7a*)[4,*]	NM_001136548	type I interferon signaling pathway	N/A	miR-192a-5p
interferon regulatory factor 7b (*irf7b*)[3,*]	FJ517644	type I interferon signaling pathway	N/A	N/A
TANK-binding kinase 1 (*tbk1*)[4]	NM_001256722	regulation of type I interferon production	miR-146a-5p	miR-146a-5p
suppressor of IKK-epsilon (*sike1*)[4]	NM_001140308	inhibitory role in virus-triggered TLR3-dependent interferon activation pathways (Huang et al., 2005)	miR-146a-1-2-3p miR-8159-5p	miR-146a-1-2-3p miR-146a-3-3p miR-183-2-3p
mitogen-activated protein kinase kinase kinase 8 (*map3k8*)[4]	NM_001173785	transducing signals from TLRs to regulate TNF and IL1B production (Mielke et al., 2009).	N/A	miR-192a-5p miR-200b-3p miR-725-3p miR-725-3p
Transcripts encoding cytokines or involved in cytokine mediated pathways				
interleukin 1 beta (*il1b*)[3]	AY617117	inflammatory response; cytokine-mediated signaling pathway	N/A	N/A

tumor necrosis factor alpha (*tnfa*)[4]	NM_001123617	inflammatory response; tumor necrosis factor-mediated signaling pathway	miR-8159-5p	miR-146d-1-3p miR-192a-5p miR-725-3p
interleukin 8a (*il8a*; alias *cxcl8a*)[4]	NM_001140710	inflammatory response; induction of positive chemotaxis	N/A	miR-194a-5p
interleukin-1 receptor type I (*il1r1*)[4]	NM_001123633	inflammatory response; interleukin-1-mediated signaling pathway	N/A	miR-725-5p miR-novel-16-5p
interleukin-10 receptor beta chain precursor (*il10rb*)[4]	BT059022	inflammatory response; interleukin-10 receptor activity	miR-221-5p	miR-183-1-3-3p miR-183-2-3p miR-221-5p miR-29b-2-5p miR-429ab-3p
interferon gamma (*ifng*)[4]	AJ841811	receptor signaling pathway via JAK-STAT; defense response to virus	N/A	miR-725-3p miR-727a-3p
interferon regulatory factor 9 (*irf9*)[4]	NM_001173719	regulating the downstream expression of ISGs within the type I IFN response pathway (Paul et al., 2018)	miR-135bd-5p miR-30e-1-2-3p	N/A
C-X-C chemokine receptor type 3 (*cxcr3*)[4]	NM_001140493	chemokine-mediated signaling pathway; regulation of leukocyte migration	miR-8159-5p	N/A
Transcripts playing key roles as immune effectors or regulators				
interferon-induced GTP-binding protein Mx a (*mxa*)[4]	NM_001123690	antiviral innate immune response; response to type I interferon	miR-181a-5-3p	N/A
interferon-induced GTP-binding protein Mx b (*mxb*)[3]	NM_001139918	antiviral innate immune response; response to type I interferon	N/A	N/A
interferon stimulated gene 15a (*isg15a*)[3]	BT049918	defense response to virus; response to type I interferon	N/A	N/A
cathelicidin antimicrobial peptide b (*campb*)[4]	NM_001123573	antibacterial humoral response; cellular response to interleukin-1	N/A	miR-183-1-3-3p
B-cell lymphoma 6 protein homolog (*bcl6*)[4]	NM_001140313	positive regulation of apoptotic process; regulation of immune system process	miR-27d-1-5p	miR-194a-5p
MAP kinase-activated protein kinase 3 (*mapk3*)[4]	NM_001139792	MAPK cascade; apoptotic process	N/A	miR-146d-1-3p miR-183-2-3p miR-29b-2-5p miR-725-3p miR-novel-16-5p
tumor necrosis factor receptor superfamily member 6 precursor (*tnfrsf6; alias fas*)[4]	NM_001173649	extrinsic apoptotic signaling pathway	miR-135bd-5p	miR-192a-5p miR-722-3p

BCL2/adenovirus E1B interacting protein 3-like (*bnip3l*)[4]	NM_001141679	positive regulation of apoptotic process	miR-146a-5p	miR-146a-5p miR-29b-2-5p
dynamin-1-like protein (*dnm1l*)[4]	NM_001173563	positive regulation of apoptotic process	miR-462a-3p miR-462b-3p	N/A
heat shock protein HSP 90-beta (*hsp90ab1*)[4]	NM_001146473	chaperone-mediated protein complex assembly; MHC class II protein complex binding	N/A	miR-200b-3p
integrin beta-2 (*itgb2*)[4]	NM_001165324	cell adhesion mediated by integrin; neutrophil migration	miR-146a-5p	miR-146a-5p miR-183-2-3p miR-29b-2-5p

[1]Genes were functionally annotated based on selected gene ontology (GO) terms from *Homo sapiens* putative orthologues or published studies. [2]pIC- or bacterin-responsive miRNAs predicted to target a given candidate gene. Genes noted with N/A (i.e. not applicable) were not predicted target mRNAs of pIC- and/or bacterin-responsive miRNAs. Immunogen-responsive miRNAs were identified and their predicted targets were conducted in Xue et al. (2019). [3]Additional candidate immune biomarkers (n = 8). [4]Predicted target genes (i.e. mRNAs) of the pIC- and/or bacterin-responsive miRNAs (n = 23). **irf7* paralogues are located on different chromosomes (ssa16 for *irf7a* and ssa10 for *irf7b*), and they are 89.4% identical at the nucleotide level.

tlr9, *myd88*, *irf7b*, *il1b*, *mxb*, *isg15a*) were also included in the qPCR analysis to further evaluate the immune responses from the immunogen challenges and the immune modulating property of the functional feed (i.e. CpG diet).

5.3.4 qPCR analysis

The qPCR experiment included a total of 67 head kidney RNA samples from pre-injection (i.e. T0), and PBS-, bacterin-, and pIC-injected fish fed the control or CpG diet (8-9 samples per treatment). First-strand cDNA templates for qPCR were synthesized in 20 µL reactions from 1 µg of DNaseI-treated, column-purified total RNA using random primers (250 ng; Invitrogen/Life Technologies), dNTPs (0.5 mM final concentration; Invitrogen/ Life Technologies) and M-MLV reverse transcriptase (200 U; Invitrogen/Life Technologies) with the manufacturer's first strand buffer (1× final concentration) and DTT (10 mM final concentration) at 37°C for 50 min. PCR amplifications were performed in 13 µL reactions using 1× Power SYBR Green PCR Master Mix (Applied Biosystems/Life Technologies), 50 nM of both the forward and reverse primers, and the indicated cDNA quantity (see below). The real-time qPCR analysis program for all primer pairs consisted of 1 cycle of 50°C for 2 min, 1 cycle of 95°C for 10 min and 40 cycles of 95°C for 15 sec and 60°C for 1 min, with fluorescence detection at the end of each 60°C step.

The sequences of all primer pairs used in qPCR analyses are presented in **Supplemental Table S5.1**. Each primer pair was quality tested using the ViiA 7 Real Time PCR system (384-well format) (Applied Biosystems/Life Technologies). Quality testing ensured that a single product was amplified (dissociation curve analysis) and that there was no primer-dimer present in the no-template control. Amplification efficiencies (Pfaffl,

2001) were calculated using three cDNA templates that were pooled post-cDNA synthesis: one pool of 4 PBS-injected samples, one pool of 4 pIC-injected samples, and one pool of 4 bacterin-injected samples. The reported efficiencies (**Supplemental Table S5.2**) are an average of the three values. Standard curves were generated using 5-point 1:3 dilution series starting with cDNA representing ten ng of input total RNA.

To select these control genes, the expression of 6 candidate normalizers [i.e. *60S ribosomal protein 32* (*rpl32*; BT043656), *β-actin* (*actb*; BG933897), *elongation factor 1-alpha 2* (*ef1a2*; BT058669), *eukaryotic translation initiation factor 3 subunit D* (*eif3d*; GE777139), *polyadenylate-binding protein 1* (*pabpc1*; EG908498) and *ATP-binding cassette sub-family F member 2* (*abcf2*; BT071904)] was measured in all individuals involved in the study and then analyzed using *geNorm* (Vandesompele et al., 2002). *ef1a2* (geNorm M = 0.198) and *pabpc1* (geNorm M = 0.196) were determined to be the most stable normalizer genes across treatments.

After completing the primer quality test and normalizer gene selection, qPCR analyses of transcript expression levels of the target genes were performed using the ViiA 7 Real Time PCR system (Applied Biosystems/Life Technologies). Diluted cDNAs corresponding to 5 ng of input RNA were used as templates in the PCR reactions to measure the C_T values of genes of interest (GOIs) and normalizer genes by QuantStudio Real-Time PCR Software. The GOIs and normalizer genes were tested in triplicate and a no-template control for each target was included. The relative quantity (RQ) of each transcript was determined using a qBase relative quantification framework (Hellemans et al., 2007; Xue et al., 2019; Xue et al., 2021), with normalization to both *pabpc1* and *ef1a2*,

and with amplification efficiencies incorporated. The RQs of each GOI were first calibrated to the sample that had the lowest normalized gene expression. For pre-injection samples (i.e., T0 samples), the RQs of each GOI were re-calibrated against fish fed the control diet, while for IP-injected groups, the RQs of each GOI were re-calibrated against PBS-injected fish fed the control diet.

5.3.5 Statistical analyses

All qPCR data (i.e., RQs) were subjected to Grubbs' test to identify potential outliers and then $\log_2$-transformation to meet the normality assumption. The normality of the qPCR data (i.e., $\log_2$ RQ values) was analyzed using the Shapiro-Wilk and Kolmogorov-Smirnov normality tests. In total, 36 RQ values were identified as statistical outliers in the entire dataset (i.e., out of 2077 RQ values), and excluded from the study. Each mRNA of interest had a minimum of 7 samples per treatment. For pre-injection samples, miRNA expression differences between diet groups were determined using Student's *t*-test ($p < 0.05$). For IP-injected groups, miRNA expression differences between treatments and diets were determined using two-way analysis of variance (ANOVA), followed by a Dunnett's test to assess the effect of immunogens within each dietary group (i.e., pIC/bacterin *vs* PBS), and a Student's *t*-test to assess the dietary effect within treatment groups ($p < 0.05$). All of the statistical tests above were performed in Prism v7.0 (GraphPad Software Inc., La Jolla, CA, USA). Principal coordinates analysis (PCoA), permutational multivariate ANOVA (PERMANOVA), and similarity of percentages analysis (SIMPER) were performed using PRIMER (Version 6.1.15; PRIMER-E Ltd, Ivybridge, UK) to explore the differences in qPCR-analyzed transcript expression among samples from fish

fed different diets (control *vs* CpG) and in different treatment groups (pre-injection, PBS-injected, pIC-injected and bacterin-injected). All variables were standardized by the total of each variable in PRIMER prior to analyses.

Pearson correlation and hierarchical clustering analyses were conducted to identify the relationships between head kidney miRNA expression and the expression of immune-relevant mRNAs that are predicted targets of these miRNAs. The head kidney miRNA expression data were previously published by Xue et al. (2019). The linear regression analyses were performed with IBM SPSS Statistics, whereas the hierarchical clustering was carried out with PRIMER (Version 6.1.15; PRIMER-E Ltd., Ivybridge, UK) using Pearson correlation resemblance matrices. The significance of the regression was determined by an F-test ($p < 0.05$).

5.4 Results

5.4.1 Effects of pIC and *A. salmonicida* bacterin treatments on the expression of immune-relevant putative target genes of miRNA biomarkers

qPCR results of 12 transcripts encoding pattern recognition receptors (PRRs) or involved in PRR signaling pathways are shown in **Figure 5.1**. Eight of these transcripts (*tlr5a*, *tlr7*, *tlr9*, *myd88*, *irf3*, *irf5*, *irf7a*, *irf7b*) had significant induction by pIC injection when compared with the PBS-injected salmon fed the respective diet (**Figure 5.1A-C, E-I**). The expression of *irf7b* in response to pIC was more strongly induced (up to 54-fold) than the other seven genes including another *irf7* paralogue (i.e. *irf7a*) (up to 15-fold). Five transcripts encoding PRRs [*tlr5a*, *clra*, *irf5* (fish fed CpG diet only), *irf7b* and *tbk1* (fish

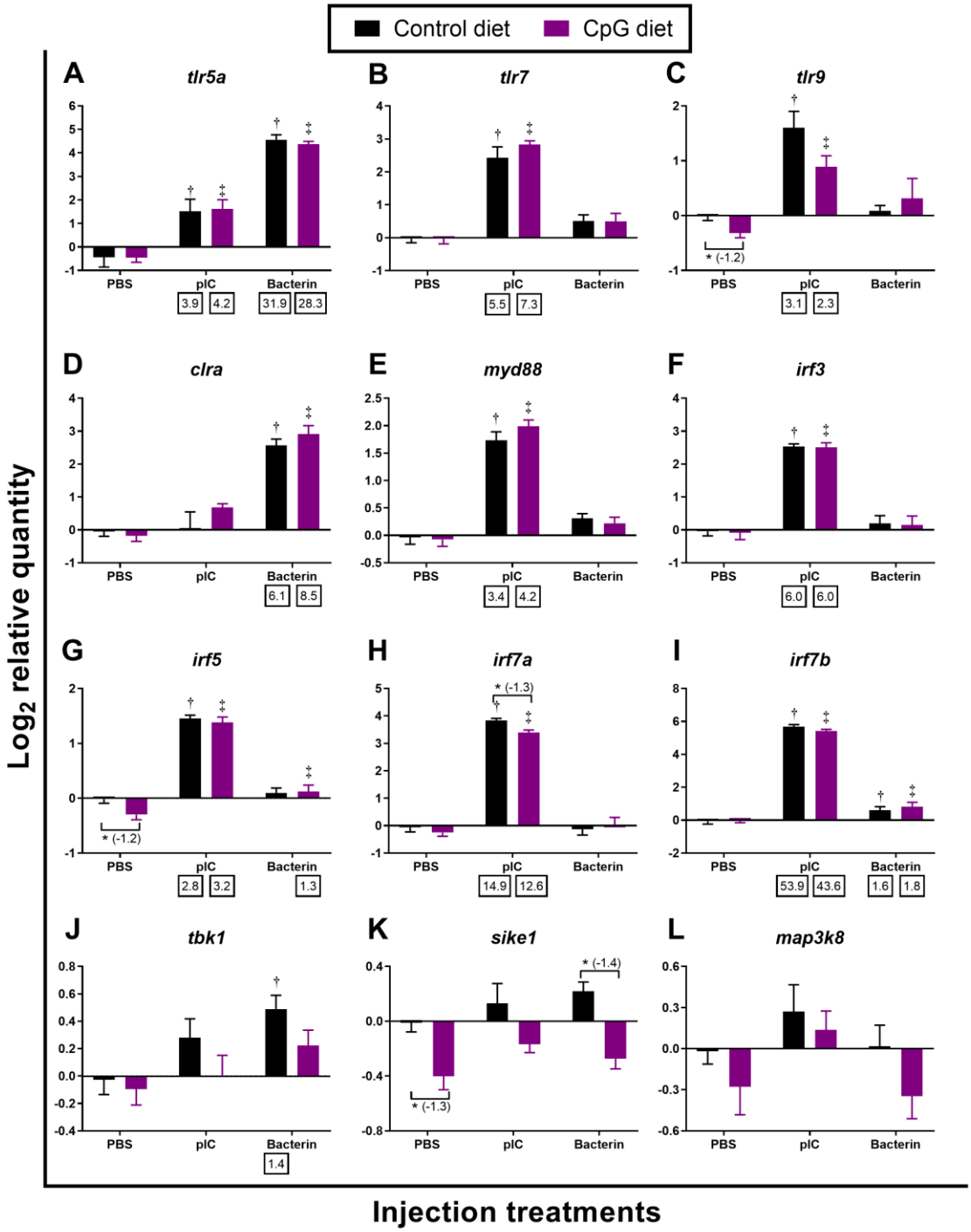
Control diet
CpG diet
A
tlr5a
B
tlr7
C
tlr9
D
clra
E
myd88
F
irf3
G
irf5
H
irf7a
I
irf7b
J
tbk1
K
sike1
L
map3k8
PBS
pIC
Bacterin
3.9
4.2
31.9
28.3
5.5
7.3
3.1
2.3
6.1
8.5
3.4
4.2
6.0
6.0
2.8
3.2
1.3
14.9
12.6
53.9
43.6
1.6
1.8
1.4
* (-1.2)
* (-1.3)
* (-1.4)
Log2 relative quantity
Injection treatments

Figure 5.1. qPCR analyses of transcripts encoding pattern recognition receptors (PRRs) or involved in PRR signaling pathways (n = 8–9). Average $\log_2$ RQs with SE bars are plotted. An asterisk (*) represents a significant difference between diets in each injection treatment ($p < 0.05$) with fold-change given in brackets. Fold-change between diets was calculated as 2^{A-B} as in Xue et al. (2019), where A is the mean of $\log_2$ RQ from the CpG fed group, and B is the mean of $\log_2$ RQ from the injection-matched control fed group. For down-regulated mRNAs, fold-change values were inverted (-1/fold-change). A dagger (†) or diesis (‡) represents a significant difference between the pIC/*A. salmonicida* bacterin-injected salmon and the diet-matched PBS-injected control ($p < 0.05$) with fold-change indicated below the x-axis. Fold up-regulation or down-regulation between injections was calculated as 2^{A-B}, where A is the mean of $\log_2$ RQ from the pIC or bacterin groups, and B is the mean of $\log_2$ RQ from the diet-matched PBS group. (**A**) *toll-like receptor 5a*; (**B**) *toll-like receptor 7*; (**C**) *toll-like receptor 9*; (**D**) *C type lectin receptor A*; (**E**) *MYD88 innate immune signal transduction adaptor*; (**F**) *interferon regulatory factor 3*; (**G**) *interferon regulatory factor 5*; (**H**) *interferon regulatory factor 7a*; (**I**) *interferon regulatory factor 7b*; (**J**) *TANK-binding kinase 1*; (**K**) *suppressor of IKK-epsilon*; (**L**) *mitogen-activated protein kinase kinase kinase 8*.

fed control diet only)] had significant induction by bacterin injection when compared with the PBS-injected salmon fed the respective diet (**Figure 5.1A,D,G,I,J**). The expression of *tlr5a* and *clra* in response to bacterin was more strongly induced (6- to 32-fold) than *irf5* (1.3-fold), *irf7b* (up to 1.8-fold), and *tbk1* (1.4-fold).

qPCR results of eight transcripts encoding cytokines or involved in cytokine mediated pathways are shown in **Figure 5.2**. All eight genes [*il1b*, *tnfa*, *il8a* (fish fed CpG diet only), *il1r1*, *il10rb*, *ifng*, *irf9*, *cxcr3*] had significant induction by pIC injection when compared with the PBS-injected salmon fed the respective diet (**Figure 5.2**). The expression of *il1b* and *ifng* in response to pIC was more strongly induced (8.7- to 27.4-fold) than the other six genes (1.5- to 4.0-fold). Seven transcripts (*il1b*, *tnfa*, *il8a*, *il10rb*, *ifng*, *irf9*, *cxcr3*) studied within this category had significant induction by bacterin injection when compared with the PBS-injected salmon fed respective diet (**Figure 5.2A-C, E-H**). The expression of *il1b* and *il8a* in response to bacterin was more strongly induced (8.3- to 20.8-fold) compared with the other five genes (1.4- to 6.0-fold).

qPCR results of 11 transcripts playing key roles as immune effectors or regulators are shown in **Figure 5.3**. Eight of these genes (*mxa*, *mxb*, *isg15a*, *campb*, *bcl6*, *mapk3*, *tnfrsf6*, *hsp90ab1*) had significant induction by pIC injection compared with the PBS-injected salmon fed respective diet (**Figure 5.3A-G, J**). *isg15a* showed the highest induction (up to 966-fold), followed by *mxa* and *mxb* (28.7- to 39.4-fold), then *campb*, *bcl6*, *mapk3*, *tnfrsf6* and *hsp90ab1* (1.3- to 7.8-fold). The injection of pIC significantly down-regulated the expression of *bnip3l* by ~1.5-fold in both diet groups (**Figure 5.3H**). Four transcripts [*campb*, *bcl6*, *bnip3l*, *hsp90ab1* (fish fed CpG diet only)] studied within

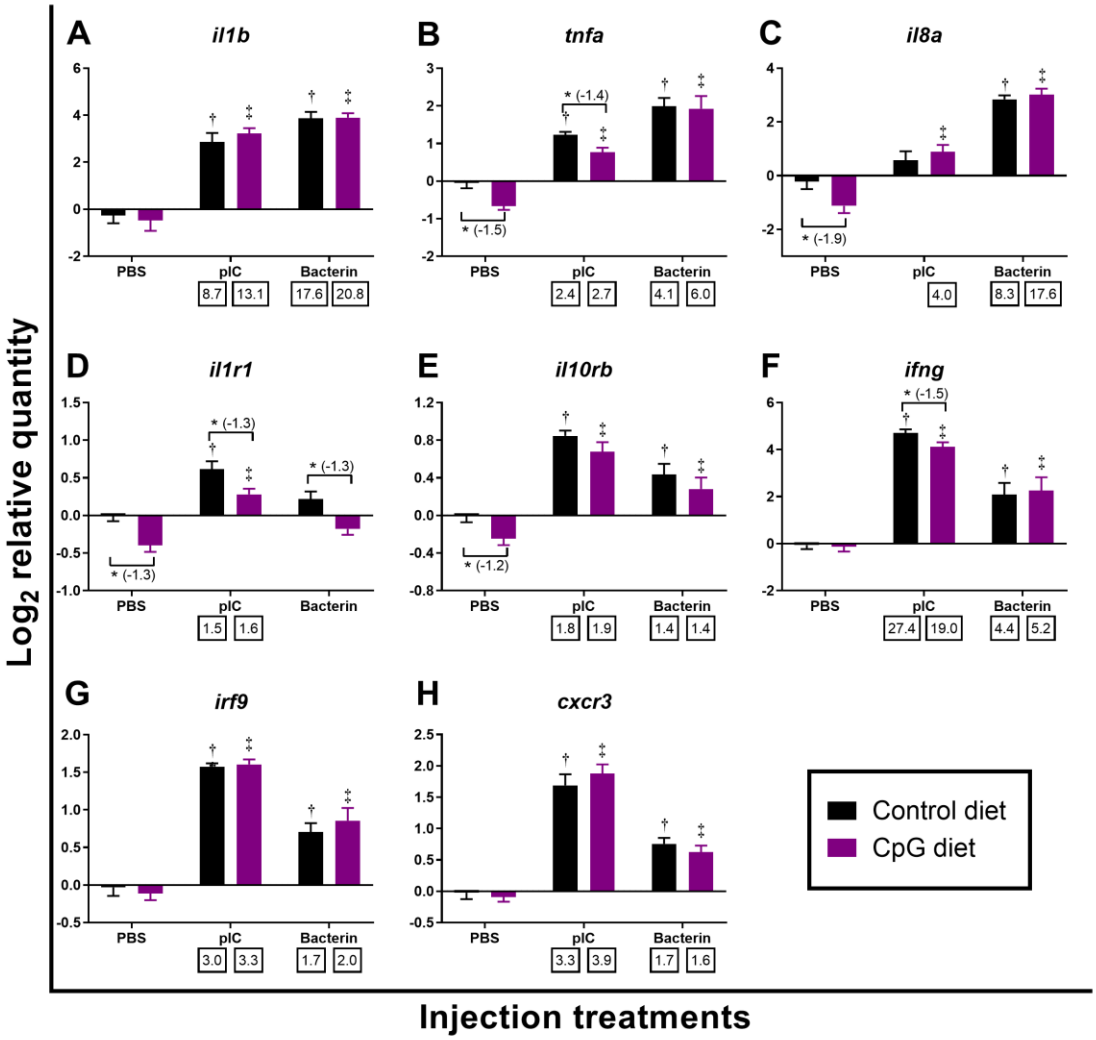

Figure 5.2. qPCR analyses of transcripts encoding cytokines or involved in cytokine mediated pathways (n = 8–9). An asterisk (*) represents a significant difference between diets in each injection treatment ($p < 0.05$) with fold-change given in brackets. Fold-change between diets was calculated as 2^{A-B} as in Xue et al. (2019), where A is the mean of $\log_2$ RQ from the CpG fed group, and B is the mean of $\log_2$ RQ from the injection-matched control fed group. For down-regulated mRNAs, fold-change values were inverted (-1/fold-change). A dagger (†) or diesis (‡) represents a significant difference between the pIC/*A. salmonicida* bacterin-injected salmon and the diet-matched PBS-injected control ($p < 0.05$) with fold-change indicated below the x-axis. Fold up-regulation or down-regulation between injections was calculated as 2^{A-B}, where A is the mean of $\log_2$ RQ from the pIC or bacterin groups, and B is the mean of $\log_2$ RQ from the diet-matched PBS group. (**A**) *interleukin 1 beta*; (**B**) *tumor necrosis factor alpha*; (**C**) *interleukin 8a*; (**D**) *interleukin-1 receptor type I*; (**E**) *interleukin-10 receptor beta chain precursor*; (**F**) *interferon gamma*; (**G**) *interferon regulatory factor 9*; (**H**) *C-X-C chemokine receptor type 3*.

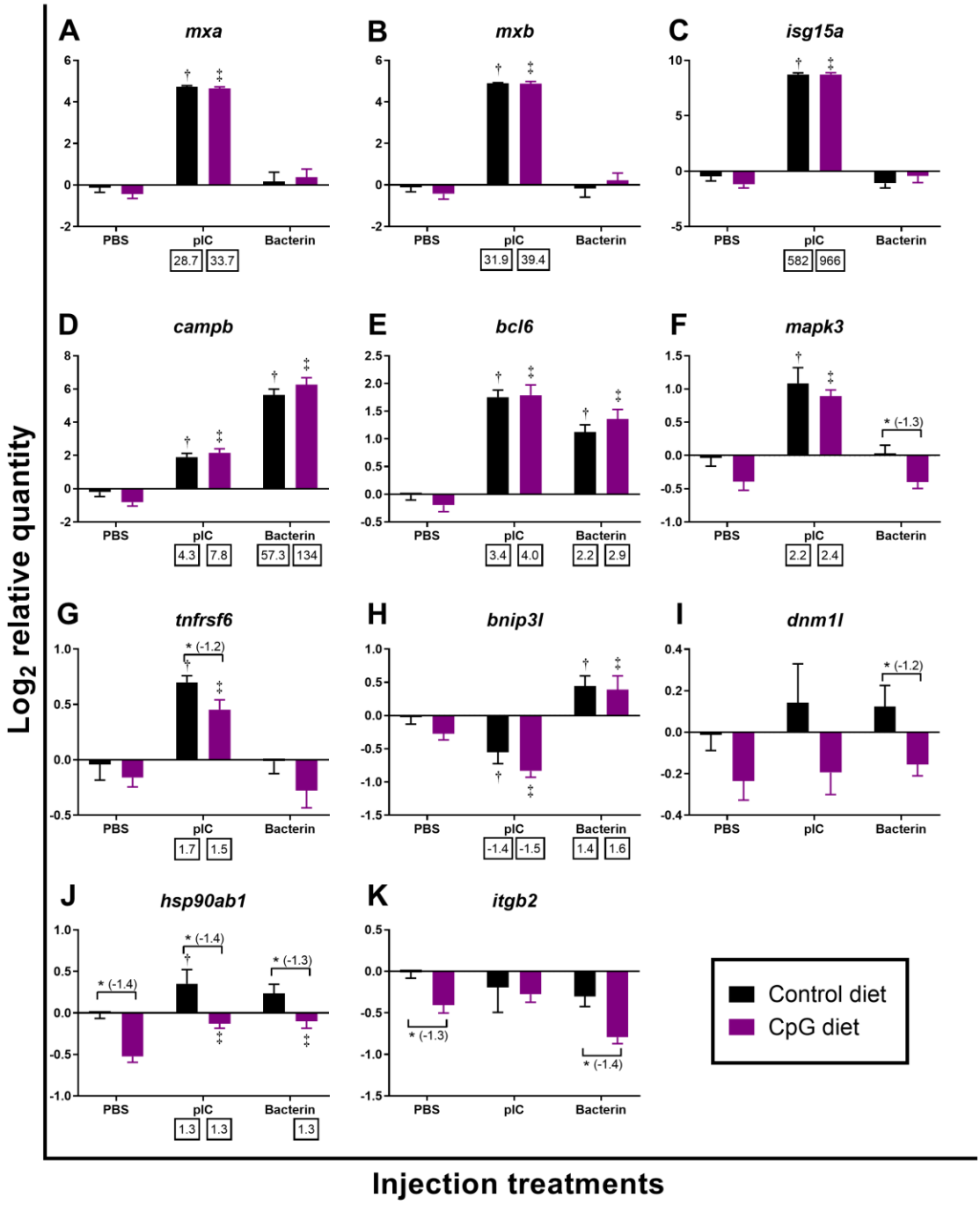
A
mxa
B
mxb
C
isg15a
D
campb
E
bcl6
F
mapk3
G
tnfrsf6
H
bnip3l
I
dnm1l
J
hsp90ab1
K
itgb2
PBS
pIC
Bacterin
28.7
33.7
31.9
39.4
582
966
4.3
7.8
57.3
134
3.4
4.0
2.2
2.9
2.2
2.4
1.7
1.5
-1.4
-1.5
1.4
1.6
1.3
1.3
1.3
* (-1.2)
* (-1.3)
* (-1.4)
Control diet
CpG diet
Log2 relative quantity
Injection treatments

Figure 5.3. qPCR analyses of transcripts encoding immune effectors and regulators (n = 8–9). Average $\log_2$ RQs with SE bars are plotted. An asterisk (*) represents a significant difference between diets in each injection treatment ($p < 0.05$) with fold-change given in brackets. Fold-change between diets was calculated as 2^{A-B} as in Xue et al. (2019), where A is the mean of $\log_2$ RQ from the CpG fed group, and B is the mean of $\log_2$ RQ from the injection-matched control fed group. For down-regulated mRNAs, fold-change values were inverted (-1/fold-change). A dagger (†) or diesis (‡) represents a significant difference between the pIC/*A. salmonicida* bacterin-injected salmon and the diet-matched PBS-injected control ($p < 0.05$) with fold-change indicated below the x-axis. Fold up-regulation or down-regulation between injections was calculated as 2^{A-B}, where A is the mean of $\log_2$ RQ from the pIC or bacterin groups, and B is the mean of $\log_2$ RQ from the diet-matched PBS group. (**A**) *interferon-induced GTP-binding protein Mx a*; (**B**) *interferon-induced GTP-binding protein Mx b*; (**C**) *interferon stimulated gene 15a*; (**D**) *cathelicidin antimicrobial peptide b*; (**E**) *B-cell lymphoma 6 protein homolog*; (**F**) *MAP kinase-activated protein kinase 3*; (**G**) *tumor necrosis factor receptor superfamily member 6 precursor*; (**H**) *BCL2/adenovirus E1B interacting protein 3-like*; (**I**) *dynamin-1-like protein*; (**J**) *heat shock protein HSP 90*-beta; (**K**) *integrin beta-2*.

this category had significant induction by bacterin injection when compared with the PBS-injected salmon fed respective diet (**Figure 5.3D,E,H,J**). The induction of *campb* in response to bacterin was much stronger (up to 134-fold) than that of *bcl6*, *bnip3l*, and *hsp90ab1* (1.3- to 2.9-fold).

5.4.2 Impact of diets on the expression of immune-relevant putative target genes of miRNA biomarkers

The impact of the diet containing functional ingredient CpG ODN 1668 on the expression of immune-relevant putative target genes of previously identified miRNA biomarkers (pIC- and *A. salmonicida* bacterin-responsive in Atlantic salmon) was investigated in both pre- and post-injection head kidney samples. The CpG diet affected the transcript levels of 6 genes analyzed among pre-injection samples; all of these genes (*tlr9*, *irf5*, *map3k8*, *il1r1*, *dnm1l*, and *hsp90ab1*) were significantly down-regulated by the CpG diet (-1.3 to -1.6-fold, **Figure 5.4C,G,L,P,AC,AD**). Similar to the pre-injection samples, a number of genes in the post-injection groups had lower expression in fish fed CpG diet compared to the controls (**Figures 5.1-5.3**). Among genes encoding PRRs or are involved in PRR signaling pathways, PBS-treated fish fed CpG diet showed significantly lower expression of *tlr9*, *irf5* and *sike1* (-1.2, -1.2, -1.3-fold, respectively) than those fed the control diet (**Figure 5.1C,G,K**). In pIC-treated salmon, fish fed the CpG diet had a significantly lower transcript level of *irf7a* (-1.3-fold) than the fish fed the control diet (**Figure 5.1H**). In bacterin-treated salmon, the expression level of *sike1* was significantly lower (-1.4-fold) in fish fed the CpG diet than those fed the control diet (**Figure 5.1K**).

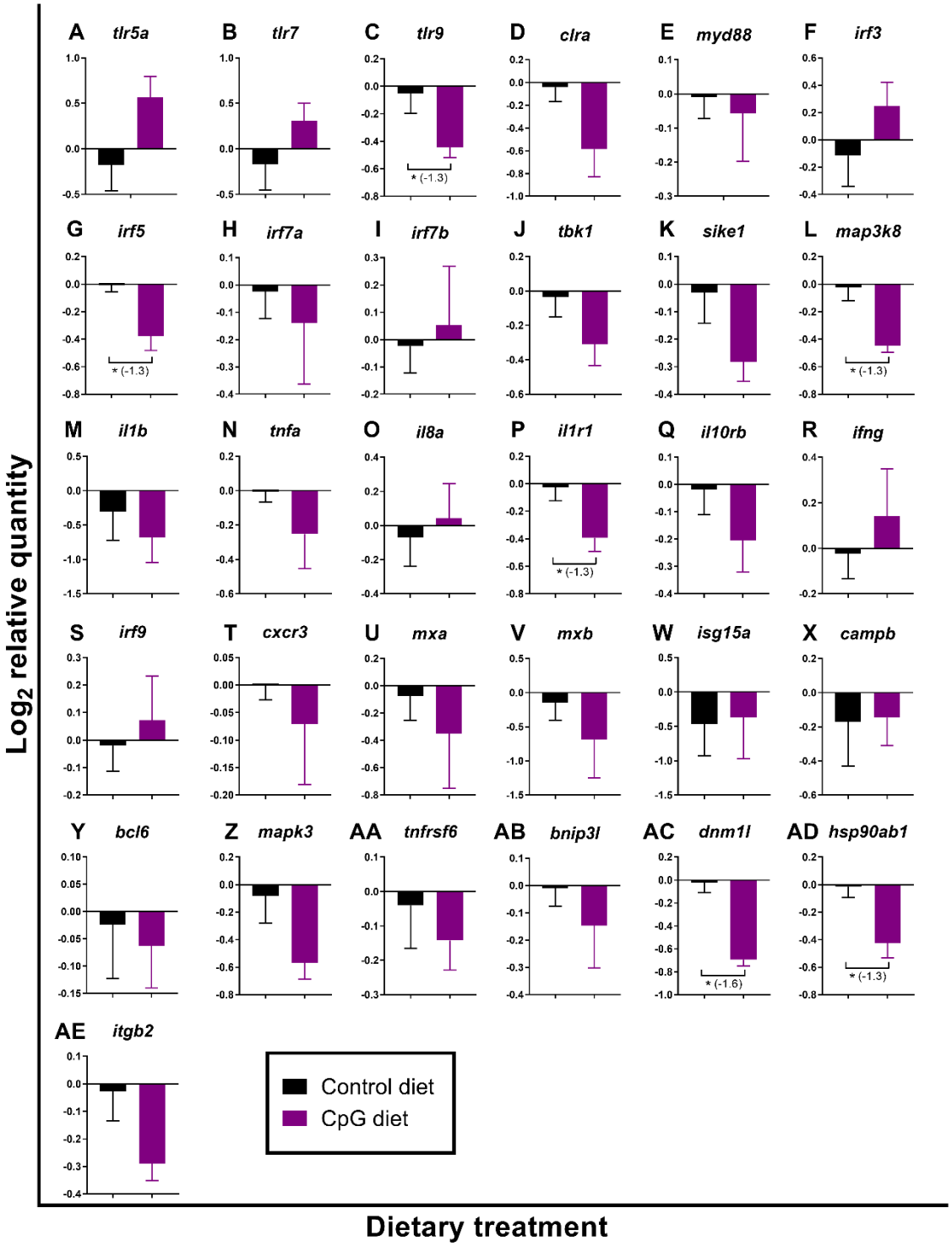
A tlr5a
B tlr7
C tlr9
D clra
E myd88
F irf3
G irf5
H irf7a
I irf7b
J tbk1
K sike1
L map3k8
M il1b
N tnfa
O il8a
P il1r1
Q il10rb
R ifng
S irf9
T cxcr3
U mxa
V mxb
W isg15a
X campb
Y bcl6
Z mapk3
AA tnfrsf6
AB bnip3l
AC dnm1l
AD hsp90ab1
AE itgb2
* (-1.3)
* (-1.6)
Control diet
CpG diet
Log2 relative quantity
Dietary treatment

Figure 5.4. qPCR analyses of basal expression (pre-injection samples) of candidate mRNAs (n = 7–8). Average $\log_2$ RQs with SE bars are plotted. An asterisk (*) indicates a significant difference between diets for a given miRNA ($p < 0.05$) with fold-change given in brackets. For qPCR fold-change calculation, overall fold up-regulation was calculated as 2^{A-B} as in Xue et al. (2019), where A is the mean of $\log_2$ RQ from the CpG fed group, and B is the mean of $\log_2$ RQ from the control fed group. For down-regulated mRNAs, fold-change values were inverted (-1/fold-change).

Among transcripts encoding cytokines or involved in cytokine-mediated pathways, PBS-treated fish fed CpG diet had significantly lower expression of *tnfa*, *il8a*, *il1r1* and *il10rb* (-1.5, -1.9, -1.3, -1.2-fold, respectively) than those fed the control diet (**Figure 5.2B-E**). In pIC-treated salmon, three transcripts (*tnfa*, *il1r1* and *ifng*) had significantly lower expression (-1.4, -1.3, -1.5-fold, respectively) in fish fed the CpG diet compared to the fish fed the control diet (**Figure 5.2B,D,F**). Only a single transcript *il1r1* had significantly lower expression (-1.3-fold) in bacterin-treated fish fed CpG diet than those fed the control diet (**Figure 5.2D**). As for genes playing key roles as immune effectors or regulators, *hsp90ab1* and *itb2* showed lower expression (-1.4 and -1.3-fold, respectively) in PBS-treated fish fed CpG diet compared to those fed the control diet (**Figure 5.3J,K**). In pIC-treated fish, dietary CpG resulted in lower transcript expression of *tnfrsf6* and *hsp90ab1* (-1.2 and -1.4-fold, respectively) compared with the control diet (**Figure 5.3G,J**). Fish fed the CpG diet showed lower levels of *mapk3*, *dnm1l*, *hsp90ab1* and *itb2* (-1.3, -1.2, -1.3, -1.4-fold, respectively) than those fed the control diet (**Figure 5.3F,I,J,K**).

5.4.3 Treatment comparisons by multivariate statistical analyses

For the pre-injection samples, the PCoA was able to segregate the two dietary groups, although relatively large variations were observed among each group (**Figure 5.5A**). PCO1 and PCO2 accounted for 32.5 and 19.5% of the variability, respectively. PCoA vectors (with $r \geq 0.70$) showed that fish fed the control diet (pre-injection) were associated with several genes, including *il1r1*, *sike1*, *irf5*, *dnm1l*, *itgb2* and *il10rb*. PERMANOVA was conducted in order to quantify the differences among samples from

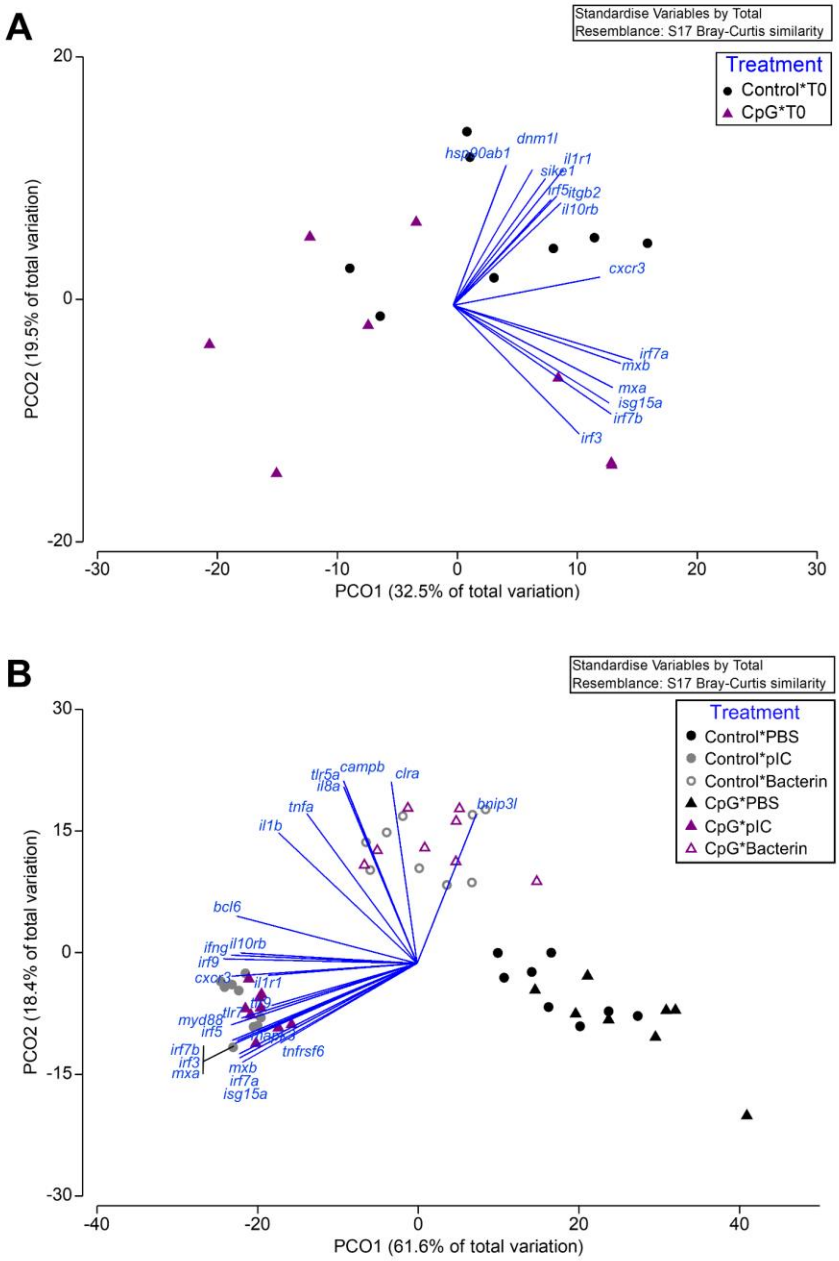

Figure 5.5. Principal coordinate analyses (PCoA) of qPCR analyzed mRNAs (RQ values) in pre-injection samples (i.e., T0 samples; **A**) and 24 h post-injection head kidney samples (**B**). Only vectors with Pearson correlation coefficients > 0.7 are shown.

fish fed different diets. The results showed that the comparisons between diets within pre-injection groups were significant based on the expression of all qPCR analyzed transcripts (**Supplemental Table S5.2).** As illustrated by SIMPER analysis, the comparison of mRNA expression between fish fed control and CpG diets within the pre-injection group was the most dissimilar (average dissimilarity = 28.27%), with 12 transcripts (e.g., *dnm1l*, *mxa*, *il10rb*, *mapk3*, *isg15a*, *tnfa*, *irf9*, *il1r1*) as the top 50% contributing variables to this dissimilarity (**Supplemental Table S5.2**).

For the post-injection groups, the PCoA was able to segregate different injection treatments (**Figure 5.5B**). PCO1 and PCO2 accounted for 61.6 and 18.4% of the variability, respectively. PCoA vectors (with $r \geq 0.70$) showed that pIC-treated fish were associated with a number of genes, including *mxb*, *irf7a*, *isg15a*, *tlr7*, *tlr9* and *mapk3*, while bacterin-treated fish were associated with a different set of genes including *bnip3l*, *clra*, *campb*, *tlr5a* and *il8a*. The overall expression differences in qPCR analyzed transcripts between dietary groups were significant for PBS- and pIC-treated fish, but not the bacterin-treated fish ($p = 0.058$), according to PERMANOVA analyses (**Supplemental Table S5.2**). The comparison of mRNA expression between fish fed control and CpG diets within PBS-injected group was the most dissimilar (average dissimilarity = 23.70%), followed by bacterin-injected group (average dissimilarity = 16.86%) and pIC-injected group (average dissimilarity = 11.40%). *sike1*, *dnm1l*, *il1rl*, *hsp90ab1*, and *mapk3* were the common contributing variables to all three dissimilarities (**Supplemental Table S5.2**). Finally, three transcripts (i.e. *il1r1*, *mapk3*, *dnm1l*) were common contributing variables to all four

pairwise dissimilarities between dietary groups (pre-injection, PBS-, pIC- and bacterin-injected groups).

5.4.4 Correlations between mRNA and miRNA levels

I attempted to explore connections between the expression changes in mRNA and miRNA. Among all injection conditions, including the pre-injection control, the highest number of significant negative correlations between miRNA and mRNA was identified within PBS-injected fish, followed by bacterin-injected fish, pre-injection control fish, and pIC-injected fish (**Supplemental Figures S5.1-5.4**). Although there were many significant correlations identified between the expression of miRNA and their putative targets (i.e. candidate mRNAs), I was particularly interested in exploring the ones representing putative miRNA-target pairs based on previous *in silico* target prediction analysis as carried out in Xue et al. (2019).

Within the pre-injection group, there were only five significant positive correlations between miRNA and mRNA expression representing putative miRNA-target pairs (e.g. *irf5* and *dnm1l* with miR-462a-3p) (**Supplemental Figure S5.1**). Although there was a large number of negative correlations between miRNA and mRNA expression identified in fish treated with PBS, only two (i.e. *il1r1* with miR-novel-16-5p and miR-725-5p) represent putative miRNA-target pairs (**Supplemental Figure S5.2**). As for fish treated with pIC, only one significant positive correlation (*bcl6* with miR-27d-1-2-5p) between miRNA and mRNA expression representing a putative miRNA-target pair was identified in the current analysis (**Supplemental Figure S5.3**). Finally, among the bacterin-injected group, the present data revealed that three significantly negative corrections (*itgb2* with

miR-29b-2-5p and miR-146a-5p; *sike1* with miR-146a-1-2-3p) between miRNA and mRNA expression in bacterin-injected fish found were putative miRNA-target pairs (**Supplemental Figure S5.4**). It is worth noting that six significant positive correlations (e.g. *irf9* with miR-30e-1-2-3p; *bcl6* with miR-27d-1-2-5p) representing putative miRNA-target pairs were also identified in fish treated with bacterin.

5.5 Discussion

5.5.1 Effects of pIC and *A. salmonicida* bacterin treatments on the expression of immune-relevant transcripts

One of the goals for the current study was to study the influence of viral mimic pIC and *A. salmonicida* bacterin stimulations on the expression of immune-relevant mRNAs, which are predicted targets of the pIC- and/or bacterin-responsive miRNAs in Atlantic salmon. Xue et al. (2019) showed that the analyses of Atlantic salmon head kidneys injected with pIC or bacterin revealed 12 and 18 miRNAs differentially expressed in pIC and bacterin groups, respectively, compared to the PBS-injected controls. The functional annotations of predicted target genes of the pIC- and/or bacterin-responsive miRNAs revealed 130 immune-relevant target genes (Xue et al., 2019). Here, I selected 23 of them and included eight additional candidate immune biomarkers for qPCR analyses to study the impact of pIC and bacterin stimulations on the transcription of these genes, using the same samples as were previously used in my miRNA study (**Chapter 4**; Xue et al., 2019).

The present study showed that pIC and bacterin stimulation changed the expression of several transcripts encoding PRRs or involved in PRR signaling pathways. Tlr5 is

generally thought to recognize flagellin found in the flagellar structure of many bacteria, including *A. salmonicida* (Tsoi et al., 2006; Moresco et al., 2011). The current qPCR study showed that head kidney *tlr5a* was induced by both pIC and *A. salmonicida* bacterin injections. Interestingly, recent infection studies in Atlantic salmon involving non-motile bacteria (e.g. *R. salmoninarum* and *P. salmonis*) also showed activation of *tlr5a* in the infected animals (Eslamloo et al., 2020; Xue et al., 2021). I hypothesize that Atlantic salmon *tlr5a* might have evolved to acquire additional immune functions compared to the mammalian orthologue. Mammalian TLR7 and TLR9, known as the endosomal PRRs, are responsible for recognizing ssRNA viruses and CpG-rich bacterial DNA/dsDNA viruses, respectively (Sato et al., 2006; De Nardo, 2015). The up-regulation of both *tlr7* and *tlr9* in the current study is similar to that reported in Atlantic salmon macrophage-like cells exposed to pIC (Eslamloo et al., 2017). Skjæveland et al. (2008) found that Atlantic salmon *tlr9* can be induced by recombinant trout Ifng (interferon gamma). This suggests that the up-regulation of *tlr9* in pIC-treated fish in the current study may be associated with a positive feedback loop resulting from the induction of *ifng* by pIC. Besides TLRs, I also found up-regulation of a transcript encoding C-type lectin receptor (i.e. *clra*) only in salmon treated with bacterin; it functions as a PRR and recognizes carbohydrate patterns present on the surface of microorganisms (Zhang et al., 2000). Similarly, in Soanes et al. (2004), Atlantic salmon infected with live *A. salmonicida* had increased hepatic *clra* expression compared with the healthy control fish.

In the current study, the up-regulation of *myd88* in pIC-treated salmon is consistent with increased expression of *tlr7* and *tlr9* as these PRRs have been shown to activate the

MyD88-dependent pathway (Eslamloo et al., 2017). It is worth noting that the expression of *myd88* was not altered by *A. salmonicida* bacterin stimulation. Although all mammalian TLRs (except TLR3) utilize the MyD88-dependent pathway (Moresco et al., 2011), the current data suggest that *tlr5a* may mediate the MyD88-independent signaling pathway. In agreement with previous work on Atlantic salmon macrophages and head kidneys with pIC stimulation (Caballero-Solares et al., 2017; Eslamloo et al., 2017), members of IRF family (i.e. *irf3*, *irf5*, *irf7a* and *irf7b*) were up-regulated by pIC in the current study. IRF3 and IRF7 are the primary family members involved in regulating the type I IFN response to viral infection, promoting the production of IFNs and interferon-stimulated genes (ISGs) (Holland et al., 2008). In addition to IRF3 and IRF7, IRF5 has also been shown to play a key role in retinoic acid-inducible gene I (RIG-I)-like receptor (RLR) and mitochondrial antiviral-signalling protein (MAVS)-mediated type I IFN expression (Lazear et al., 2013). I observed significant up-regulation (1.3- to 1.8-fold) of *irf5* and *irf7b* by bacterin in salmon head kidney. Similar to my results, previous studies also reported the up-regulation of *irf5* and *irf7* by LPS in common carp (*Cyprinus carpio* L.) head kidney leukocytes and large yellow croaker (*Larimichthys crocea*) liver, respectively (Yao et al., 2012; Zhu et al., 2016). Further, the slight up-regulation of *irf7b* found in fish treated with bacterin in the current study can be related to the increased expression of *tbk1* (1.4-fold in bacterin-injected group) as mammalian TBK1 has been shown to be a molecular bridge, linking the TLR and RLR signals to activate IRF3- and IRF7-mediated type I IFN response (Chen et al., 2017). It is worth noting that the differential regulation of *irf7* paralogues (i.e. bacterin

responsiveness of *irf7b* only; stronger induction of *irf7b* by pIC) suggests that these paralogues have undergone regulatory and potentially functional divergence.

Upon ligand recognition, TLR pathways activate signaling cascades that result in the induction of IFNs and cytokines, essential mediators of the inflammatory response (De Nardo, 2015). Il1b and Tnfa are pro-inflammatory cytokines involved in the activation of a wide range of genes expressed during inflammation (Covello et al., 2009). Il1b is predominantly produced by monocytes and macrophages, and participates in the regulation of phagocytic activity, macrophage proliferation and leukocyte migration (Peddie et al., 2001). Tnfa displays overlapping functions with Il1b; however, it also possesses the ability to induce apoptosis and necrosis (Zou and Secombes, 2016). Il8 (also referred to as Cxcl8) functions as a chemotactic factor by recruiting specific subsets of leukocytes (primarily neutrophils) to the site of infection (Seppola et al., 2008). I observed higher induction of *il1b*, *il8a* and *tnfa* in fish treated with bacterin compared with those treated with pIC, suggesting that *A. salmonicida* bacterin can cause a stronger inflammatory response. Il1r1, a receptor of Il1b, can mediate Il1b-dependent activation of NF-kappa-B, MAPK and other pathways (Slack et al., 2000). I found an up-regulation of *il1r1* in the salmon head kidney in response to pIC, but it was not responsive to bacterin. In disagreement with the present study, miiuy croaker (*Miichthys miiuy*) *il1r1* was found to be induced by both LPS and pIC (Yang et al., 2017). Moreover, the expression of IL10RB protein is essential for the signal transduction of IL10, which is a key anti-inflammatory cytokine (Shouval et al., 2014). In the present study, the up-regulation of *il10rb* in both pIC- and bacterin-injected Atlantic salmon may be necessary to prevent pathological inflammation. The up-regulation of *ifng*

by pIC and bacterin in the present study suggests that a type II IFN response was activated. As shown by Caballero-Solares et al. (2017) and Eslamloo et al. (2017), pIC can elicit both type I and II IFNs mediated antiviral responses. Irf9 plays an essential role in antiviral immunity by regulating the downstream expression of ISGs within the type I IFN response pathway (Paul et al., 2018). The up-regulation of *irf9* by both pIC and bacterin in the current study, therefore, indicated a type I IFN response. I hypothesize that the type I IFN pathway might also play important roles in mediating immune response resulting from bacterial infection/bacterin stimulation. Further, it is worth noting that pIC-treated fish in the current study exhibited more robust IFN responses (both type I and II) compared with bacterin-stimulated salmon. CXCR3 is a chemokine receptor that plays an essential role in the trafficking and migration of leukocytes at sites of infection and inflammation (Groom and Luster, 2011). Similar to the current findings, the expression of *cxcr3* was elevated in the kidney of large yellow croaker after *Vibrio anguillarum* challenge and pIC stimulation (Liu et al., 2017).

In the current study, I observed up-regulation of *mxa*, *mxb* and *isg15a* only by pIC in salmon head kidney. This is consistent with previous reports on salmon antiviral responses (Caballero-Solares et al., 2017; Eslamloo et al., 2017). Unlike the pIC stimulation, *A. salmonicida* bacterin injection did not result in the up-regulation of these antiviral effector genes. Therefore, it is unclear what the type I IFN pathway in Atlantic salmon plays in bacterial infection/stimulation. Camp (i.e. Cathelicidin) is a well-known antimicrobial peptide that was found to be important in the fight against bacterial invasion (Maier et al., 2008). The up-regulation *campb* in bacterin-treated fish was expected as it

was previously shown to be an excellent *A. salmonicida*-inducible biomarker (Kitani et al., 2019). Induction or suppression of apoptosis because of pathogen and host interaction may play a vital role in the outcome of infection. The present study analyzed a number of genes related to the apoptotic pathway (i.e. *bcl6*, *mapk3*, *tnfrsf6*, *bnip3l*) (Baron et al., 2002; Kurosu et al., 2003; Burton and Gibson, 2009; Minutoli et al., 2009; Yi et al., 2018). Of these genes, *bcl6* was induced by both pIC and bacterin injections, whereas *mapk3* and *tnfrsf6* were only induced by pIC. Interestingly, opposite expression responses of *bnip3l* to pIC (down-regulation) and bacterin (up-regulation) were observed in the current study. My previous study (**Chapter 3**) found Atlantic salmon *bnip3l* to be suppressed following *P. salmonis* infection (Xue et al., 2021). Collectively, the current results suggest that pIC and *A. salmonicida* bacterin stimulations modulate the apoptotic pathway in Atlantic salmon. Furthermore, HSPs (Heat Shock Proteins) not only function as molecular chaperones, but also play essential roles in immune system function (e.g. antigen presentation) (Srivastava, 2002; Callahan et al., 2008; Xie et al., 2015; Beemelmanns et al., 2021). A slight up-regulation of *hsp90ab1* seen with salmon injected with pIC or bacterin in the current study provide some evidence of its role in immune response and/or disease defense in Atlantic salmon.

5.5.2 Impact of diets on the expression of immune-relevant putative target genes of miRNA biomarkers

CpG ODNs found in bacterial and some viral genomes have been shown to be important immunostimulants that can enhance fish immunity and confer protection from pathogen invasion (Tassakka and Sakai, 2005). Recognition of CpG ODNs by host PRRs

occurs specifically through TLR9, resulting in activation of antiviral and antibacterial cell signaling (Cuesta et al., 2008; Strandskog et al., 2008; Liu et al., 2010). My previous work has revealed that dietary CpG ODN 1668 at an inclusion level of 10 mg kg^{-1} feed can modulate miRNA biomarkers associated with immune responses in Atlantic salmon (Xue et al., 2019). For example, CpG supplementation generally suppressed basal expression (i.e. in pre-injection samples) of many miRNAs studied (e.g. miR-192a-5p, miR-462a-3p, miR-181a-5-3p). In the post-injection groups, dietary CpG had significant impacts on the miRNA expression in both PBS and bacterin treated fish with several miRNAs (e.g., miR-181a-5-3p, miR-221-5p, miR-29b-2-5p) showing higher expression in fish fed the CpG-containing diet. To complement this recently published work on the impact of dietary CpG on miRNA expression in Atlantic salmon (Xue et al., 2019), in the present study, I analyzed 31 immune relevant mRNAs (23 of which were putative target genes of miRNA biomarkers identified from the previous research) on the pre- and post-immune stimulation head kidney samples. Importantly, all genes significantly modulated by diet had lower expression in fish fed the CpG diet regardless of injection treatments. In disagreement with the miRNA expression profiles (Xue et al., 2019), the overall expression differences in qPCR analyzed transcripts between dietary treatments were most dissimilar among pre-injection and PBS-injected fish based on the current SIMPER analyses.

Among transcripts encoding PRRs or involved in PRR signaling pathways, *tlr9* and *irf5* had lower expression in both pre- and PBS-injected fish fed the CpG diet. As discussed earlier, mammalian TLR9 is responsible for recognizing CpG-rich bacterial DNA/viral dsDNA, respectively (Sato et al., 2006). The studies on the regulation of fish *tlr9* after

stimulation with CpG ODNs via IP-injection are conflicting since both up- and down-regulation of TLR9 expression have been described, which may reflect different classes of CpG ODN or time points used in these studies (Strandskog et al., 2008; Cárdenas-Reyna et al., 2016; Jung and Jung, 2017; Angulo et al., 2018). Purcell et al. (2013) showed that Atlantic salmon fed diet containing CpG ODN 1668 had significantly decreased *tlr9* expression over time in both skin and spleen. Alongside the current results, these findings suggest that Tlr9 may be under a negative feedback loop control in Atlantic salmon. The down-regulation of *irf5* (among pre-injection and PBS-injected groups) and *irf7a* (among pIC-injected groups) by CpG diet indicate that the RLR- and MAVS-mediated type I IFN response may be attenuated by dietary CpG. Furthermore, mammalian SIKE1 interacts with IKBKE (i.e. Inhibitor of nuclear factor kappa b kinase subunit epsilon) and TBK1; it plays an inhibitory role in virus-triggered TLR3-depedent IFN activation pathways (Huang et al., 2005). In the present study, the down-regulation of *sike1* seen in PBS- and bacterin-injected fish fed CpG diet once again indicated that dietary CpG might modulate IFN-related pathways. It has been shown in mammals that MAP3K8, a serine-threonine kinase, is critical in innate immunity, transducing signals from TLRs to regulate TNFA and IL1B production (Mielke et al., 2009). The down-regulation of *map3k8* in pre-injected fish fed CpG diet found in the current study suggests that dietary CpG could potentially influence Map3k8 signaling and thereby regulate Tnfa and Il1b in Atlantic salmon.

Among the transcripts encoding cytokines or involved in cytokine-mediated pathways, *il1r1* was consistently down-regulated in fish fed CpG from all treatment groups. I hypothesize that dietary CpG is able to modulate the Il1b-dependent activation of NF-

kappa-B and MAPK pathways. In addition, the current qPCR study showed that three important inflammatory markers (i.e. *il8a*, *il10rb*, *tnfa*) had decreased expression in PBS- and pIC-treated (*tnfa* only) fish fed CpG diet, suggesting these animals might have lower inflammation. These results could also indicate that fish-fed the CpG diet might be able to resolve inflammatory responses more quickly after a generalized stress event (e.g. PBS injection) or pIC stimulation. Moreover, the down-regulation of *ifng* in pIC-treated salmon fed CpG diet found in the present study suggests that the type II IFN mediated antiviral response may be altered. Since *ifng* also plays regulatory roles in both innate and adaptive immunity (e.g. activating macrophages, enhancing antigen presentation), it is reasonable to speculate that CpG-driven immune modulation may have an impact on the adaptive responses in Atlantic salmon.

Among the transcripts playing critical roles as immune effectors or regulators, the transcript levels of *hsp90ab1* and *itgb2* were consistently down-regulated in fish fed CpG from all treatment groups (except *itgb2* among pIC-injected fish). As discussed earlier, *hsp90ab1* may play additional roles in immune responses (e.g. antigen presentation). Moreover, in mammalian species as well as zebrafish, adhesion molecules of the β_2 integrin family (e.g. ITGB2, also referred to as CD18) are necessary for neutrophil recruitment to sites of inflammation (Bader et al., 2021). My qPCR data on *hsp90ab1* and *itgb2* suggest that dietary CpG might modulate other immune system functions in Atlantic salmon, such as antigen presentation and neutrophil recruitment. Lastly, the down-regulation of apoptosis-relevant genes (i.e. *mapk3*, *dnm1l*, *tnfrsf6*) among pre-, pIC- and/or bacterin-

injected fish fed CpG diet indicates that the apoptotic pathway may be suppressed by dietary CpG in Atlantic salmon.

5.5.3 Correlations between mRNA and miRNA levels

miRNAs have been well-documented to cause transcriptional degradation and/or translational repression (Huntzinger and Izaurralde, 2011; Herkenhoff et al., 2018). It has also been previously shown that the miRNA-mRNA regulatory network is very complex (Zhang et al., 2016b). A single miRNA can regulate multiple target mRNAs, while a given mRNA can be targeted by various miRNAs (Xu et al., 2020). Here, I attempted to explore connections between the expression changes in mRNA and miRNA. Among all injection conditions, including the pre-injection control, the highest number of significant negative correlations between miRNA and mRNA was identified within PBS-injected fish, followed by bacterin-injected fish, pre-injection control fish, and pIC-injected fish (**Supplemental Figures S5.1-5.4**). Among PBS-injected fish, many transcripts had lower expression in fish fed the CpG diet while these fish had higher expression for a number of miRNAs, as shown by Xue et al. (2019). This is consistent with the negative correlations between miRNAs and mRNAs found in PBS-treated fish. In the current study, PBS was used to control for the handling stress (e.g. netting, light anesthesia, and injection associated stress) caused during immune stimulations. Espelid et al. (1996) showed that IP injection of PBS/handling stress elevated the level of cortisol in serum collected from Atlantic salmon, and the serum cortisol returned to background levels after approximately five hours. As suggested by other studies (Andreassen and Høyheim, 2017; Eslamloo et al., 2018), the large number of negative correlations between miRNAs and mRNAs found in PBS-treated

fish in the current study may further support the notion that miRNAs fine-tune the expression of stress- and/or immune-responsive transcripts.

I acknowledge that there may be some false positives or false negatives among the predicted targets of miRNAs. However, among all significant correlations between miRNA and mRNA expression in PBS-injected fish, only two negative correlations found (i.e. *il1r1* with miR-novel-16-5p and miR-725-5p) represent putative miRNA-target pairs based on previous *in silico* target prediction analysis as carried out in Xue et al. (2019). This result suggests that miR-novel-16-5p and miR-725-5p might negatively regulate *il1r1* transcript level in Atlantic salmon in response to general stress. As mentioned earlier, *il1r1* plays a key role in modulating many important immune pathways, including the activation of NF-kappa-B pathway (Slack et al., 2000). It is also worth noting that three significant negative correlations (*itgb2* with miR-29b-2-5p and miR-146a-5p; *sike1* with miR-146a-1-2-3p) between miRNA and mRNA expression in *A. salmonicida* bacterin-injected fish were putative miRNA-target pairs. Collectively, my study suggests that miRNAs (e.g. miR-novel-16-5p, miR-725-5p, miR-29b-2-5p, miR-146a-1-2-3p) might suppress stress- and immune-related expression of defense-relevant genes.

Among the pre- and pIC-injection groups, there were a number of positive correlations between miRNA and mRNA expression representing putative miRNA-target pairs (e.g. *irf5* and *dnm1l* with miR-462a-3p in pre-injection fish; *bcl6* with miR-27d-1-2-5p in pIC-injected fish). As noted by others (Eslamloo et al., 2018; Xiong et al., 2019; Smith et al., 2021), positive correlations between miRNA-target pairs are commonly seen as some miRNAs may influence their putative targets at the translational level. In addition,

a positive correlation between a miRNA-target pair can be explained by the feed forward loop mechanism that regulates miRNA and its target mRNA in the same direction (Xiong et al., 2019). Andreassen and Høyheim (2017) proposed a similar miRNA and mRNA interaction model (e.g. expression dynamics) for miRNAs associated with immune responses in teleost fish. For instance, the increase in miRNA expression along with the increase in target (i.e. mRNA) expression is needed to ensure a balanced immune response. Future studies related to experimental validations of target genes (e.g. a dual luciferase assay) are required to fully understand the regulatory roles of miRNA in Atlantic salmon.

5.6 Conclusions

To complement my recent published work on miRNA (Xue et al., 2019), the present study explored the impact of viral mimic pIC and *A. salmonicida* bacterin stimulations on the expression of immune-relevant predicted target genes of miRNAs that were previously identified as pIC- and/or *A. salmonicida* bacterin-responsive in Atlantic salmon. The current qPCR data showed that pIC and/or bacterin stimulations significantly modulated the majority of the predicted target genes involved in various immune pathways. Immunogen-specific expression patterns were also observed. For example, higher induction of pro-inflammatory genes (e.g. *il1b*, *il8a* and *tnfa*) in bacterin-injected fish suggests that *A. salmonicida* bacterin stimulation caused a stronger inflammatory response compared with pIC. On the other hand, pIC-treated fish in the current study showed stronger IFN responses (both type I and II) compared with bacterin-stimulated salmon. Significant modulations of immune-relevant transcripts by dietary CpG were also evident, with higher impacts seen among pre-injection and PBS-injected fish based on the current

results. Surprisingly, all genes that showed significant modulation by diet had lower expression in CpG diet fed fish regardless of injection treatments. Future studies are needed to evaluate the effects of dietary immunostimulant CpG ODN 1668 on Atlantic salmon responses to viral and bacterial infections. Lastly, the significant correlations representing putative miRNA-target pairs found in the current study provide further insights into how miRNAs might regulate the expression of critical immune-relevant genes and pathways.

5.7 Supplemental materials

Supplemental Table S5.1. qPCR primers.

Transcript (gene symbol)	Primer sequence 5'-3'[1]	Efficiency (%)	Size (bp)[2]	GenBank accession number
Genes of interest				
toll-like receptor 5a (*tlr5a*)[3]	F:ATCGCCCTGCAGATTTTATG R:GAGCCCTCAGCGAGTTAAAG	99.7	103	AY628755
toll-like receptor 7 (*tlr7*)[4]	F:CACCAACACAGAGCTGGAGA R:GCCTTGGAAAACTTGCTGAG	99.9	184	HF970585
toll-like receptor 9 (*tlr9*)	F:ATTCAGCAGGTAGGGAAGGA R:CCAGGGCCCTCATATGACTA	102.4	97	NM_001123653
C type lectin receptor A (*clra*)[3]	F:CGAATCTTCAATCATGGAGAAG R:TTCAGCCCCTGGGTATTTTG	86.7	117	NM_001123579
MYD88 innate immune signal transduction adaptor (*myd88*)	F:TTCCTGACGGTGTGTGACTAC R:GGCCCTCTGTGATGATTGGTT	86.2	127	NM_001136545
interferon regulatory factor 3 (*irf3*)[4]	F:ACAAACAGCTGGGAACCAAC R:ATTGGATATTGCCGTTGCTC	92.2	108	NM_001172282
interferon regulatory factor 5 (*irf5*)	F:AACTGCTTTGTGTGAGGGGAT R:AGAGGATACAGCAGTCTGGG	97.6	169	NM_001139852
interferon regulatory factor 7a (*irf7a*)[4]	F:CCAGTGCCACCAGTCCTAAT R:GGTGATCTCCAAGTCCCAGA	94.6	105	BT045216
interferon regulatory factor 7b (*irf7b*)[4]	F:GTCAGTGGTAAAATCAACACGC R:CACCATCATGAAACGCTTGGT	93.3	99	FJ517644
TANK-binding kinase 1 (*tbk1*)	F:TGGACTCCATTACGGCCATC R:AGGCGATACTTCATGGCACA	97.6	166	NM_001256722
suppressor of IKK-epsilon (*sike1*)	F:CCGAGAACTGTGGCTGTCTT R:CCAGTTGGCTTTGCACTTCC	93.2	167	NM_001140308
mitogen-activated protein kinase kinase kinase 8 (*map3k8*)[5]	F:GGTGAACGTGTGACTGATGC R:GGCAGCTACAGAAACCACCT	96.0	144	NM_001173785
interleukin 1 beta (*il1b*)[6]	F:GTATCCCATCACCCCATCAC R:TTGAGCAGGTCCTTGTCCTT	96.6	119	AY617117
tumor necrosis factor alpha (*tnfa*)	F:TGCCATGGTAACACCACAGT R:AGATCTGGGACCACGCTAGA	104.3	111	NM_001123617
interleukin 8a (*il8a*; alias *cxcl8a*)[7]	F:GAAAGCAGACGAATTGGTAGAC R:GCTGTTGCTCAGAGTTGCAAT	102.6	99	BT046706
interleukin-1 receptor type I (*il1r1*)	F:TCGACACATCATGTTGGGGG R:GTGTTCTTGGCCATGGGAGA	95.9	82	NM_001123633
interleukin-10 receptor beta chain precursor (*il10rb*)	F:GAACACACCACTCTAGGCCC R:CCTCCTGACCGTCTTTCCAG	89.3	157	BT059022
interferon gamma (*ifng*)[4]	F:CCGTACACCGATTGAGGACT R:GCGGCATTACTCCATCCTAA	100.8	133	AJ841811
interferon regulatory factor 9 (*irf9*)	F:CTGAGCTATGGCATCTGGGAG R:TCTTCACTGCGGAAGTCCTG	92.8	168	NM_001173719
C-X-C chemokine receptor type 3 (*cxcr3*)[5]	F:GGTGTTGGTGCTGGTCTTTT R:GCGAACGTAACCACCAGACT	92.2	150	NM_001140493
interferon-induced GTP-binding protein Mx a (*mxa*)[4]	F:CTGAAAAGCGGAGTTCGTCT R:CTCCCTCGATCCTCTGGTTA	90.0	112	U66475
interferon-induced GTP-binding protein Mx b (*mxb*)[4]	F:ACGCACCACTCTGGAGAAAT R:CTTCCATTTCCCGAACTCTG	97.6	184	BT044881
interferon stimulated gene 15a (*isg15a*)[4]	F:AAAGTGGCCACAACAAAGCAG R:ATAGGAGCGGGCTCCGTAATC	92.9	140	BT049918
cathelicidin antimicrobial peptide b (*campb*)[3]	F:AGACTGGCAACACCCTCAAC R:TTGCCTCTTCTTGTCCGAAT	103.2	112	AY360357

B-cell lymphoma 6 protein homolog (*bcl6*)	F:TGTCGCAGGTTCATCAAGTC R:CACCCTATCCAGAACCCTGA	99.4	117	NM_001140313
MAP kinase-activated protein kinase 3 (*mapk3*)	F:ATGTGGCTCCTGAGGTTTTG R:TCCTGATCCTCCGTTTCATC	96.8	156	NM_001139792
tumor necrosis factor receptor superfamily member 6 precursor (*tnfrsf6*; alias *fas*)	F:GCCTGTGCATTTTGTGTACC R:CACAGAGACAGCATGCCATT	95.3	153	NM_001173649
BCL2/adenovirus E1B interacting protein 3-like (*bnip3l*)	F:GCCTGGGTTTTGATTATGAAGGG R:AAGCAGATTCCCTCCAGTGC	100.5	88	NM_001141679
dynamin-1-like protein (*dnm1l*)	F:ATCGTCCGCAAGAGCATTCA R:TGCAGACGCTCCTTCACAAA	100.1	80	NM_001173563
heat shock protein HSP 90-beta (*hsp90ab1*)	F:AGCACAATGATGACGAGCAG R:CCACCTCCTTGACCCTCTTC	94.0	162	NM_001146473
integrin beta-2 (*itgb2*)	F:GGGAAGTGCATCGAGTGTCT R:AGTTCTCCACATCCCTCACG	94.4	142	NM_001165324
Normalizer genes				
elongation factor 1 alpha-2 (*ef1a2*)[8]	F:GCACAGTAACACCGAAACGA R:ATGCCTCCGCACTTGTAGAT	96.6	132	BT058669
polyadenylate-binding protein 1 (*pabpc1*)[4]	F:TGACCGTCTCGGGTTTTTAG R:CCAAGGTGGATGAAGCTGTT	92.0	108	EG908498

[1]F: forward primer; R: reverse primer.
[2]Amplicon size.
[3]qPCR assay was published previously (Eslamloo et al. 2020. Fish Shellfish Immunol. 98: 937-949).
[4]qPCR assay was published previously (Caballero-Solares et al. 2017. Fish Shellfish Immunol. 64: 24-38).
[5]qPCR assay was published previously (Eslamloo et al. 2017. BMC Genomics 18: 706).
[6]qPCR assay was published previously (Eslamloo et al. 2020. Front. Immunol. 11: 2487).
[7]qPCR assay was published previously (Zanuzzo et al. 2020. Front. Immunol. 11: 1009).
[8]qPCR assay was published previously (Katan et al. 2019. Comp. Biochem. Physiol. Part D Genomics Proteomics 30: 290-304).

Supplemental Table S5.2. Permutational multivariate ANOVA (PERMANOVA) and similarity of percentages analysis (SIMPER) of analyzed transcripts.

	CpG *vs* Control[3]			
	Pre-injection	PBS	pIC	Bacterin
p (perm)[1]	0.014	0.007	0.012	0.058
Average dissimilarity (%)[2]	28.27	23.70	11.40	16.86
Contributing variables (top 50%)	*dnm1l* *mxa* *il10rb* *mapk3* *isg15a* *tnfa* *irf9* *il1r1* *mxb* *tlr5a* *irf3* *myd88*	*hsp90ab1* *sike1* *il1r1* *dnm1l* *mapk3* *tnfa* *tnfrsfb* *il8a* *map3k8* *tbk1* *il10rb*	*dnm1l* *hsp90ab1* *tlr9* *sike1* *mapk3* *tbk1* *il1r1* *cxcr3* *bnip3l*	*sike1* *dnm1l* *bnip3l* *ifng* *il1rl* *hsp90ab1* *tnfa* *tlr9* *il10rb* *tnfrsfb* *mapk3*

[1]p (perm) is the statistical significance value obtained from PERMANOVA with 9999 permutations.
[2]Average dissimilarity and contributing variables (top 50%) were obtained through SIMPER.
[3]Dietary effects were evaluated within each injection treatment.

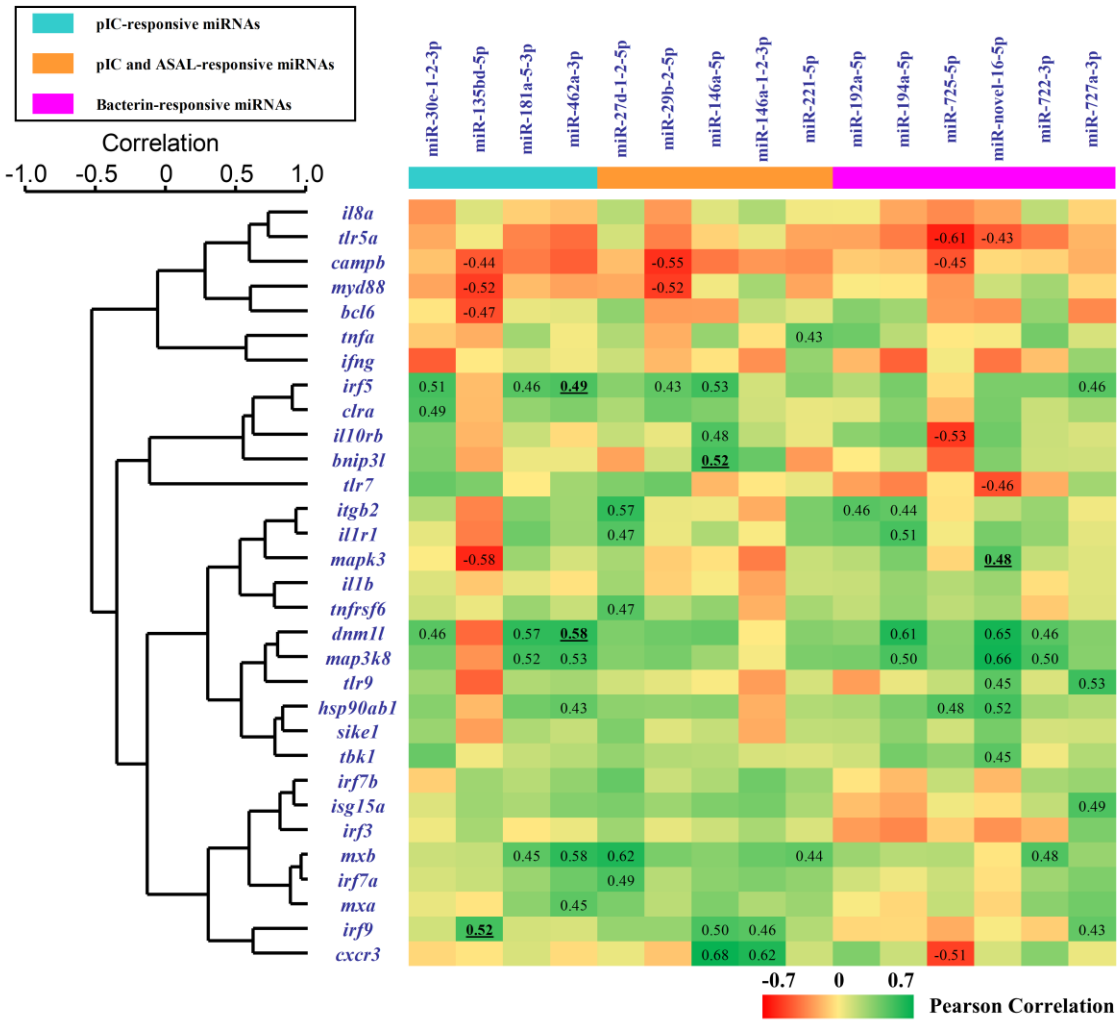

Supplemental Figure S5.1. Matrix representing Pearson's correlation coefficients between head kidney mRNA expression (row; Log_2 RQ) and miRNA expression (columns; Log_2 RQ) in pre-injected group (T0). mRNA data were arranged based on hierarchical clustering analyses (PRIMER, Version 6.1.15, Ivybridge, UK). miRNA data were arranged based their responsiveness to immunogen injections. Pearson's correlation coefficients with significant regressions ($p < 0.05$) are shown. Pearson's correlation coefficients with bold font and underline represent putative miRNA-target pairs based on previous *in silico* target prediction analysis (Xue et al. 2019).

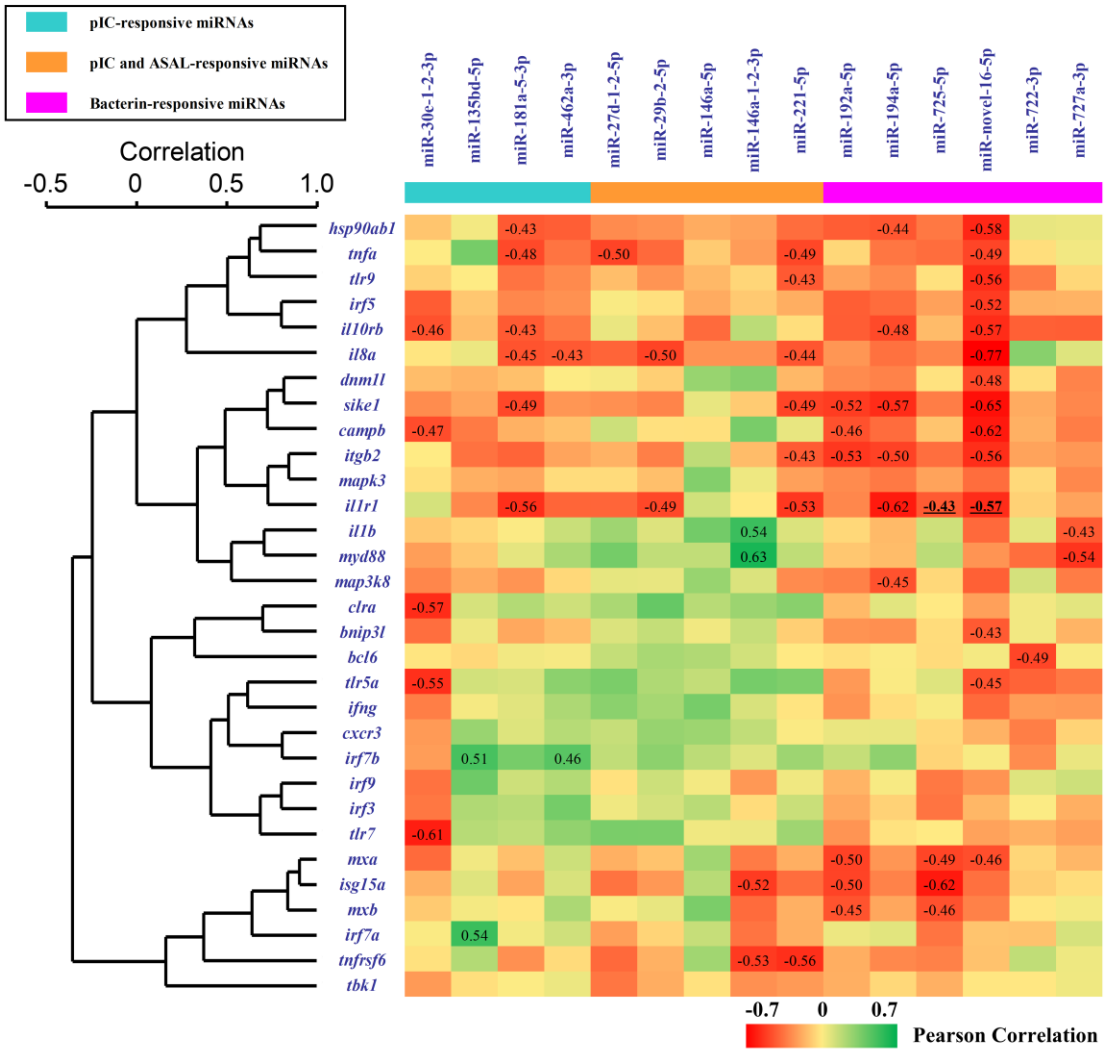

Supplemental Figure S5.2. Matrix representing Pearson's correlation coefficients between head kidney mRNA expression (row; Log_2 RQ) and miRNA expression (columns; Log_2 RQ) in PBS-injected salmon. mRNA data were arranged based on hierarchical clustering analyses (PRIMER, Version 6.1.15, Ivybridge, UK). miRNA data were arranged based their responsiveness to immunogen injections. Pearson's correlation coefficients with significant regressions ($p < 0.05$) are shown. Pearson's correlation coefficients with bold font and underline represent putative miRNA-target pairs based on previous *in silico* target prediction analysis (Xue et al. 2019).

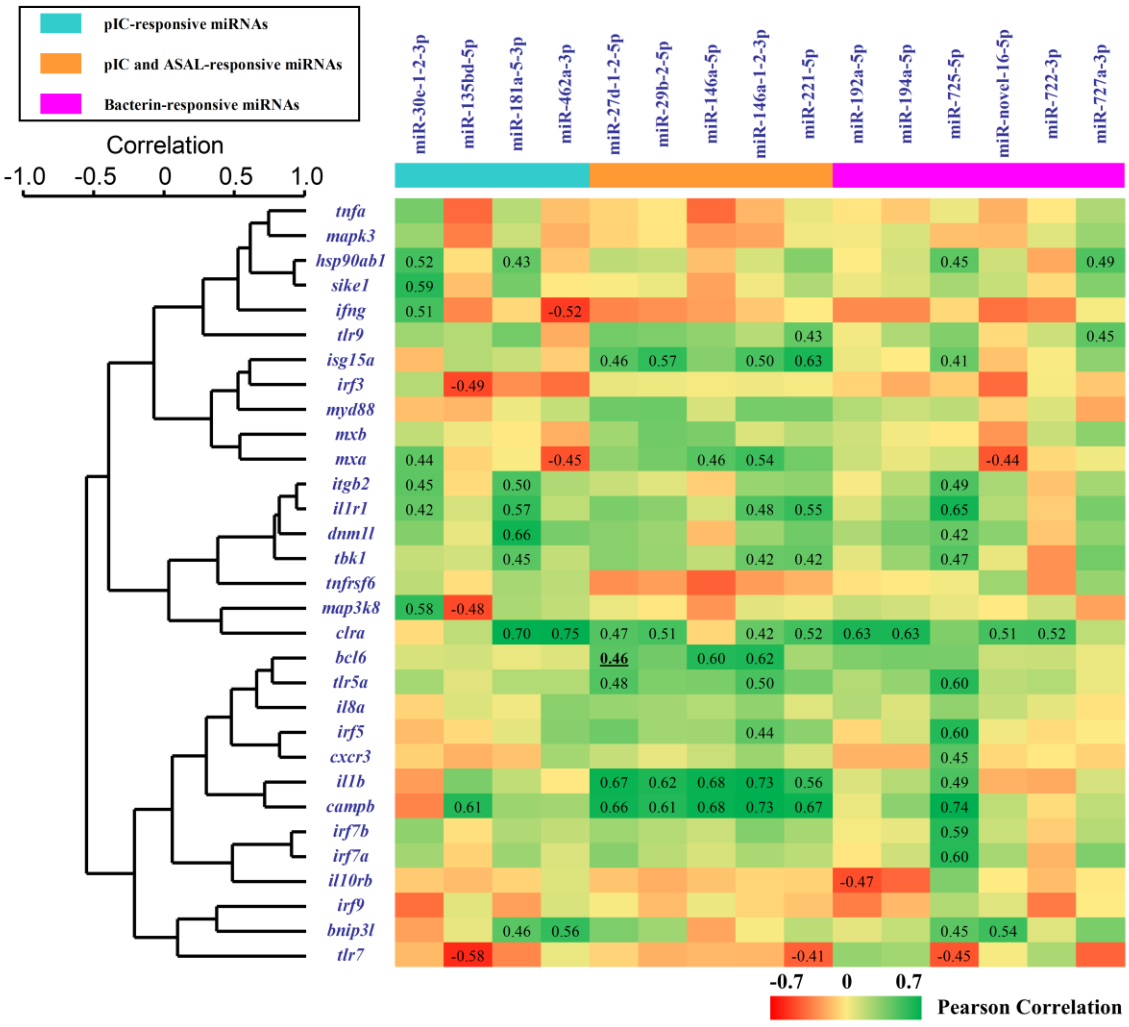

Supplemental Figure S5.3. Matrix representing Pearson's correlation coefficients between head kidney mRNA expression (row; Log_2 RQ) and miRNA expression (columns; Log_2 RQ) in pIC-injected salmon. mRNA data were arranged based on hierarchical clustering analyses (PRIMER, Version 6.1.15, Ivybridge, UK). miRNA data were arranged based their responsiveness to immunogen injections. Pearson's correlation coefficients with significant regressions ($p < 0.05$) are shown. Pearson's correlation coefficients with bold font and underline represent putative miRNA-target pairs based on previous *in silico* target prediction analysis (Xue et al. 2019).

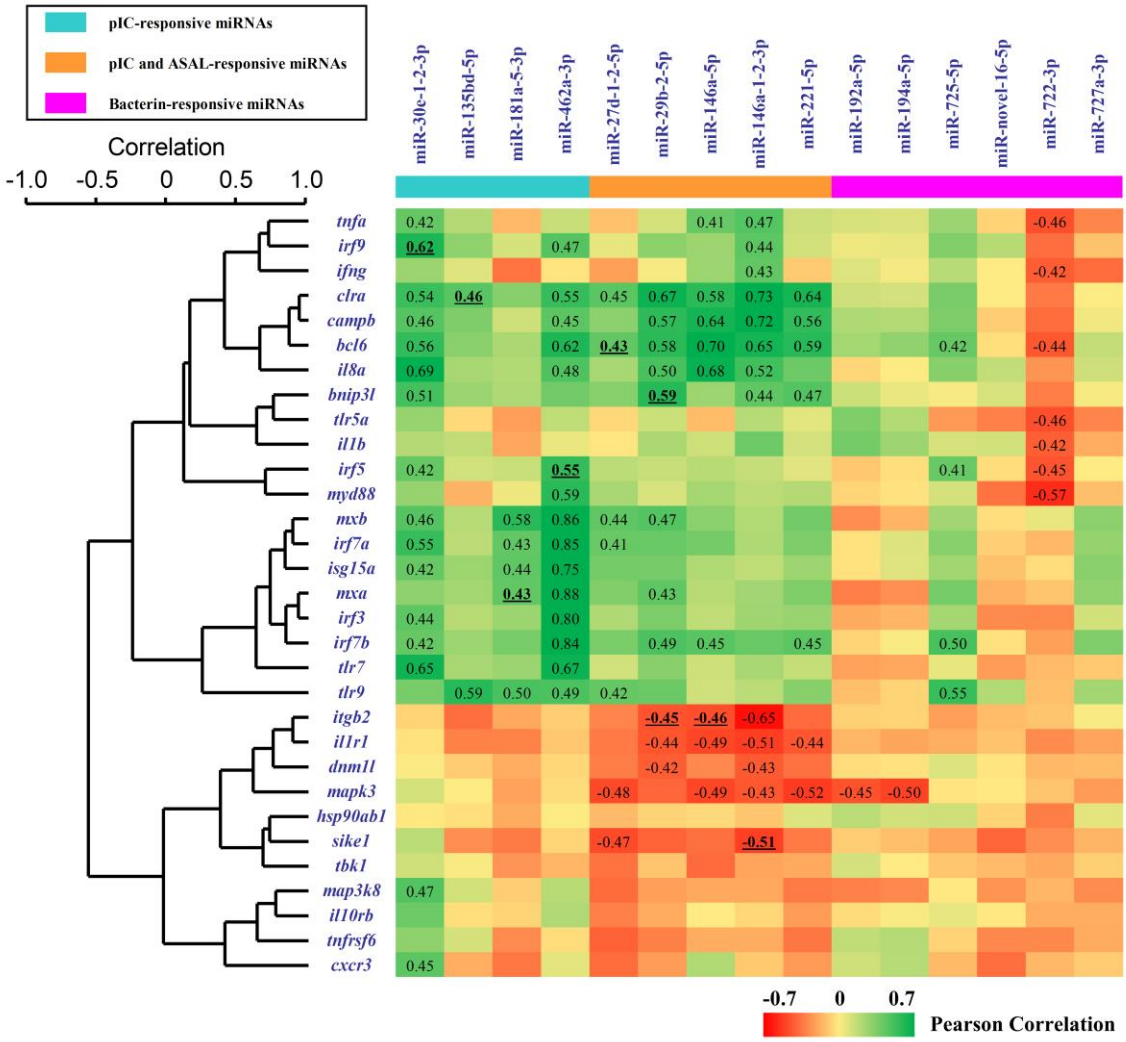

Supplemental Figure S5.4. Matrix representing Pearson's correlation coefficients between head kidney mRNA expression (row; Log_2 RQ) and miRNA expression (columns; Log_2 RQ) in *A. salmonicida* bacterin-injected salmon. mRNA data were arranged based on hierarchical clustering analyses (PRIMER, Version 6.1.15, Ivybridge, UK). miRNA data were arranged based their responsiveness to immunogen injections. Pearson's correlation coefficients with significant regressions ($p < 0.05$) are shown. Pearson's correlation coefficients with bold font and underline represent putative miRNA-target pairs based on previous *in silico* target prediction analysis (Xue et al. 2019).

5.8 References

Andreassen, R., Høyheim, B., 2017. miRNAs associated with immune response in teleost fish. Dev. Comp. Immunol. 75, 77-85.

Andreassen, R., Woldemariam, N.T., Egeland, I.Ø., Agafonov, O., Sindre, H., Høyheim, B., 2017. Identification of differentially expressed Atlantic salmon miRNAs responding to salmonid alphavirus (SAV) infection. BMC Genomics 18, 349.

Angulo, C., Alamillo, E., Hirono, I., Kondo, H., Jirapongpairoj, W., Perez-Urbiola, J.C., Reyes-Becerril, M., 2018. Class B CpG-ODN2006 is highly associated with IgM and antimicrobial peptide gene expression through TLR9 pathway in yellowtail *Seriola lalandi*. Fish Shellfish Immunol. 77, 71-82.

Bader, A., Gao, J., Rivière, T., Schmid, B., Walzog, B., Maier-Begandt, D., 2021. Molecular insights into neutrophil biology from the zebrafish perspective: lessons from CD18 deficiency. Front. Immunol. 12, 677994.

Baron, B.W., Anastasi, J., Thirman, M.J., Furukawa, Y., Fears, S., Kim, D.C., Simone, F., Birkenbach, M., Montag, A., Sadhu, A., 2002. The human programmed cell death-2 (PDCD2) gene is a target of BCL6 repression: implications for a role of BCL6 in the down-regulation of apoptosis. Proc. Natl. Acad. Sci. U. S. A. 99, 2860-2865.

Beemelmanns, A., Zanuzzo, F.S., Xue, X., Sandrelli, R.M., Rise, M.L., Gamperl, A.K., 2021. The transcriptomic responses of Atlantic salmon (*Salmo salar*) to high temperature stress alone, and in combination with moderate hypoxia. BMC Genomics 22, 261.

Burton, T.R., Gibson, S.B., 2009. The role of Bcl-2 family member BNIP3 in cell death and disease: NIPping at the heels of cell death. Cell Death Differ. 16, 515-523.

Caballero-Solares, A., Hall, J.R., Xue, X., Eslamloo, K., Taylor, R.G., Parrish, C.C., Rise, M.L., 2017. The dietary replacement of marine ingredients by terrestrial animal and plant alternatives modulates the antiviral immune response of Atlantic salmon (*Salmo salar*). Fish Shellfish Immunol. 64, 24-38.

Callahan, M.K., Garg, M., Srivastava, P.K., 2008. Heat-shock protein 90 associates with N-terminal extended peptides and is required for direct and indirect antigen presentation. Proc. Natl. Acad. Sci. U. S. A. 105, 1662-1667.

Cárdenas-Reyna, T., Angulo, C., Hori-Oshima, S., Velázquez-Lizárraga, E., Reyes-Becerril, M., 2016. B-cell activating CpG ODN 1668 enhance the immune response of Pacific red snapper (*Lutjanus peru*) exposed to *Vibrio parahaemolitycus*. Dev. Comp. Immunol. 62, 72-81.

Carrington, A.C., Secombes, C.J., 2006. A review of CpGs and their relevance to aquaculture. Vet. Immunol. Immunopathol. 112, 87-101.

Chen, S.N., Zou, P.F., Nie, P., 2017. Retinoic acid‐inducible gene I (RIG‐I)‐like receptors (RLR s) in fish: current knowledge and future perspectives. Immunology 151, 16-25.

Covello, J.M., Bird, S., Morrison, R.N., Battaglene, S.C., Secombes, C.J., Nowak, B.F., 2009. Cloning and expression analysis of three striped trumpeter (*Latris lineata*) pro-inflammatory cytokines, TNF-α, IL-1β and IL-8, in response to infection by the ectoparasitic, *Chondracanthus goldsmidi*. Fish Shellfish Immunol. 26, 773-786.

Covello, J.M., Friend, S.E., Purcell, S.L., Burka, J.F., Markham, R.J.F., Donkin, A.W., Groman, D.B., Fast, M.D., 2012. Effects of orally administered immunostimulants on inflammatory gene expression and sea lice (*Lepeophtheirus salmonis*) burdens on Atlantic salmon (*Salmo salar*). Aquaculture 366, 9-16.

Cuesta, A., Esteban, M.A., Meseguer, J., 2008. The expression profile of TLR9 mRNA and CpG ODNs immunostimulatory actions in the teleost gilthead seabream points to a major role of lymphocytes. Cell. Mol. Life Sci. 65, 2091-2104.

De Nardo, D., 2015. Toll-like receptors: activation, signalling and transcriptional modulation. Cytokine 74, 181-189.

Eslamloo, K., Caballero-Solares, A., Inkpen, S.M., Emam, M., Kumar, S., Bouniot, C., Avendaño-Herrera, R., Jakob, E., Rise, M.L., 2020. Transcriptomic profiling of the adaptive and innate immune responses of Atlantic salmon to *Renibacterium salmoninarum* infection. Front. Immunol. 11, 2487.

Eslamloo, K., Inkpen, S.M., Rise, M.L., Andreassen, R., 2018. Discovery of microRNAs associated with the antiviral immune response of Atlantic cod macrophages. Mol. Immunol. 93, 152-161.

Eslamloo, K., Xue, X., Hall, J.R., Smith, N.C., Caballero-Solares, A., Parrish, C.C., Taylor, R.G., Rise, M.L., 2017. Transcriptome profiling of antiviral immune and dietary fatty acid dependent responses of Atlantic salmon macrophage-like cells. BMC Genomics 18, 706.

Espelid, S., Løkken, G.B., Steiro, K., Bøgwald, J., 1996. Effects of cortisol and stress on the immune system in Atlantic Salmon (*Salmo salar* L.). Fish Shellfish Immunol. 6, 95-110.

Ewart, K.V., Belanger, J.C., Williams, J., Karakach, T., Penny, S., Tsoi, S.C., Richards, R.C., Douglas, S.E., 2005. Identification of genes differentially expressed in Atlantic salmon (*Salmo salar*) in response to infection by *Aeromonas salmonicida* using cDNA microarray technology. Dev. Comp. Immunol. 29, 333-347.

Groom, J.R., Luster, A.D., 2011. CXCR3 in T cell function. Exp. Cell Res. 317, 620-631.

Guo, C., Cui, H., Ni, S., Yan, Y., Qin, Q., 2015. Comprehensive identification and profiling of host miRNAs in response to Singapore grouper iridovirus (SGIV) infection in grouper (*Epinephelus coioides*). Dev. Comp. Immunol. 52, 226-235.

Hellemans, J., Mortier, G., De Paepe, A., Speleman, F., Vandesompele, J., 2007. qBase relative quantification framework and software for management and automated analysis of real-time quantitative PCR data. Genome Biol. 8, R19.

Herkenhoff, M.E., Oliveira, A.C., Nachtigall, P.G., Costa, J.M., Campos, V.F., Hilsdorf, A.W., Pinhal, D., 2018. Fishing into the MicroRNA transcriptome. Front. Genet. 9, 88.

Holland, J., Bird, S., Williamson, B., Woudstra, C., Mustafa, A., Wang, T., Zou, J., Blaney, S., Collet, B., Secombes, C., 2008. Molecular characterization of IRF3 and IRF7 in rainbow trout, *Oncorhynchus mykiss*: functional analysis and transcriptional modulation. Mol. Immunol. 46, 269-285.

Hori, T.S., Gamperl, A.K., Nash, G., Booman, M., Barat, A., Rise, M.L., 2013. The impact of a moderate chronic temperature increase on spleen immune-relevant gene

transcription depends on whether Atlantic cod (*Gadus morhua*) are stimulated with bacterial versus viral antigens. Genome 56, 567-576.

Huang, J., Liu, T., Xu, L.G., Chen, D., Zhai, Z., Shu, H.B., 2005. SIKE is an IKK ε /TBK1 - associated suppressor of TLR3 - and virus - triggered IRF - 3 activation pathways. EMBO J. 24, 4018-4028.

Huntzinger, E., Izaurralde, E., 2011. Gene silencing by microRNAs: contributions of translational repression and mRNA decay. Nat. Rev. Genet. 12, 99-110.

Jung, M.-H., Jung, S.-J., 2017. CpG ODN 1668 induce innate and adaptive immune responses in rock bream (*Oplegnathus fasciatus*) against rock bream iridovirus (RBIV) infection. Fish Shellfish Immunol. 69, 247-257.

Kitani, Y., Hieu, D.Q., Kiron, V., 2019. Cloning of selected body surface antimicrobial peptide/protein genes of Atlantic salmon and their responses to *Aeromonas salmonicida*. Fish. Sci. 85, 847-858.

Kurosu, T., Fukuda, T., Miki, T., Miura, O., 2003. BCL6 overexpression prevents increase in reactive oxygen species and inhibits apoptosis induced by chemotherapeutic reagents in B-cell lymphoma cells. Oncogene 22, 4459-4468.

Lang, A.S., Rise, M.L., Culley, A.I., Steward, G.F., 2009. RNA viruses in the sea. FEMS Microbiol. Rev. 33, 295-323.

Lazear, H.M., Lancaster, A., Wilkins, C., Suthar, M.S., Huang, A., Vick, S.C., Clepper, L., Thackray, L., Brassil, M.M., Virgin, H.W., 2013. IRF-3, IRF-5, and IRF-7 coordinately regulate the type I IFN response in myeloid dendritic cells downstream of MAVS signaling. PLoS Pathog. 9, e1003118.

Liu, C.-S., Sun, Y., Hu, Y.-H., Sun, L., 2010. Identification and analysis of a CpG motif that protects turbot (*Scophthalmus maximus*) against bacterial challenge and enhances vaccine-induced specific immunity. Vaccine 28, 4153-4161.

Liu, X., Kang, L., Liu, W., Lou, B., Wu, C., Jiang, L., 2017. Molecular characterization and expression analysis of the large yellow croaker (*Larimichthys crocea*) chemokine receptors CXCR2, CXCR3, and CXCR4 after bacterial and poly I:C challenge. Fish Shellfish Immunol. 70, 228-239.

Løvoll, M., Wiik-Nielsen, C.R., Tunsjø, H.S., Colquhoun, D., Lunder, T., Sørum, H., Grove, S., 2009. Atlantic salmon bath challenged with *Moritella viscosa* – Pathogen invasion and host response. Fish Shellfish Immunol. 26, 877-884.

Maier, V.H., Dorn, K.V., Gudmundsdottir, B.K., Gudmundsson, G.H., 2008. Characterisation of cathelicidin gene family members in divergent fish species. Mol. Immunol. 45, 3723-3730.

Maisey, K., Montero, R., Christodoulides, M., 2017. Vaccines for piscirickettsiosis (salmonid rickettsial septicaemia, SRS): the Chile perspective. Expert Rev. Vaccines 16, 215-228.

Meza, K., Inami, M., Dalum, A.S., Lund, H., Bjelland, A.M., Sørum, H., Løvoll, M., 2019. Comparative evaluation of experimental challenge by intraperitoneal injection and cohabitation of Atlantic salmon (*Salmo salar* L) after vaccination against *Piscirickettsia salmonis* (EM90 - like). J. Fish Dis. 42, 1713-1730.

Mielke, L.A., Elkins, K.L., Wei, L., Starr, R., Tsichlis, P.N., O'Shea, J.J., Watford, W.T., 2009. Tumor progression locus 2 (Map3k8) is critical for host defense against Listeria monocytogenes and IL-1β production. J. Immunol. 183, 7984-7993.

Minutoli, L., Antonuccio, P., Polito, F., Bitto, A., Squadrito, F., Di Stefano, V., Nicotina, P.A., Fazzari, C., Maisano, D., Romeo, C., 2009. Mitogen-activated protein kinase 3/mitogen-activated protein kinase 1 activates apoptosis during testicular ischemia–reperfusion injury in a nuclear factor-κB-independent manner. Eur. J. Pharmacol. 604, 27-35.

Moresco, E.M.Y., LaVine, D., Beutler, B., 2011. Toll-like receptors. Curr. Biol. 21, R488-R493.

Murray, A.G., Munro, L.A., Wallace, I.S., Allan, C.E.T., Peeler, E.J., Thrush, M.A., 2012. Epidemiology of *Renibacterium salmoninarum* in Scotland and the potential for compartmentalised management of salmon and trout farming areas. Aquaculture 324-325, 1-13.

Paul, A., Tang, T.H., Ng, S.K., 2018. Interferon regulatory factor 9 structure and regulation. Front. Immunol. 9, 1831.

Peddie, S., Zou, J., Cunningham, C., Secombes, C.J., 2001. Rainbow trout (*Oncorhynchus mykiss*) recombinant IL-1β and derived peptides induce migration of head-kidney leucocytes in vitro. Fish Shellfish Immunol. 11, 697-709.

Pfaffl, M.W., 2001. A new mathematical model for relative quantification in real-time RT–PCR. Nucleic Acids Res. 29, e45-e45.

Purcell, S.L., Friend, S.E., Covello, J.M., Donkin, A., Groman, D.B., Poley, J., Fast, M.D., 2013. CpG inclusion in feed reduces sea lice, *Lepeophtheirus salmonis*, numbers following re‐infection. J. Fish Dis. 36, 229-240.

Rehmsmeier, M., Steffen, P., Höchsmann, M., Giegerich, R., 2004. Fast and effective prediction of microRNA/target duplexes. RNA 10, 1507-1517.

Rozas, M., Enríquez, R., 2014. Piscirickettsiosis and *Piscirickettsia salmonis* in fish: a review. J. Fish Dis. 37, 163-188.

Sato, A., Linehan, M.M., Iwasaki, A., 2006. Dual recognition of herpes simplex viruses by TLR2 and TLR9 in dendritic cells. Proc. Natl. Acad. Sci. U. S. A. 103, 17343-17348.

Seppola, M., Larsen, A.N., Steiro, K., Robertsen, B., Jensen, I., 2008. Characterisation and expression analysis of the interleukin genes, IL-1β, IL-8 and IL-10, in Atlantic cod (*Gadus morhua* L.). Mol. Immunol. 45, 887-897.

Sernapesca, 2021. Informe Sanitario de Salmonicultura en Centros Marinos 2020. Servicio Nacional de Pesca y Acuicultura.

Shouval, Dror S., Biswas, A., Goettel, Jeremy A., McCann, K., Conaway, E., Redhu, Naresh S., Mascanfroni, Ivan D., Al Adham, Z., Lavoie, S., Ibourk, M., Nguyen, Deanna D., Samsom, Janneke N., Escher, Johanna C., Somech, R., Weiss, B., Beier, R., Conklin, Laurie S., Ebens, Christen L., Santos, Fernanda G.M.S., Ferreira, Alexandre R., Sherlock, M., Bhan, Atul K., Müller, W., Mora, J.R., Quintana, Francisco J., Klein, C., Muise, Aleixo M., Horwitz, Bruce H., Snapper, Scott B., 2014. Interleukin-10 receptor signaling in innate immune cells regulates

mucosal immune tolerance and anti-inflammatory macrophage function. Immunity 40, 706-719.
Skjæveland, I., Iliev, D.B., Zou, J., Jørgensen, T., Jørgensen, J.B., 2008. A TLR9 homolog that is up-regulated by IFN-γ in Atlantic salmon (*Salmo salar*). Dev. Comp. Immunol. 32, 603-607.
Slack, J.L., Schooley, K., Bonnert, T.P., Mitcham, J.L., Qwarnstrom, E.E., Sims, J.E., Dower, S.K., 2000. Identification of two major sites in the type I interleukin-1 receptor cytoplasmic region responsible for coupling to pro-inflammatory signaling pathways. J. Biol. Chem. 275, 4670-4678.
Smith, N.C., Umasuthan, N., Kumar, S., Woldemariam, N.T., Andreassen, R., Christian, S.L., Rise, M.L., 2021. Transcriptome profiling of Atlantic salmon adherent head kidney leukocytes reveals that macrophages are selectively enriched during culture. Front. Immunol. 12, 709910.
Soanes, K.H., Figuereido, K., Richards, R.C., Mattatall, N.R., Ewart, K.V., 2004. Sequence and expression of C-type lectin receptors in Atlantic salmon (*Salmo salar*). Immunogenetics 56, 572-584.
Srivastava, P., 2002. Interaction of heat shock proteins with peptides and antigen presenting cells: chaperoning of the innate and adaptive immune responses. Annu. Rev. Immunol. 20, 395-425.
Strandskog, G., Skjæveland, I., Ellingsen, T., Jørgensen, J.B., 2008. Double-stranded RNA-and CpG DNA-induced immune responses in Atlantic salmon: comparison and synergies. Vaccine 26, 4704-4715.
Tassakka, A.C.M.A.R., Sakai, M., 2005. Current research on the immunostimulatory effects of CpG oligodeoxynucleotides in fish. Aquaculture 246, 25-36.
Tsoi, S., Park, K.C., Kay, H.H., O'Brien, T.J., Podor, E., Sun, G., Douglas, S.E., Brown, L.L., Johnson, S.C., 2006. Identification of a transcript encoding a soluble form of toll-like receptor 5 (TLR5) in Atlantic salmon during *Aeromonas salmonicida* infection. Vet. Immunol. Immunopathol. 109, 183-187.
Vandesompele, J., De Preter, K., Pattyn, F., Poppe, B., Van Roy, N., De Paepe, A., Speleman, F., 2002. Accurate normalization of real-time quantitative RT-PCR data by geometric averaging of multiple internal control genes. Genome Biol 3, research0034.0031.
Woldemariam, N.T., Agafonov, O., Høyheim, B., Houston, R.D., Taggart, J.B., Andreassen, R., 2019. Expanding the miRNA repertoire in Atlantic salmon; discovery of isomiRs and miRNAs highly expressed in different tissues and developmental stages. Cells 8, 42.
Woldemariam, N.T., Agafonov, O., Sindre, H., Høyheim, B., Houston, R.D., Robledo, D., Bron, J.E., Andreassen, R., 2020. miRNAs predicted to regulate host anti-viral gene pathways in IPNV-challenged Atlantic salmon fry are affected by viral load, and associated with the major IPN resistance QTL genotypes in late infection. Front. Immunol. 11, 2113.
Xie, Y., Song, L., Weng, Z., Liu, S., Liu, Z., 2015. Hsp90, Hsp60 and sHsp families of heat shock protein genes in channel catfish and their expression after bacterial infections. Fish Shellfish Immunol. 44, 642-651.

Xiong, P., Schneider, R.F., Hulsey, C.D., Meyer, A., Franchini, P., 2019. Conservation and novelty in the microRNA genomic landscape of hyperdiverse cichlid fishes. Sci. Rep. 9, 13848.

Xu, P., Wu, Q., Yu, J., Rao, Y., Kou, Z., Fang, G., Shi, X., Liu, W., Han, H., 2020. A systematic way to infer the regulation relations of miRNAs on target genes and critical miRNAs in cancers. Front. Genet. 11, 278.

Xu, T., Chu, Q., Cui, J., Huo, R., 2018. MicroRNA-216a inhibits NF-κB-mediated inflammatory cytokine production in teleost fish by modulating p65. Infect. Immun. 86, e00256-00218.

Xue, X., Caballero-Solares, A., Hall, J.R., Umasuthan, N., Kumar, S., Jakob, E., Skugor, S., Hawes, C., Santander, J., Taylor, R.G., Rise, M.L., 2021. Transcriptome profiling of Atlantic salmon (*Salmo salar*) parr with higher and lower pathogen loads following *Piscirickettsia salmonis* infection. Front. Immunol. 12, 789465.

Xue, X., Woldemariam, N.T., Caballero-Solares, A., Umasuthan, N., Fast, M.D., Taylor, R.G., Rise, M.L., Andreassen, R., 2019. Dietary immunostimulant CpG modulates microRNA biomarkers associated with immune responses in Atlantic salmon (*Salmo salar*). Cells 8, 1592.

Yang, Q., Chu, Q., Zhao, X., Xu, T., 2017. Characterization of IL-1β and two types of IL-1 receptors in miiuy croaker and evolution analysis of IL-1 family. Fish Shellfish Immunol. 63, 165-172.

Yao, C.-L., Huang, X.-N., Fan, Z., Kong, P., Wang, Z.-Y., 2012. Cloning and expression analysis of interferon regulatory factor (IRF) 3 and 7 in large yellow croaker, *Larimichthys crocea*. Fish Shellfish Immunol. 32, 869-878.

Yi, F., Frazzette, N., Cruz, A.C., Klebanoff, C.A., Siegel, R.M., 2018. Beyond Cell Death: New Functions for TNF Family Cytokines in Autoimmunity and Tumor Immunotherapy. Trends Mol. Med. 24, 642-653.

Zhang, B.C., Zhou, Z.J., Sun, L., 2016a. pol-miR-731, a teleost miRNA upregulated by megalocytivirus, negatively regulates virus-induced type I interferon response, apoptosis, and cell cycle arrest. Sci. Rep. 6, 28354.

Zhang, G., Yin, S., Mao, J., Liang, F., Zhao, C., Li, P., Zhou, G., Chen, S., Tang, Z., 2016b. Integrated analysis of mRNA-seq and miRNA-seq in the liver of *Pelteobagrus vachelli* in response to hypoxia. Sci. Rep. 6, 22907.

Zhang, H., Robison, B., Thorgaard, G.H., Ristow, S.S., 2000. Cloning, mapping and genomic organization of a fish C-type lectin gene from homozygous clones of rainbow trout (*Oncorhynchus mykiss*). Biochim. Biophys. Acta, Gene Struct. Expression 1494, 14-22.

Zhu, Y., Qi, C., Shan, S., Zhang, F., Li, H., An, L., Yang, G., 2016. Characterization of common carp (*Cyprinus carpio* L.) interferon regulatory factor 5 (IRF5) and its expression in response to viral and bacterial challenges. BMC Vet. Res. 12, 127.

Zou, J., Secombes, C.J., 2016. The function of fish cytokines. Biology 5, 23.

CHAPTER 6: Summary and general conclusions

6.1 Summary

Aquaculture is becoming the main supplier of seafood for human consumption due to a flat or decreasing global capture fisheries in the face of the rising human population (FAO, 2020). Atlantic salmon is one of the most economically important species in many countries such as Canada, Chile, the United Kingdom and Norway (Houston and Macqueen, 2019). However, Atlantic salmon farming faces several issues and challenges, such as disease outbreaks and the limited supply of fish oil (FO), affecting the sustainability of the industry. The increasing demand and limited supply of FO have resulted in the high substitution of FO with alternatives. The main substitutes of FO today are terrestrial or vegetable oils (VO), which lack long-chain polyunsaturated fatty acids (LC-PUFAs) but are rich in short-chain PUFAs (Xue et al., 2015). The dietary requirement of ω3 LC-PUFA in Atlantic salmon has been subjected to several studies and is found to vary greatly depending on life stage, experimental setting and parameters assessed (Ruyter et al., 2000; Glencross et al., 2014; Rosenlund et al., 2016; Sissener et al., 2016; Bou et al., 2017a; Bou et al., 2017b). However, studies on the determination of ω3 LC-PUFA requirements in Atlantic salmon were mostly conducted based on growth and survival. Other parameters such as fish health and immunity need to be considered when determining the nutritional requirement of EPA and DHA.

The first goal of my thesis was to determine the optimal dietary requirement of ω3 LC-PUFA for Atlantic salmon that promotes growth and health. To accomplish this objective, in **Chapter 2** (Xue et al., 2020), a 14-week feeding trial was conducted with salmon fed three different experimental diets containing increasing levels of DHA + EPA

(0, 1.0, and 1.4% of the diet, as formulated) in the presence of high linoleic acid to assess growth performance. At the end of the trial, Atlantic salmon fed diet ω3LC0 (i.e. 0% of DHA+EPA) showed significantly lower final weight and weight gain, and higher feed conversion ratio compared with ω3LC1.0 and ω3LC1.4 diet groups. I then used 44K microarrays to study molecular mechanisms involved in salmon's response to increasing dietary DHA and EPA levels. A total of 200 differentially expressed probes were identified in the pairwise comparisons of the liver transcriptome of salmon fed the three experimental diets. The transcriptome results were confirmed by qPCR analyses of 22 microarray-identified transcripts. Overall, my results showed that the experimental diets modulated the transcript expression of genes involved in carbohydrate metabolism, fatty acid synthesis, redox homeostasis, and immunity. For example, critical genes involved in fatty acid metabolism (e.g. LC-PUFA synthesis) were up-regulated in fish fed ω3LC0 compared with both other groups (i.e. ω3LC1.0 and ω3LC1.4). Hierarchical clustering and linear regression analyses of liver qPCR and fatty acid composition data showed that fatty acid biosynthesis-related genes (i.e. *fadsd5*, *fadsd6a*, *fasb*) were positively correlated with ω6 fatty acids, and negatively correlated with ω3 fatty acids and two important fatty acid ratios (EPA/ARA and ω3/ω6), suggesting that these genes can regulate both ω3 and ω6 LC-PUFA synthesis pathways. The linear regression analyses also showed that the transcript expression of antiviral genes (*irf3*, *mxb*, *ifit5*) correlated negatively with hepatic EPA/ARA and ω3/ω6 ratios and EPA and positively with 20:3ω6 (dihomo-γ-linolenic acid; DGLA), suggesting these fatty acid-related factors can modulate genes involved in interferon-mediated pathways. In contrast to antiviral transcript expression, several essential genes of

antibacterial response (e.g. *lect2a*, *lyz2*) were up-regulated in the liver of fish fed ω3LC1.4 diet compared with ω3LC1.0 group, suggesting that a higher dietary level of DHA + EPA may be associated with stronger expression of antibacterial genes.

Based on growth performance alone, 1.0% ω3 LC-PUFA seemed to be the minimum requirement for Atlantic salmon. However, fish fed ω3LC1.0 and ω3LC1.4 diets had similar hepatic fatty acid profiles, but marked differences in the transcript expression of genes related to molecular pathways such as redox homeostasis (*mgst1*) and immune responses (*mxb*, *igmb*, *irf3*, *lect2a*, *srk2*, *lyz2*). Several recent studies on the topic in Atlantic salmon showed that higher dietary levels of DHA and EPA (i.e. >1.0%) influenced macrophage gene expression (Eslamloo et al., 2017), enhanced growth (Rosenlund et al., 2016), supported normal intestine structure and health (Bou et al., 2017a; Bou et al., 2017b; Løvmo et al., 2021), and promoted fish robustness under demanding environmental conditions (Bou et al., 2017b). Taken together, our data suggest that ~1.0% of dietary ω3 LC-PUFA is sufficient to sustain the optimal growth performance of Atlantic salmon. However, this level may not be enough to maintain good health and survival compared with fish fed diets containing a higher amount of DHA and EPA, especially under commercial growing conditions, and warrants further investigation. The results from **Chapter 2** has provided new insights into the dietary requirement of DHA and EPA, and their impact on physiologically important pathways in addition to lipid metabolism in Atlantic salmon.

In addition to the limited supply of FO, infectious diseases have resulted in substantial mortality and financial losses to aquaculture worldwide, affecting the growth

and sustainability of the industry (Rodger, 2016). As mentioned earlier in the current thesis, Piscirickettsiosis or salmonid rickettsial septicemia (SRS) caused by the intracellular Gram-negative bacterial pathogen, *Piscirickettsia salmonis*, is one of the most economically significant diseases of Atlantic salmon aquaculture (Rise et al., 2004; Rozas and Enríquez, 2014). Occurrences of this pathogen have also been reported in farmed salmonids in Norway, Scotland, Ireland and Canada (Meza et al., 2019b; Jones et al., 2020). In Chile, the existence of two distinct *P. salmonis* genogroups, LF-89-like and EM-90-like strains, has been reported (Nourdin-Galindo et al., 2017; Saavedra et al., 2017; Meza et al., 2019b). Saavedra et al. (2017) found that EM-90-like isolates, similar to LF-89-like ones, are highly prevalent and disseminated across Chilean marine farms. Studies revealed differences between these two genogroups concerning geographic distribution, antibiotic susceptibility and host specificity, and may link to the genomic divergences (Nourdin-Galindo et al., 2017; Saavedra et al., 2017). As a result, there has been a growing interest in studying the piscirickettsiosis resulting from EM-90-like isolates (Rozas-Serri et al., 2017; Rozas-Serri et al., 2018a; Rozas-Serri et al., 2018b; Meza et al., 2019a; Meza et al., 2019b). However, the molecular mechanisms involved in *P. salmonis* pathogenesis are not entirely known, and the transcriptomic responses of Atlantic salmon parr in freshwater to an EM-90-like isolate have not been explored.

The second goal of my thesis was to explore the head kidney transcriptomic responses of Atlantic salmon parr to an EM-90-like *P. salmonis* isolate and fill the gaps in the current knowledge regarding piscirickettsiosis outbreaks involving such isolates. In **Chapter 3** (Xue et al., 2021), Atlantic salmon parr were infected with an EM-90-like

isolate through intraperitoneal injection. The infected fish showed ~30% cumulative mortality by the end of the trial (42 days post-injection, DPI). Head kidney samples collected from multiple time points post-injection were included in qPCR analyses to study the temporal patterns of pathogen level and host immune responses. Two infection phenotypes [lower (L-SRS) and higher (H-SRS) infection level] at 21 DPI were detected by multivariate analyses of pathogen load and levels of 4 antibacterial biomarker transcripts. I then selected five fish from each group (Control, L-SRS, and H-SRS) for transcriptome profiling using cGRASP-designed 44K salmonid oligonucleotide microarrays. I identified 1,636 and 3,076 DEPs in the L-SRS and H-SRS groups compared with the control group, respectively (FDR = 1%). Transcriptome results were confirmed by qPCR analyses of 42 microarray-identified transcripts. A large number of innate and adaptive immune processes were activated based on gene ontology (GO) term enrichment analyses of SRS-responsive genes, while a small number of GO terms related to general physiological processes was also enriched. Furthermore, the comparison of individuals with differing levels of infection (H-SRS *vs* L-SRS) generated insights into the biological processes possibly involved in natural resistance to *P. salmonis*. As suggested by several previous studies of bacterial (Škugor et al., 2009; Braden et al., 2019) and viral diseases (Jørgensen et al., 2008; Timmerhaus et al., 2012; Martinez-Rubio et al., 2014) in salmonids, a more pronounced immune response against infection at a late stage observed in H-SRS fish suggests that at least part of these responses was exaggerated and not protective. It is worth mentioning that similar to the result reported in my thesis, Moraleda et al. (2021) also showed that *bnip3* (an apoptotic biomarker gene) was repressed by *P.*

salmonis infection and it was also found to be one of key genes involved in resistance to SRS. Finally, this study (**Chapter 3**) demonstrated a low mortality EM-90-like *P. salmonis* infection model, broadened the current understanding of molecular pathways underlying *P. salmonis*-triggered responses of Atlantic salmon, and provided qPCR-validated many SRS-responsive molecular biomarkers, which are valuable tools for future research aimed at improving farmed Atlantic salmon resistance to SRS.

miRNAs are known to play important immunoregulatory roles in teleosts (Andreassen and Høyheim, 2017; Andreassen et al., 2017; Eslamloo et al., 2018; Herkenhoff et al., 2018). Studies investigating miRNA responses to different pathogen infections or other immune stimuli can improve our understanding of miRNAs involved in immunity (Andreassen and Høyheim, 2017; Wang et al., 2018). It is well known that microbial cell components (e.g., lipopolysaccharide, peptidoglycan, RNAs, and DNAs), recognized by animal immune cells as pathogen-associated molecular patterns (PAMPs), can elicit host immune responses to fight the invading pathogen (Vallejos-Vidal et al., 2016). In fish, immunogens: polyriboinosinic polyribocytidylic acid (pIC, a PAMP-like synthetic dsRNA analogue) and formalin-killed typical *Aeromonas salmonicida* (a PAMP-containing bacterin) have been used to study antiviral and antibacterial immune responses, respectively (Akira et al., 2006; Robertsen, 2006; Feng et al., 2009; Hori et al., 2013; Eslamloo et al., 2016; Caballero-Solares et al., 2017). However, the impact of pIC and *A. salmonicida* bacterin on the expression of miRNAs in Atlantic salmon has not been documented previously.

In **Chapter 4** (Xue et al., 2019), I used small RNA deep sequencing and qPCR analyses to identify and confirm pIC- and/or *A. salmonicida* bacterin-responsive miRNAs in the head kidney of salmon. DESeq2 analyses identified 12 and 18 miRNAs differentially expressed in pIC and bacterin groups, respectively. Many of the miRNAs identified herein are involved in immune responses, as shown in many similar teleost immune/pathogen challenge studies. Fifteen of these miRNAs were studied by qPCR; nine remained significant by qPCR. Five miRNAs (miR-27d-1-2-5p, miR-29b-2-5p, miR-146a-5p, miR-146a-1-2-3p, miR-221-5p) were shown by qPCR to be significantly induced by both pIC and bacterin. The predicted target gene analyses of pIC- and/or bacterin-responsive miRNAs identified 130 immune-relevant genes. The pathways mapped to these target genes include NOD-like receptor signaling pathway, Toll-like receptor signaling pathway, RIG-I-like receptor signaling pathway, and cytokine–cytokine receptor interaction pathway, confirming that the pIC- and/or bacterin-responsive miRNAs identified herein are relevant to the host-pathogen immune response.

As discussed in the previous sections, one of the approaches to fighting disease problems in intensive culture systems is to incorporate functional feeds into health management (Tacchi et al., 2011; Kiron, 2012; Martin and Król, 2017). Functional feeds are able to enhance fish health and/or growth by incorporating additional functional ingredients (e.g. immunostimulant) beyond the basic nutritional requirements of the animal (Martin and Król, 2017). CpG ODN has been used in aquaculture to mitigate fish diseases by enhancing the non-specific immune system. However, the impact of dietary CpG on the expression of miRNAs associated with antiviral and antibacterial responses in Atlantic

salmon was previously unknown. Another goal of this chapter was to evaluate the immune-modulating properties of dietary CpG by studying the expression changes of putative antiviral and antibacterial responsive miRNAs identified through sequencing in pre- and post-stimulation individuals. In pre-injection samples, six miRNAs (e.g., miR-181a-5-3p, miR-462a-3p, miR-722-3p) had significantly lower expression in fish fed CpG diet than the control diet. In contrast, several miRNAs (e.g., miR-146a-1-2-3p, miR-192a-5p, miR-194a-5p) in the PBS- and bacterin-injected groups had significantly higher expression in CpG-fed fish. Multivariate statistical analyses further confirmed that the CpG diet had a greater impact on miRNA expression in bacterin-injected compared with pIC-injected fish. Finally, this study (**Chapter 4**) broadened the current understanding of miRNAs involved in immune responses of Atlantic salmon and the immune-modulating properties of dietary CpG, and provided qPCR-validated immune-relevant miRNA biomarkers that will be valuable in future research.

The final goal of my thesis was to gain a more complete picture of the impact of pIC, *A. salmonicida* bacterin, and dietary CpG on the immune responses of Atlantic salmon. In **Chapter 5**, I report a complementary qPCR study that investigated the impact of the pIC, *A. salmonicida* bacterin and dietary CpG on the expression of immune-relevant mRNAs (n = 31) using the same samples as were previously used in the miRNA chapter (Xue et al., 2019). Twenty-three of these genes were predicted target transcripts of the pIC- and/or *A. salmonicida* bacterin-responsive miRNAs in Atlantic salmon identified in the earlier study (**Chapter 4**). The qPCR data showed that pIC and/or bacterin stimulations significantly modulated most of the predicted target genes involved in various immune

pathways (e.g. TLR-mediated pathway). Several genes (e.g. *tnfa*, *il10rb*, *ifng*, *irf9*, *cxcr3*, *campb*) were shown by qPCR to be significantly modulated by both stimulations while others appeared to be stimulus specific [e.g. *irf3*, *irf7a*, *il1r1*, *mxa*, *mapk3* (pIC only); *clra* (bacterin only)]. Atlantic salmon with *A. salmonicida* bacterin stimulation had a stronger inflammatory response (e.g. higher expression of *il1b*, *il8a* and *tnfa*) compared with the pIC-treated group, while salmon stimulated with pIC showed stronger interferon responses. The expression levels of several immune-relevant transcripts (e.g. *tlr9*, *irf5*, *il1r1*, *hsp90ab1*, *itgb2*) were repressed by dietary immunostimulant CpG, especially among pre-injection and PBS-injected fish. Furthermore, significant correlations between mRNA and miRNA expression representing putative miRNA-target pairs were found, providing further insights into how miRNAs might fine-tune the expression of immune-relevant mRNAs.

6.2 Perspectives and future research

In **Chapter 2**, I used microarrays to profile the hepatic transcriptome response of Atlantic salmon to varying levels of DHA and EPA, and provided new insights into the dietary requirement of DHA and EPA, and their impact on physiologically important pathways (e.g. redox, immune responses) in addition to lipid metabolism in Atlantic salmon. Future studies should perform functional/cellular assays to measure the redox status [e.g. the reduced (GSH) and oxidized (GSSG) glutathione levels] in the liver of salmon fed different levels of LC-PUFA. Future research such as environmental/live pathogen challenge in a biocontainment facility is also needed to assess further the potential effects of dietary DHA and EPA on fish physiology and health and define the optimal

requirement in Atlantic salmon. Furthermore, I showed that the transcript expression changes of antiviral genes might be regulated by hepatic ω3/ω6 and EPA/ARA ratios. Therefore, the interactions between levels of DHA + EPA, PUFA (e.g. ALA or LA), and ω3/ω6 and EPA/ARA ratios on Atlantic salmon health warrant further investigation. The liver was the only target tissue used in **Chapter 2**. As such, future research should involve other organs such as the intestine and head kidney to develop a better understanding of the dietary requirement of DHA and EPA in Atlantic salmon.

In **Chapter 3**, I demonstrated a low mortality EM-90-like *P. salmonis* infection model, and broadened the current understanding of molecular pathways underlying *P. salmonis*-triggered responses of Atlantic salmon. I showed that SRS influenced host cellular immunity, and cytoskeletal remodeling may be essential in promoting immune cell mobility and migration. Future studies are needed to better understand the function of cytoskeletal remodeling during piscirickettsiosis. The activation of iron withholding response (or nutritional immunity) in *P. salmonis*-infected fish was evidenced; however, such activation increases iron intracellular storage that may be detrimental for the host and more beneficial to the pathogen. Future studies should investigate the cellular iron content in the infected animals to elucidate the potential mechanism of iron withholding response in regulating Atlantic salmon resistance to *P. salmonis*. Examination of earlier and later time points (e.g. 2 DPI, 42 DPI) and other relevant tissues (e.g. spleen and liver) are necessary for future research to fully elucidate mechanisms responsible for different infection phenotypes (L-SRS and H-SRS) and protection against *P. salmonis* infection. Further, it should be noted that aspects such as route of infection and infection level during

natural SRS outbreaks may differ from the IP injection model. As such, future studies should also employ a cohabitation challenge model to validate the results obtained in the current thesis. As illustrated by previous studies in identifying Atlantic salmon genetic resistance to ISAV and LF-89 *P. salmonis* (Li et al., 2011; Moraleda et al., 2021), respectively, further study should aim at mapping the quantitative trait loci (QTL) affecting resistance to EM-90-like *P. salmonis* and compared with the *P. salmonis*-responsive genes identified in this thesis, to define the functional mechanisms underpinning genetic resistance.

In **Chapter 4**, I successfully identified and confirmed nine pIC- and/or *A. salmonicida* bacterin-responsive miRNAs in the head kidney of Atlantic salmon. However, only 50% (5 out of 10) of deep sequencing-identified *A. salmonicida* bacterin-responsive miRNAs were confirmed by qPCR analyses. In order to reduce the likelihood of false negatives, future miRNA deep sequencing studies could employ higher numbers of biological replicates (e.g. n = 6). Although the *in silico* target gene prediction provided some insights on the potential regulatory roles of immune-responsive miRNAs (i.e. pIC- and/or bacterin-responsive miRNAs identified in this thesis), future research should validate the target genes by experimental approaches as suggested by Andreassen and Høyheim (2017). For example, a dual luciferase assay is commonly used to detect a true miRNA:mRNA binding site (Nicolas, 2011). The miRNAs identified in the current thesis should also be further functionally characterized using *in vitro* assays (gene silencing or overexpression) and evaluating if these miRNAs interfere with viral and bacterial replication in Atlantic salmon.

In **Chapter 5**, I conducted a complementary qPCR study to evaluate the impact of the pIC and *A. salmonicida* bacterin immune stimulations, and CpG-containing functional feed on the expression of immune-relevant mRNAs, with the majority of them being identified as predicted target transcripts from **Chapter 4**. Future research could investigate the whole transcriptome responses (both miRNA and mRNA) of Atlantic salmon to dietary CpG using a 44K microarray or RNA-seq approach. Further, since only the immunogens (i.e. pIC and *A. salmonicida* bacterin) were used to trigger immune responses in **Chapters 4** and **5** of this thesis, future studies should involve live pathogen challenges in a biocontainment facility (similar to the method used in **Chapter 3**) to examine the beneficial effects of dietary immunostimulant CpG ODN 1668 on Atlantic salmon in modulating viral and bacterial infections.

Finally, the current thesis focused on the study of changes in mRNA expression in responses to diet, infection, and other immune stimulations. However, as suggested by other researchers (e.g. Dixon et al., 2018), changes in transcript levels do not always translate into alterations at the protein level. It is vital for future research to develop antibodies against proteins encoded by some of the key dietary- and immune-responsive genes identified in the current thesis and to validate the main findings from the present study. Future research could also apply high-throughput multi-omics approaches (e.g. transcriptomics, proteomics, and metabolomics) to provide a complete understanding of how diet and infections affect Atlantic salmon metabolism, physiology and health.

6.3 References

Akira, S., Uematsu, S., Takeuchi, O., 2006. Pathogen recognition and innate immunity. Cell 124, 783-801.

Andreassen, R., Høyheim, B., 2017. miRNAs associated with immune response in teleost fish. Dev. Comp. Immunol. 75, 77-85.

Andreassen, R., Woldemariam, N.T., Egeland, I.Ø., Agafonov, O., Sindre, H., Høyheim, B., 2017. Identification of differentially expressed Atlantic salmon miRNAs responding to salmonid alphavirus (SAV) infection. BMC Genomics 18, 349.

Bou, M., Berge, G.M., Baeverfjord, G., Sigholt, T., Østbye, T.-K., Romarheim, O.H., Hatlen, B., Leeuwis, R., Venegas, C., Ruyter, B., 2017a. Requirements of n-3 very long-chain PUFA in Atlantic salmon (*Salmo salar* L): effects of different dietary levels of EPA and DHA on fish performance and tissue composition and integrity. Br. J. Nutr. 117, 30-47.

Bou, M., Berge, G.M., Baeverfjord, G., Sigholt, T., Østbye, T.-K., Ruyter, B., 2017b. Low levels of very-long-chain n-3 PUFA in Atlantic salmon (*Salmo salar*) diet reduce fish robustness under challenging conditions in sea cages. J Nutr Sci 6, E32.

Braden, L.M., Whyte, S.K., Brown, A.B., Vaniderstine, C., Letendre, C., Groman, D., Lewis, J., Purcell, S., Hori, T., Fast, M.D., 2019. Vaccine-induced protection against furunculosis involves pre-emptive priming of humoral immunity in Arctic charr. Front. Immunol. 10, 120.

Caballero-Solares, A., Hall, J.R., Xue, X., Eslamloo, K., Taylor, R.G., Parrish, C.C., Rise, M.L., 2017. The dietary replacement of marine ingredients by terrestrial animal and plant alternatives modulates the antiviral immune response of Atlantic salmon (*Salmo salar*). Fish Shellfish Immunol. 64, 24-38.

Dixon, B., Barreda, D.R., Sunyer, J.O., 2018. Perspective on the development and validation of Ab reagents to fish immune proteins for the correct assessment of immune function. Front. Immunol. 9, 2957.

Eslamloo, K., Inkpen, S.M., Rise, M.L., Andreassen, R., 2018. Discovery of microRNAs associated with the antiviral immune response of Atlantic cod macrophages. Mol. Immunol. 93, 152-161.

Eslamloo, K., Xue, X., Booman, M., Smith, N.C., Rise, M.L., 2016. Transcriptome profiling of the antiviral immune response in Atlantic cod macrophages. Dev. Comp. Immunol. 63, 187-205.

Eslamloo, K., Xue, X., Hall, J.R., Smith, N.C., Caballero-Solares, A., Parrish, C.C., Taylor, R.G., Rise, M.L., 2017. Transcriptome profiling of antiviral immune and dietary fatty acid dependent responses of Atlantic salmon macrophage-like cells. BMC Genomics 18, 706.

FAO, 2020. The state of world fisheries and aquaculture 2020. Food and Agriculture Organization of the United Nations, Rome.

Feng, C.Y., Johnson, S.C., Hori, T.S., Rise, M., Hall, J.R., Gamperl, A.K., Hubert, S., Kimball, J., Bowman, S., Rise, M.L., 2009. Identification and analysis of differentially expressed genes in immune tissues of Atlantic cod stimulated with formalin-killed, atypical *Aeromonas salmonicida*. Physiol. Genomics 37, 149-163.

Glencross, B.D., Tocher, D.R., Matthew, C., Bell, J.G., 2014. Interactions between dietary docosahexaenoic acid and other long-chain polyunsaturated fatty acids on performance and fatty acid retention in post-smolt Atlantic salmon (*Salmo salar*). Fish Physiol. Biochem. 40, 1213-1227.

Herkenhoff, M.E., Oliveira, A.C., Nachtigall, P.G., Costa, J.M., Campos, V.F., Hilsdorf, A.W., Pinhal, D., 2018. Fishing into the MicroRNA transcriptome. Front. Genet. 9, 88.

Hori, T.S., Gamperl, A.K., Nash, G., Booman, M., Barat, A., Rise, M.L., 2013. The impact of a moderate chronic temperature increase on spleen immune-relevant gene transcription depends on whether Atlantic cod (*Gadus morhua*) are stimulated with bacterial versus viral antigens. Genome 56, 567-576.

Jones, S.R., Long, A., MacWilliams, C., Polinski, M., Garver, K., 2020. Factors associated with severity of naturally occurring piscirickettsiosis in netpen‐and tank‐reared juvenile Atlantic salmon at a research aquarium in western Canada. J. Fish Dis. 43, 49-55.

Jørgensen, S.M., Afanasyev, S., Krasnov, A., 2008. Gene expression analyses in Atlantic salmon challenged with infectious salmon anemia virus reveal differences between individuals with early, intermediate and late mortality. BMC Genomics 9, 179.

Li, J., Boroevich, K.A., Koop, B.F., Davidson, W.S., 2011. Comparative genomics identifies candidate genes for infectious salmon anemia (ISA) resistance in Atlantic salmon (*Salmo salar*). Mar. Biotechnol. 13, 232-241.

Løvmo, S.D., Whatmore, P., Sundh, H., Sigholt, T., Madaro, A., Bardal, T., Olsen, R.E., 2021. Effects of Atlantic salmon (*Salmo salar*) fed low- and high HUFA diets on growth and midgut intestinal health. Aquaculture 539, 736653.

Martin, S.A.M., Król, E., 2017. Nutrigenomics and immune function in fish: new insights from omics technologies. Dev. Comp. Immunol. 75, 86-98.

Martinez-Rubio, L., Evensen, Ø., Krasnov, A., Jørgensen, S.M., Wadsworth, S., Ruohonen, K., Vecino, J.L., Tocher, D.R., 2014. Effects of functional feeds on the lipid composition, transcriptomic responses and pathology in heart of Atlantic salmon (*Salmo salar* L.) before and after experimental challenge with Piscine Myocarditis Virus (PMCV). BMC Genomics 15, 462.

Meza, K., Inami, M., Dalum, A.S., Bjelland, A.M., Sørum, H., Løvoll, M., 2019a. Development of piscirickettsiosis in Atlantic salmon (*Salmo salar* L.) smolts after intraperitoneal and cohabitant challenge using an EM90‐like isolate: A comparative study. J. Fish Dis. 42, 1001-1011.

Meza, K., Inami, M., Dalum, A.S., Lund, H., Bjelland, A.M., Sørum, H., Løvoll, M., 2019b. Comparative evaluation of experimental challenge by intraperitoneal injection and cohabitation of Atlantic salmon (*Salmo salar* L) after vaccination against *Piscirickettsia salmonis* (EM90‐like). J. Fish Dis. 42, 1713-1730.

Moraleda, C.P., Robledo, D., Gutiérrez, A.P., Del-Pozo, J., Yáñez, J.M., Houston, R.D., 2021. Investigating mechanisms underlying genetic resistance to Salmon Rickettsial Syndrome in Atlantic salmon using RNA sequencing. BMC Genomics 22, 156.

Nicolas, F.E., 2011. Experimental validation of microRNA targets using a luciferase reporter system, MicroRNAs in Development. Springer, pp. 139-152.
Nourdin-Galindo, G., Sánchez, P., Molina, C.F., Espinoza-Rojas, D.A., Oliver, C., Ruiz, P., Vargas-Chacoff, L., Cárcamo, J.G., Figueroa, J.E., Mancilla, M., 2017. Comparative pan-genome analysis of *Piscirickettsia salmonis* reveals genomic divergences within genogroups. Front. Cell. Infect. Microbiol. 7, 459.
Robertsen, B., 2006. The interferon system of teleost fish. Fish Shellfish Immunol. 20, 172-191.
Rodger, H.D., 2016. Fish disease causing economic impact in global aquaculture, Fish vaccines. Springer, pp. 1-34.
Rosenlund, G., Torstensen, B.E., Stubhaug, I., Usman, N., Sissener, N.H., 2016. Atlantic salmon require long-chain n-3 fatty acids for optimal growth throughout the seawater period. J Nutr Sci 5, e19.
Rozas-Serri, M., Ildefonso, R., Peña, A., Enríquez, R., Barrientos, S., Maldonado, L., 2017. Comparative pathogenesis of piscirickettsiosis in Atlantic salmon (*Salmo salar* L.) post‐smolt experimentally challenged with LF‐89‐like and EM‐90‐like *Piscirickettsia salmonis* isolates. J. Fish Dis. 40, 1451-1472.
Rozas-Serri, M., Peña, A., Arriagada, G., Enríquez, R., Maldonado, L., 2018a. Comparison of gene expression in post‐smolt Atlantic salmon challenged by LF‐89‐like and EM‐90‐like *Piscirickettsia salmonis* isolates reveals differences in the immune response associated with pathogenicity. J. Fish Dis. 41, 539-552.
Rozas-Serri, M., Peña, A., Maldonado, L., 2018b. Transcriptomic profiles of post-smolt Atlantic salmon challenged with *Piscirickettsia salmonis* reveal a strategy to evade the adaptive immune response and modify cell-autonomous immunity. Dev. Comp. Immunol. 81, 348-362.
Ruyter, B., Røsjø, C., Einen, O., Thomassen, M., 2000. Essential fatty acids in Atlantic salmon: effects of increasing dietary doses of n-6 and n-3 fatty acids on growth, survival and fatty acid composition of liver, blood and carcass. Aquac. Nutr. 6, 119-127.
Saavedra, J., Hernandez, N., Osses, A., Castillo, A., Cancino, A., Grothusen, H., Navas, E., Henriquez, P., Bohle, H., Bustamante, F., 2017. Prevalence, geographic distribution and phenotypic differences of *Piscirickettsia salmonis* EM‐90‐like isolates. J. Fish Dis. 40, 1055-1063.
Sissener, N., Waagbø, R., Rosenlund, G., Tvenning, L., Susort, S., Lea, T., Oaland, Ø., Chen, L., Breck, O., 2016. Reduced n-3 long chain fatty acid levels in feed for Atlantic salmon (*Salmo salar* L.) do not reduce growth, robustness or product quality through an entire full scale commercial production cycle in seawater. Aquaculture 464, 236-245.
Škugor, S., Jørgensen, S.M., Gjerde, B., Krasnov, A., 2009. Hepatic gene expression profiling reveals protective responses in Atlantic salmon vaccinated against furunculosis. BMC Genomics 10, 503.

Timmerhaus, G., Krasnov, A., Takle, H., Afanasyev, S., Nilsen, P., Rode, M., Jørgensen, S.M., 2012. Comparison of Atlantic salmon individuals with different outcomes of cardiomyopathy syndrome (CMS). BMC Genomics 13, 205.

Vallejos-Vidal, E., Reyes-López, F., Teles, M., MacKenzie, S., 2016. The response of fish to immunostimulant diets. Fish Shellfish Immunol. 56, 34-69.

Wang, M., Jiang, S., Wu, W., Yu, F., Chang, W., Li, P., Wang, K., 2018. Non-coding RNAs function as immune regulators in teleost fish. Front. Immunol. 9, 2801.

Xue, X., Caballero-Solares, A., Hall, J.R., Umasuthan, N., Kumar, S., Jakob, E., Skugor, S., Hawes, C., Santander, J., Taylor, R.G., Rise, M.L., 2021. Transcriptome profiling of Atlantic salmon (*Salmo salar*) parr with higher and lower pathogen loads following *Piscirickettsia salmonis* infection. Front. Immunol. 12, 789465.

Xue, X., Hall, J.R., Caballero-Solares, A., Eslamloo, K., Taylor, R.G., Parrish, C.C., Rise, M.L., 2020. Liver transcriptome profiling reveals that dietary DHA and EPA levels influence suites of genes involved in metabolism, redox homeostasis, and immune function in Atlantic salmon (*Salmo salar*). Mar. Biotechnol. 22, 263-284.

Xue, X., Hixson, S.M., Hori, T.S., Booman, M., Parrish, C.C., Anderson, D.M., Rise, M.L., 2015. Atlantic salmon (*Salmo salar*) liver transcriptome response to diets containing *Camelina sativa* products. Comp. Biochem. Physiol. D: Genomics Proteomics 14, 1-15.

Xue, X., Woldemariam, N.T., Caballero-Solares, A., Umasuthan, N., Fast, M.D., Taylor, R.G., Rise, M.L., Andreassen, R., 2019. Dietary immunostimulant CpG modulates microRNA biomarkers associated with immune responses in Atlantic salmon (*Salmo salar*). Cells 8, 1592.